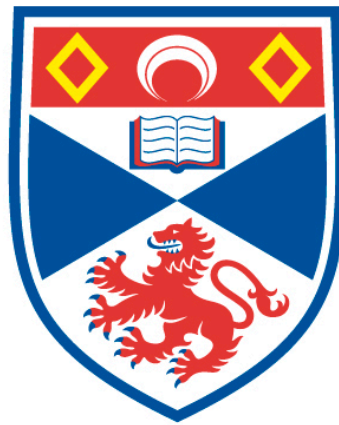


# DETECTING MYCOBACTERIAL CELL STATES USING PHOTONICS

Robert James Hunter Hammond

A Thesis Submitted for the Degree of PhD  
at the  
University of St Andrews



2016

Full metadata for this item is available in  
St Andrews Research Repository  
at:

<http://research-repository.st-andrews.ac.uk/>

Identifiers to use to cite or link to this thesis:

DOI: <https://doi.org/10.17630/10023-17007>  
<http://hdl.handle.net/10023/17007>

This item is protected by original copyright

# DETECTING MYCOBACTERIAL CELL STATES USING PHOTONICS

ROBERT JAMES HUNTER HAMMOND

THESIS SUBMITTED TO THE  
UNIVERSITY OF ST ANDREWS  
FOR THE DEGREE OF  
DOCTOR OF PHILOSOPHY (PHD)

MARCH 2016

MEDICAL AND BIOLOGICAL SCIENCES BUILDING  
UNIVERSITY OF ST ANDREWS  
NORTH HAUGH  
ST ANDREWS

### 1. Candidate's declarations:

I, Robert J H Hammond, hereby certify that this thesis, which is approximately 70,000 words in length, has been written by me, and that it is the record of work carried out by me, or principally by myself in collaboration with others as acknowledged, and that it has not been submitted in any previous application for a higher degree.

I was admitted as a research student in July 2012 and as a candidate for the degree of Doctor of Philosophy in July 2016; the higher study for which this is a record was carried out in the University of St Andrews between 2012 and 2016.

Date 29/08/2016                      signature of candidate

### 2. Supervisor's declaration:

I hereby certify that the candidate has fulfilled the conditions of the Resolution and Regulations appropriate for the degree of Doctor of Philosophy in the University of St Andrews and that the candidate is qualified to submit this thesis in application for that degree.

Date 29/08/2016                      signature of supervisor

### 3. Permission for electronic publication: *(to be signed by both candidate and supervisor)*

In submitting this thesis to the University of St Andrews we understand that we are giving permission for it to be made available for use in accordance with the regulations of the University Library for the time being in force, subject to any copyright vested in the work not being affected thereby. We also understand that the title and the abstract will be published, and that a copy of the work may be made and supplied to any bona fide library or research worker, that my thesis will be electronically accessible for personal or research use unless exempt by award of an embargo as requested below, and that the library has the right to migrate my thesis into new electronic forms as required to ensure continued access to the thesis. We have obtained any third-party copyright permissions that may be required in order to allow such access and migration, or have requested the appropriate embargo below.

The following is an agreed request by candidate and supervisor regarding the publication of this thesis:

#### PRINTED COPY

a) ~~No embargo on print copy~~

b) Embargo on all or part of print copy for a period of 1 year (maximum five years) on the following ground(s):

- Publication would be commercially damaging to the researcher, or to the supervisor, or the University
- Publication would preclude future publication
- Publication would be in breach of laws or ethics

c) ~~Permanent or longer term embargo on all or part of print copy for a period of ... years (the request will be referred to the Pro-  
Provost and permission will be granted only in exceptional circumstances).~~

#### Supporting statement for printed embargo request:

#### ELECTRONIC COPY

a) ~~No embargo on electronic copy~~

b) Embargo on all or part of electronic copy for a period of 1 year (maximum five years) on the following ground(s):

- Publication would be commercially damaging to the researcher, or to the supervisor, or the University
- Publication would preclude future publication
- Publication would be in breach of law or ethics

c) ~~Permanent or longer term embargo on all or part of electronic copy for a period of ... years (the request will be referred to  
the Pro- Provost and permission will be granted only in exceptional circumstances).~~

#### Supporting statement for electronic embargo request:

Date 29/08/2016                      signature of candidate                      signature of supervisor

*Please note initial embargoes can be requested for a maximum of five years. An embargo on a thesis submitted to the Faculty of Science and Medicine is rarely granted for more than two years in the first instance, without good justification. The Library will not lift an embargo before confirming with the student and supervisor that they do not intend to request a continuation. In the absence of an agreed response from both student and supervisor, the Head of School will be consulted. Please note that the total period of an embargo, including a continuation, is not expected to exceed ten years.*

*Where part of a thesis is to be embargoed, please specify the part and the reason.*

# Abstract

Tuberculosis is an ancient disease with evidence of *Mycobacterium tuberculosis* bacilli being found in mummies from ancient Egypt. There are also contemporary cases of tuberculosis, worldwide, every day. Like a good parasite *Mycobacterium tuberculosis* can hide within its host undetected for long periods of time. This state of quiescence has numerous names but in this research we will be referring to mycobacterial dormancy.

This study investigates the continuing problem of dormancy and associated antibiotic resistance in *Mycobacterium tuberculosis* (MTB). We focussed on closely related research surrogates of MTB; *M. smegmatis*, *M. fortuitum*, *M. marinum* and *M. bovis* (BCG). Phenotypic resistance is defined as antibiotic resistance that arises as a function of an organism's specific phenotype, rather than its genome and the genes it *could* express. Dormancy in MTB can arise when a culture of *in vitro* bacteria ages to the stationary phase or becomes otherwise stressed. *In vivo* the conditions surrounding dormancy are less well understood.

Dormancy is an ill-defined state of being suggested for MTB characterised by a down shift in metabolic function and a resistance to chemotherapy. It has been noted that a similar phenotype is found in MTB cells that are expressing lipid bodies- lipid rich cells.

We aimed to create a device that could differentiate between lipid rich and lipid poor cells rapidly using photonic technology. In so doing we created a rapid cell quantifying device, SLIC, which we have used and evaluated extensively with both mycobacteria and common nosocomial pathogens.

As another approach we attempted to separate lipid rich from lipid poor cells. This was achieved using a novel buoyant density separation methodology in combination with an adapted lipophilic staining regimen. In combination these two techniques allowed us to generate discreet populations of  $\geq 95\%$  purity which we were then able to experiment on individually.

Due to our novel separation methodology we were able to discover that lipid rich cells are much more resistant to the current anti-tuberculosis frontline treatment ( $\approx 40\times$  more

resistant). We showed that lipid rich cells down regulate certain nucleic acid markers associated with a quiescent cell state. We were also able to discover that lipid rich cells occur in young unstressed cultures indicating that the accumulation of lipid bodies is a natural part of the mycobacterial cell cycle. This hints at a possible reason for relapse in non-immunocompromised patients that maintain their drug regimen over the entire term.

Given what we have achieved over the course of this work I believe that we are closer to understanding the effects of mycobacterial dormancy on the *Mycobacterium tuberculosis* bacilli *in vivo*. Combining this with the invention of SLIC and its capacity to rapidly detect bacteria at unprecedentedly low concentrations we are closer to being able to diagnose and treat patients faster and with less wasted antibiotics than was previously possible.

# Acknowledgements

I would like to address my acknowledgements to the University of St Andrews for giving me the opportunity to study this PhD and for all the financial, material and moral support.

I am extremely grateful for all the help and support I received from my supervisor Professor Stephen H Gillespie. On numerous occasions I would be stuck with a problem or have a burning question and, although constantly called upon for his expertise, Professor Gillespie managed to make time and ceaselessly encouraged me to be a better scientist and always to think critically.

My special thanks also go to my colleagues without whom my work would not only have been impossible, but significantly less enjoyable;

Dr Katarina Oravcova, Mr John Kennedy, Dr Eoghan Farmer, Mr Vincent Baron, Dr Han Xiao, Dr Wilber Sabiiti, Mr Prince Agyirey-Kwakye, Dr Janet Cox-Singh, Mr Scott Millar, Dr Ruth Bowness, Mrs Souad Alateah, Dr Catriona Harkins and Dr Kerry Pettigrew.

In particular I want to thank Katarina for her tireless understanding, help, direction and advice.

John, Vince, Eoghan, Scott, Sophie and Stef for their entirely limited help and sympathy, but mostly for their friendship and support.

Janet, Han, Wilber and Prince for their professional guidance and use of their expertise.

And all others, friends and colleagues, present within labs 248 and 249 and without, the experience of working with you has made these last 3 years some of the most enjoyable of my life.

A special remark must be made for Ms Marion Ponthus, organiser supreme, without whom the group would cease to function.

Many thanks to Dr Simon Young who performed the mass spectrometry on extracted whole-cell lipid for us both effectively and quickly.

My thanks to Dr Simon Powis for the use of his flow cytometer and to Dr Elaine Campbell for teaching me all about its use and data analysis. In addition many thanks are owed to Dr Melissa Andrews for the use of her microscope without which the work would have been impossible.

My thanks also go out to the department of Medicine and Biological Sciences and the School of Biology at St Andrews University, especially Mr Henry Rae, a constant wellspring of unhelpful inspiration and a fantastic and unlimited resource. And finally the people who make the building run and keep it open for us to study, work and learn, thank you all.

I must thank PreDiCT-TB, not for their monetary or material contributions, but for allowing me amongst their ranks to exchange names and ideas with great academics in the field of tuberculosis research.

Throughout my academic career and beforehand my parents have been there to support me; I thank them for their guidance and their care. From them I get my stubbornness and my pathological curiosity.

I would like to thank my Partner, Fiancé and anchor for many years now, Siobhan Dunn, for her unwavering support though the good times and the bad. Through the trials and tribulations of our studies and many other circumstances we have overcome, Thank you.  
(TAS; 526;9-22)

There are many more I would like to mention but time and space are limited.

Dedicated to my Father, David Wayne Hammond. The biggest man I ever knew.



# List of abbreviations

ABS	Acrylonitrile butadiene styrene
BDS	Buoyant density separation
Ct	Cycle threshold – PCR measure of positivity
D <sub>2</sub> O	diDuterium monoxide (heavy water)
DAG	Diacylglycerol(s)
DMSO	Dimethyl sulfoxide
DNA	Deoxyribonucleic acid
FitC	Fluorescein isothiocyanate
FLIC	Fluorescent Light Integrating Collector
GMM	Glucose monomycolate(s)
24h	24 hours
HIV	Human immunodeficiency virus
hSLIC	Heated SLIC
ICL	Isocitratelase
IF	Immunofluorescence
IgA	Immunoglobulin A (dimer)
IgM	Immunoglobulin M (pentamer)
λ	Lambda, - Wavelength
LB	Lipid body
LJ	Lowenstein-Jensen agar
LP	Lipid poor
LR	Lipid rich
MA	Mycolic acid(s)
MBC	Minimum bactericidal concentration

MDR-TB	Multi drug resistant TB
MGIT	Mycobacterial growth indicator tube
MIC	Minimum inhibitory concentration
mm	millimetre(s)
MRC	Medical research council
mRNA	Messenger RNA
MTB	Mycobacterium tuberculosis (bacteria)
MTBC	MTB complex
mV	Millivolt(s)
NAG	N-acetyl-glucosamine
NGM	N-acetyl-muramic acid
nm	nanometre(s)
OD <sub>600</sub>	Optical density at 600 nm
PBS	Phosphate buffered saline
PCR	Polymerise chain reaction
PIM	Phosphatidylmyo-inositol mannoside(s)
PLA	Polylactic acid
qPCR	Quantitative PCR
RGD	Rayleigh-Gans Debye light scattering
RNA	Ribonucleic acid
RNAseq	RNA sequencing- next generation, real time RNA quantification and profiling
RPF	Resuscitation promotion factor
rRNA	Ribosomal RNA
SILAC	Stable isotope labelling by amino acids in cell culture
SLIC	Scattered Light Integrating Collector
SNP	Single nucleotide polymorphism

TAG	Triacylglycerol(s)
TB	Tuberculosis (disease)
tmRNA	Transfer messenger RNA
TSO	Total scattering output
WHO	World Health Organisation
XDR-TB	Extensively drug resistant TB
ZN	Zeihl – Neelsen

# List of figures

Figure 1.1. Mycobacterium spp. Stained with Auramine-O .....	18
Figure 1.2. Image taken from Max Planck Gesellschaft (Society) showing an interesting ‘double membrane’ feature .....	24
Figure 2.1. A schematic of a nephelometer .....	41
Figure 2.2. Bacterial presence test.. .....	65
Figure 2.3. Total scattering output for four species of Mycobacterium; <i>M. smegmatis</i> , <i>M.</i> <i>fortuitum</i> , <i>M. marinum</i> and BCG.....	67
Figure 2.4. Total scattering output for a dilution series of <i>Mycoplasma pneumoniae</i> .. .....	69
Figure 2.5. Total scattering output of 3 example species. 3 of the 23 clinically relevant species tested over a serial dilution series. Bacterial concentration for each culture was at approximately $5 \times 10^6$ prior to first dilution. ....	70
Figure 2.6. graph displaying the 1000 fold difference in sensitivity between SLIC and spectrophotometry.. .....	72
Figure 2.7. TSOs for rapidly dividing bacterial species- <i>Escherichia coli</i> , <i>Serratia marcescens</i> and <i>Staphylococcus epidermidis</i> . .....	74
Figure 2.8 Examples of clinically relevant species treated with drugs they are resistant to over time in SLIC. ....	77
Figure 2.9. Examples of rapid susceptibility testing of clinically relevant species in SLIC.....	78
Figure 2.10. Rapid drug susceptibility data for BCG.. .....	80

Figure 2.11. hSLIC preliminary data. ....	82
Figure 2.12. Preliminary FLIC data. ....	83
Figure 2.13. Fluorescence microscopy of sample as displayed in Figure 2.12 . ....	84
Figure 2.14. Schematic of two possible end results of scattered laser light in the SLIC. ....	87
Figure 2.15. Typical scattering pattern emitted by a sample containing few bacteria. Bright central spot is the main focal point of the exiting laser beam. ....	88
Figure 2.16. Comparison of SLIC to other commercial products currently on the market for establishing bacterial number and their relative time to positivity (TTP) times in minutes. ....	90
Figure 3.1. Schematic depicting differential centrifugation in action, sequentially removing larger particles with every round of centrifugation. ....	102
Figure 3.2 Schematic diagram of the assembly used to centrifuge D <sub>2</sub> O and bacterial samples for separation ....	110
Figure 3.3. Difference in density of 10 <sup>9</sup> cells/ml of M. smegmatis culture. ....	113
Figure 3.4. Percentage of samples extracted from top fraction of 75% D <sub>2</sub> O- 25% H <sub>2</sub> O solution that yield greater than or equal to 90% purity of lipid rich cells. ....	114
Figure 3.5. flow cytometry data depicting the differences between LR and LP extractions form the BDS methodology. ....	116
Figure 3.6. Representative raw flow cytometry dot plots. ....	118
Figure 3.7. Raw flow cytometry side scatter data. ....	121

Figure 3.8. <i>M. smegmatis</i> cells separated by D <sub>2</sub> O fractionation and measured for side scatter (granularity) in a flow cytometer when unstained.....	122
Figure 4.1. Molecular structure of Nile red. ....	134
Figure 4.2. Excitation and emission spectra of EvaGreen dye bound to dsDNA in pH 7.3 buffer. ....	149
Figure 4.3. Nile red fluorescence of polar lipids at 645 nm, Nile red fluorescence of non-polar lipids at 527 nm .....	156
Figure 4.4. Graph displaying the number of flow cytometry events of an intensity greater or equal to 3 arbitrary units of <i>Mycobacterium smegmatis</i> after FitC staining and incubation for either 72 hours .....	158
Figure 4.5. Graph of a 400h long experiment displaying the relative concentrations detected of pre16S RNA, tmRNA, 16s RNA and the CFU value of <i>M. smegmatis</i> .....	160
Figure 4.6. Quantity of non-polar lipid fluorescence increasing over time relative to the quantity of detected red fluorescence and the CFU value. ....	163
Figure 4.7. lipid profiles across 6 time points from 72-288 hours.....	164
Figure 4.8. Concentrations of drugs required to completely sterilise cultures of mycobacteria, LR and LP Vs. old and young cultures .....	167
Figure 4.9. Images of human lung sections stained with Nile red.....	169
Figure 5.1. Figure displaying a growth curve of <i>M. smegmatis</i> over 10 days.. ....	187
Figure 5.2. Comparison of TLC results from a whole lipid extraction of four mycobacterial species in different culture stages; young (mid-exponential phase) and old (late stationary phase). ....	188

Figure 5.3. Figure displaying the Rf values for every successful TLC experiment colour coded to their respective lipid family.....	191
Figure 5.4. Gross ion counts for numerous lipid species recovered from a Bligh and Dyer extraction of lipid rich and lipid poor BCG.. .....	192
Figure 5.5. Data from Figure 5.4 displayed separately. ....	193
Figure 5.6. Data from Figure 5.4 displayed in terms of the absolute difference in the relative ion counts. ....	194
Figure 5.7 Nile red stained fluorescence micrograph of the difference between ‘fed’ and ‘unfed’ cultures.....	198
Figure 5.8. TLC of Bligh and Dyer extracted whole cell lipids from samples of ‘fed’ and ‘unfed’ BCG and <i>M. smegmatis</i> against the control lipid that was fed to the cells. ....	199
Figure 5.9. <i>M. fortuitum</i> cells grown under hypoxic conditions.....	206
Figure 6.1. The newest version of the SLIC.....	217

# List of tables

Table 1.1. Slow growing mycobacteria classified by their ability to produce pigments..	14
Table 2.1. Species tested in SLIC.	61
Table 2.2. Limit of detection for all clinically relevant microorganisms tested.....	71
Table 2.3. Chi <sup>2</sup> data from Figure 2.7. ....	76
Table 2.4. Time to positivity values along with accepted doubling times for each of the clinically relevant species tested. ....	79
Table 3.1. Student's T-test p values for data displayed in Figure 3.8. ....	122
Table 4.1. Physical properties of Nile red .....	135
Table 4.2. ingredients and volumes for all constituents of all RNA qPCR reactions. ....	150
Table 4.3. Sequences for the primers used including the internal control devised and optimised in house. ....	151
Table 4.4. ingredients and volumes for all constituents of all DNA qPCR reactions. ....	151
Table 4.5. Minimum bactericidal concentration (MBC) for M. smegmatis from published literature versus the lipid poor and lipid rich samples obtained for this study treated with the same regimen as described in the literature. ....	154
Table 4.6. Fold increase in MBC concentration required to clear LR cells compared with LP cells.. ....	154
Table 4.7. Table displaying the raw values for the data shown in Figure 4.8.. ....	166



Table 4.8. Values for MBCs of cultures of <i>M. smegmatis</i> grown to either later stationary phase (old) or mid exponential phase (young), separated into LR and LP (LR only show here) and treated with increasing quantities of drugs until there was no detectable growth.....	170
Table 5.1. Table showing the accepted R <sub>f</sub> values for the solvent system used in Figure 5.2 and the associated predicted lipid position. m. ....	189
Table 5.2. Mass to charge ratios for all lipid species displayed in Figure 5.4 and accompanying identifiers .....	197
Table 6.1. Discrepancy between the numerical readout from the lock-in amplifier and the digital oscilloscope which is the presumed source of the distortions in the SLIC data found at high mV ranges. ....	216

# Contents

<b>ABSTRACT</b>	<b>I</b>
<b>ACKNOWLEDGEMENTS</b>	<b>III</b>
<b>LIST OF ABBREVIATIONS</b>	<b>VI</b>
<b>LIST OF FIGURES</b>	<b>IX</b>
<b>LIST OF TABLES</b>	<b>XIII</b>
<b>1 GENERAL INTRODUCTION</b>	<b>1</b>
1.1 Tuberculosis	1
1.2 Tuberculosis risk factors	2
1.3 Transmission of tuberculosis	3
1.4 Pathology of Tuberculosis	4
1.4.1 Pathogenesis of MTB	4
1.4.2 Development of granuloma	6
1.4.3 Latency, reactivation/re-infection to produce secondary disease	6
1.4.4 Breakdown of caseous lesions, erosion into bronchi and TB infection	7
1.4.5 Treatment and control of TB	8
1.4.6 Primary and Secondary Tuberculosis	9
1.4.7 Latent TB	10
1.5 Epidemiology of TB	11
1.6 Taxonomy	12
1.7 Clinical tuberculosis	14
1.7.1 Signs and Symptoms of Pulmonary TB	15
1.8 Genome and Genotypes	15
1.9 Diagnosis of TB	15
1.9.1 Sputum microscopy	16
1.9.2 Sputum smear microscopy to detect TB Bacilli	17
1.9.3 Fluorescence microscopy to detect TB Bacilli	18
1.10 Cultivation of Mycobacteria	19
1.11 Identification of mycobacteria in culture	21

<b>1.12</b>	<b>The genus Mycobacterium</b>	<b>21</b>
<b>1.13</b>	<b>Morphology and staining of MTB</b>	<b>22</b>
<b>1.14</b>	<b>MTB cell envelope</b>	<b>22</b>
<b>1.15</b>	<b>Lipid bodies in Bacteria</b>	<b>25</b>
1.15.1	Lipid storage in prokaryotes	26
1.15.2	Lipid bodies in mycobacteria	27
<b>1.16</b>	<b>Growth characteristics of MTB in hypoxic environments</b>	<b>28</b>
1.16.1	Lipid metabolism	29
1.16.2	Responses to external stresses and stimuli	30
1.16.3	Antimicrobials - Anti-TB drug regimens	31
<b>1.17</b>	<b>Phenotypic drug resistance</b>	<b>34</b>
<b>1.18</b>	<b>Hypothesis, Aims and Objectives</b>	<b>35</b>
<b>1.19</b>	<b>Specific objectives</b>	<b>36</b>
<b>2</b>	<b>SLIC</b>	<b>37</b>
<b>2.1</b>	<b>Introduction to bacterial detection technologies</b>	<b>37</b>
<b>2.2</b>	<b>Direct methods</b>	<b>37</b>
2.2.1	Basic Cell detection – Microscopy	37
2.2.2	Basic Cell detection – Growth assays	39
<b>2.3</b>	<b>Light based cell detection</b>	<b>41</b>
2.3.1	Nephelometry	41
2.3.2	qPCR	43
2.3.3	Flow Cytometry	43
2.3.4	Spectrophotometry	45
2.3.5	Dynamic Light Scattering	46
<b>2.4</b>	<b>Introduction to SLIC</b>	<b>48</b>
2.4.1	Static Light Scattering	48
2.4.2	Rayleigh-Gans-Debye scattering	50
2.4.3	Integrating sphere	54
2.4.4	Lock-in Amplifier	55
<b>2.5</b>	<b>Methods</b>	<b>57</b>
<b>2.6</b>	<b>SLIC</b>	<b>57</b>
2.6.1	Development of the SLIC	57
2.6.2	Bacterial detection	58
2.6.3	Bacterial scattering at differing concentrations	59
2.6.4	Rapid antibiotic susceptibility testing	60
2.6.5	Self-incubating SLIC (hSLIC)	61
2.6.6	Detecting presence of lipid rich cells (SLIC fluorescence)	62

<b>2.7</b>	<b>Results</b>	<b>64</b>
2.7.1	SLIC calibration with biological material	65
2.7.2	Concentration dependant scattering test (lower limit of detection)	66
2.7.3	Rapid antibiotic susceptibility testing	72
2.7.4	hSLIC	80
2.7.5	Detecting presence of lipid rich cells (SLIC fluorescence- FLIC)	82
<b>2.8</b>	<b>Discussion</b>	<b>85</b>
2.8.1	SLIC calibration with biological material	85
2.8.2	Concentration dependant scattering test	85
2.8.3	Rapid susceptibility test	89
2.8.4	Rapid MIC/MBC testing of LR vs. LP	91
2.8.5	hSLIC	92
2.8.6	FLIC	93
<b>3</b>	<b>SEPARATION</b>	<b>95</b>
<b>3.1</b>	<b>Introduction to separation methodologies</b>	<b>95</b>
<b>3.2</b>	<b>Adherence</b>	<b>95</b>
<b>3.3</b>	<b>Density</b>	<b>96</b>
<b>3.4</b>	<b>Antibody binding</b>	<b>98</b>
<b>3.5</b>	<b>Filtering</b>	<b>101</b>
<b>3.6</b>	<b>Differential centrifugation</b>	<b>101</b>
<b>3.7</b>	<b>Introduction to D<sub>2</sub>O separation (buoyancy dependant separation, BDS)</b>	<b>103</b>
3.7.1	Isopycnic centrifugation	103
3.7.2	Percoll ©	104
3.7.3	D <sub>2</sub> O	105
<b>3.8</b>	<b>Methods</b>	<b>108</b>
3.8.1	Buoyant density separation	108
3.8.2	One <i>g</i> separation	108
3.8.3	Centrifuge (~200 <i>g</i> ) separation	109
3.8.4	Isolation and identification of different phenotypic states	111
3.8.5	Granularity data	112
<b>3.9</b>	<b>Results</b>	<b>113</b>
3.9.1	D <sub>2</sub> O	114
3.9.2	Comparing efficiency to purity of the separation technique	115
3.9.3	Confirmation – granularity results	118
<b>3.10</b>	<b>Discussion</b>	<b>123</b>
3.10.1	Mycobacterial separation via D <sub>2</sub> O solution	123
3.10.2	Yields and efficiencies of BDS methodologies	124
3.10.3	Significance of our findings	126
3.10.4	Relevance to presence of mycobacterial lipid bodies	127

3.10.5	Disadvantages of BDS methods	128
3.10.6	Flow cytometry data	130
3.10.7	Centrifuge separation	131
3.10.8	Conclusion	132
<b>4</b>	<b>LIPID RICH MYCOBACTERIA</b>	<b>133</b>
<b>4.1</b>	<b>Introduction to Bacterial Dormancy</b>	<b>133</b>
<b>4.2</b>	<b>Nile red</b>	<b>134</b>
<b>4.3</b>	<b>Lipids</b>	<b>136</b>
<b>4.4</b>	<b>Chemotherapy</b>	<b>138</b>
<b>4.5</b>	<b>Methods</b>	<b>142</b>
4.5.1	Lipid-rich bacteria analysis	142
4.5.2	FitC staining	142
4.5.3	Determination of antibiotic susceptibility	142
4.5.4	Staining	143
4.5.5	Flow cytometry	144
4.5.6	Human lung tissue	144
4.5.7	Old Lipid-rich cells versus young lipid-rich cells	145
4.5.8	Long term experiments	146
4.5.9	PCR	147
4.5.10	qPCR protocol	150
4.5.11	DNA	151
<b>4.6</b>	<b>Results</b>	<b>153</b>
4.6.1	Determination of antibiotic susceptibility	153
4.6.2	Staining	154
4.6.3	FitC	157
4.6.4	Long term experiments	159
4.6.5	Old Lipid-rich cells versus young lipid-rich cells	165
4.6.6	Human lung tissue exhibiting LR cells	168
<b>4.7</b>	<b>Discussion</b>	<b>171</b>
4.7.1	Susceptibility	171
4.7.2	Staining	174
4.7.3	Flow data	176
4.7.4	As a function of time – when to LBs form?	177
4.7.5	Lung	179
4.7.6	Old Lipid-rich cells versus young lipid-rich cells	180
<b>5</b>	<b>LIPIDOMICS</b>	<b>181</b>
<b>5.1</b>	<b>Introduction to lipidomics</b>	<b>181</b>
5.1.1	TLC	182
5.1.2	Mass Spectrometry	182

<b>5.2</b>	<b>Methods</b>	<b>184</b>
5.2.1	Lipidomics	184
5.2.2	Artificial lipid accumulation	186
<b>5.3</b>	<b>Results</b>	<b>188</b>
5.3.1	TLC	188
5.3.2	Mass spectrometry	192
5.3.3	Artificial lipid accumulation	198
<b>5.4</b>	<b>Discussion</b>	<b>200</b>
<b>6</b>	<b>GENERAL DISCUSSION</b>	<b>208</b>
6.1	SLIC	214
6.2	Detection methodologies	219
6.3	Separation	220
6.4	Lipid accumulation	222
6.5	Lipidomics	228
6.6	Conclusions	231
<b>7</b>	<b>FUTURE WORK</b>	<b>233</b>
<b>8</b>	<b>REFERENCES</b>	<b>238</b>

# 1 General introduction

## 1.1 Tuberculosis

Tuberculosis (TB) is one of the oldest recognised human diseases (Tripathi, Tewari et al. 2005). Throughout human history it has had many names; Consumption, phthisis, scrofula (cervical lymphadenitis), Pott's disease (spinal tuberculosis), lupus vulgaris (cutaneous tuberculosis) and the White Plague have all been used to describe the disease caused by *Mycobacterium tuberculosis*. The name 'tuberculosis' is drawn from the Latin word "tubercle" meaning a small lump. The seminal microbiologist Robert Koch discovered the "tubercle bacillus" in 1882 (Sakula 1983). In 1993 TB was acknowledged as a "global health emergency" by the World Health Organisation (WHO).

TB is associated with poverty and is often a secondary infection associated with Human Immunodeficiency Virus (HIV) (Coker and Miller 1997). TB can also present as the primary infection with a secondary infection of its own such as *Haemophilus influenza* or *Listeria spp* (Kahnert, Hopken et al. 2007).

TB is predominantly a disease of the lungs but can affect other bodily tissues such as the liver and kidneys (Narayana 1982, Wu, Wang et al. 2013). Forms of tuberculosis that affect tissues other than the lungs are known as extrapulmonary tuberculosis, pulmonary tuberculosis is TB of the lungs (Mehta, Dutt et al. 1991).

A cough is the most common symptom of pulmonary TB (see section 1.4) however it is possible that at an early stage in the infection the patients are asymptomatic and when a cough does develop it can be unproductive (Li, Bai et al. 1999, Chintu and Mwaba 2003). When sputum is produced it is often used to confirm a tuberculosis diagnosis in conjunction with chest X-rays and (in rare cases) a tuberculin skin test (van Cleeff, Kivihya-Ndugga et al.

2005, Lalvani 2007). Using sputum to confirm a TB diagnosis is an old technique but still widely used (Steingart, Henry et al. 2006) and is only possible with the use of staining reagents; the Kinyoun hot and cold techniques, Ziehl Neelsen and Auramine O are all widely used acid fast staining methodologies (Thadepalli, Rambhatla et al. 1977, Githui, Kitui et al. 1993, Caviedes, Lee et al. 2000, Van Deun, Hamid Salim et al. 2005, Steingart, Henry et al. 2006, Marais, Brittle et al. 2008). For initial diagnosis of pulmonary TB, a series of three sputum need to be collected, ideally before drug therapy is started (Ssengooba, Kateete et al. 2012).

## **1.2 Tuberculosis risk factors**

Infectivity risk for tuberculosis is increased in households containing a tuberculosis sufferer or areas in which those who have been in contact with a tuberculosis sufferer are again in close contact (Wood, Johnstone-Robertson et al. 2010). There are documented cases of TB being spread in public transport, especially on airplanes (Kenyon, Valway et al. 1996). As with many diseases the old and the young are most at risk (Stead and Lofgren 1983, Wood, Johnstone-Robertson et al. 2010) along with immunocompromised individuals (Coker and Miller 1997). Other contributing factors to an individual's susceptibility to TB are their nutritional state, drug use and socioeconomic background (the latter is often a compounding factor) (Cundall 1986, Mangtani, Jolley et al. 1995, Chan, Tian et al. 1996, Cantwell, McKenna et al. 1998). There is even limited evidence that gender can play a role in TB susceptibility (Hudelson 1996). Irrespective of the state of the individual at the time of infection it is generally true that individuals infected with non-DRTB are not infectious to others for at least 2 weeks (Griffith and Kerr 1996).



### 1.3 Transmission of tuberculosis

Transmission of tuberculosis occurs mainly by aerosolised droplets liberated during coughing, sneezing, speaking, singing or laughing (Kenyon, Valway et al. 1996, King 2001, Roy and Milton 2004, Morawska 2006, Tang, Li et al. 2006, Jones-Lopez, Namugga et al. 2013). The main source of these aerosolised droplets is an individual suffering from active pulmonary TB. Apart from a patient suffering with laryngeal TB singing (Rieder 2009), a sneeze is the second most infectious of the expulsion events and can express up to 1 million bacilli in less than a second. A cough can release as many as 3500 organisms and talking between 0 and 200 (Paul A. Jensen 2015). The infectious dose of tuberculosis could be as low as five - ten intact and healthy bacilli (Balasubramanian, Wiegeshaus et al. 1994, Nicas, Nazaroff et al. 2005) therefore all of these routes could potentially propagate an infection in a new host. Expelled droplets can range from 0.5 - ~30µm in diameter. Droplets >20µm will fall directly to the ground whereas droplets in the 5-20µm range can hang in the air for seconds to minutes (Papineni and Rosenthal 1997). These droplets could then potentially be inhaled by surrounding individuals. *Mycobacterium tuberculosis* is quickly killed by UV radiation (up to a log7 reduction in bacilli numbers after 30 second exposure (David, Jones et al. 1971)), naturally occurring in the form of strong daylight. This means that in geographic areas with long periods of strong sunlight, areas nearer the equator for example, the bulk of transmission occurs indoors or under shade where settled droplets of infected saliva can be re-aerosolised by human movement and inhaled -or inhaled directly. Familial clustering of cases of TB has been noted for a long time (OPIE and McPHEDRAN 1926, Verver, Warren et al. 2004). There is also evidence of clustering in other areas of high human concentration such as schools (Ewer, Deeks et al. 2003) and universities (Alonso-Echanove, Granich et al. 2001), works places (Nardell, Keegan et al. 1991, Bowden and

McDiarmid 1994) and airplanes (Mangili and Gendreau 2005). The smallest droplets (0.5 - 5  $\mu\text{m}$ ) can enter the lower passages of the lungs directly and cause a more immediate infection.

When TB bacilli begin to establish an infection, immune cells such as macrophages and lymphocytes will start to migrate to the point of infection. If the immune system fails to clear the bacilli either because the patient is immune compromised or because of MTB's capacity to survive within host macrophages then the patient will develop primary pulmonary TB.

## **1.4 Pathology of Tuberculosis**

### **1.4.1 Pathogenesis of MTB**

MTB enters the human host via aerosolised droplets that are inhaled into the alveoli and are internalised by alveolar macrophages. Once inside macrophages MTB replicates and forms a preliminary lesion called a *Ghon focus* (Bermudez and Goodman 1996). While a *Ghon focus* is formed some bacilli may migrate to the hilar lymph nodes and form an inflammatory infection there which causes the lymph node to distend. This along with the *Ghon focus* forms the primary infection site (Parrish, Dick et al. 1998, Jeong and Lee 2008). MTB can spread from this stage but, much more commonly, at a later stage of infection to the kidneys, brain or bone via the blood (Fountain 1954, EASTWOOD, CORBISHLEY et al. 2001).

Macrophages are thought to be the primary location within which pathogenic mycobacteria are able to replicate (Cosma, Sherman et al. 2003). In the airways, alveolar macrophages phagocytose the bacteria and attempt to destroy them by fusion of the vesicle in which the bacteria are located (the phagosome) by fusing it with a pre-existing vesicle (the lysosome) to form a phagolysosome. MTB however is able to prevent this from occurring through as yet unknown mechanisms (Goren, D'Arcy Hart et al. 1976, Deretic, Singh et al. 2006). Once

infected with MTB macrophages release chemokines to recruit neutrophils and monocytes to the site of infection (Peters and Ernst 2003). At the site of infection monocytes will differentiate into macrophages in the cavities or dendritic cells in the tissues. These dendritic cells will then migrate to the draining lymph nodes, where mycobacterial antigens are presented to T cells (Russell 2011). When T lymphocytes are activated, they produce cytokines such as interferon gamma (IFN- $\gamma$ ) that can activate macrophages to produce antimicrobial substances.

Russell (Russell 2007) reported that MTB has adapted strategies to survive in the naive macrophage through mechanisms that result in the modulation of the host cell function and prevent macrophage activation by arresting the development of a localized immune response. The normal maturation process of the phagosome into digestive, bactericidal organelle involves progressive acidification, accumulation of hydrolytic enzymes and fusion with lysosomal compartments (Clemens and Horwitz 1995, Honer zu Bentrup and Russell 2001, Huang, Zhou et al. 2012). However, *MTB* is able to arrest the maturation of the phagosome and prevent its fusion with lysosomal compartments, thereby maintaining the pH at 6.4. MTB is also able to modulate the adaptive immune response by subverting the MHC class II presentation pathway (Voskuil, Bartek et al. 2011).

In recent years a lot of work has been focussed on resuscitation promotion factors (RPFs). RPFs are a family of secreted proteins produced by *Mycobacterium tuberculosis* that stimulate mycobacterial growth. Some mouse infection studies have shown that RPFs support bacterial survival and disease reactivation post-dormancy. It is currently unknown whether RPFs influence human infection (Mukamolova, Turapov et al. 2010).

### **1.4.2 Development of granuloma**

Once endocytosed MTB bacilli will reside in an endocytic vacuole called the phagosome. Antigen presenting cells begin antigen processing and presentation after approximately 10 days of infection. The processed components of the MTB antigen are, at this point, called adjuvants and are presented to antigen-specific T lymphocytes. These T lymphocytes undergo clonal proliferation, cytokine release, recruitment of cells and finally granuloma formation (Saunders and Cooper 2000). Initially thought to be exclusively beneficial to the host, the role of the granuloma is now found to be more complex (Ramakrishnan 2012). A granuloma is constantly remodelled, due to the balance between pro-and anti-inflammatory immune signals at the site of infection (Russell 2011). Once infection is established adaptive immunity begins to activate. This means more cells are recruited to the site of infection. The granuloma then becomes a more organized and stratified structure with a macrophage-rich centre surrounded by lymphocytes that in turn may be covered with a fibrous outer layer (Russell, Barry et al. 2010). The classically described caseous granuloma indicates a central necrotic region with a core of foamy macrophages that may become hypoxic.

### **1.4.3 Latency, reactivation/re-infection to produce secondary disease**

Throughout this work the term latency will refer only to the tuberculosis disease state and not the responsible bacteria (Lipworth, Hammond et al. 2016). The bacteria that take part in latent disease are often given the name dormant. This is not necessarily strictly accurate but for the purposes of discussion it is assumed that a patient with latent disease is infected with a high proportion of dormant cells. Dormancy has been defined as “a reversible state of low metabolic activity in a unit that maintains viability” (Kaprelyants and Kell 1993). Latency could last for most of an individual’s lifetime and the individual may never exhibit disease

symptoms. In approximately 5% of cases (10% in the immunocompromised) (Salina, Waddell et al. 2014) the patient will undergo an activation event and the disease will manifest overt symptoms. This is sometimes called a *reactivation* event or relapse, although these two ideas are not synonymous. Relapse in the context is a misnomer as relapse is not possible unless the patient has undergone antibiotic therapy.

Associated TB risk factors include immunocompromised individuals; either through co-infection or through malnutrition and age. Individuals with HIV often develop a TB coinfection either through reactivation of a pre-existing infection or a new infection from a hospital, clinic or the community; a primary infection.

The progression of an MTB infection to an active infection can occur when a granuloma starts to degrade, bringing oxygen and other nutrients to the bacteria in the granuloma (Dye, Bassili et al. 2008). If the granulomatous structure fails MTB cells and infected macrophages can spread to other areas of the body. At each point where these freed cells can establish an infection lesions are formed that destroy local tissue (Cheney 1909, Schubert, Haltaufderheide et al. 1992, Kannaperuman, Natarajarathinam et al. 2013).

#### **1.4.4 Breakdown of caseous lesions, erosion into bronchi and TB infection**

In primary TB infection the initial outcomes; spontaneous cure, active disease or inactive disease are based largely on the strength of cell mediated immune response (Smith 2003). Once an infection is well established and granulomatous lesions have formed liquefaction of the granuloma can occur. It is currently not known the exact processes that lead to granuloma liquefaction but many suspect it to be enzymatically mediated (Dannenberg and Sugimoto 1976). After a liquefaction event the bacilli may be able to reach and to

disseminate to other tissue and organs through the circulatory and lymphatic system. This can lead rapidly to extra-pulmonary tuberculosis infection (Smith 2003). After a liquefaction event the patient is no longer a simple carrier of disease but is now once again infectious. If the liquefaction of caseous granulomas has been extensive then it is thought that this can lead to a severe increase in morbidity to, and infectivity of, the patient.

Caseation of a granuloma can be regarded as a host defence mechanism even though bacilli have been found to still be viable. These cells are embedded in the area of coagulative necrosis within a lesion. MTB may remain viable for long periods in caseous material. Only calcification of the granuloma is known to give a high likelihood of the internalised bacilli being no longer infectious in the long term (Gawne-Cain and Hansell 1996). Caseous granulomas are difficult places for MTB cells to survive. They have low pH, high concentrations of reactive oxygen and nitrogen species and are low in molecular oxygen (Dannenberg and Sugimoto 1976, Sherman, Sabo et al. 1995, Via, Lin et al. 2008). These conditions stress any embedded MTB cells and could contribute to the emergence of the dormancy phenotype (Deb, Lee et al. 2009, Voskuil, Bartek et al. 2011).

#### **1.4.5 Treatment and control of TB**

The major aims of TB treatment are to cure the patient, control transmission of the disease and to stop the disease entering latent phase. This last is itself highly challenging as the concentrations of drug required to clear all dormant bacteria are thought to be toxic to the host (Hammond *et al*, 2015). Treatment of TB requires 6 months of intensive therapy to complete and two or more anti-TB drugs that work differently are administered to prevent the bacteria becoming drug resistant. There are two phases during the treatment of TB

namely the intensive and continuation phases (Gosling, Uiso et al. 2003, van Ingen, Aarnoutse et al. 2011).

#### **1.4.6 Primary and Secondary Tuberculosis**

Primary TB is defined as an infection event in which MTB bacilli enter the respiratory tract and are subsequently phagocytosed by macrophages where they are either killed, become dormant and non-replicating or begin to replicate within the macrophage. Classically there will be an acquired immune response via type IV hypersensitivity, this leads to an up regulation of the quantity of lymphocytes in the patients' blood (Dannenberg 1991). During the initiation of the type IV hypersensitivity response infected macrophages are taken up into the lymph nodes of the host body and retained there (Ferrero, Biswas et al. 2003). If the immune system is fully competent then a full type IV hypersensitivity reaction can take place and the majority of TB cells will be killed but at the cost of severe local damage and inflammation to the affected area. This occurs because the hyper-sensitised macrophages produce TNF in abundance which recruits monocytes which then differentiate into epithelioid histiocytes and block the affected area (Shi and Pamer 2011). This total and competent immune reaction is thought to occur relatively rarely and is referred to as 'spontaneous curing' (Millington, Gooding et al. 2010). When the immune system is competent but no spontaneous cure event takes place the scene is set for a latent TB disease state where the infected individual can carry the bacilli for decades and unless they become seriously ill the disease will never manifest (Lin and Flynn 2010). If the immune system *is* in some way compromised at the time of infection or shortly thereafter then active pulmonary TB will occur.

Secondary TB occurs in one of two ways; a carrier can become immunocompromised and either a novel infection begins or a relapse ensues or an already infected person is re- or double infected with a new strain of the disease or a drug resistant version. In both these scenarios the immune system is compromised and the patient has already been exposed to TB bacilli. This means that they in all likelihood have a granuloma or lesion containing 'dormant' bacteria. When the secondary infection asserts itself the monocyte barrier protecting the host from the phagocytosed bacilli can break causing severe trauma to the plural tissue via the secondary immune response. This can lead to blood in the sputum, night sweats, chronic coughing and cachexia (Hunter, Olsen et al. 2006).

#### **1.4.7 Latent TB**

As discussed briefly above the case for spontaneous cure is rare, far more common is an infected individual carrying TB cells in their lungs but suffering no active disease, this is latent TB. Individuals with latent TB are not infectious to others but can become so if the disease reactivates (Comstock, Livesay et al. 1974). Little is known about the physiology of MTB bacilli once in a latent infection within the host lung (Boshoff and Barry 2005). We have gone some way to demonstrate the functioning of MTB in *post mortem* lung tissue but much more work must be done. It appears that bacilli that are not replicating and could be said to be 'dormant' express intracytoplasmic lipid inclusion bodies (lipid bodies- LB) and can be said to be lipid rich (LR) (Deb, Lee et al. 2009, Daniel, Burnett School of Biomedical Sciences et al. 2011). The expression of these lipid bodies seems to be an indication of the cells metabolic state, we have shown that cells that express LBs have a much higher



tolerance to antibiotic therapy than lipid poor (LP) cells. This could account for the long duration of therapy that is required to treat a patient of latent TB. Another theory put forward by Wayne and Sohaskey (Wayne and Sohaskey 2001) is that the latent cells and the host immune system are in a constant state of flux. They theorise that this could be due to ongoing interactions with the immune system. Macrophages that had previously up taken MTB cells die by apoptosis and release bacteria into the pulmonary environment which are re-phagocytosed by healthy macrophages. This allows for a period of replication during which the immune system is 're-awakened' and then a period of quiescence until the next apoptotic event. The risk of developing active TB from being a latent TB carrier was calculated to be approximately 10% per year per carrier if that individual was an HIV sufferer. This figure compared with 10% over a lifetime with an individual uninfected with HIV (Kawamura, Grinsdale et al. 2012).

## **1.5 Epidemiology of TB**

TB is a global problem with most of the burden borne by poor and developing nations. According to the WHO 2013 report an estimated 8.6 million new cases of TB were reported globally and 1.3 million people died of tuberculosis (~24% of who were HIV positive) (Organisation 2013). Africa, especially sub-Saharan Africa, and Asia carry the heaviest burdens of TB with south east Asia becoming the most densely populated with TB positive people (Lienhardt, Glaziou et al. 2012). In the same study the WHO reported that the incidence of TB is declining globally due, in part, to renewed research efforts and funding strategies and greater availability of frontline drugs (Organisation 2013). In addition to this the WHO reported that the total mortality rate was declining, by 41% as of the date of the report (Organisation 2013).

In Africa HIV co-infection is the largest contributing factor to increasing TB prevalence (Gandhi, Moll et al. 2006). The combined effects of a lack of sexual education, poor medical and research facilities and high traveling costs mean that more people contract HIV and many suffering with it are not able to control the disease effectively. This leads to an increase in the number of preventable TB cases and deaths resulting from TB infection (Corbett, Watt et al. 2003). It is estimated that in ten years from 2015-2025 that TB will reduce the GDP of developing nations across the world by approximately \$1 trillion USD and will account for a 7% drop in productivity in those nations stunting the growth of countries that are attempting to become global centres for research or industry (Alliance 2015). In developed nations the effect of TB on the economy is still high; a report in the European Respiratory Journal found that in Germany standard outpatient costs were approximately €1,197 for adults and €1,006 for children. The same report found that MDR-TB costs were considerably higher; up to €36,543 (Diel, Rutz et al. 2012). When bundled with the reported loss of productivity, the total economic burden of TB in Germany is €52,259 per patient (Diel, Rutz et al. 2012).

## **1.6 Taxonomy**

*Mycobacterium* is a genus of Actinobacteria in the family Mycobacteriaceae. In 1896 Lehmann and Neumann anticipated that the genus *Mycobacterium* would contain the disease causing tubercle bacillus and leprosy (Goodfellow and Magee 1998). The standards required to enter any potentially newly discovered bacteria into the *Mycobacterium* clade are fairly strict; acid-fastness of the bacteria, the presence of mycolic acids containing 60–90 carbon atoms and a guanine and cytosine content of the DNA of 61 to 71 mol % based on the 16S rRNA sequences (Tortoli 2006) are all required.

### 1.6.1 Classification of slow growing mycobacteria

The slow growing mycobacteria are classified in to 3 groups based on their pigment production when exposed to light or in the dark. There are also non-chromogenic slow growing mycobacteria (Rogall, Flohr et al. 1990, Brown-Elliott and Wallace 2002).

Group	Classification by pigment production	Species	
		Rough (matt) colonies	Smooth (shiny) colonies
I	Nonchromagenic	<i>M. africanum</i>	<i>M. branderi</i>
		<i>M. bovis</i>	<i>M. heidelbergense</i>
		<i>M. leprae</i>	<i>M. intracellulare</i>
		<i>M. lepraemurium</i>	<i>M. malmoense</i>
		<i>M. microti</i>	<i>M. avium avium</i>
		<i>M. pinnipedi</i>	<i>M. avium paratuberculosis</i>
		<i>M. shottsii</i>	<i>M. avium silvaticum</i>
		<i>M. tuberculosis</i>	<i>M. genavense</i>
			<i>M. montefiorensense</i>
			<i>M. ulcerans</i>
II	Photochromagenic	<i>M. kansasii</i>	<i>M. asiaticum</i>
			<i>M. marinum</i>
III	Scotochromagenic	<i>M. cookii</i>	<i>M. conspicuum</i>
		<i>M. flavescens</i>	<i>M. botniense</i>
		<i>M. gordonae</i>	<i>M. farcinogenes</i>

			M. heckeshornense
			M. interjectum
			M. kubicae
			M. lentiflavin
			M. nebraskense
			M. palustre

Table 1.1. Slow growing mycobacteria classified by their ability to produce pigments.

Nonchromagenic – no pigment produced. Photochromagenic – pigment (yellow carotenoid) produced upon exposure to light. Scotochromagenic – yellow pigment produced in darkness.

## 1.7 Clinical tuberculosis

Depending on the site of infection the clinical presentation of TB will be different. Whether or not clinical disease progresses depends upon a number of factors. Some of these factors include the host's defences; whether the individual is immunocompromised by illness or medical treatment. If a vaccine was given at any stage of the host's life, the availability of treatment options and stresses of the environment all play a part in the development of disease (Lonnroth, Jaramillo et al. 2009). Persistent coughing is generally recognised as the universal indicator of pulmonary tuberculosis. When the cough becomes productive and bacilli are found within it TB can be confirmed. Aside from a productive cough there are a number of other common symptoms of active TB such as fever, night sweats, loss of appetite, weakness, weight loss, malaise and haemoptysis (Murray, Murray et al. 1978, Organization 2013). Chest X-rays are still widely used to assist with tuberculosis diagnosis (van Cleeff, Kivihya-Ndugga et al. 2005), these can show cavities and/or lesions in advanced disease. Cavities are known to be hypoxic stressful environments for MTB (Rustad, Harrell et

al. 2008, Daniel, Maamar et al. 2011). It is in these lesions what we theorise that lipid-loaded MTB phenotypes could reside.

### **1.7.1 Signs and Symptoms of Pulmonary TB**

The most obvious symptom of tuberculosis infection is a persistent and sometimes productive cough lasting longer than 2 weeks (Steen and Mazonde 1998). Expectoration of sputum in pulmonary TB infection is common after the early stages of the disease. Sputum containing blood is a clear indication that there is a possible tuberculosis infection along with other signs such as weight loss, chest pains, shortness of breath as well as wheezing, fever, night sweats and a general fatigue or malaise (Miller, Asch et al. 2000).

### **1.8 Genome and Genotypes**

The sequence of the MTB H37Rv consists of 4,411,532 bp and was sequenced in 1998 by the Sanger Institute (Cole, Brosch et al. 1998). The MTB genome has a high G+C content of 65.6%, a parameter which is associated with an aerobic lifestyle (Naya, Romero et al. 2002).

### **1.9 Diagnosis of TB**

Diagnosis of TB is possible via useful means, some of which have been touched on above. The clinical symptom of chronic coughing for more than 2-3 weeks with or without production is, by itself, not enough for a diagnosis. Laboratory tools are used to specifically find and test mycobacteria for acid fastness and drug sensitivity. Sputum is the most commonly used as it is produced in the natural disease state and therefore does not require invasive step such as lavages or needle biopsy and in a heavily infected patient there can exceed  $10^8$  bacteria per millilitre of sputum (Garton, Waddell et al. 2008).

### **1.9.1 Sputum microscopy**

In order to directly observe TB bacilli from a patient the easiest way (for the patient in the case of pulmonary TB) is to expel sputum naturally via coughing. Sputum induction can also be used. This consists of administration of an aerosol of lukewarm sterile hypotonic physiological saline at approximately 3-5%. This will often produce deep coughing which will, in many cases, also produce a watery, saliva-like sputum. Sputum induction is commonly used in patients who cannot cough strongly enough for themselves to produce sputum (Anderson, Inhaber et al. 1995, Conde, Loivos et al. 2003). This can be due to numerous factors such as the exhaustion from excessive coughing or from disturbed sleep. It can also result from a shortness of breath and decreased lung capacity due to pleural effusion or oedema or secondary infection with another respiratory pathogen. The wasting associated with TB can also be too advanced and the patient simply not having the muscular strength to expel sputum (Parry, Kamoto et al. 1995, Shata, Coulter et al. 1996, Zar, Tannenbaum et al. 2000).

The current methodology for sputum collection is known as spot-morning-spot (SMS) and is recommended by the WHO to gain the most efficacious bacilli rich samples (WHO 2001). However this method has its detractors (Rao 2009). For the SMS method the first and third samples are collected at a healthcare facility such as hospital or clinic. The middle sample, the morning sample, is usually collected at home by the patient (Kivihya-Ndugga, van Cleeff et al. 2003).

### **1.9.2 Sputum smear microscopy to detect TB Bacilli**

Direct sputum microscopy is still used globally as the primary method of TB diagnosis, however this ignores several large flaws in the method. Some of these flaws consist of; the detection of dead bacilli, the lack of thorough quantification and bacilli misidentified or missed entirely (Harries, Maher et al. 1998, Steingart, Henry et al. 2006, Getahun, Harrington et al. 2007) all of these problems being compounded in the case of HIV co-infection. This being true the method does have merit- the stains used are designed to be specific for acid fast bacteria and have relatively low levels of non-specific binding if used properly. The sputum smear is also non-infectious once fixed to a slide and is inexpensive and rapid but these advantages are all dependant on a skilled operator able to process many samples at once without contaminating their surroundings or themselves (Steingart, Henry et al. 2006, Paul A. Jensen 2015). The two main procedures used are the Ziehl-Neelson (ZN) stain and the Auramine-O stain. ZN staining is non-fluorescent and therefore more suited to less well funded clinics without a fluorescent microscope. This however does make the principal identification more difficult as in an Auramine-O slide and acid fast bacteria fluoresce brightly and a diagnosis can be made more swiftly with greater accuracy. It has been noted that the relative quantity of TB bacilli in a sputum sample must be high for a positive identification to be made with ZN staining – on the order of 10,000 bacilli per mL of sample (Hobby, Holman et al. 1973).

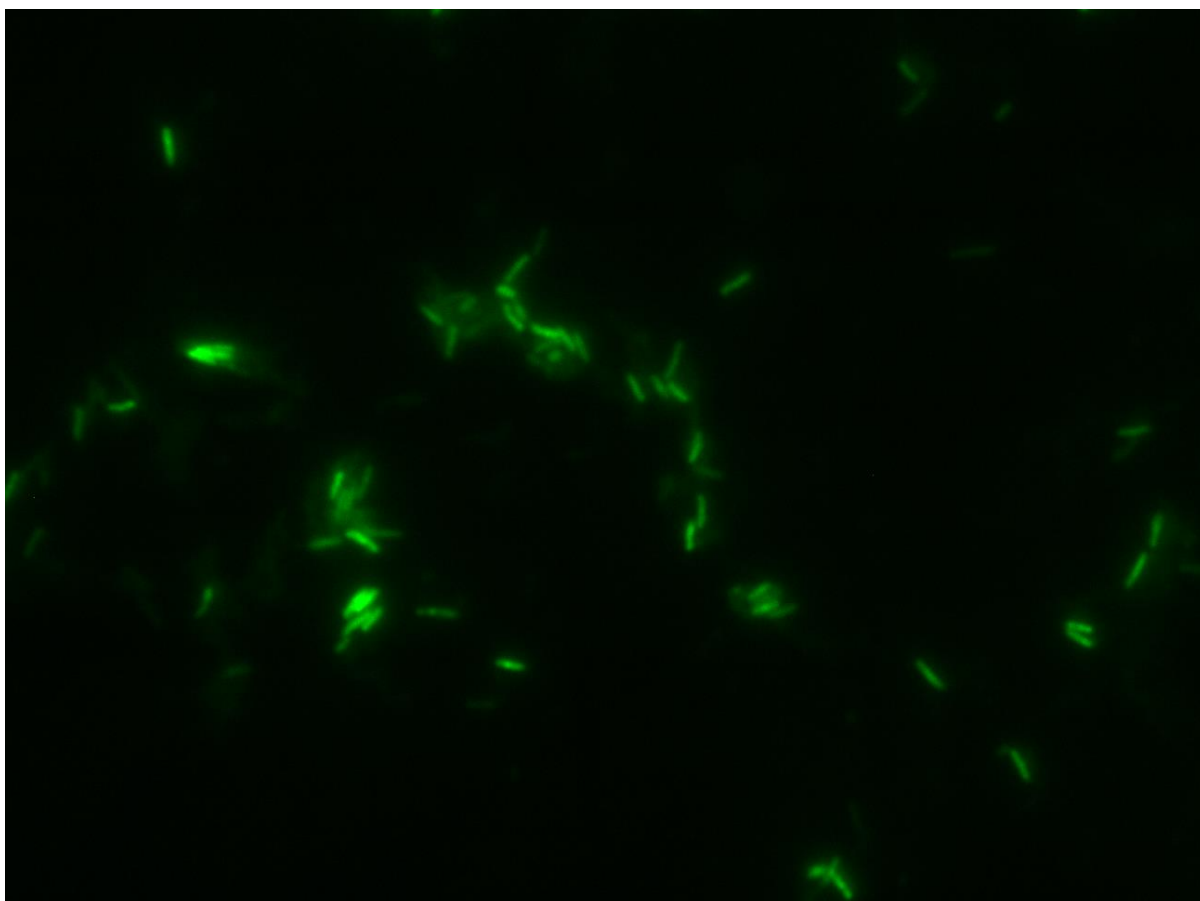


Figure 1.1. Mycobacterium spp. Stained with Auramine-O

### **1.9.3 Fluorescence microscopy to detect TB Bacilli**

In 1937 Hagemann first described the use of fluorescent dyes to identify acid fast bacilli in clinical samples (Truant, Brett et al. 1962). The most common stain used to identify TB bacilli in sputum is Auramine-O which fluoresces green-yellow. Potassium permanganate is often used as a counterstain which will not bind to the acid fast TB bacilli and make visible any other bacteria in the sputum smear. If the smear is not in a complete monolayer then the potassium permanganate can quench the Auramine-O fluorescence so care must be taken during smear preparation. When conventional light microscopy is used with ZN staining to detect TB in sputum at least a 5 minute microscopic examination is required before concluding that sample is negative for acid fast bacilli (IUATLD 2000). A systematic review by



WHO/IUATLD found that fluorescence microscopy on average increased the possible sensitivity by 10% over conventional ZN microscopy. They also found that reading a fluorescent stained smear takes only 25% of the time taken to read a ZN stained smear (Laifangbam, Singh et al. 2009).

While Auramine-O staining is effective it does not report on the state of the bacteria, simply their presence. One major drawback of Auramine-O staining is that if a cell loses its acid fastness due to age or stress Auramine-O will no longer display that cell as a bright fluorescent event (Daniel, Maamar et al. 2011). This is of particular concern in aged laboratory cultures or in chronically infected TB patients.

Nile red has been used for many years as a lipophilic stain for identifying intracellular lipid droplets (Fowler and Greenspan 1985, Greenspan and Fowler 1985, Greenspan, Mayer et al. 1985, Fowler, Brown et al. 1987). During the course of this investigation we found that Nile red, without the use of a counterstain, can not only report on the presence of mycobacteria in *post mortem ex vivo* human tissue but also report on the phenotypic state of the TB bacilli found there. Using Nile red as a probe allowed us to see that some of the cells in the most 'stressful' areas of the lung (cavities and inside macrophages) were displaying lipid bodies, a sign of their metabolic down-shift and apparent stress. This technique was used liberally in all investigations in pure culture throughout this work.

### **1.10 Cultivation of Mycobacteria**

Culture of MTB is the standard method by which a definitive diagnosis of TB infection is made globally. This is changing with the advent of devices such as the BACTEC, MGIT and Phoenix (Becton Dickinson) and the VITEK (bioMérieux) but culture, while slow, still has greater sensitivity and specificity ranges than these devices- sensitivity from 80-85% and

specificity regularly at 100% (Ichiyama, Shimokata et al. 1993). This is due largely to a skilled operator with a lot of experience growing the cultures and being able to identify them with the use of other techniques in addition to plate and liquid based growth media.

Culture is still the gold standard for MTB detection. The reasons for this are twofold; culture can detect samples with as few as 10 cells per ml, no current commercial technology can compare with that degree of sensitivity. Another reason is that agar or broth grown MTB can be used for morphological or characteristic identification, drug susceptibility, epidemiological studies and genetic studies to trace an outbreak or establish if a particular patient has been re-infected or has suffered a relapse (Yeager, Lacy et al. 1967).

There are three culture types in two categories: solid media, which includes Middlebrook 7H10 and 7H11 and Lowenstein-Jensen (LJ) agar which contains egg. The second category is liquid based media which includes Middlebrook 7H9 and 7H12 and the media used in MGIT tubes. In developing nations LJ media is used most commonly as the media discourages growth by contaminants that are not acid fast bacilli due to the inclusion of malachite green. WHO recommends the use of LJ media for this same reason (R. Ananthanarayan 2009). Growth on LJ media appears after approximately 2-6 weeks depending on numerous factors such as the phase of growth of the individual bacilli and the fitness of the population as a whole and the bacteria individually (Caviedes, Lee et al. 2000, Tanoue, Mitarai et al. 2002). A negative result cannot be reported until there has been no growth on the LJ media for 8 weeks. This is a considerable problem as contamination is counted as growth and the vast majority of contaminants will grow more quickly than MTB meaning that sterility is of the utmost importance. This significant 56 day lag between sample collection and negative result is the reason for the development of some of the devices listed above. We have also

created, during the course of this work, our own MTB detection mechanism that has a similar degree of sensitivity to culture but is significantly faster at detecting growth even than machines such as the MGIT (2 days) and can be used to conduct drug susceptibility tests. We believe this represents a significant step forward with MTB detection and TB therapy.

### **1.11 Identification of mycobacteria in culture**

Mycobacteria, in general, can be identified primarily by their slow growth rates, even those species identified as “rapidly growing” (*M. smegmatis* and *M. fortuitum* for example) (Gordon and Smith 1953, Hall-Stoodley and Lappin-Scott 1998) can take 2-3 days to appear on solid agar. In more slowly growing species the difference is even more pronounced. On an ostensibly MTB culture plate if any colonies appeared before 14 days we would be highly suspicious of the colonies identity. Aside from this MTB can be identified by its rough, matt appearance as well a lack of pigment on Middlebrook agars and a “buff, rough and tough” (matt and brown) appearance on LJ media (Kawkab Adris Mahmod , Middlebrook and Cohn 1958). Aside from gross techniques such as macro- and microscopic observation there are also a number of nucleic acid methods available such as qPCR, spoligotyping and DNA and RNA sequencing (Driscoll 2009).

### **1.12 The genus Mycobacterium**

The name mycobacterium is derived from the fungal like growth characteristic that all mycobacteria share. With few examples all mycobacteria are slender, slightly curved or straight rod-shaped organisms on the order of 1-4µm long and 0.25-0.8µm wide. Mycobacteria are divisible into two major groups; slow and rapid growers where rapid growers will appear as microcolonies on an agar plate within 48-73 hours whereas slow growers (which MTB is one) will not appear for more than 2 weeks.

The mycobacteria show high tolerance to environmental stresses and inhabit various environments such as water, soil, plants and mosses, animals and humans. Many of these species are non-pathogenic to human but can cause disease in animals and some are totally environmental and/or saprophytic. Some of the pathogenic mycobacteria are *M.leprae*, *M.ulcerans* and of course MTB (Ducati, Ruffino-Netto et al. 2006). The MTB complex includes strains of five species: MTB, *M.canettii*, *M.africanum*, *M.microti*, and *M.bovis* and two subspecies *M.caprae* and *M.pinnipedii* (Lawn and Zumla 2011). Recently, new MTB lineage “the Woldia lineage” was found and reported in Ethiopia (Berg, Firdessa et al. 2009, Firdessa, Berg et al. 2013).

### **1.13 Morphology and staining of MTB**

As the name would suggest the tubercle bacillus is bacillus in shape; a rod 1-3µm in length and 0.5-0.8µm in width. This shape and size and change slightly given different culture conditions, when starved of oxygen or nutrients, for example, TB cells can become characteristically shorter and fatter (Deb, Lee et al. 2009, Daniel, Maamar et al. 2011) and, as discussed above, can gain intercellular lipid bodies. TB cells can also appear as V or Y type variants under microscopic examination. The V shape is often attributed to the post-fission ‘snapping’ of the two daughter cells separating (Farnia, Mohammad et al. 2010). The Y shape sometimes observed is due to the branching nature of the expansion of the growing cells, often if they have become attached to a surface rather than living planktonically (Velayati, Farnia et al. 2010). This could also account for the fungus-like growth patterning that gave the mycobacterial clade their name.

### **1.14 MTB cell envelope**

The *M. tuberculosis* cell envelope is a structure that has been the subject of investigation for many years. It is often said that mycobacteria possess a “mycolic acid outer layer” (Deng,

Mikusova et al. 1995) but that diminishes the truth of the matter. The mycobacterial cell envelope is a complex structure comprising peptidoglycan, arabinoglycan and mycolic acids with a secondary structure of lipids associated with polysaccharides which appear free of the cell wall proper on the external cell surface (Brennan 2003). Peptidoglycan is common to all eubacteria and is the basis of the well-known gram stain invented by Hans Christian Gram in Berlin in 1884 (Austrian 1960, Salton and Kim 1996). Peptidoglycan is made of repeating subunits of N-acetyl-glucosamine (NAG) and N-acetyl-muramic acid (NAM) bound with  $\beta$ -(1,4) glycosidic bonds. Strings of NAG-NAM complexes are held together by peptide bonds between the NAM molecules (Vollmer, Blanot et al. 2008). This is true of the majority of eubacteria however this basic structure is altered in mycobacteria. The classic NAG-NAM structure is interspersed with N-glycol-muramic acid (NGM) in place of some of the NAM making a NAG-NGM complex. The reason for this change is as yet unknown but it has been suggested that the presence of the NGM increases the hydrogen bonding within the peptidoglycan layer creating a more rigid structure less easily damaged by mechanical stress (Hett and Rubin 2008).

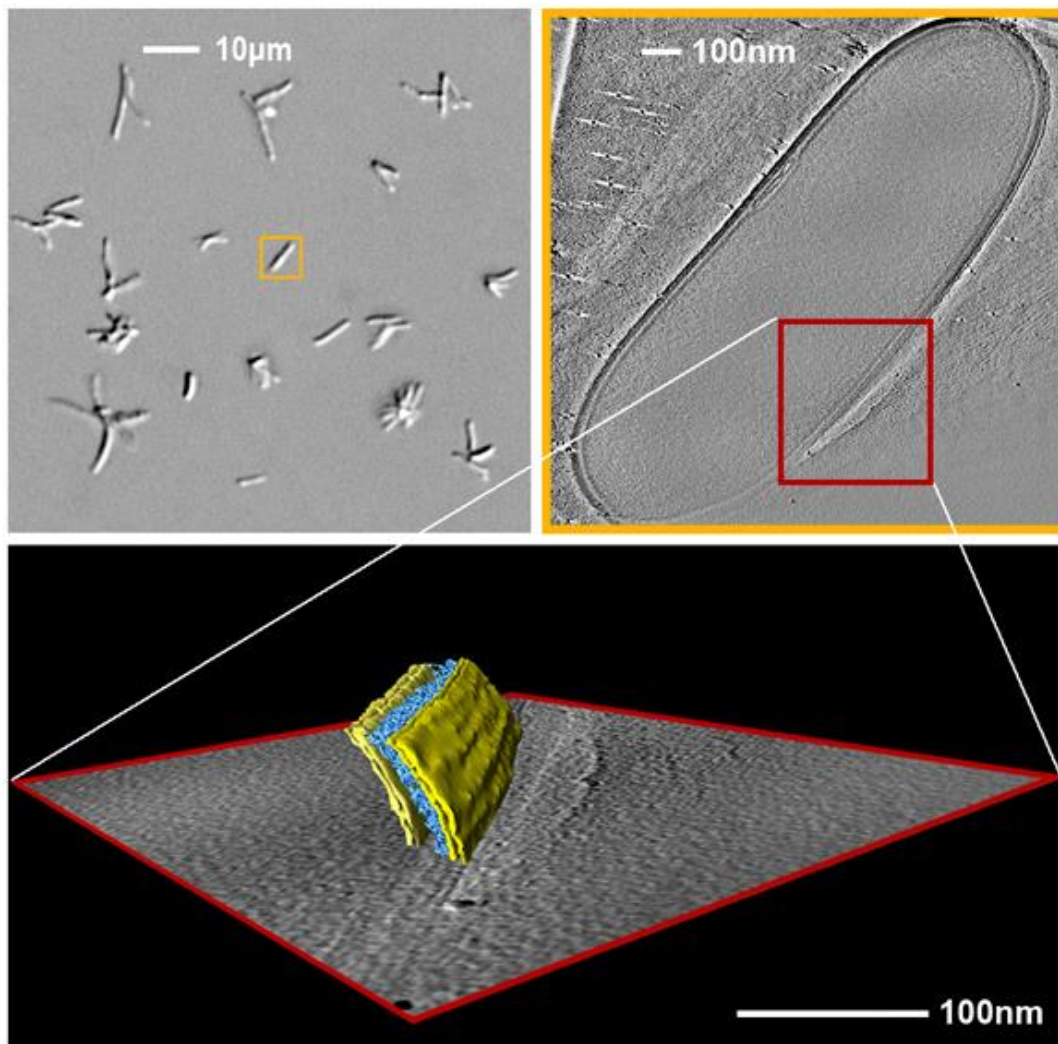


Figure 1.2. Image taken from <http://www.mpg.de/569661/pressRelease20080304> Max Planck Gesellschaft (Society) showing that there is still ongoing interest in the construction of the MTB cell envelope and showing an interesting 'double membrane' feature

Mycolic acids are  $\alpha$ -branched- $\beta$ -hydroxy fatty acids with carbon chains from 20- 90 carbons in length. Mycolic acids were first isolated from mycobacteria (hence the name) but have subsequently been found in actinobacter of the suborder Corynebacterineae including the genera *Nocardia*, *Gordonia*, *Rhodococcus*, *Dietzia*, *Corynebacterium*, and of course *Mycobacterium* (Teramoto, Tamura et al. 2013). Mycolic acids in mycobacterium and related species have been shown to contain functional group such as cyclopropane rings, methoxy-, keto-, epoxy- or ester-groups. These differences between mycolic acid subgroups (including carbon chain length) are the basis of some chemotaxonomic markers to

differentiate genera (Goodfellow, Minnikin et al. 1982). When found in *Corynebacterium* mycolic acids are generally known as corynomycolic acids. Mycobacterial mycolic acids are from 60-90 carbons long whereas corynomycolic acids are generally 20-36 carbons long.

Arabinogalactan is a dimer of arabinan and galactan in a furanose state. These dimers are attached to the peptidoglycan layer. Unlike with peptidoglycan arabinogalactan is not made of repeating monomers but is arranged with galactan molecules in 1-5 and 1-6 linkages. An arabinan molecule is bound to the 5<sup>th</sup> position of the galactan in the 1-5 links. This is repeated for approximately 30 units, and forms a structural motif that is covalently bound by an N-acetylglucosaminosyl-rhamnosyl linked to peptidoglycan (Hett and Rubin 2008).

### **1.15 Lipid bodies in Bacteria**

In 1945, Knaysi found that fatty deposits (droplets) formed in the cytoplasmic membrane in living cells of *Bacillus cereus* (Knaysi 1945). In 1946 Burdon (Burdon 1946) demonstrated that Sudan Black B was useful in elucidating intracellular fatty material in bacteria. One of the attributes used to characterise the genus *Mycobacterium* is their high lipid content, mostly in the lipid-rich cell envelopes (Liu, Barry et al. 1996, Takayama, Wang et al. 2005). It has been shown that the lipid inclusions within mycobacteria are a mixture of numerous whole lipids and fatty acids including unique mycobacterial fatty acids, triacylglycerols (TAG) and wax esters (WE) (Garton, Christensen et al. 2002, Garton, Waddell et al. 2008, Daniel, Burnett School of Biomedical Sciences et al. 2011).

Lipid bodies were demonstrated by our group in both pure culture 'fed' with specific lipid or with a general mixture. They have also been shown in young and old cultures (mid exponential phase and late stationary phase, respectively) of numerous mycobacterial species including MTB. We have also demonstrated the existence of lipid bodies in *ex vivo post mortem* tissue from a TB sufferer.

We have shown that the presence of lipid bodies is indicative of a metabolic slow-down with this being specifically shown in these LB containing cells being more resistant to antimicrobials than their lipid poor counterparts (Hammond *et al*, 2015).

Two distinctive characteristics of human TB are the frequent occurrence of latent infection and the extended period required for chemotherapy. It is unknown whether the phenotypic state of MTB in the human host is responsible for these phenomena.

### **1.15.1 Lipid storage in prokaryotes**

Lipids have many roles in the metabolome of bacteria and other prokaryotes. In bacteria they are a major constituent of membranes and cell envelopes and can act as storage material. It is well documented that many prokaryotic species can accumulate lipophilic compounds as inclusion bodies in their cytoplasm (Waltermann and Steinbuchel 2005). Some of these lipophilic compounds, found across the taxonomy of microorganisms, are; poly $\beta$ -hydroxybutyrate, triacylglycerols and wax esters. Although apparently a useful carbon store lipid inclusions, or bodies, are only found within a few prokaryotes (Murphy and Vance 1999, Alvarez and Steinbuchel 2002).

Triacylglycerol inclusions (TAGs) are the principal lipid storage in numerous different eukaryotic clades of life such as moulds, yeasts and algae. One study found that 87% of lipid bodies found in the test species lipid bodies were composed primarily if not entirely of TAGs (Waltermann and Steinbuchel 2005). The other components of the TAG lipid bodies include diacylglycerols (DAGs) (5%), free fatty acids (5%), phospholipids (1.2%), and proteins (0.8%) (Waltermann and Steinbuchel 2005, Waltermann, Stoveken *et al.* 2007). Triacylglycerol is a fatty acid with tri-esters of glycerol is a highly efficient way of storing fatty acids (Alvarez



and Steinbuchel 2002). Triacylglycerol have been shown to almost completely fill the cells of the species in which they are found, mostly the members of actinomycetes group, primarily *Mycobacterium*, *Nocardia*, *Rhodococcus* and *Streptomyces* (Waltermann, Stoveken et al. 2007). These TAG-rich lipid bodies are thought to act mainly as energy and carbon storage. Other theories for LBs have been suggested, such as deposits for toxic or surplus fatty acids from phospholipid biosynthesis. It was demonstrated that MTB is capable of accumulating TAGs under both dormancy and virulence conditions indicating that TAG accumulation probably plays a role in pathogenicity (Garton, Christensen et al. 2002, Daniel, Deb et al. 2004) or is at least a natural part of the mycobacterial cell cycle.

Wax esters (WE): are similarly found in only a few prokaryote species and are synthesised by the same set of key enzymes as TAGs; acyl-coenzyme A as an acyl donor and long chain fatty alcohols or diacylglycerols as acyl acceptors. Specifically for wax ester synthesis diacylglycerol acyltransferases are used (Waltermann, Stoveken et al. 2007). The major function of TAG and WEs is thought to be to provide energy and carbon in times of starvation or when there is another environmental pressure. They are also thought to be used for removal of potentially toxic fatty acids during the growth of bacteria (Alvarez and Steinbuchel 2002).

### **1.15.2 Lipid bodies in mycobacteria**

Schafer and Lewis (Schaefer and Lewis 1965) demonstrated that uptake of oleic acid or its ester Tween resulted in notable accumulation of LBs and increase in optical density in culture. Microscopic study of *Mycobacterium* species including *M. avium* (Peyron, Vaubourgeix et al. 2008), *M. leprae* (Mattos, Lara et al. 2011), *M. kansasii* (Kremer, de Chastellier et al. 2005), *M. smegmatis* (Anuchin, Mulyukin et al. 2009), *M. fortuitum*

(Sirakova, Dubey et al. 2006), *M. marinum* (Hammond et al, 2015) , *BCG* (D'Avila, Melo et al. 2006) and MTB confirmed the presence of lipid bodies. *BCG* was reported to be capable of adapting to a microaerobic or hypoxic environment *in vitro* by shifting down to a non-replicating dormant state similar to MTB (Boon and Dick 2002). Christensen et al (Christensen, Garton et al. 1999) observed the interactions between fluorescent lipid probes (nile red, acridine orange) and mycobacteria and reported that a substantial proportion of the cells contained intracellular lipophilic inclusions. The proposed compounds were poly- $\beta$ -hydroxybutrate (PHB), triacylglycerols (TAGs) and wax esters and the latter were shown to be a major component (Garton, Christensen et al. 2002, Deb, Lee et al. 2009, Daniel, Maamar et al. 2011).

### **1.16 Growth characteristics of MTB in hypoxic environments**

MTB is an aerobic organism that will not grow in anaerobic environments. In hypoxic environments where the oxygen concentration is maintained around 1% there is a noticeable increase in turbidity which does not correspond to an increase in CFU count over time (Wayne and Hayes 1996). This could be due to a number of factors; the presence of a greater number of cells but not ones that would grow on agar- so called viable-non-culturable cells, a large bloom of cells growing in this low oxygen environment but dying shortly before sampling took place or, the reason that Wayne and Hayes used in their 1996 paper- a thickening in the cell wall of the mycobacteria (Wayne and Hayes 1996). It has been noted before that in hypoxic environments *in vitro* mycobacteria will become short and fat (Deb, Lee et al. 2009, Daniel, Maamar et al. 2011) and if this were detectable by simple turbidity reading this represents a simple way to track the phenotypic changes taking place in MTB in under hypoxia. At a concentration of 0.06% a microaerophilic environment is

defined and this threshold denotes the switch from an aerobic to an anaerobic metabolism (Wayne and Lin 1982). Two populations of MTB at different dissolved oxygen concentrations are given the names NRP1 (higher O<sub>2</sub> content) and NRP2 (lower O<sub>2</sub> content). It has been noted, again by Wayne *et al*, that in a shift from NRP1 to NRP2 a phenotypic resistance to isoniazid and rifampicin was expressed (Wayne and Hayes 1996). It has been hypothesised that as well as a hypoxic environment that the MTB bacilli living in the human lung may also be in a nutrient poor environment at times, depending on the state of the infection and the competency of the host immune system (Peyron, Vaubourgeix *et al.* 2008). The Cornell model that describes a latent MTB infection and was first devised by McCrune and Colleagues at Cornell University in the 1950s (Flynn and Chan 2001). The Cornell model simulates the *in vivo* conditions of human latent infection in which very few bacteria can be detected within the lung. It was the Cornell model that first showed the importance of fatty acid metabolism in MTB infections in the human host and the implications therein (de Wit, Wootton *et al.* 1995, Hampshire, Soneji *et al.* 2004).

### **1.16.1 Lipid metabolism**

Isocitratelase (icl) is an enzyme that catalyses the conversion of acetyl-CoA to succinate in the glyoxylate cycle. It is used by bacteria that are metabolically dependant on fatty acids (Kornberg and Beevers 1957). Two MTB icl homologues exist; icl1 and icl2. It is not known where the fatty acids utilized by MTB originate. It is likely that they are found in the cells immediate environment. This has been shown to be the case when bacilli are encapsulated in macrophages, particularly if these macrophages go on to become foamy. Bentrup and Russel theorise that fatty acids may be acquired from the lipid rich host-cell debris in mature

granulomas (Honer zu Bentrop and Russell 2001). Lung surfactant is also rich in fatty acids and can be internalized by macrophages where MTB can utilise it. MTB may also be able to utilize macrophage triacylglycerol stores that are prepared during phagocytosis (Munoz-Elias and McKinney 2005). Alternatively, MTB may metabolize fatty acids stored as TAG directly from its microenvironment (Deb, Lee et al. 2009, Daniel, Maamar et al. 2011).

The  $\beta$ -oxidation cycle is the principal pathway for the degradation of fatty acids in bacteria and eukaryotes (Gonzalez-Mariscal, Garcia-Teston et al. 2014). Successive rounds of  $\beta$ -oxidation in bacteria yield acetyl-CoA that is channelled into the citric acid cycle (Munoz-Elias and McKinney 2006). The  $\beta$ -oxidation cycle generates one molecule of Flavin adenine dinucleotide (FADH<sub>2</sub>), Nicotinamide-adenine dinucleotide (NADH) and acetyl-CoA which are a form of cellular energy currency (Brown and Marnett 2011). Acetyl-CoA can be directed into the glyoxylate shunt pathway and lead the flux of carbon into gluconeogenesis. These pathways allow MTB to acquire and conserve carbon from fatty acid. The glyoxylate shunt pathway is a metabolic pathway in which acetate is oxidized to produce ATP

### **1.16.2 Responses to external stresses and stimuli**

Once phagocytosed by a macrophage MTB bacilli are in a very harsh environment. Hypoxia (Vandal, Nathan et al. 2009), nutrient depletion (Lorenz and Fink 2002), reactive oxygen and nitrogen species (Voskuil, Bartek et al. 2011) and acidic conditions (Vandal, Nathan et al. 2009) are all present inside even an unfused phagolysosome. In many mycobacteria the oxidative stress response is mediated by the *oxyR* gene (Master, Springer et al. 2002). The oxidative stress response differs across mycobacteria so the category 2 mycobacteria such as *M. smegmatis* that is commonly used in laboratories as an analogue for MTB may not be

the most appropriate model in this circumstance. It was found by Sherman *et al* (Sherman, Sabo et al. 1995) that *M. smegmatis* could mount an effective oxidative stress response but MTB could not. Mycobacteria, pathogenic to humans or environmental, are likely to encounter acidic conditions in their host or in the soil or water microenvironmental niches they live. This means that they must have an effective pH regulation complex. When MTB is exposed to an acidic pH it has been shown that a large number of genes show differential expression (Ragno, Romano et al. 2001). When confronted with a drug challenge it is known that MTB and other mycobacteria can mutate rapidly, especially in the *rrdr* region of the *RpoB* gene which confers resistance to rifampicin (Mboowa, Namaganda et al. 2014).

### **1.16.3 Antimicrobials - Anti-TB drug regimens**

The first anti-TB drug in clinical use, 1945 was streptomycin (BOGEN 1948). Streptomycin monotherapy, however, resulted in the emergence of bacterial resistance and treatment failure (McKinney, Honer zu Bentrup et al. 2000). Streptomycin was first introduced in 1944 to combat TB but by 1946 cases of streptomycin resistant disease were occurring widely (Raviglione 2009).

Isoniazid (INH), Rifampicin (RIF), Pyrazinamide (PYZ), and Ethambutol (ETB) are the modern drugs used during the intensive treatment phase for acute TB. These drugs are administered orally, daily for two months. In the continuation phase, INH and RIF are given for a further 4 months, either daily or 3 times per week. Vilcheze and Jacobs (Vilcheze and Jacobs 2007) documented that INH plays a critical role in the initial killing of replicating bacteria and has been in use since 1952. Isoniazid is a prodrug and requires activation by catalase-peroxidase enzyme (*KatG*) for it to become active. Rifampicin and pyrazinamide are believed to

eradicate dormant or non-replicating bacteria (Wayne 1994, Zhang, Wade et al. 2003, Zhang 2004) which make them important in tackling latent disease. In order to largely avoid the problem of MTB becoming resistant to the therapeutics being used a combination therapy is always used to treat TB in the modern era.

TB drug resistance can take place when the anti-TB drugs are not correctly taken. This is a not-uncommon occurrence among patients in developing nations. This phenomenon, called drug or therapy non-adherence, can occur due to infrastructure issues within the patient's country of residence. Other reasons are patients selling their drugs, believing those issuing the drugs are in fact trying to do them harm and the superstitious belief the witch-doctors hold more effective cures. One of the most common reasons for patients not correctly taking their drugs, irrespective of socio-economic level is the belief that once the symptoms have abated that they are cured. This is particularly untrue because, as stated above, latent TB is not only common but a well-established part of the TB lifecycle.

Clinicians issuing therapy can also be to blame. Dosing TB drugs is relatively straight forward but errors can occur with the length of time of treatment is issued being inappropriately shortened or if the drugs provided are of poor quality (Goble, Iseman et al. 1993, Quy, Lan et al. 2003, Gandhi, Moll et al. 2006). The WHO defines drug resistance as a "decrease in susceptibility of sufficient degree to be distinguishable from a wild type strain that has never been exposed to the drug" (WHO 2001). When 1% or more of any isolated sample of organisms are found to be resistant to any anti-TB drug, therapeutic success is unlikely to occur. When this drug susceptibility threshold is reached the strain is considered resistant to the drug. Drug-resistant TB was recognized shortly after the introduction of anti-TB chemotherapy in 1946 (Crofton and Mitchison 1948). In 1948, TB drug resistance was first reported by the British Medical Research Council (MRC) that revealed the treatment

outcome of patient treated with streptomycin was similar to those not treated at all. (BOGEN 1948). Although TB drug resistance continued to occur little attention was given to this important problem until the 1990s (Frieden, Sterling et al. 1993).

Mycobacterial drug resistance can occur and present in two ways; Primary anti-TB drug resistance is a type of resistance that occurs in patients who are anti-TB drug naïve. When the history of treatment is doubtful it is called initial resistance which is a mixture of primary resistance and undisclosed acquired resistance. The second and by far the most common form of resistance is acquired resistance. This type of resistance occurs amongst patients that had previous treatment (more than one month) (Baek, Li et al. 2011, Shi, Zhang et al. 2011, Sarathy, Dartois et al. 2012, Dutta, Pinn et al. 2014, Zumla, Gillespie et al. 2014).

MTB can present as resistant in a few ways; mono-resistance is the MTB strain being resistant to only one drug. Any more than one drug resistance is termed multi drug resistance (MDR). Extensively drug resistant (XDR) strains of MTB are occurring worldwide with alarming rapidity. MDRTB is defined as not responding to at least isoniazid and rifampicin. XDRTB is resistant to these two drugs as well as any member of the quinolone family *and* at least one of the second-line injectable anti-TB drugs kanamycin, capreomycin or amikacin (WHO 2006).

Global TB drug resistance prevalence data shows that isoniazid and streptomycin resistance was found in 35 countries in 1994. The overall prevalence of TB drug resistance was 9.9% with a median of 1% MDR-TB by the same year (Diseases and Surveillance 2000). In some developing countries such as Mozambique, Cote D'Ivoire, Cameron, Argentina, the Dominican Republic, and Mexico the prevalence of MDR-TB among new cases was reported more than 3% by the year 2000 (Diseases and Surveillance 2000).

Primary MDR-TB was first reported in Ethiopia as 2% in samples taken from Addis Ababa and Harer (Yimer, Agonafir et al. 2012). The incidence of MDR-TB was estimated 2.3% by the year 2003 by the WHO (Organization 2013).

### **1.17 Phenotypic drug resistance**

Bacterial antibiotic tolerance is the capacity of a bacterium to resist the killing action of antibiotics. This differs from drug resistance in that drug resistance involves an increase in the minimum inhibitory concentration mediated by a phenotypic change that is transient (Lewis 2006). While drug resistance can be caused through mutation or epigenetic triggers, antibiotic tolerance is a mode of survival in adverse environments through a transient state (Lewis 2008), in the case of mycobacteria this could be dormancy.

During antibiotic treatment the killing pattern of the antibiotic could be considered biphasic. This is because in situations such as naturally occurring biofilms there will be less drug penetration and therefore less drug delivered to some of the cells present in the biofilm. This means there are two phases to the killing action, one in which the cells that were dosed correctly are killed but their cohorts are essentially treated with less drug and therefore are not killed and in fact could become resistant to the applied drug rapidly (Lewis 2008). The concept of a biofilm is somewhat applicable to a TB infection. If there are indeed dormant cell(s) amongst actively multiplying cells then these are the cells that will become resistant to any applied drug as they are not immediately killed. Persister cells are thought to be tolerant to antibiotics without having acquired genetic modifications (Keren, Kaldalu et al. 2004).

In the case of mycobacteria dormancy refers to a non-replicating state influenced by an external stimulus. This state is thought to be fully reversible (resuscitation) (Chao and Rubin 2010).



### **1.18 Hypothesis, Aims and Objectives**

The central hypothesis of this work has shifted as time has passed. Originally I was tasked with developing a technology that could distinguish different cell states from one another in mycobacteria. In attempting to accomplish this we developed a highly sensitive laser spectrophotometer (SLIC) which we have now filed with the patent office. In parallel with this work and because of the original remit we have also developed buoyant density separation method that will separate lipid loaded cells from lipid poor cells and a modified Nile red staining regimen for identifying lipid rich cells.

With this in mind the central hypothesis of this work has become two fold;

Can we use our SLIC device to differentiate slow growing and fast growing mycobacteria and can we further use it to make highly sensitive measurements of mycobacteria responding to drugs- drug susceptibility testing (DST).

In addition to this and incorporated with it we hypothesised that lipid rich and lipid poor cells were phenotypically different and that lipid rich cells were metabolically slowed-down and more dormant so we used antimicrobial drugs in the SLIC to test this theory.

### **1.19 Specific objectives**

To establish a robust protocol for the use of SLIC with a range of bacteria, including but not limited to, mycobacteria for antibiotic susceptibility testing, microbial cell enumeration and growth analysis.

To separate and identify lipid rich from lipid poor cells to a very high purity (>95%).

Test separated cells with front-line anti-tuberculosis drugs and fluoroquinolones for the purpose of establishing any differences in MIC and MBC (minimum inhibitory concentration and minimum bactericidal concentration).

To genetically test the difference between lipid rich and lipid poor populations, specifically their mutation rates to rifampicin and their levels of expressed tmRNA, pre16sRNA, and 16s RNA.

To test the differences between whole cell lipids extracted from lipid rich and lipid poor populations with both thin layer chromatography (TLC) and mass spectrometry.

## 2 SLIC

### 2.1 Introduction to bacterial detection technologies

There are many bacterial detection methodologies that have been used for, in some cases, over 100 years (Gram 1884, Austrian 1960). The techniques that will be summarised below fall into two main categories: direct and indirect.

### 2.2 Direct methods

#### 2.2.1 Basic Cell detection – Microscopy

##### *2.2.1.1 Microscopy*

The oldest method for detecting bacterial cells that requires the least expertise is with observation via light microscopy. This technique, however, has many major drawbacks in trying to gain useful information from the sample that is being observed (Bianchi and Giuliano 1996). The most important of these failures is the inability to differentiate between living/viable and dead cells. At the time of observation all cells should be dead (if the slide was heat fixed and stained) but there is no way of knowing (outside of any obvious gross cell wall deformities etc.) which, if any, cells were dead prior to the microscopic investigation (Porter, Diaper et al. 1995).

##### *2.2.1.2 Staining*

There are various fluorescence and staining techniques available to a microbiologist attempting to 'type' the unknown bacteria being investigated however there are many more that could arguably fit under the umbrella of 'staining'. The most relevant to the ongoing work this report is concerned with will be briefly summarised below but it is

important to note that there are many more that could be useful but have simply been omitted at this time to allow for the more immediately obvious techniques to be discussed.

To stain a bacterial culture or to grow it on differential and/or selective media is a classic and simple method for differentiating between genera and often species of bacteria (LEIFSON 1951). It is effective, but with today's rapid or real-time techniques is at least a little dated (LEIFSON 1951, Auty, Gardiner et al. 2001). It is however worth mentioning as it is a starting point for some very useful fluorescence techniques; such as fluorescence in-situ hybridisation (FISH) and fluorescence microscopy.

The use of certain stains is able to surmount the problem discussed earlier with the differentiation of living and dead cells; a mix of propidium iodide and a nucleic acid staining compound known as SYTO will, by a colour differential, show living and dead cells clearly side-by-side (Penney, Powers et al. 2009, Bruckner 2012).

Staining is also the first step in some types of flow cytometry (Nicoletti, Migliorati et al. 1991), a very accurate technique that can be used for cell counting, sorting and biomarker detection amongst other applications (Amann, Binder et al. 1990).

#### ***2.2.1.3 Immuno-fluorescence***

Immuno-fluorescence (IF) is a useful technique that allows specific antigens on a cell to be detected using fluorescently labelled antibodies, allowing for the detection of a mutant colony of cells in an emulsified mixture of wild type cells of the same species, for example (Brathwaite, Ross et al. 1993). IF's power lies in its specificity and its ability to elucidate tiny populations of cells in overwhelming quantities of near identical cells (Heesemann and Laufs

1985), however as with all of the previously outlined techniques, it has significant drawbacks. Antibodies must be raised to the specific antigen and there is no way of knowing whether the antigen on the surface of the bacteria will still be present a few generations later, especially in a bacterial cell with a small genome and high antigenic variation, such as TB (Su, Heatwole et al. 1995, Cole, Brosch et al. 1998). Also there is no way of being sure that all the antibody or all the antigen has reacted or has reacted with its target antigen exclusively therefore a false negative, false positive or a falsely lower or higher result could easily be obtained (Gratama, Department of Clinical and Tumor Immunology et al. 1999).

It is also worth noting the extremely useful technique of green fluorescent protein (GFP) insertion. GFP insertion is both relatively easy and reliable and also has an excellent track record with reason to believe that it gives a very high yield of transfected bacteria if the GFP is introduced into the genome properly and in a suitably essential gene (Tombolini, Department of Biochemistry et al. 2006).

## **2.2.2 Basic Cell detection – Growth assays**

### **2.2.2.1 CFU Count**

The most straight forward method of detecting and enumerating viable cells is a colony-forming unit (CFU) count (Putman, Burton et al. 2005) where a sample of culture is serially diluted and aliquoted typically in 10 $\mu$ L droplets, in triplicate, onto the surface of an agar plate and incubated. The individual dots that grow will be colonies and some simple mathematics can reveal the original numbers of CFUs in in 1mL of culture (displayed as CFU/ml). This method also has significant drawbacks; the time taken to allow the bacteria to grow could be vital to the survival of a patient if this sample had come from a clinical

setting, the veracity of the colonies growing on the plate being from one species can only be judged by the microbiologist doing the counting and as many bacterial colonies grow grossly similarly (depending on the media) there is the possibility of contamination that could skew the result, this can only be rectified by further testing which is time consuming (Coulombel 2004) and potentially expensive.

These two techniques are reliable but outdated yet they remain a staple of lab work. An electronic version with a higher throughput rate and, most importantly, a far faster result time is desperately needed not only in a research setting but also in a clinical setting where such a technology would render the need to grow cells (especially slow growing cells such as *Mycobacterium tuberculosis*) obsolete.

#### **2.2.2.2 Oxygen depletion test (MGIT)**

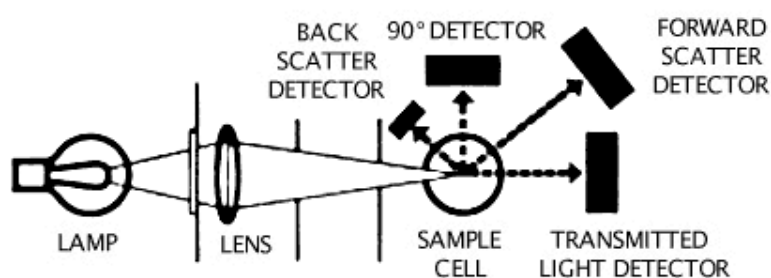
*Mycobacterium spp* are aerobic organisms (Shi, Sohaskey et al. 2005) and as such consume oxygen to respire. In a closed system where the quantity of oxygen is fixed any respiring mycobacteria will consume oxygen in relative proportion to their cell number and physiological state. This is the basis of the MGIT (mycobacterial growth indicator tube) test (Hanna, Ebrahimzadeh et al. 1999, Tunney, Patrick et al. 1999). A colour change occurs as the concentration of oxygen is depleted in the tube and a photonic emission test grants this colour change a numerical value. In this way oxygen concentrations in the tubes can be monitored as growth of mycobacteria is monitored. There are various flaws with this test; chiefly that it required absolute confidence that only mycobacteria are present in the tube, other bacteria are aerobic and faster growing and could therefore out compete any mycobacteria growing in the tube and give a false positive. Another flaw, from the

perspective of this project, is the time, facilities and expertise required to operate the machine that reads the MGIT. *Mycobacterium tuberculosis* is very slow growing and therefore the quantity of oxygen consumed will be very low when the cell number are low and will not quickly increase. Unless the confidence intervals of the test are very tight a small variation in detected oxygen over the course of a few hours could cause a false positive or negative. The MGIT tubes themselves are self-contained units carrying all the reagents necessary to grow mycobacteria but the machine to measure the colour change is very large and expensive and therefore prohibitive to poorer nations and clinics.

## 2.3 Light based cell detection

### 2.3.1 Nephelometry

Nephelometry is an older technique used widely in the detection of water- and air-borne pollutants (BICK 1963) and in clinical settings (Jula, Puukka et al. 1999) for both the detection of cells and smaller particles such as antibodies (Knight and Pritchard 1982).



Courtesy of National Academies Press –  
[http://www.nap.edu/openbook.php?record\\_id=12658&page=212](http://www.nap.edu/openbook.php?record_id=12658&page=212)

Figure 2.1. A schematic of a nephelometer

Nephelometry can, as above be used with a lamp (more recently an LED) and a focussing lens however it will work with a laser as the photon source and this does away with the

need of the focussing lens (Harmoinen, Hällström et al. 2009). The detection setup can also be different from the above schematic, a integrating sphere can be placed after the incident beam has interacted with the sample to allow for more of the diffracted light to be collected and therefore the acquisition of more data is possible (Varma, Moosmiller et al. 2003).

Nephelometry is a similar practice to the desired end result of this study however it differs in a few important ways; Nephelometry is used on both gases and liquids but must be optimised to a particular particle (size, shape, orientation, charge, etc.) (Vercellotti, McCarthy et al. 1985) however the proposed method of data collection, with the sample mounted within the integrating sphere and in the path of the laser, allows for the total amount of light that is scattered to be collected (excluding the small and statistically insignificant amount that escapes along the incident or transmission beam paths). Few nephelometry protocols allow for a beam dump at the end of the beam-line after the incident beam has interacted with the sample, this is possibly an error. As the above schematic shows there are multiple detectors that, through uncomplicated mathematics, can show the intensity of light leaving the photon source, the intensity that reaches the transmitted light detector and the quantity of light that is scattered in 3 different directions (although all along a 2-dimensional plane). In order to greatly simplify the methodology it is necessary only to place the sample within an integrating sphere that has been coated with a diffusive substance, with one detector within the sphere but baffled from the direct influence of the beam, collecting the diffracted light. The remainder of the light beam being dumped into a matt black beam dump so as to completely remove the problem of back reflection onto and through the sample.



### **2.3.2 qPCR**

qPCR, or quantitative polymerase chain reaction, is a useful laboratory technique that has become standard practise in many labs world-wide. It is also known as real-time PCR and is essentially a basic PCR reaction which will amplify the target DNA via the use of primers for the specific regions of DNA under study, the addition of free nucleotides and the enzyme DNA polymerase. While a nucleic acid and molecular quantification technique it still falls beneath the umbrella of photonic quantification as qPCR is dependent on fluorescence for its rapid detection capacity.

The significant difference with qPCR is that the quantity of DNA being amplified and therefore the quantity of DNA present in the sample under investigation is directly detected by one of two methods; either a fluorescent molecule is added to the reaction that intercalates with the DNA as it is being amplified and is activated and fluoresces only after being intercalated into the DNA helix. The second method is a DNA probe consisting of fluorescent oligonucleotides that only fluoresce when bound to their complimentary DNA are included in the reaction. In order to use the information gleaned via qPCR it is necessary to create a standard curve based on DNA samples of known concentrations to compare the fluorescence intensities of the standards versus the experimental samples.

### **2.3.3 Flow Cytometry**

Flow cytometry is a simple and highly sensitive method as described above; it manages to surpass a problem with nephelometry; without a flow system the keep the particles in

constant motion there is potential for the particles to settle under gravity and/or if the sample contains live bacteria and is long-term there is potential for a biofilm to form on the walls of the sample vessel without constant agitation.. This is overcome by using a glass or plastic tube with a much wider bore than is required (as using a smaller bore tube would be extremely fragile while being difficult and expensive to manufacture) and passing a 'sheath flow' down the wall of the tube to reduce the bore, the sample liquid is then allowed to pass down the tube, the flow of the sheath carrying with it the sample without the two ever mixing as the sheath and the sample have differing viscosities and therefore will not interact with each other (Shuler, Aris et al. 1972). If the sheath fluid is [refractive] index matched to the sample tube in the spectrum of the laser light being used then the experiment will be even more accurate (Eisert, Ostertag et al. 1975).

At the simplest level the cells are detected simply as present in the flow through the detection of the scattered laser light. Classically there will be a photon detector mounted in the trajectory of the incident beam in order to collect the forward scattered light, there will also be a range of detectors at 90 degrees to the beam-line to collect scattered light at. There is also usually a number of fluorescence detectors to identify whether the laser light has excited the cells (or compounds contained within or without them) to emit light at a longer wavelength, this, as mentioned above, is sometimes woven into the experiment specifically to allow detection of particular cells or traits in cells amongst a multitude of similar cells (Amann, Binder et al. 1990).

The information it is possible to glean from a well calibrated flow cytometer is much more complex and subtle than simply if the cells are present, however. It is possible to detect the shape and size of the nucleus, the proteins present on the cell surface or the granularity of the cytoplasm, for example (Jung, Schauer et al. 1993).

### **2.3.3.1 FACS**

Fluorescence activated cell sorting (FACS) is a sub-set of flow cytometry which is very useful if a heterogeneous mixture of cells needs to be separated for the continued study of one particular cell set (i.e. separating leucocytes from whole blood, which is, incidentally, a gross over-simplification). This is achieved through the unique scattering and fluorescence patterns emitted by each cell as it passes through the laser beam-line. The sample is sent through the flow cytometer as described above, with the fluorescence of each cell being measured. Directly thereafter a vibration is applied to the flow tube in order to separate the flow into individual droplets, each containing one cell (this is achieved through careful calibration of the vibrating mechanism), these droplets are then electrically charged based on their fluorescence reading and deflected based on the charge applied to them via an electrostatic deflector and then collected for study. (Trojan, Duc et al. 1996)

The system is highly sophisticated and some derivation therein could be of use in the later stages of this study as it would be helpful to be able to differentiate between any sloughed off epithelial cells from clinical sputum samples and the TB cells actually under investigation.

### **2.3.4 Spectrophotometry**

A Spectrophotometer is a staple bench-top lab tool and while not capable of detecting individual cells or even colonies like some of the devices or techniques outlined thus far it does deserve a mention as it is extremely useful when roughly quantifying the concentration of bacteria in a liquid culture during serial dilutions or similar practices. The main difference between the light based techniques discussed so far and then spectrophotometer is that while the scattered light is collected in a flow cytometer and

spectrophotometer displays its results as a function of the light *transmitted* to the detector, the more turbid the sample, the less light that can penetrate and therefore the lower the light intensity, which scales linearly with the turbidity of the sample (Zhao, Wu et al. 2007). Simply, the spectrophotometer consists of a light source that passes through a monochomator to allow only one wavelength of light to pass through the sample. The choice of light wavelength its tailored to what it is the researcher wishes to understand about the sample, but for bacterial concentration in a sample of media the classic wavelength is approximately 600nm (Soukos, Som et al. 2005). The use of a blank is normal in the use of a spectrophotometer, if the bacteria in question were grown in Brain Heart Infusion (BHI) media then the BHI used would be kept sterile and stored until the culture had grown sufficiently, the culture would then be aliquotted into cuvettes to fit the spectrophotometer as would the sterile BHI, the blank would then be set as the BHI and the reading from the bacterial samples would then be as a percentage of the light *not* scattered by bacteria (Otte, Leiden et al. 2012).

Although not as refined as the other techniques spectrophotometer readings have their place as a vital microbiological tool.

### **2.3.5 Dynamic Light Scattering**

Dynamic light scattering is a more complex but related form of light based data collection that is also known as quasi-elastic light scattering. Dynamic light scattering, as the name suggests is concerned with the dynamics of the particles in suspension. Typical results show a time dependant trace of light intensity being refracted and reflected by the particles in suspension undergoing Brownian motion (Urban and Schurtenberger 1998, Schatzel, Drewel

et al. 1999), therefore random movements of the particle are tracked. One of the major problems with dynamic light scattering is the issue of multiple scattering events occurring within the sample vessel (Pusey 1999) If one photon enters the vessel from the subject laser and is then refracted between numerous particles the information about one particular particle is lost and instead very noisy data is gathered with too many scattering events occurring at any given time (Schatzel, Drewel et al. 1999). There are a few ways to correct for this, the first and crudest is to use a latitudinal approach for the laser beam-line. If a long and thin cuvette is used then the laser only passes through a very small volume of sample and therefore will scatter very little. This approach used in conjunction with the second approach; using a lock-in amplifier and a reference signal exactly matching the frequency at which the laser is oscillating allows the noise in the data to be filtered out and the true scattered light (that is to say, the light that has been scattered only once) is measured (Goldburg 1999).

This technique may well be implemented in this study when the details of the static light scattering experiments have been fully analysed. When the proposed device is completed a dynamic light scattering array may be the first of a battery of tests used to establish the usability of the sample before any further information is gleaned from it. It could be extremely useful in ascertaining the gross size and shape of particles in the sample and therefore if it is likely that any of the particles are TB cells.

## **2.4 Introduction to SLIC**

The detection of bacteria in human effluent is a difficult, dangerous task which can also be time and resource consuming. An inexpensive device capable of quantifying the bacterial load in an infected human sample quickly with minimal reagents and training required is something developing countries are in great need of. Here we outline such a device based upon known photonic techniques which is robust and inexpensive to produce.

### **2.4.1 Static Light Scattering**

Flow cytometry is a more complex and targeted version of static light scattering, flow cytometry has faculties that static light scattering cannot achieve as a result of the dynamic nature of the technique, however static light scattering has many advantages over flow cytometry, not least size and cost. Static light scattering is relatively cheap and easy to set up and there no concern with flowing liquids and bacterial contamination as all work can be done on attenuated or dead bacteria. There is of course the possibility of incorporating a flow element into the static light scattering system and that can improve results however it is not necessary as it is in flow cytometry.

Static light scattering is usually used in physical chemistry to ascertain the molecular weight of a molecule or macromolecule and to discover the radius of gyration which is concerned with the root mean square distance of the periphery of any mobile particle from its centre of gravity or rotational axis (Debye 1944, Zimm 1945), this is found with numerous photon detectors at various angles around the sample.

Static light scattering is also commonly utilized to determine the size of particle suspensions in the sub- $\mu\text{m}$  and supra- $\mu\text{m}$  ranges, via the Lorenz-Mie and Fraunhofer diffraction systems, respectively.

For static light scattering experiments a laser is shone in a solution containing colloidal particles. Classically one or many detectors are used to measure the scattering intensity at one or many angles. The angular dependence is required to obtain accurate measurements of both molar mass and size for all particles of radius above 1-2% the incident wavelength. Hence simultaneous measurements at several angles relative to the direction of incident light, known as multi-angle light scattering (MALS) or multi-angle laser light scattering (MALLS), is generally regarded as the standard implementation of static light scattering.

The work undertaken herein is concerned primarily with Rayleigh-Gans-Debye (RGD) scattering. RGD scattering is light scattering by particles larger than the wavelength of the light used. Broadly, two other scattering formulations exist; these are Mie scattering and Rayleigh scattering.

Rayleigh scattering is described as elastic light scattering. Optical elastic scattering is characterised as Rayleigh scattering and no other form. In Rayleigh scattering a photon penetrates a medium composed of particles whose sizes are smaller than the wavelength of the incident photons. The energy (and therefore the wavelength) of the incident photon is conserved and only its direction is changed. The scattering intensity is proportional to the fourth power of the reciprocal wavelength of the incident photon ( $\lambda^{-4}$ ).

Mie scattering is primarily used when the incident beam wavelength is similar to that of the scattering particle. Some of these theories are applicable to this work as the centre of rotation for cells used in this study is approximately 500nm and the incident beam used is

635nm. However, many of these formulations rely upon homogeneous spheres in dilute solution to suppress the effects of multiple scattering events. This is simply not something we can guarantee in a bacterial system therefore we are primarily concerning ourselves with RGD scattering

### **2.4.2 Rayleigh-Gans-Debye scattering**

Static light scattering is a simple method used in physical chemistry for determining the molecular weight of a molecule or macromolecule. It is also useful when determining the radius of gyration which is concerned with the root mean square distance of the periphery of any mobile particle from its centre of gravity or rotational axis (Debye 1944, Zimm 1945), this is normally found with numerous photon detectors at various angles around the sample (dynamic light scattering). In this instance we are concerned with bacterial samples, not those of a chemical nature.

Static laser light scattering is the effect a particle in the path of a laser beam has on the light in that beam, namely scattering it in all directions. The angle and intensity of the scatter carries information about the particle intercepting the laser.

If the particles have a different refractive index ( $n$ ) than the surrounding media they will scatter the laser light. In order to understand which direction the light will scatter it is important to consider that light is an electromagnetic wave. The corresponding oscillating electric field of this wave deforms the electronic cloud of the atoms making up the particle. As a result, the oscillating electrons emit ("scatter") electromagnetic radiation. Each small volume struck by the laser light in a sample will scatter light according to the aforementioned mechanism, thus the intensity measured will be the sum of all such



contributions. With this explanation in mind it can be seen that a homogeneous sample wouldn't scatter any light. For every small volume scattering a wave with a phase ( $\phi$ ) on the direction connecting it to the detector, we can find another small volume at a distance such that its scattered light has a phase of  $\phi + \pi(2n+1)$ . This results in destructive interference. On the other hand, if the sample in the cuvette is not homogeneous, i.e. contains colloidal particles or polymer chains, this argument doesn't apply as the two volumes might have different properties in terms of dielectric constant, such as their polarizabilities. The two volume elements will scatter the light with the same phase but different amplitudes, thus interference will not be completely destructive.

One simple yet very useful theory describing the light scattering of colloidal samples is the so-called Rayleigh-Gans-Debye (RGD) theory. Its basic assumption is that light is not reflected at the medium-particle boundary nor is it attenuated within the particle. This is true if the following conditions are met.

$$|1-m| \ll 1$$

$$\frac{2\pi n_s}{\lambda} a |1-m| \ll 1$$

here  $\lambda$  is the wavelength of light and  $m \equiv n_p/n_s$  is the relative refractive index i.e. the ratio of the refractive index of the colloidal particles to that of the suspending medium, and  $a$  is the characteristic size of the colloidal object.

These two conditions do indeed hold true for our model;

$$2\pi n_s / \lambda = 0.0132, a \approx 500 \text{ nm, therefore;}$$

$$= 6.580 * |1-m|,$$

$$m \equiv n_p/n_s, n_p/n_s = 1.083, 1-m = 0.083, \text{ therefore;}$$

$$= 0.546 < 1 \text{ is correct.}$$

We use the value of  $a$  as 500 nm because the units must remain the same throughout the equation (nm of both  $a$  and  $\lambda$ ) and because this is the largest unmoving area of a cell. We know that mycobacterial cells are approximately  $2\mu\text{m}$  long and  $0.5\mu\text{m}$  (500nm) wide. A mycobacterial cell moving under Brownian motion would be tumbling in liquid media about an axis. As the cells can be thought of as rounded cylinders a tumbling cylinder will move around its rotational axis. Irrespective of where this is on the cell the non-moving axis will be a sphere approximately 500nm in diameter.

The equations regarding RGD scattering continue but hereafter begin to include angle of scattering terms. These terms are not required for our system as we have placed our sample inside an integrating sphere with a single photodetector. We have shown that the placement of the photodetector within the inner face of the sphere is unimportant as it is baffled from the direct beam of the laser and collects light only from the scattered and diffused light from the titanium dioxide (III) inner coating. If we were to create another scattering rig that was concerned with the angle of scattering we may well glean more information about the size and shape of the cells within the sample cuvette but as we have not built such a rig at this stage we need not discuss the necessary equations here.

There are two curious features of the SLIC seen at very high and very low concentrations of bacteria.

At the threshold between approximately 100,000-10,000 cells per mL there is an amplification of the signal seen from the SLIC. Another phenomenon is a certain amount of quenching of the scattering signal seen at very high concentrations of bacteria. Both of these phenomena are justifiable by two possible explanations;

RGD scattering is dependent on the wavelength of the incident beam being smaller than the particle size *and* on there being a lack of multiple scattering events. Where there are a large number of cells multiple scattering events (where one photon scatters off many individual particles) are unavoidable. This causes a chain reaction when a threshold of cells is reached and the quantity of scattering observed is increased significantly. This effect is short lived (on a logarithmic scale) as when the concentration of cells reaches approximately  $10^7$  there is a quenching effect of the signal. This is due to absorption of the beam by the massive quantity of organic matter present. At the point where absorption becomes a serious issue to the reliability of the signal a standard spectrophotometer can be used to gain an accurate result, below this threshold the SLIC is significantly more sensitive.

A bacterial culture placed in the path of a laser would scatter light based on the number and morphology of the cells present within that culture. The technology we have developed here outstrips any commercially available photonic bacterial quantification apparatus by several orders of magnitude.

This has been achieved through the use of an integrating sphere as part of the detection equipment and novel geometries therein. In a nephelometer (a device used primarily to discover air purity and quality) the sample is placed out-with the integrating sphere and light scattered forward is collected inside the sphere. This is acceptable if the only information necessary comes from the forward scattering angles, as all other information is lost, but in this technology we capture all light from all angles and therefore all of the information, this is one of the sources of our sensitivity, another is the application of a lock-in amplifier.

### 2.4.3 Integrating sphere

An integrating sphere (or an Ulbricht sphere) is a hollow sphere treated on the inside with a diffuse coating allowing for the equal transmission of light around the internal cavity of the sphere. The use of an integrating sphere in collecting all, or almost all, of the scattered light means that very little information is lost (KUPPENHEIM 1955, Kawaguchi, Imai et al. 1997).

Integrating spheres are common in photonics and are used industrially to measure the output of light bulbs and other radiation emission apparatus. The integrating sphere in this study has been adapted to allow the sample in question to be removed and replaced easily.

The radiation source, a 635nm laser, shines through the sphere and is dumped on the other side meaning that only the light scattered by the biological sample will be detected. The usefulness of an integrating sphere stems from the fact that it is light impermeable. This, however, is an interesting point when different wavelengths of radiation are considered. An integrating sphere must be impermeable to the wavelength of light that is being used within it and diffuse the same wavelength of light evenly throughout its internal cavity. This necessitates the internal surface of the sphere to be smooth and uniform, otherwise light will reflect and refract at non uniform and unpredictable angles. An integrating sphere, ideally, would have less than 5% of its surface area taken up with ports and support material (Ducharme, Daniels et al. 1997). This may not immediately seem to be a problem; however, there *must* be ports in the sphere to allow for the changing of the sample and for the application of measurement apparatus. If the internal surface was not uniform then light could be scattered or directed onto one or more of the detectors giving a false positive or a falsely higher than anticipated result (Goebel 1967, Ducharme, Daniels et al. 1997).

#### 2.4.4 Lock-in Amplifier

Lock-in amplifiers work by being supplied with a reference signal (in this case from a Keithly 3390 50MHz arbitrary waveform generator oscillating at 10kHz). This signal is the only input that will register and therefore this gives us another stratum of accuracy as unlike spectrophotometers which need a cover and a lack of light to work correctly the SLIC can be operated in bright direct light and near other electrical devices as electrical noise will have no effect either.

Another aspect of this work is the differentiation of cell sub-groups. This could be a sub-population that is resistant to an antibiotic or a population which is morphologically, phenotypically or genetically different to the whole. Detection of these sub-groups is important in bacteriology as a whole but is especially important when mycobacterial diseases are considered, in particular *Mycobacterium tuberculosis*; TB. The specific sub-population we are concerned with when discussing TB is the dormant cells (also known as latent cells or persister cells). There is evidence to suggest that dormant TB cells express triacylglyceride (TAG) (Reed, Gagneux et al. 2007, Young, Gideon et al. 2009, Daniel, Maamar et al. 2011) and waxy esters (Sirakova, Dubey et al. 2006, Deb, Burnett School of Biomedical Sciences et al. 2009, Sirakova, Burnett School of Biomedical Sciences et al. 2012) both of which are non-polar lipids. Cells that express these groups have been termed 'lipid rich cells' (their counterparts, those cells without lipid bodies are 'lipid poor cells'). Work has been done to elucidate the composition of these lipid bodies and to visualise them (Daniel, Maamar et al. 2011) and while these have been somewhat successful we believe that we have discovered a more effective way of differentiating between lipid rich and lipid poor

cells. This was first achieved under a fluorescent microscope but now has been shown to work with the aid of this highly sensitive technology (the SLIC).

## 2.5 Methods

### 2.5.1 SLIC

#### 2.5.1.1 *Development of the SLIC*

The SLIC methodology went through considerable evolution with a first second and third iterations.

The first iteration of SLIC was micro-milled from modelling foam and coated on the inside with a diffusive titanium oxide (II) coating. A second spherical collector was made as used as a beam dump. The Sphere was coated with a matt-black coating to absorb light that entered the beam dump so as to stop any back-reflection that might give a false-positive result. At this stage it was established that the lock-in amplifier and signal generator were essential to the sensitivity of the SLIC. The first crude laser mount was created and the first tests were under taken. These encouraging data lead us to produce more robust versions of the SLIC for use in the biohazard category 2 laboratory with live bacteria.

SLIC version 2 was 3D printed and mounted to a floating photonic table. Version 2 consisted of a hollow sphere that was again given the diffusive titanium oxide II coating on the inside. The plastic that the integrating sphere was built from was a translucent white and diffusive in its own right. However due to the translucent aspect there were issues with some of the scattered laser light escaping. To combat this we coated the outer face of the sphere with a reflective metal sheeting to give us our first total internal diffusive chamber. The laser mount was completely re-designed and a circuit designed to not allow the laser to dim over time so we got constant readings from the SLIC until the power failed entirely. The version 2 had intricate internal architecture that was required to hold the sample vessel in the same place for every experiment to lessen experimental error. This internal structure was cumbersome and so in the version 3 it was removed. As this version was mounted to the

photonic bench only dead microbial samples were used. This too was rectified with the version 3.

Version 3 of the SLIC was mounted to a fixed and screw threaded board (a breadboard) that allowed the SLC to be moved without de-aligning the laser or other components. This meant it could, for the first time be moved to the biohazard lab. The internal stricker was removed and replaced with a cap-loading system which allowed for the same degree of reproducibility with sample position in the beam line but interfered with the transmission of the signal much less. At this point we realised that a data logging software option would be advisable so we added a digital oscilloscope to the rig and a computer to record the data meaning we could not log the data coming from the SLIC in real time and check for errors or contaminants in the sample as we measured them. Version 3 also had all the features of the previous models but the reflective metal sheeting was placed inside the sphere to ensure that no light was absorbed by the plastic or lost through minute cracks or fissures in the outer structure.

A slight change was made to version 3 to give us version 3.1 where we changed the sample loaded to completely remove any change in sample position as this was found to be a significant source of error. Also a 3D printed beam dump was produced (modelled on commercially available beam dumps) and the power supply stabilised to achieve maximum reproducibility even on 24 hour experimental runs.

#### **2.5.1.2 Bacterial detection**

Specimens of *Mycobacterium fortuitum*, *M. smegmatis* and *M. bovis* (BCG) were grown in 14mL round bottomed growth tubes in sterile culture medium (middlebrook 7H9) with 0.5% Tween 80 in a shaking incubator at 210 RPM, 37°C and ambient CO<sub>2</sub>/O<sub>2</sub> concentrations.



Cultures were left to grow for various lengths of time ranging from 72 hours to several months. This resulted in cultures of various concentrations of live-dormant, live-active or dead bacteria. Samples of these cultures were aliquoted at 3 x 1mL into sterile Microcentrifuge tubes. 3 x 1 mL of sterile media was aliquoted into another three sterile Microcentrifuge tubes. All of these samples (culture and pure media) were then vortexed vigorously for a few seconds and pipetted into standard 1.5 mL cuvettes and loaded into the SLIC. Measurements were recorded over 30 seconds and checked in real-time for aberrations (indicating airborne contamination; i.e. dust). This was repeated for each sample in triplicate. Measurements recorded were averaged to gain a single figure for each sample and these were statistically checked against the sterile media as a standard.

#### **2.5.1.3 Bacterial scattering at differing concentrations**

Samples of *M. smegmatis* and *M. fortuitum* were collected as above and serially diluted in sterile PBS from neat culture to  $10^{-10}$  and measured in the SLIC and analysed as above. When the results indicated that there was no signal (the signal was the same as the standard) this was noted. All samples (including the standard) were plated onto BHI agar and incubated for 72hrs at 37°C. When colonies had grown these were counted and cross checked with the results from the SLIC. Where no colonies had grown this indicated no viable cells were present, these results tallied with the SLIC results when no signal was measured indicating both a 100% accuracy rate and the limit of detection to which the SLIC could measure. When the colony count was only 4-10 CFU the SLIC could detect cells indicating an unprecedented sensitivity with light-based technology. As a secondary form of cellular concentration validation qPCR was conducted on the 16s ribosomal DNA from the original cultures. These were found to tally with the SLIC results.

#### **2.5.1.4 Rapid antibiotic susceptibility testing**

Cultures of *M. smegmatis* and *M. fortuitum* were grown to known density (concentration confirmed via CFU counting on BHI agar plates) were harvested at 500µL and added to tubes of new, pre-warmed sterile media. One tube was dosed with a concentration of antimycobacterial antibiotic 2 x higher than the MIC (isoniazid at 40mg/ml) and one was left without antibiotic. One tube of sterile media was also treated with antibiotic and another left without any additives. These tubes were all then sampled immediately (1mL removed and 1mL of sterile media added) and allowed to incubate for 30 minutes at 210 RPM and 37°C after which another sample was removed and media added to maintain a constant volume. This was repeated for 5 hours with every sample measured in the SLIC immediately after extraction. The results show that after 3 hours it is possible to distinguish the dosed from the antibiotic-free samples for *M. smegmatis* and *M fortuitum*.

This experiment was also repeated with samples of *Escherichia coli* in which it was found that antibiotic susceptibility was evident after only 45-60 minutes (sampled every 15 minutes).

<b>Mycobacteria</b>	<b>Gram negatives</b>	<b>Gram positives</b>
M. smegmatis	P. aeruginosa	E. faecium
M. fortuitum	H influenzae	S. aureus (MRSA)
M. bovis (BCG)	K pneumoniae	S. aureus (MSSA)
M. marinum	E. coli	E. faecalis
M. komossense	C. koseri	S. pyogenes
	P. mirabilis	S. pneumoniae
	S. maltophilia	S. agalactiae
	E. aerogenes	
	A. baumannii	

Table 2.1. Species tested in SLIC. It was found that all species, irrespective of gram-status or morphology, gave similar results- a linear relationship when diluted serially until the limit of detection was reached.

#### **2.5.1.5 Self-incubating SLIC (hSLIC)**

A new version of SLIC was built that could self-incubate samples directly from frozen stock, culture or recovered from patient (e.g. Mouth or skin swab). The capacity of this new version was tested against a frozen culture of *E. coli* taken directly from glycerol stock. Internal temperature was closely regulated via three wire-wound resistors wired in series (the heat source), an internal thermistor and a feedback loop programmed into a raspberry pi designed to keep the temperature at  $37^{\circ}\text{C} \pm 0.5^{\circ}\text{C}$ . Measurements were made every 2 minutes and the data shown in Figure 2.7 are the median data points across 10 minute intervals.

For species tested see Table 2.1

#### **2.5.1.6 Detecting presence of lipid rich cells (SLIC fluorescence)**

A different spherical collector was built using an UP! 3D printer and polylacticacid (PLA) plastic, this was then coated internally with a diffusive layer of titanium oxide paint and coated on the outside with a reflective layer to allow as little light as possible to escape the sphere. Two LEDs were then attached, one with peak emission at 430nm (blue) and another with peak emission at 510nm (green). These LEDs were wired directly to the Keithly 3390 50MHz arbitrary waveform generator which was set, as before, to 10kHz. This locked on to the Stanford SR530 Lock-in amplifier which was receiving inputs from two photodiodes, both shielded by custom coloured plastic filters, one in the red range and one in the green range. Samples of *M. smegmatis* were prepared by removing an aliquot of 100µL from an old culture expected to contain a high proportion of lipid rich cells and a younger culture expected to contain many fewer lipid rich cells. These samples were spotted onto a BHI agar plate and allowed to grow statically at 37°C for 72h to quantify the number of recoverable cells present to allow results to be adjusted after the experiment to account for differences in cell density. Both remaining lipid rich and lipid poor samples (70µl) were stained with Nile red dissolved in ethanol to a final concentration of 500µg/mL with agitation for 30 minutes. They were then centrifuged for 3 minutes at 20,000g and the supernatant removed and kept. The pellet was resuspended in 100% ethanol, vortexed and spun again at 20,000g for 3 minutes. This was repeated a further two times. The remaining pellet was resuspended in 20µL of sterile PBS (a 3.5 fold concentration) and 2x 10µL was spotted onto 2 clean glass slides. These were then heat fixed and allowed to cool. The remaining spot was washed briefly with 70% ethanol and then dH<sub>2</sub>O to remove any remaining unbound Nile red. Both slides were then allowed to dry and one viewed under a fluorescent microscope to ascertain by counting the number of lipid rich cells present. A clean slide was placed inside the sphere

and had its fluorescence measurements read as a blank. The other slide was placed inside the fluorescence sphere and green vs. red readings were taken to ascertain relative abundance of lipid rich to lipid poor cells. This was compared against the microscopic investigation and the blank slide value was subtracted to give a relative green to red ratio.

## 2.6 Results

Current light scattering arrays for sale commercially rely on detection techniques such as absorption of the incident beam by the sample or collection of scattered light from one position. The interactions of particles with a laser beam are well understood from their k-vectors (*Kachan, Ponyavina et al. 2001*), to the differences in the scattering patterns of spherical to elongated shapes (*Zhou, Burger et al. 2001*) and the effect of size on scattering angle (*Prashant K. Jain, Kyeong Seok Lee et al. 2006*).

All of these effects are important in the design of standard scattering arrays however the technique described here does not rely on many of these principals, instead it relies on the use of an integrating sphere. In order to take advantage of this fact and measure the total scattering output (TSO) a sample of bacteria were grown in middlebrook media (7H9) with 0.5% Tween 80 added to discourage clumping of the bacteria. These samples were grown for varying lengths of time; from 48hours to several months, and measured intermittently. CFU counts and qPCR results were conducted in tandem to ascertain by more standard methods the bacterial load of a sample and to confirm the SLIC results.

### 2.6.1 SLIC calibration with biological material

After each SLIC iteration was assembled and completed it required calibration with both standardised calibration media (data not shown) and with live biological samples. The first stage of this was to establish the SLIC could identify samples containing concentrations of bacteria detectable by other photonic technologies (such as spectrophotometry). The data shown below in

Figure 2.2 is from the most recent version of SLIC as part of routine calibration. This was done to establish the limit of detection.

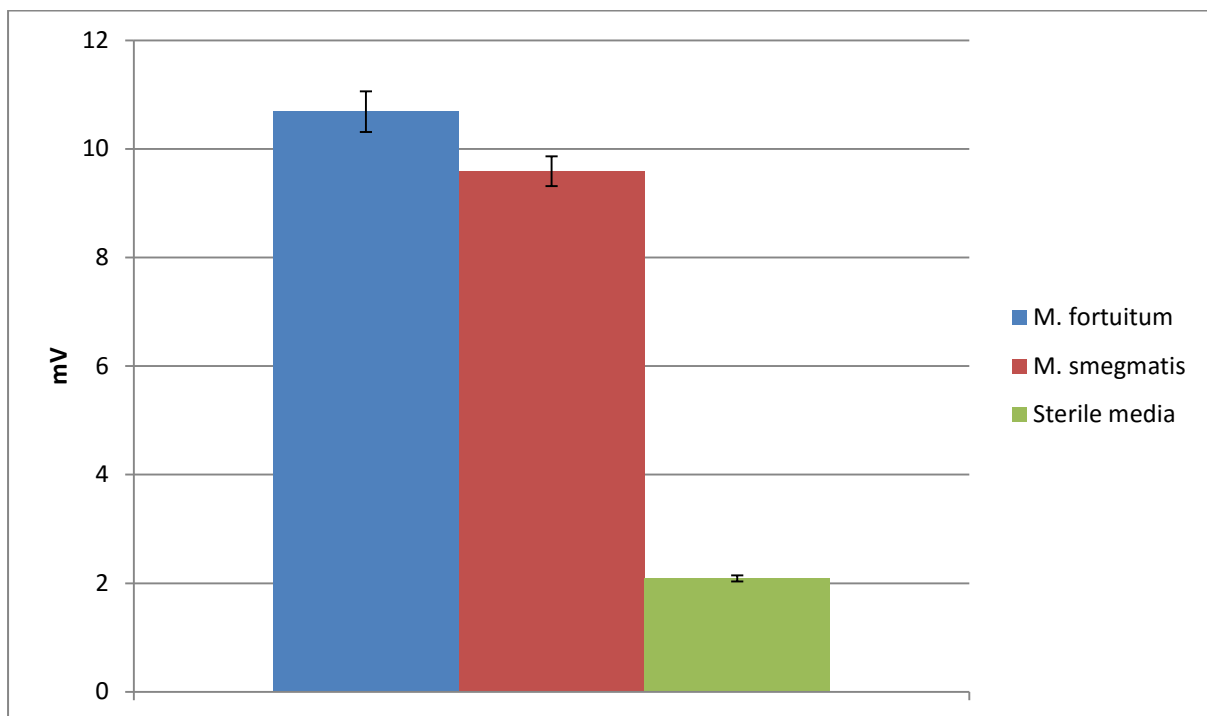


Figure 2.2. Bacterial presence test. Samples of *M. smegmatis* and *M. fortuitum* were taken from mature culture and washed twice with sterile media and then resuspended to their original concentrations. These samples were measured against sterile media. The data is the average of 6 experiments and shows that the SLIC can differentiate between media containing bacteria and media that is free of bacteria. n=6. Error bars are 2 standard deviations from the mean.

Samples of bacteria were removed from culture and pipetted into 1.5mL plastic cuvettes and loaded into the SLIC. After measurement the samples were pipetted onto BHI agar plates for CFU counting. After colonies had grown the density of the culture was established. The results clearly show that over multiple experiments (results here are averages of 6 experiments) the quantity of detected light (TSO) was consistently higher in samples which contain bacteria. Results here are adjusted to reflect the same concentration of bacteria in both *M. fortuitum* and *M. smegmatis* samples-  $4.0 \times 10^7$ .

### **2.6.2 Concentration dependant scattering test (lower limit of detection)**

This experiment was carried out as the final stage of calibration of the SLIC against live microorganisms. This test was first performed with the second iteration of SLIC and was designed to discover the SLIC's lower limit of detection. Samples used in these experiments were always of known bacterial concentration (established by CFU and spectrophotometry) so that SLIC results could be related directly to CFU and spectrophotometry results and the true limit of detection established. As described samples were serially diluted from neat culture to  $10^{-10}$  and then measured for the TSO (figure 2.3).



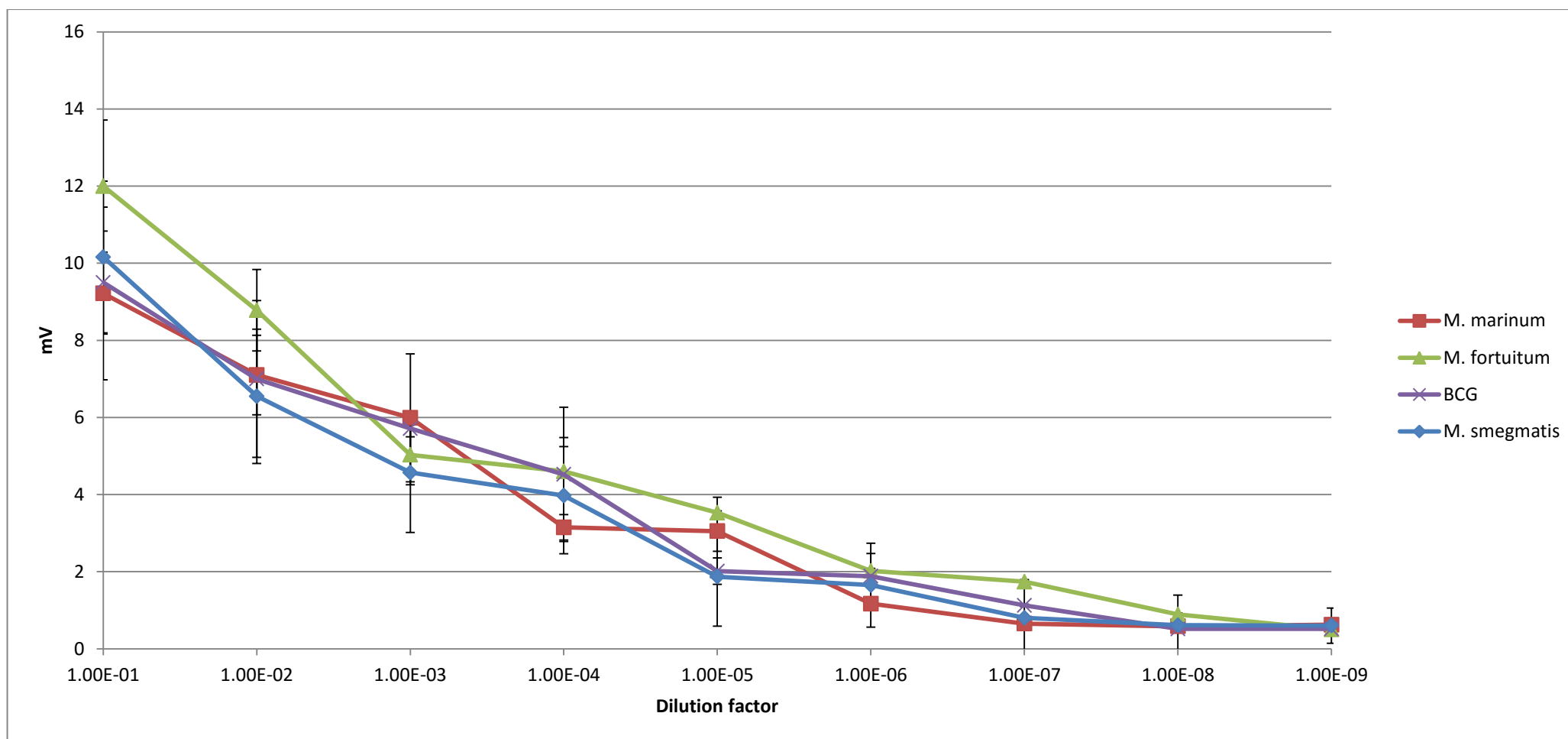


Figure 2.3. Total scattering output for four species of Mycobacterium; *M. smegmatis*, *M. fortuitum*, *M. marinum* and BCG. As the dilution factor decreases and the quantity of bacteria rises so does the mV value. This value is derived from the photodiode that receives the light signal and translates it into electrical energy that the lock-in amplifier can read; the more light detected the higher the voltage. Both cultures were at  $\sim 10^8$  cells per millilitre.  $n=3$ . Error bars are mean  $\pm$  2 standard deviations.

Concentration dependant scattering tests were also carried out with organisms other than mycobacteria. As we hope to open the scope of SLIC beyond mycobacterial infections and, eventually, to bring it to market we needed to validate the technology and techniques against other clinically relevant species (many of these species can be seen in Table 2.2. Our choice of organisms was also influenced by literature searches that reported the most difficult bacteria to detect (Nikfarjam and Farzaneh 2012). With these two criteria in mind we chose to attempt the rapid detection of *Mycoplasma pneumoniae* as a test organism for difficult to detect bacteria. Mycoplasmas are difficult to detect with classical methods because they are highly fastidious and do not readily grow and classical media, they are slow growing and also are very small; 100nm in diameter. The size of the mycoplasma cell presented an interesting challenge for the SLIC as it is calibrated to detect cells larger than half the wavelength of the light used (635nm laser = 317.5 nm minimum scattering cross section). If the particle in question is smaller than ~320nm the scattering is no longer classed as RGD. We were unsure if the SLIC would be able to detect particles as small as the mycoplasma cells but as Figure 2.4 shows we found a strong linear relationship between scattering output and dilution series.

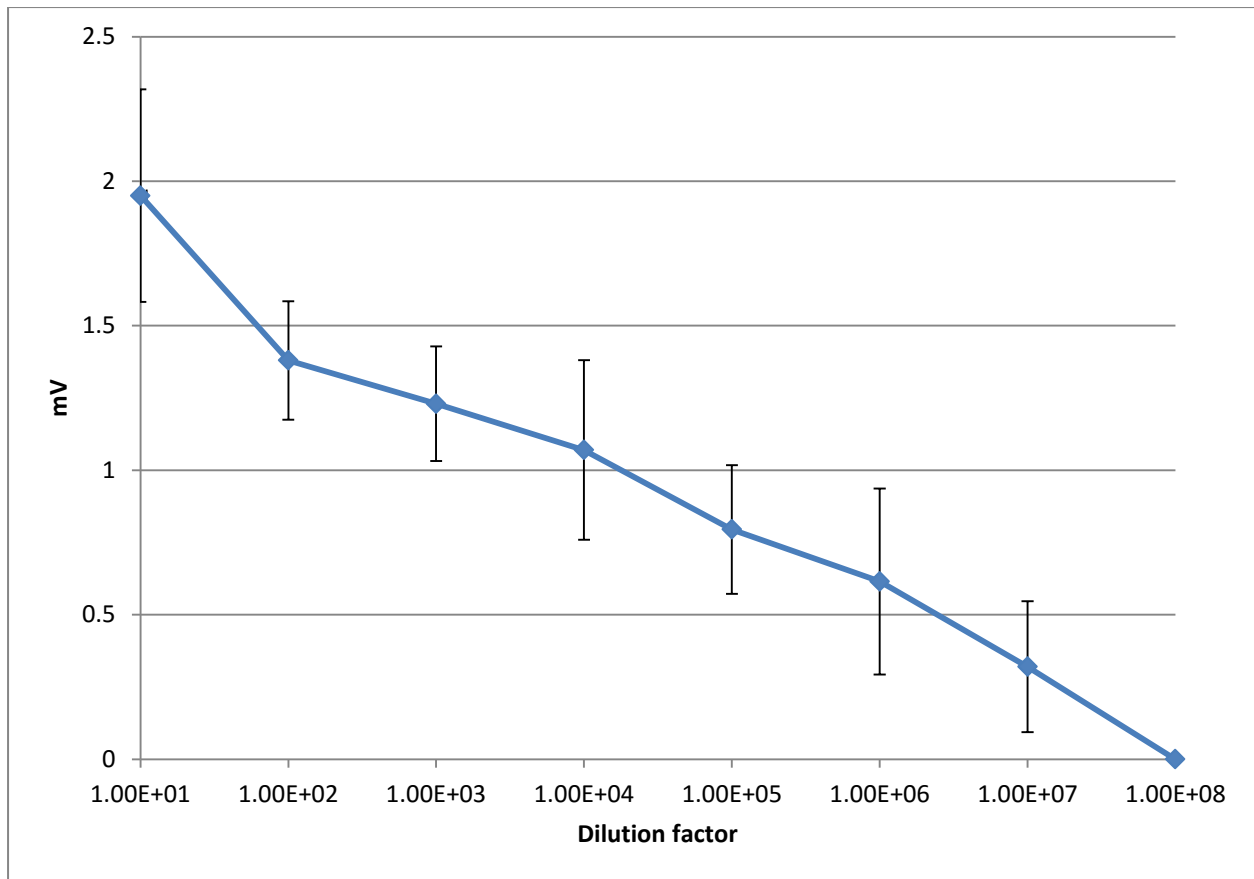


Figure 2.4. Total scattering output for a dilution series of *Mycoplasma pneumoniae*. As the dilution factor rises and the total number of bacteria decreases the signal decreases linearly. Error bars represent 2 standard deviations from the mean. n=3.

This strongly positive result is likely due to the relationship between particle size and light scattering. Large particles ( $>\lambda$ ) will scatter light more forwards and backwards than small particles ( $<\lambda$ ). Small particles will scatter more light at an approximately  $90^\circ$  angle from the emission source. In this case that means that very few of the scattered photons are leaving the integrating sphere along the beamline and are therefore being measured more readily (see Figure 2.10).

Data from some of the clinically relevant species we chose to analyse are shown below (Figure 2.5)

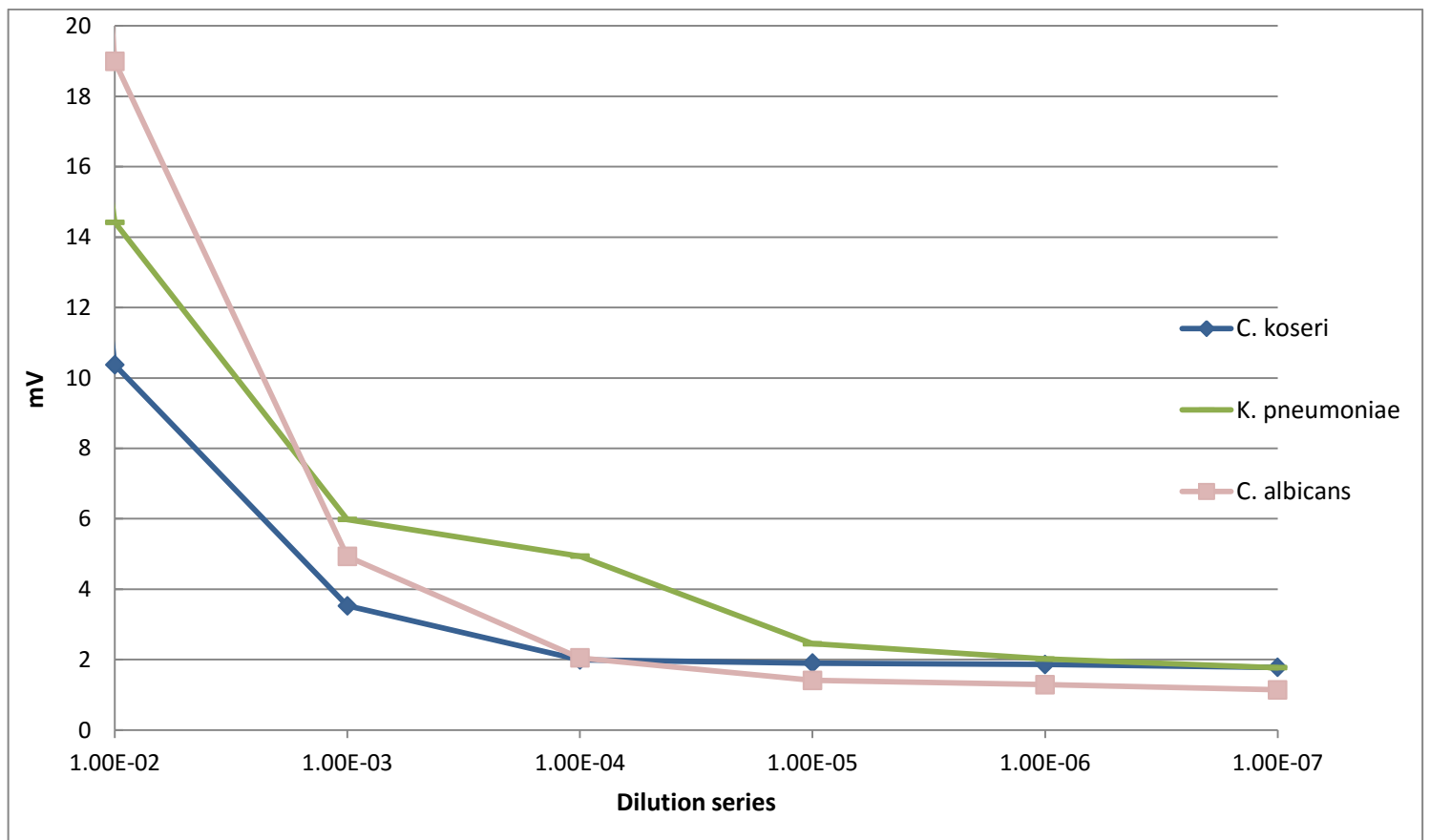


Figure 2.5. Total scattering output of 3 example species. 3 of the 23 clinically relevant species tested over a serial dilution series. Bacterial concentration for each culture was at approximately  $5 \times 10^6$  prior to first dilution.

Figure 2.5 shows that the same patterns found in mycobacteria (Figure 2.3) are found in non-mycobacterial, clinically relevant species. The patterns are that, even with very different morphologies, laser scattering signals the species tested above still decrease in proportion with the quantity of cells present over a serial dilution series. This was true of all species tested (Table 2.2).

Bacterium	limit of detection (CFU/ml)
<i>C. koseri</i>	10
<i>C. perfringens</i>	100
<i>E. clocae</i>	100
<i>S. pneumoniae</i>	10
<i>E. coli</i> 35218	10
<i>E. coli</i> 25922	100
<i>A. baumannii</i>	100
<i>E. faecium</i>	10
<i>K. pneumoniae</i> 1706	10
<i>K. pneumoniae subsp. pneumoniae</i> 700603	10
<i>K. pneumoniae</i> 705	100
<i>P. mirabilis</i>	10
<i>E. faecalis</i>	100
<i>S. maltophilia</i>	100
<i>S. pyogenes</i>	100
<i>H. influenzae</i>	10
<i>S. genitalium</i>	100
<i>P. aeruginosa</i>	10
<i>E. aerogenese</i>	100
<i>C. albicans</i>	100
MRSA 29213	10
MRSA 43300	100
<i>S. aureus</i>	100

Table 2.2. Limit of detection for all clinically relevant microorganisms tested

In order to evaluate SLIC against other commonly used systems a direct comparison was required. Samples of bacteria were aliquoted into cuvettes and diluted in a 10 fold series. The results can be seen in

Figure 2.3 showing that SLIC is, in this instance, 1000 times more sensitive than the spectrophotometer. The signal from the spectrophotometer is lost at  $10^5$  times diluted whereas the signal is lost in SLIC at  $10^8$  time diluted. The 'true' concentration of bacteria was established by CFU plate and was found to be  $7 \times 10^8$  CFU/mL. This means that the SLIC was detecting 7 cells per mL whereas the spectrophotometer lost signal when there was still 7000 cells in the tested media.

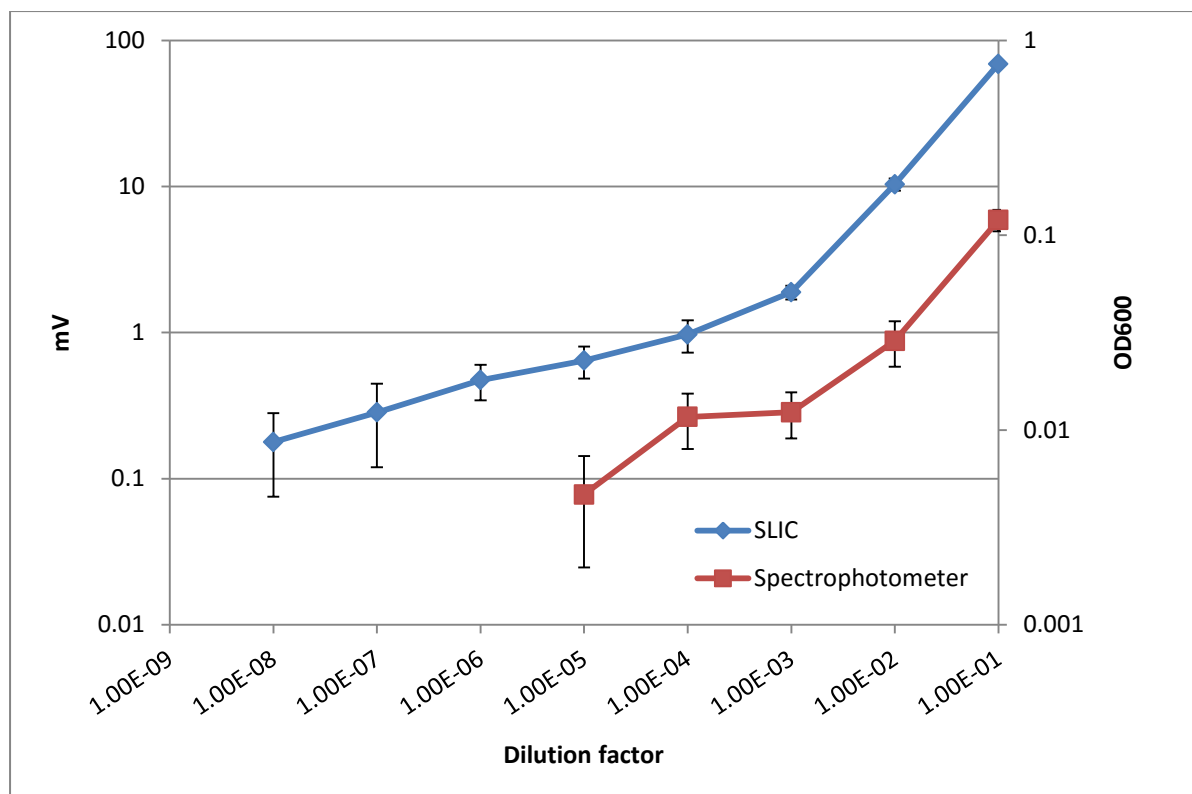


Figure 2.3. Graph displaying the 1000 fold difference in sensitivity between SLIC and spectrophotometry. The signal was lost in the spectrophotometer after the sample was diluted by  $10^5$  times. In the SLIC signal remained until the sample was diluted by  $10^8$  times. The actual number of cells was found to be  $7 \times 10^8$  by Miles and Misra CFU plating. Error bars represent two standard deviations from the mean.  $n=3$ .

### 2.6.3 Rapid antibiotic susceptibility testing

In addition to SLIC's ability to be a highly accurate cell counter it also has the capacity to determine the differences between minute changes in actively growing bacterial populations. This ability is useful when rapidly determining the change in bacterial load in antibiotic studies (Figure 2.4, Figure 2.10 and

Figure 2.5) as a change of 10-100 individual bacteria can have a significant outcome. In a rapidly replicating bacterium such as *Escherichia coli* it is possible to see a statistically significant difference between a culture that has been treated with an antibiotic and one

that has not after only 45-60 minutes of free growth at 37°C from a starting concentration of approximately  $10^3$  cells (Table 2.4). This equates roughly to 2 generations or doubling time points. This means that the cells of the untreated population have grown from  $1 \times 10^4$  cells to  $4 \times 10^4$  cells, a difference which is imperceptible to modern rapid quantification technologies and would take considerably longer to elucidate using molecular methods such as PCR or metabolic methods such as MGIT.

In order to discover the full capabilities of SLIC in this role SLIC was tested exhaustively against a range of microorganisms.

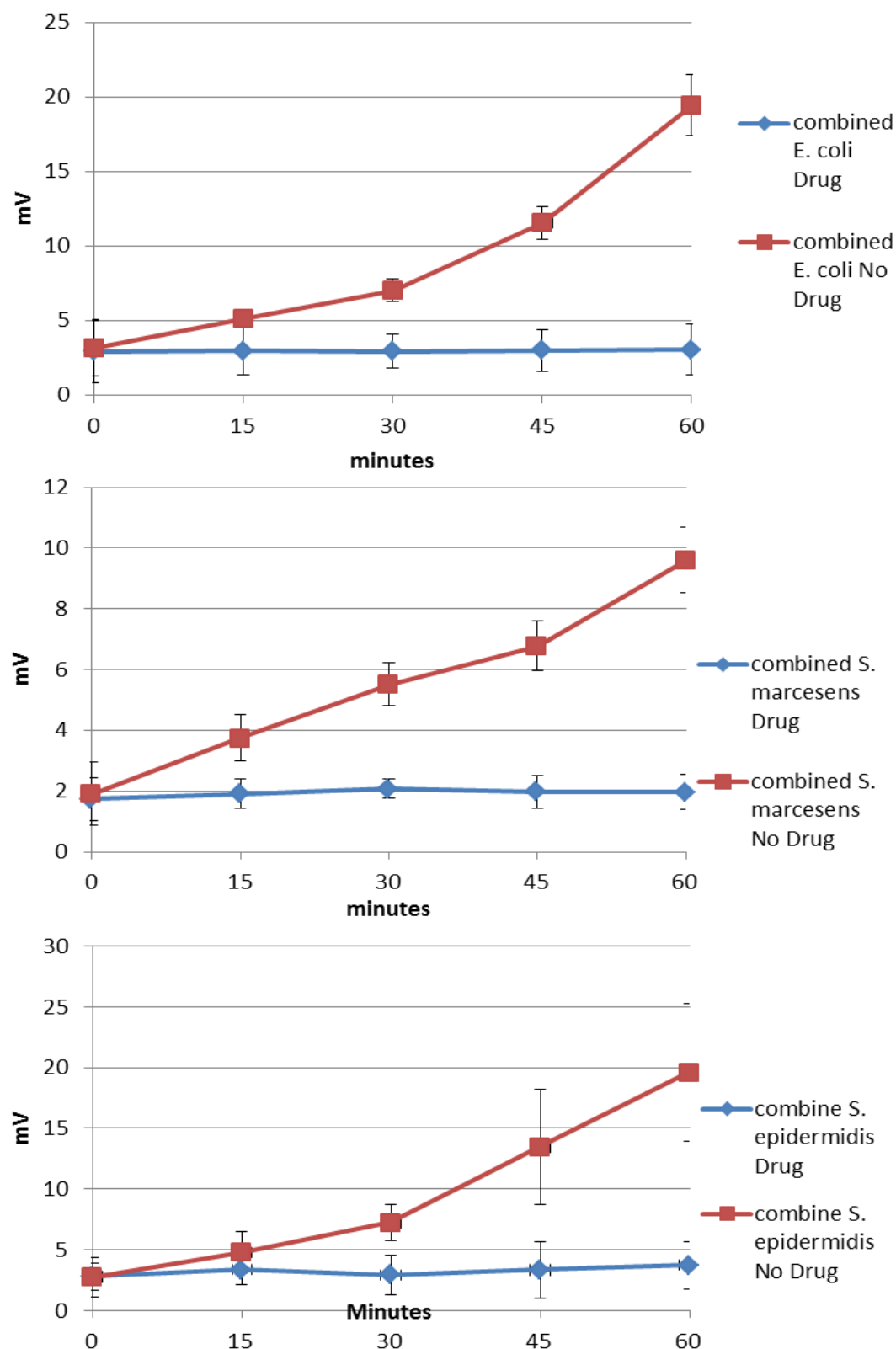


Figure 2.4. TSOs for rapidly dividing bacterial species- *Escherichia coli*, *Serratia marcescens* and *Staphylococcus epidermidis*. These species were treated with 20ug/mL of ciprofloxacin and then allowed to grow freely without any inhibition. The statistical differences are indicated by the error bars (2 standard deviations from the mean) and it can be seen that at 45 minutes there is a significant statistical difference between the two populations this can also be seen in



	Minutes						
	0	15	30	45	60	75	90
<i>E. coli</i> P value =	0.934	0.180	0.025	<0.001	<0.001	<0.001	<0.001
<i>S. marcescens</i> P value =	0.836	0.239	0.039	0.006	<0.001	<0.001	<0.001
<i>S. epidermidis</i> P value =	0.894	0.521	0.018	<0.001	<0.001	<0.001	<0.001
<b><i>P. aeruginosa</i></b> <b>P value =</b>	<b>0.981</b>	<b>0.984</b>	<b>0.991</b>	<b>0.413</b>	<b>0.019</b>	<b>&lt;0.001</b>	<b>&lt;0.001</b>
<b>MRSA</b> <b>P value =</b>	<b>0.311</b>	<b>0.976</b>	<b>0.868</b>	<b>0.761</b>	<b>0.052</b>	<b>&lt;0.001</b>	<b>&lt;0.001</b>
<b><i>K. pneumoniae</i></b> P value =	<b>0.794</b>	<b>0.935</b>	<b>0.997</b>	<b>0.796</b>	<b>0.514</b>	<b>&lt;0.001</b>	<b>&lt;0.001</b>
<i>C koseri</i> P value =	0.966	0.930	0.496	0.132	<0.001	<0.001	<0.001
<i>P. mirabilis</i> P value =	0.998	0.987	0.968	0.978	<0.001	<0.001	<0.001
<b><i>E faecium</i></b> <b>P value =</b>	<b>0.915</b>	<b>0.990</b>	<b>0.994</b>	<b>0.756</b>	<b>0.005</b>	<b>&lt;0.001</b>	<b>&lt;0.001</b>
<i>E aerogenes</i> P value =	0.521	0.750	0.833	0.247	<0.001	<0.001	<0.001
<i>S pyogenes</i> P value =	0.021	0.094	0.970	0.003	<0.001	<0.001	<0.001
<i>S pneumoniae</i> P value =	0.841	0.840	0.001	<0.001	<0.001	<0.001	<0.001
<i>S. maltophillicia</i> P value =	0.854	0.337	0.836	0.500	<0.001	<0.001	<0.001
<b><i>S agalacticae</i></b> <b>P value =</b>	<b>0.857</b>	<b>0.116</b>	<b>0.809</b>	<b>0.401</b>	<b>0.165</b>	<b>&lt;0.001</b>	<b>&lt;0.001</b>
<i>S. aureus</i> P value =	0.992	0.798	0.003	<0.001	<0.001	<0.001	<0.001
<i>H influenzae</i> P value =	0.976	0.001	<0.001	<0.001	<0.001	<0.001	<0.001
<i>E faecalis</i> P value =	0.342	0.487	0.678	<0.001	<0.001	<0.001	<0.001
<i>A baumannii</i> P value =	0.531	0.874	0.286	0.986	<0.001	<0.001	<0.001
<i>S. pneumoniae</i> P value =	0.322	0.006	0.188	<0.001	<0.001	<0.001	<0.001
<i>S. agalacticae</i> P value =	0.977	0.972	0.994	0.997	<0.001	<0.001	<0.001

<i>S. aureus</i> P value =	0.108	0.894	0.310	0.001	<0.001	<0.001	<0.001
<i>A. baumannii</i> P value =	<b>0.519</b>	<b>0.904</b>	<b>0.879</b>	<b>0.065</b>	<b>0.001</b>	<b>&lt;0.001</b>	<b>&lt;0.001</b>

Table 2.3. Displays Chi<sup>2</sup> data from Figure 2.4 plus all other susceptibility data gathered on clinically significant pathogens tested. It can be seen that at for nearly all species there is a significant difference in the dataset at 60 minutes indicating that there is a statistically significant difference between the treated and the untreated samples. Those samples that do not show a significant difference in P value at 60 minutes are highlighted in bold. All samples show a significant difference at 75 minutes.

After the above experiments were completed the procedure for clarifying TTPs of rapidly dividing microorganisms was optimised and we moved onto testing a greater range of microbe samples. These were collected from the infection wards of local hospitals and their specific drug susceptibility profiles were established using SLIC. These profiles were then matched against the NHS database for each isolate. It was found that SLIC was able to determine with 100% accuracy the susceptibility profiles of the bacterial species tested.

Figure 2.5 displays the results of two experiments that were undertaken as part of this drug susceptibility profiling.

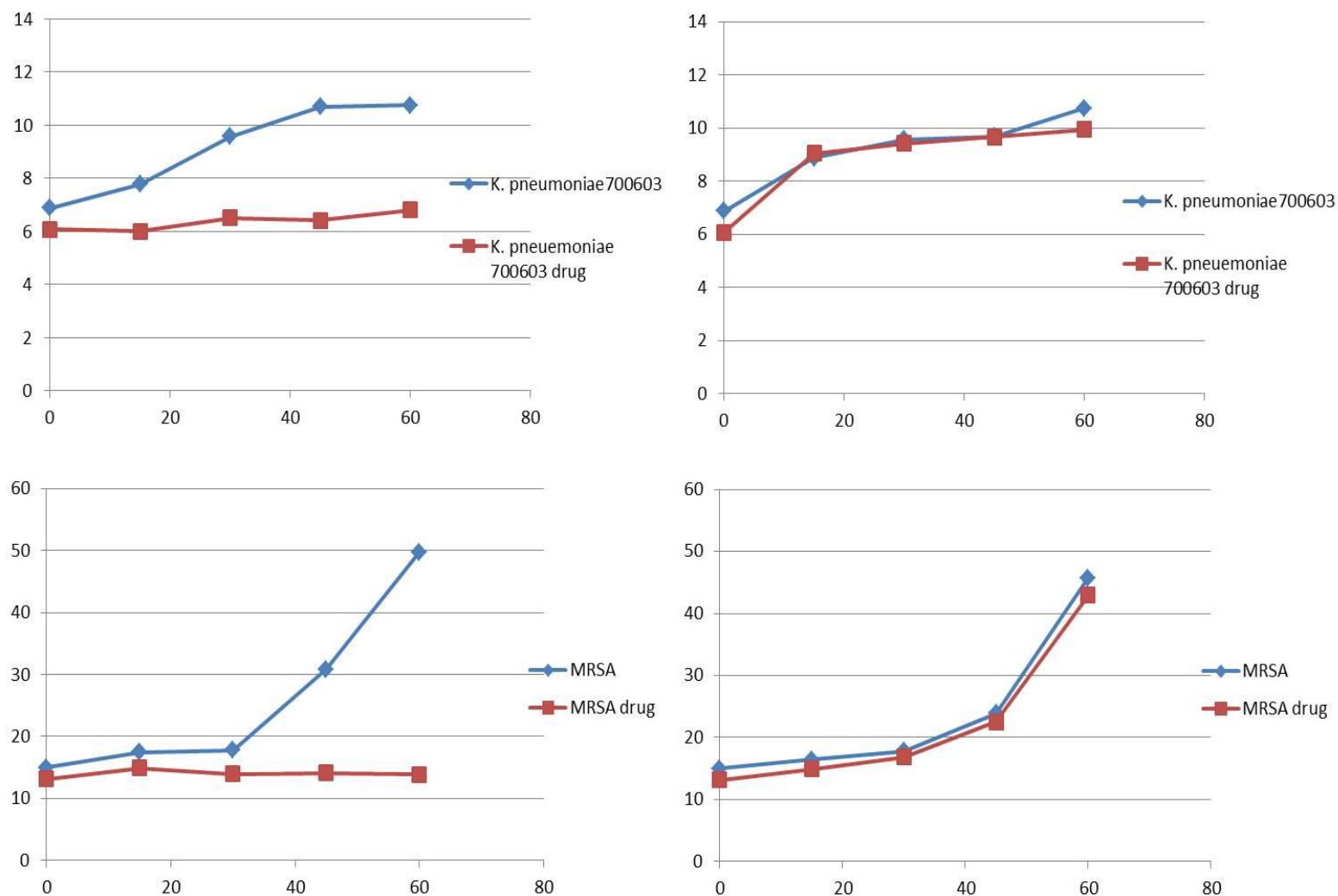


Figure 2.5 Examples of clinically relevant species treated with drugs they are resistant to over time in SLIC (right side). Examples of clinically relevant species treated with drugs they are susceptible to over time in SLIC (left side). Sample of MRSA was exposed to methicillin to confirm its status as MRSA and *K. pneumoniae* 700603 was exposed to ampicillin which this strain is resistant to. These samples were treated identically to those that appear in Figure 2.9 and Table 2.4.

Figure 2.5 displays examples of experiments in which a drug was found that the tested organisms were susceptible to. In all cases this allowed us to use the baseline measurement of non-growth (the red lines) as statistical markers to establish earliest TTPs for these species. The TTPs for all species tested are shown in Table 2.4.

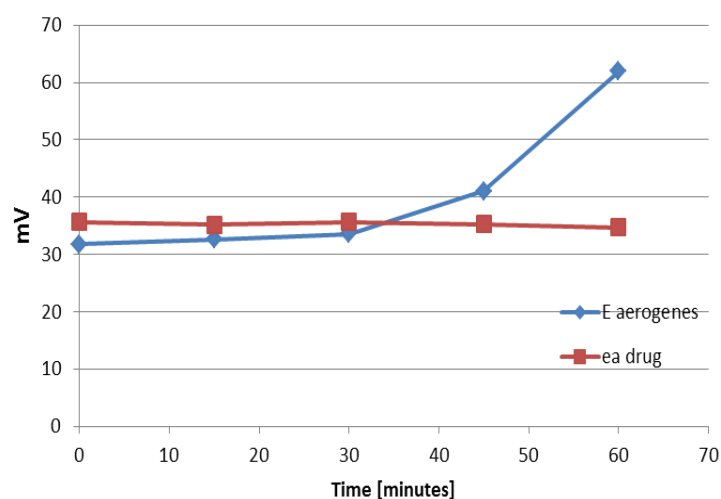
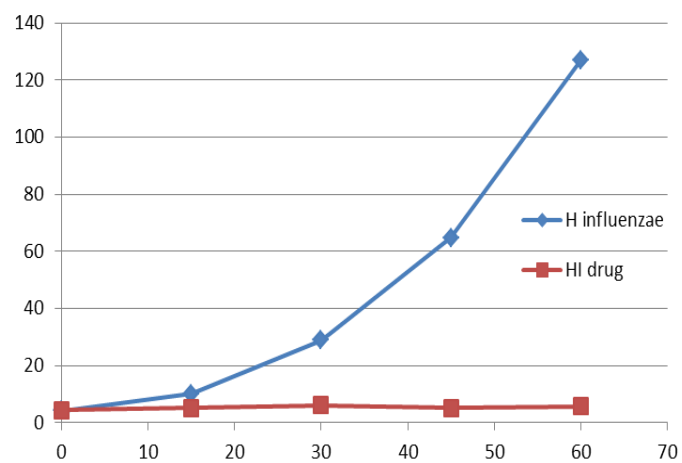
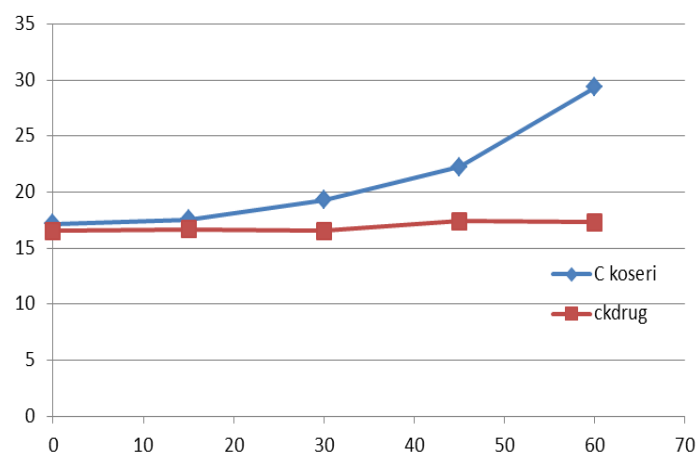
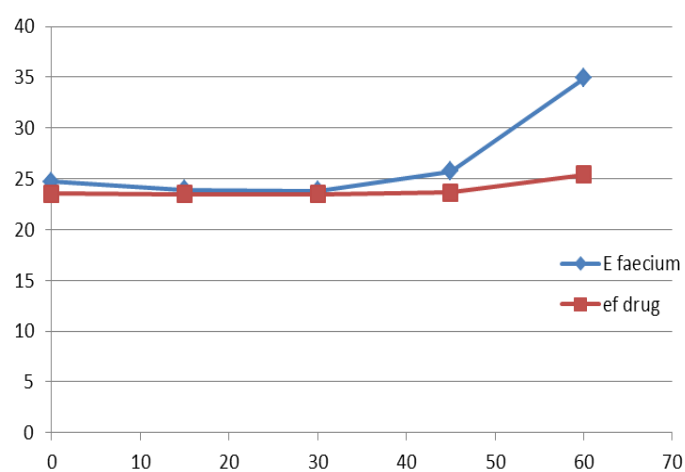
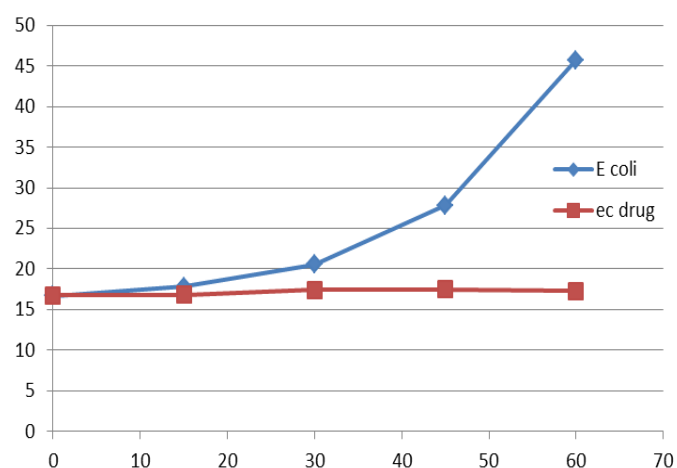
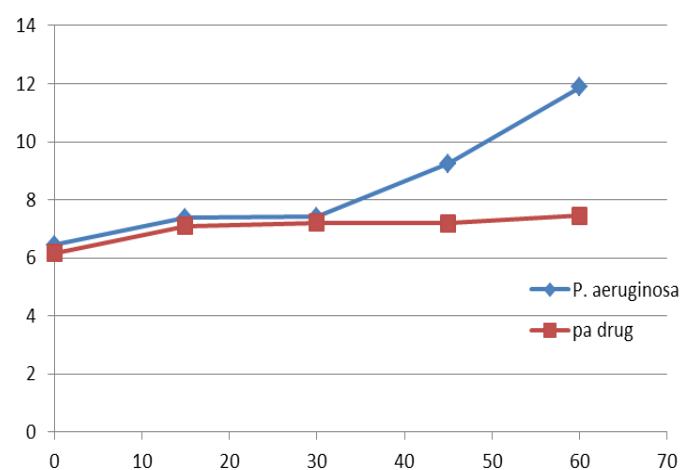


Figure 2.5. Examples of rapid susceptibility testing of clinically relevant species in SLIC. Each sample was inoculated into 1mL of pre-warmed media at  $3 \times 10^2$  cells/mL and incubated for the indicated length of time at which point they were sacrificed and measured in SLIC.  $n=3$ . Error bars are two standard deviations from the mean.

Bacterium	Time to significant result – [mins]	Generation time [mins]
<i>C. koseri</i>	45	22-37
<i>S. pneumoniae</i>	45	20-30
<i>E. coli</i> 35218	45	20-38
<i>E. coli</i> 25922	45	20-38
<i>E. faecium</i>	60	48
<i>K. pneumoniae</i> 1706	75	40
<i>K. pneumoniae subsp. pneumoniae</i> 700603	75	40
<i>K. pneumoniae</i> 705	75	40
<i>P. mirabilis</i>	60	28
<i>E. faecalis</i>	45	26
<i>S. maltophilia</i>	60	63
<i>S. pyogenes</i>	45	25
<i>H. influenzae</i>	30	23
<i>P. aeruginosa</i>	45	38
<i>E. aerogenes</i>	60	30
<i>C. albicans</i>	90	77
MRSA 29213	60	28-40
MRSA 43300	60	28-40
<i>S. aureus</i>	45	27

Table 2.4. Time to positivity values along with accepted doubling times for each of the clinically relevant species tested. TTPs are based upon significant statistical differences that were calculated as in Table 2.3

As we had established a robust testing platform for multiple organisms we then tested this protocol against our organism of most interest. As we did not have access to MTB at this stage we tested against the closest surrogate organism we had access to, *M. bovis* BCG. As BCG has the same doubling time as MTB it is a good surrogate for these types of experiments. We found that we were able to differentiate between a growing and non-growing culture in less than two generations, a result which is in agreement with previous data shown above.

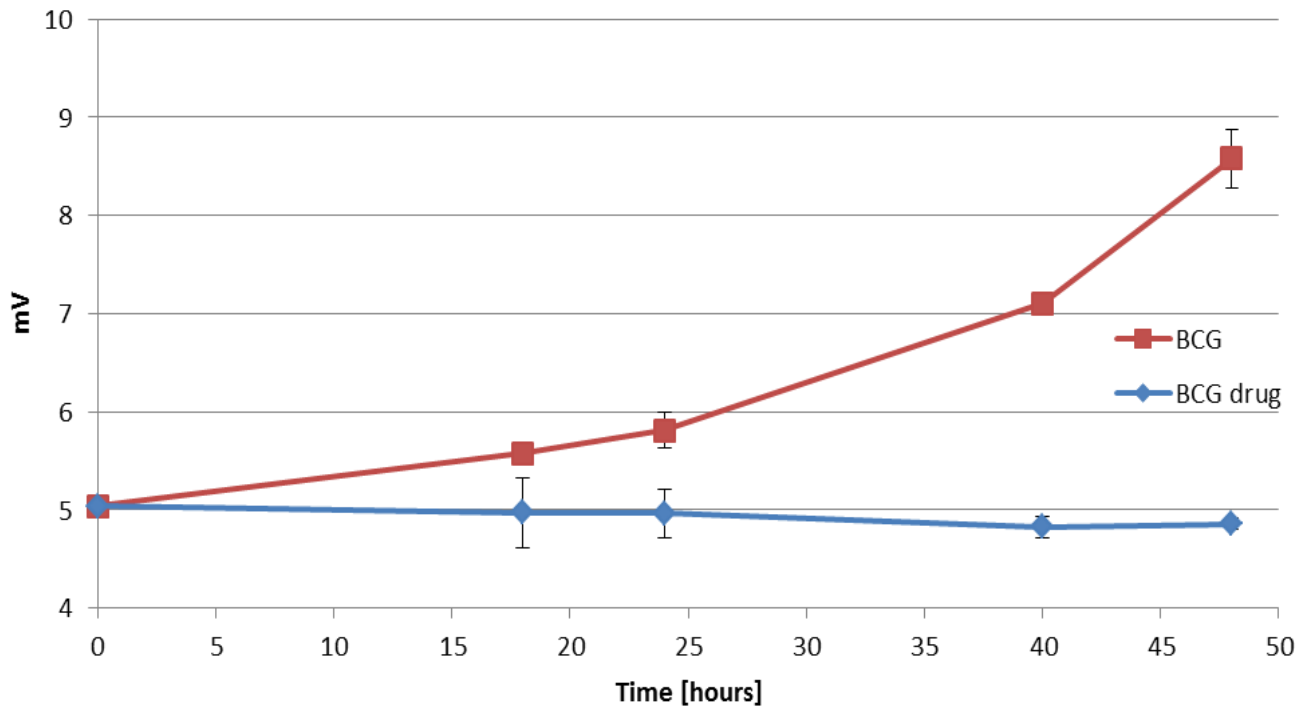


Figure 2.6. Rapid drug susceptibility data for BCG. Samples in this study were treated the same as those above in Figure 2.9. SLIC has been shown to detect statistically significant differences between a growing and non-growing culture in less than 2 generations.  $n=3$ . Error bars are two standard deviations from the mean.

#### 2.6.4 hSLIC

Thus far we had shown that SLIC was a useful and sensitive cell counter and that this capacity could be used to elucidate rapid bacterial susceptibilities of individual or combined drugs and rapid times to positivity for all species of microorganism tested

A later iteration of the SLIC is a version that does not require samples to be removed and heated separately. We added a heating element to the SLIC with a feedback loop to a raspberry pi rig to negatively regulate the temperature and keep it at a constant 37°C. This allowed us to run a preliminary experiment shown in Figure 2.7. This figure illustrates that without any agitation or outside influence the SLIC, completely automatically, is able to read

the concentrations of growing bacteria within it in real time. This is a significant step forward meaning that we are able now to grow bacteria completely aseptically without having to interfere with the SLIC at all. The SLIC will generate automatic growth curves and susceptibility data without the necessity of the operator changing reagents or being involved in any way except to receive the results at the end of the experiment.

The hSLIC has been used to incubate a sample of *E.coli* taken from glycerol stock culture at -80°C and added to cold media. This gives a long lag phase which can be seen in Figure 2.7. Figure 2.7 displays the first instance of the SLIC technology being used to create data automatically without any operator input beyond adding the sample and turning the system on. This is an important breakthrough as it paves the way for automatic SLIC system development in the future.

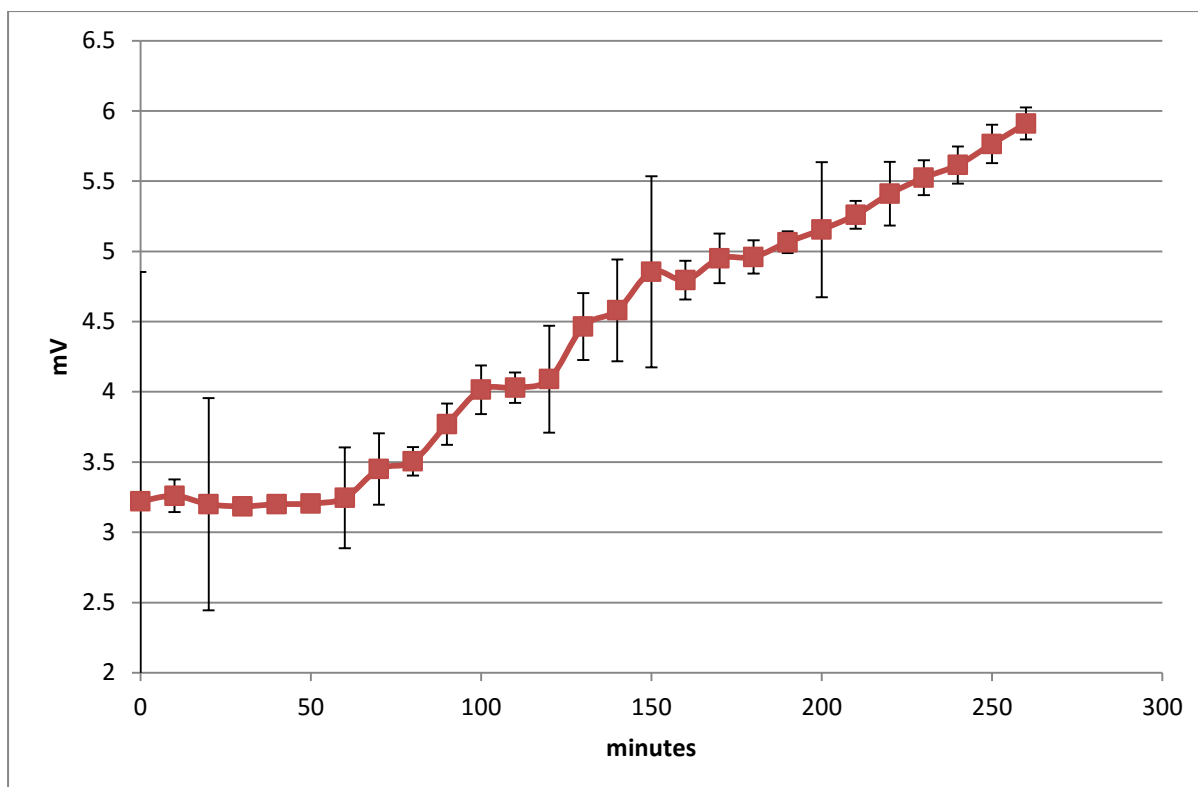


Figure 2.7. hSLIC preliminary data. *E. coli* taken from glycerol stock at  $-80^{\circ}\text{C}$  and incubated into cold media at  $4^{\circ}\text{C}$  showing a long lag period of 60 minutes but thereafter obvious exponential phase growth. Data logged automatically. Data shown are 10 minute median points. Raw data was collected every 120 seconds.  $n=10$ . Error bars indicate 2 standard deviations from the median.

## 2.6.5 Detecting presence of lipid rich cells (SLIC fluorescence- FLIC)

After having shown that SLIC is capable of all the tasks above we decided to take the work a step further and create a SLIC version that could detect small traces of fluorescent light- the FLIC.

The main purpose for the development of the FLIC was aimed at our own work with mycobacteria (see page 133). We theorise that the emergence of lipid bodies in mycobacterial cells is an indicator of dormancy. Lipid bodies are small when compared to the volume of the whole cell but can be made to fluoresce vividly green/yellow with the



stain Nile red. The new fluorescence sphere was built to attain the high sensitivity achieved with the SLIC and it seems to have accomplished this. Figure 2.8 displays the data from an experiment on a one month old culture assumed to contain lipid rich cells.

Figure 2.9 shows the fluorescence micrograph of the same sample clearly showing both red and green fluorescence, fluorescence which has been detected in the new rig.

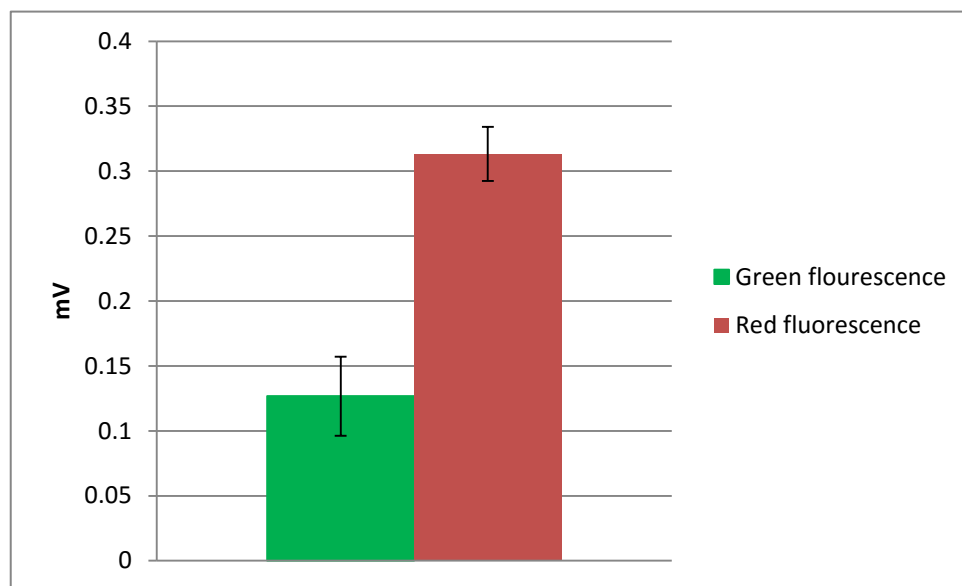


Figure 2.8. Preliminary FLIC data. Samples of *M. smegmatis* were stained with Nile red and spotted onto a glass slide. A clean glass slide was measured first and its fluorescence value was subtracted from the sample value to give the above results.  $n=3$ . Error bars indicate standard error from the mean. Green:red ratio = 2:5

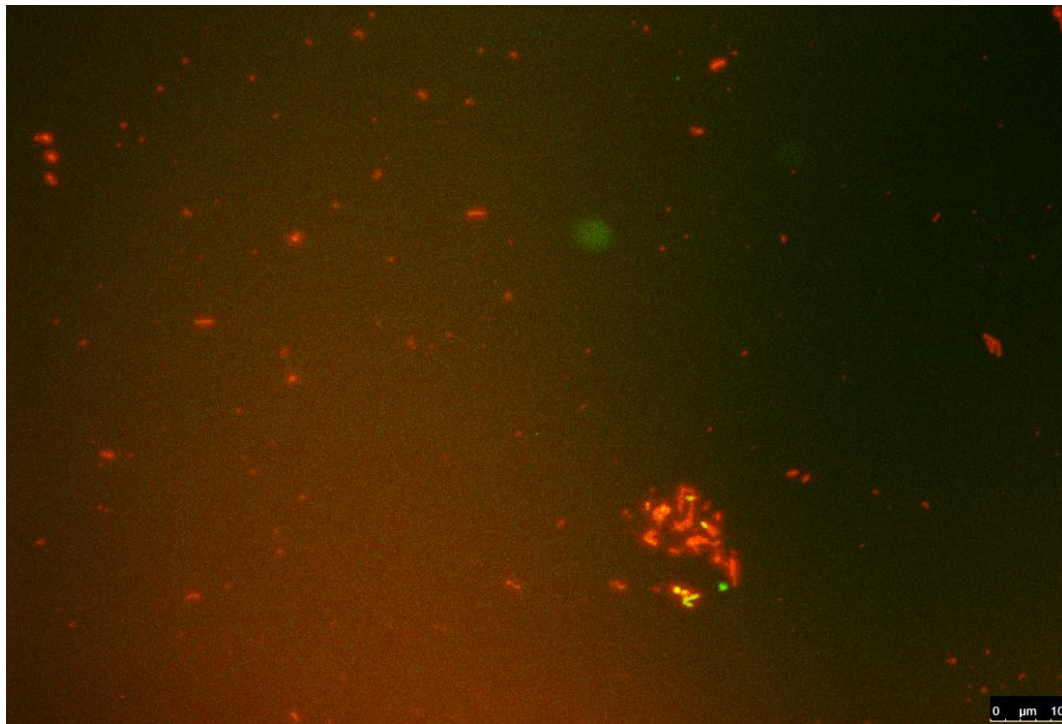


Figure 2.9. Fluorescence microscopy of sample in displayed in Figure 2.8 treated identically but visualised under a Lieca DM550 automated light microscope. Filters used; L5; Blue, excitation range 480/40 nm, emission 527/30 nm. TX2; Green, excitation range 560/40 nm, emission 645/75 nm. Imaged merged in the microscope's native software; LAS AF.

With this data we have shown that the SLIC technology is applicable across a range of light collecting disciplines. We are able to detect a relatively small number of bacteria fluorescing at a specific wavelength amongst a relatively huge number of bacteria fluorescing at another, entirely discrete, wavelength. The magnitude of this development is important to appreciate as it opens the possibility, not only of SLIC and its derivatives to become commercial successes, but for an entirely new form of light detection technology to emerge.

## 2.7 Discussion

### 2.7.1 SLIC calibration with biological material

Once we had established that SLIC was not able to differentiate between cell morphologies we attempted to use SLIC to differentiate between cultures with different *numbers* of bacterial cells. We first loaded blank buffer into the SLIC followed by a sample containing bacteria. The SLIC was able to detect the difference between them. We began to reduce the concentrations of bacteria present until the SLIC could no longer differentiate between the blank and the diluted sample. At this bacterial concentration we realised we had reached the SLIC's limit of detection. As the limit of detection appeared to be at a very small number of bacterial cells in suspension we realised that the SLIC had the potential to be a highly useful cell counting device.

The differences shown in Figure 2.2 between *M. smegmatis* and *M. fortuitum* are not due to a difference in cell number; by CFU counting these cultures had the same number of cells per millilitre. The difference in the signal is likely due to the difference in the cellular morphology. This difference is not, currently, reproducible enough to allow robust differentiation between species but this is an aim of the future development of the SLIC.

### 2.7.2 Concentration dependant scattering test

Once it was established that the SLIC could discriminate very tiny changes in bacterial number we began to test the limits of its capabilities. The data shown in Figure 2.3 illustrates the sensitivity of the SLIC. All of these mycobacterial cultures were grown to approximately  $1 \times 10^7$  CFU/mL. The data displayed shows that the SLIC's limit of detection is

approximately 10 cells per millilitre. For a photonic system this is an unprecedented level of sensitivity.

We believe we have an understanding of how the device reaches this degree of sensitivity even with the vast majority of the laser light leaving the sphere via the exit port (see Figure 2.10).

SLIC compares favourably with other rapid cell quantification technologies. As seen in Figure 2.16 of the newer technologies available on the market, SLIC is approximately 20 times faster than the fastest machines to detection of cellular growth (TTP). In the case of older technologies such as spectrophotometry, the sensitivity of SLIC is 100-1000 times greater for solutions of low particle density allowing for more accurate quantification of cultures containing few bacterial cells.

When comparing SLIC against less rapid technologies such as qPCR, SLIC has not been as rigorously tested, however it still compares favourably with regards to sensitivity. Where SLIC is less effective, when compared to qPCR, is the level of specificity acquired. SLIC cannot detect the difference between two species of bacteria if they are at the same concentration in CFU/mL. qPCR can do this, providing that the reaction has been set up correctly with the correct primers, etc. With regards to this last SLIC is once again an attractive platform for users as it requires no special reagents and only minimal training.

When considering the limit of detection of current bacterial quantification technologies SLIC is more accurate, sensitive and faster to TTP

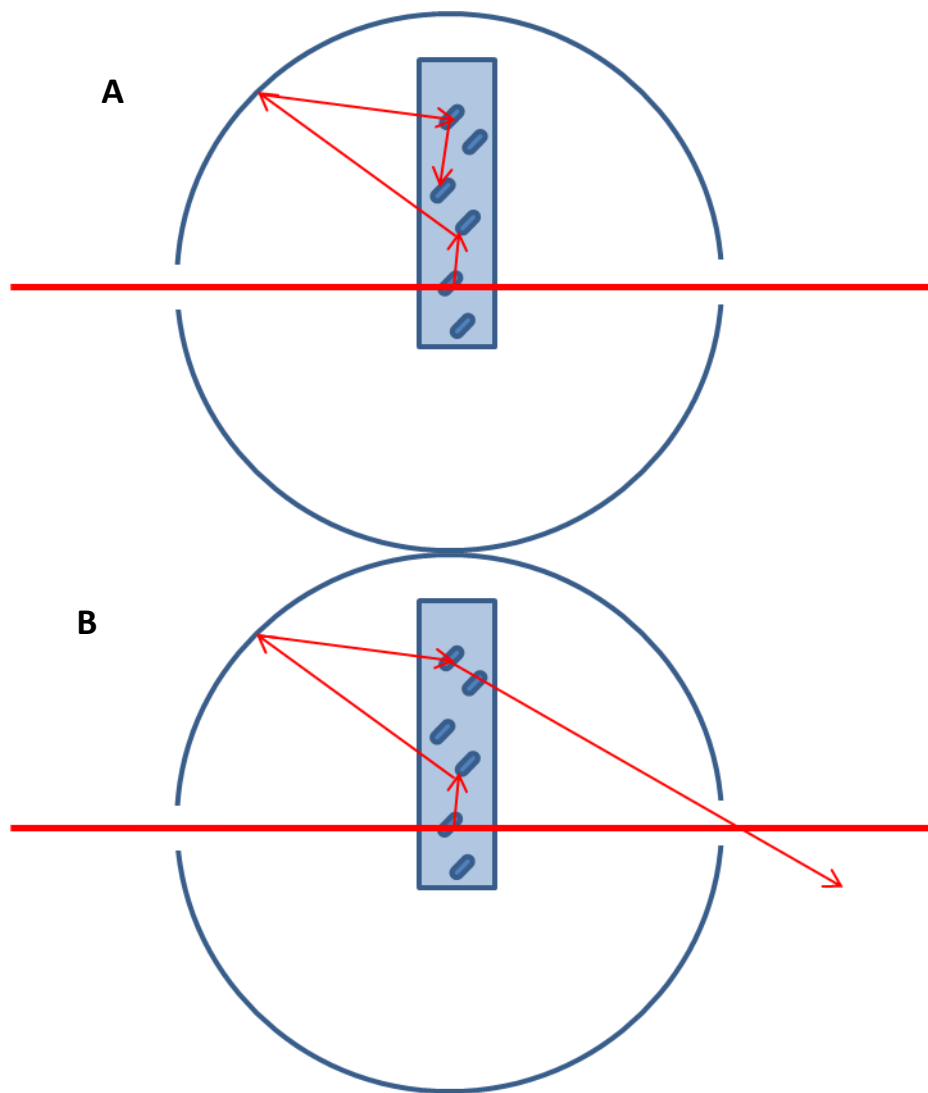


Figure 2.10. Schematic of two possible end results of scattered laser light in the SLIC. A displays one of two scenarios we believe are the cause of the SLIC's sensitivity. The laser beam line passes through a relatively small quantity of the sample. Typically we use samples of between  $700\mu\text{L}$  and  $1000\mu\text{L}$ . The beam volume over the width of the cuvette ( $10\text{mm}$ ) is  $30\text{mm}^3$ . This is 3% of the total volume of the sample if we use  $1000\mu\text{L}$  ( $1000\mu\text{L}=1000\text{mm}^3$ ).

Figure 2.10A and B show two scenarios that explain the sensitivity of the device. In A the laser beam line (thick red line) passes through the sample interacting with only one cell. However a photon from that interaction scatters and interacts with another cell which again scatters the light, this occurs until the photons energy diminishes to a point that it can be

absorbed. In the case of B the photons scatter and are re-scattered, absorbed or leave the sphere via the exit or entry port leaving a tell-tale signature scattering pattern (Figure 2.11).

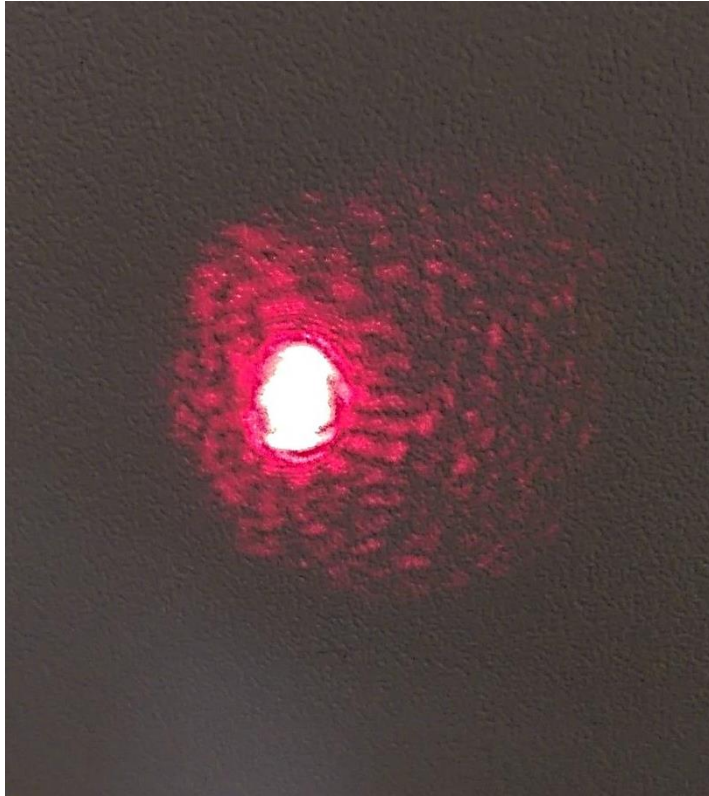


Figure 2.11. Typical scattering pattern emitted by a sample containing few bacteria. Bright central spot is the main focal point of the exiting laser beam.

The variances in the shapes of the curves in

Figure can be explained by the dissimilar scattering of the different bacterial morphologies.

As mentioned above these data are not robust enough to clearly determine the phenotype or species based only on our scattering data but we are working towards that goal. The different morphologies appear to allow better or worse degrees of sensitivity but always within an order of magnitude of the 'true' number of cells as defined by CFU. This is true even of smaller particles such as *Mycoplasma spp.* which are  $0.1\mu\text{m}$  in diameter cocci bacteria. Indeed these smallest of free living cells actually give a more linear result than

some larger cells as the small particles scatter more sideways (lower K vectors) than particles larger than the wavelength of the light (635 nm laser).

These data led us to the use of SLIC to discriminate between cellular populations that were changing very little or very slowly; such as MTB.

## **2.7.3 Rapid susceptibility test**

### **2.7.3.1 Rapid growers**

Before testing the SLIC with mycobacteria in general and slow growing mycobacteria in particular we tested the SLIC's ability to conduct a clinical laboratory standard test- a susceptibility test. This was done with three clinically significant bacteria; *E. coli*, *S. marcescens* and *S. epidermidis*. We found that when one culture was dosed with a drug (ciprofloxacin) concentration high enough to inhibit growth and the other identical culture was allowed to grow freely over the course of one hour there was significant statistical difference between the growing and non-growing culture in approximately 30 minutes. This is less than 2 generations for all species tested. We went on to test the SLIC in this same way with 23 clinical isolates of 18 different species found in a local hospital. In two generations or less we were able to detect the difference between a growing and non-growing culture for all species tested. All inoculum sizes were less than the detectable limit on a Shimadzu UV-1601 and by CFU counting were all between 300-700 cells/mL. This data represents a huge step forward for susceptibility testing in hospitals and clinical settings the world over. The degree of accuracy we are obtaining from limited sample sizes in a short period of time is what is needed in microbiology testing facilities. Indeed we have shown that SLIC is faster and more accurate than the current commercial competition (see Figure 2.16).

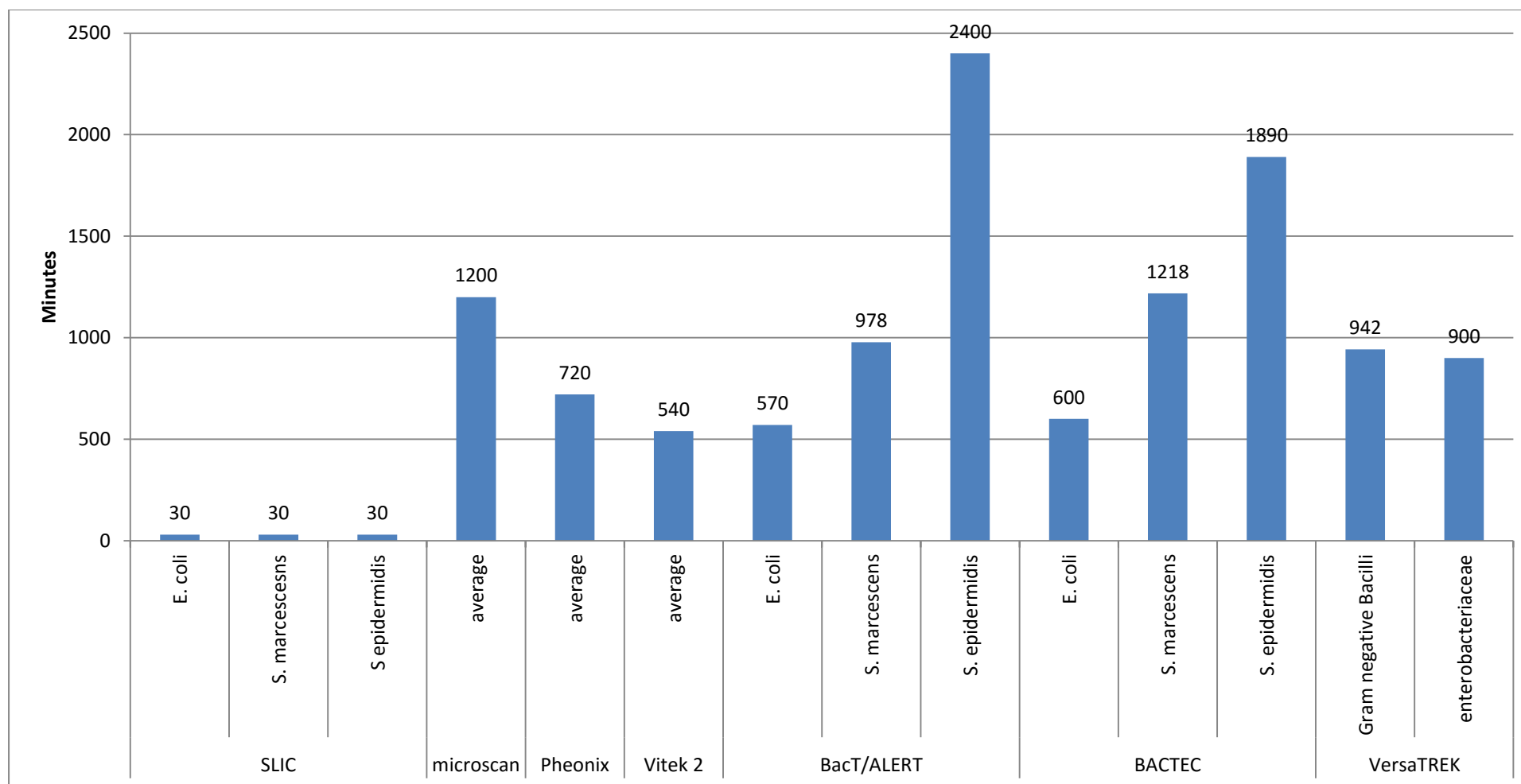


Figure 2.12. Comparison of SLIC to other commercial products currently on the market for establishing bacterial number and their relative time to positivity (TTP) times in minutes for three rapidly dividing bacteria. TTP in this context is defined as the first time point at which a statistically significant difference can be found between an exponentially growing and a non-growing culture.



### **2.7.3.2 *Mycobacteria***

Once we had established the protocol for rapidly growing bacteria we turned to our main focus; mycobacteria, and attempted to discern growing from non-growing at a similarly early stage- approximately two generations growth time.

As

Figure and Figure 2.10 show we were able to discern a statistically significant difference for BCG over the time frame of 2 generations (48 hours). This is an important result as it shows that for slow growing mycobacteria (of which MTB is one) can be detected in our system in significantly less time than is currently possible with growth methodologies. PCR and other nucleic acid protocols are faster than 48 hours and can give the genes associated with particular antibiotic susceptibilities but this method allows the bacteria to grow and be tracked in real-time. This means that changes can be made to the growing bacterial population and more data can be gleaned from the cultures as they grow. It also means that it is possible to check for contamination in real time, a major problem with slow growing organisms.

### **2.7.4 Rapid MIC/MBC testing of LR vs. LP**

Susceptibility testing is useful in a clinical setting but a common task in a research laboratory is to discover the MIC or MBC of an organism. SLIC can accomplish this as well. In Chapter 4 (page 133) we show that there is a significant difference in the MBC between lipid rich and lipid poor mycobacterial cells for a range of drugs. Some of this work was accomplished with SLIC.

Figure 2.4 displays the raw data used to inform our more in-depth MBC studies carried out as part of chapter 4. It can be clearly seen that in all cases there is a significant drop in the mV signal, this is proportional to the number of bacteria present. This drop in signal indicates that there are no more living bacteria present in this sample and that the MBC has been reached somewhere between the concentration at which the signal diminishes to 0 and the previous quantity of drug.

This methodology can be applied to any culture in which one wishes to discover the concentration of drug that will kill or inhibit the growth of all or a proportion of cells present.

### **2.7.5 hSLIC**

One exciting possibility of SLIC is that it will become a commercial entity and for this to become a reality more steps had to be taken. One of the first and most important required SLIC to operate automatically and independently. For this we created the heated SLIC (hSLIC), a self-contained, automatically sampling version of SLIC. the major advantage of this new version is that samples can be loaded into and left until a growth maximum is reached, at which point the SLIC powers down and stores the sample at room temperature until collection.

What Figure 2.7 demonstrates is a lag phase of approximately 1 hour. This is to be expected as the bacteria had just been removed from the -80°C freezer in glycerol stock and added to cold media at 4°C. Even so the SLIC was able to detect growth after only a short lag phase and then exponential growth with the expected trend with little to no aberrations from the norm.

With the data from the hSLIC we have taken the first step towards making SLIC a viable commercial entity.

### **2.7.6 FLIC**

Another version of the SLIC is a fluorimeter built primarily to discriminate between NR stained cultures of mycobacteria. The theory is the same as the SLIC; a rapidly oscillating signal that the lock-in can lock in to, in this case an LED. This LED illuminates a sample of bacteria that has been stained with a fluorescent stain. The LED is at a wavelength that will cause the stain to fluoresce. This fluorescence is detected by a photodiode also linked to the lock-in amplifier that has a peak absorption at around the expected emission wavelength from the stain on the cells. This photodiode is also shielded with a coloured plastic shield that stops all but the desired wavelength of emitted light to reach it. This process is repeated with another LED and photodiode array completing the fluorescence capturing hardware. The data captured by the FLIC compares favourably with data from the flow cytometer for the same sample.

Much of the work undertaken in clinical and research laboratories is based on the collection of light as a signal of positivity. With SLIC technology in place it might be possible to lower the thresholds required for the number of photons released by a reaction in order to signal positive. This would lead to more sensitive testing possibilities with shorter waiting and lead times meaning more work could be done more quickly but research and hospital/clinic staff.

The SLIC and FLIC are essentially highly sensitive and sensitive light harvesting devices that allow any process that is concerned with capturing light increase its sensitivity by at least an order of magnitude as a consequence of the unique way in which they work.

Our laser scattering technology can detect bacterial cells at lower quantities than was previously possible with photonic technologies.

# 3 Separation

## 3.1 Introduction to separation methodologies

There are several techniques to separate both eukaryotic and prokaryotic cells. These methods can be divided into three categories; techniques that rely upon (1) adherence, (2) density and (3) antibody binding. Microfluidics are also making an impact on cell separation techniques relying upon such cell characteristics as cell elasticity and response to ultrasonic waves and membrane polarisation in a non-uniform electric field. These microfluidic techniques are mostly still nascent in design and therefore will not be discussed further. Here I will summarise the three main current technique families for cell separation;

## 3.2 Adherence

Adherence based methodologies are used mainly for the separation of living eukaryotic cells from dead and non-viable eukaryotic cell debris left after, for example, mammalian organ homogenisation. An example of this method is the isolation of dental pulp stromal cells from whole digested dental pulp. In this technique, enzymatically digested dental pulp is filtered and plated directly onto tissue culture plastic, and following a period of culture, the adherent stromal cells are passaged (Gronthos, Mankani et al. 2000). These techniques involve the washing of homogenised tissue and cell slurry with some form of growth medium directly over the interior of a plastic culture vessel. After a period of time has elapsed (>24 hours) some of the live viable eukaryotic cells in the original culture will have adhered to the culture plastic and can then be passaged and split for further study.

This example specifically and these techniques in general benefit from being very simple and cheap but are not specific unless the culture plastic is treated in some way and even then the degree of specificity possible is still not great. Another drawback is the techniques

reliance on the cells under investigation adhering and rapidly proliferating to outcompete other cell types that might attempt to adhere and grow themselves. The time taken for the initial adherence to take place is also an issue leading to some confusion over the efficiency of the separation. More recent adherence based methodologies are overcoming some of these hurdles with specific cell binding to specialised polymer surfaces and polymer bushes of various lengths grafted to glass plates. These techniques are currently still being refined. Even with these advancements adherence methodologies are still more suitable for separations in which purity is not paramount and isolation of various sub-populations is not required.

Separation of macrophages as subpopulation of leukocytes from whole human blood occurs commonly in research laboratories. It is relevant to this work tangentially as MTB can survive within macrophages *in vivo* but we will not be undertaking cell culture work as part of this study. It is, however, an excellent practical example of density based separation. Human macrophages have a native density of approximately  $1.065 \text{ g/cm}^3$ . Making a Percoll or Ficoll separation gradient to separate them is relatively trivial. Once this has been achieved pre-prepared magnetic beads can be added to the macrophages and these internalised by the cells. The macrophages are then run through a LS column and are ready for culturing.

### **3.3 Density**

Density-based techniques rely upon the inherent variances in buoyant density of different cells types, families and subpopulations. Most density-based techniques are now predicated on the use of a centrifuge but historically 1g bench top sedimentation-based methods have been employed to, for example, separate erythrocytes from whole blood based on their size and shape (Miller and Phillips 1969).

Techniques based on centrifugation are used in many laboratories. The ability to sort large numbers of cells based on their density, relative to a graduated separation medium (usually a sucrose solution), makes these techniques particularly applicable for separations involving the use of blood, which contains very high concentrations of cells (approximately  $10^9$  cells/mL).

Despite the large-scale use of density-based methods, there are still problems with specificity as the differing densities of different cell populations are, in some instances, not large enough to be able to separate out individual cell types. These problems can be overcome by performing repeated centrifugations using differing concentrations of centrifugation medium and differing angular velocities. By using these techniques it is possible to isolate different cell types from a complex mixture of bacterial and eukaryotic cells (Eisenberg, Fox et al. 1982, Hayakawa, Otoguro et al. 2000). Although technically possible these methodologies are still challenging to perform with high specificity and due to this centrifugation techniques are generally used if specificity is not absolutely necessary.

Rosetting is another eukaryotic density-based methodology used in laboratory separations (Carlson, Helmby et al. 1990) which works as a combination between antibody binding and density methods. In this method unwanted cells are labelled with antibodies that subsequently form complexes, creating immunorosettes that are much denser than the surrounding cells of interest. Following centrifugation these rosettes, containing the labelled unwanted cells, pellet leaving purified target cells. This technique can also be applied to prokaryotic culture with the addition of IgM or IgA antibodies which are a pentamer and a dimer, respectively. These antibodies can bind to and sequester unwanted cells and in the same way as rosetting, allowing centrifugation separation of the much less dense unbound cells (Viljanen, Nurmi et al. 1983).

Methods that sort cells by density can be employed when working with cultures that contain a large number of unwanted cells. This can be for the isolation of a heterogeneous mix of cells. For example Castro-Malaspina *et al* used velocity sedimentation separation to divide human bone marrow samples into populations of haematopoietic cells and stromal cells which allowed them to culture only the haematopoietic cells for further analysis and testing (Castro-Malaspina, Gay et al. 1980). It is also possible to use density separation methods for the isolation of a homogeneous subpopulation of bacterial cells which can then be used experimentally (Hammond, Baron et al. 2015), or as a pre-enrichment step prior to sorting by other methods.

### **3.4 Antibody binding**

Antibody-binding methods generally refer to the commonly used techniques of fluorescence-activated cell sorting (FACS) and magnetic-activated cell sorting (MACS). Both technologies utilise the same cellular properties for separation, namely, cell surface antigens against which antibodies are raised (Bonner, Hulett et al. 1972, Miltenyi, Muller et al. 1990). FACS separation relies on the conjugation of fluorescent labels to these antibodies, whereas MACS uses conjugation to iron oxide containing microbeads (Zborowski, Moore et al. 1996, Panchuk-Voloshina, Haugland et al. 1999). Following binding of conjugated antibodies, FACS separation is achieved by laser excitation of the bound fluorophores, with excitation above a threshold level signalling the corresponding cell to be separated. For example Schmidt *et al* used thiazole orange to differentiate between transfusion relevant bacteria in their study into blood borne nosocomial infections (Schmidt, Hourfar et al. 2006). In contrast MACS requires the cells to be placed in a magnetic field; unlabelled cells are eluted, and labelled cells are retained in the field until they are removed



from the magnet, giving the separated populations. An example of this technique is Adams *et al* using MACS to screen for specific bacterial surface markers in a continuous flow microfluidic apparatus (Adams, Kim et al. 2008). MACS is as a high throughput but low sensitivity method, there is no individual cell analysis, magnetically tagged cells are retained and non-tagged cells are eluted. FACS, however, analyses each individual cell which can be tagged with multiple antibodies. This is in contrast with MACS which is restricted to individual markers unless another process is undertaken to a secondary antibody. This individual cell analysis means that while FACS can be more specific, it is significantly slower than MACS. Sorting that takes several hours by FACS can be achieved in less than 1 hour by MACS.

Antibody binding can be adapted to other separation techniques: for example, antibodies, immobilised to polymer surfaces, have been used in microfluidic systems to capture circulating human cancer tumour cells from homogenised tissue (Adams, Okagbare et al. 2008). Similarly columns have also been developed with antibody-immobilised surfaces to enrich specific cells based on antigen binding affinity such as Molloy *et al* who used this technique to reduce the concentration of pathogenic *Pseudomonas* species present in food and water samples (Molloy, Brydon et al. 1995).

Antibody-based methods of separation are currently the standard practise for the selection of individual cell populations, and both FACS and MACS can be used to isolate cell populations to high purity. FACS and MACS rely on cell surface markers which limits their applications. If no antibody is available commercially or no antibody can be successfully raised to the antigen in question then these techniques cannot be used.

Another feature of flow cytometry generally, as opposed to FACS and MACS specifically, is the generation of side scatter data. Side scatter is an intrinsic property of cells in a flow

cytometer beamline and indicates the degree of granularity, or deviation from transparency, the cell exhibits. Granularity data was gathered for all samples processed in the flow cytometer. One of the effects of lipid body accumulation is an increase in side scatter. This is due to an increase in apparent granularity (Grossman, Verbsky et al. 2004) as they are large internal vesicles that increase the relative granularity. This was an important discovery that we used to confirm some of our other results regarding the presence of lipid bodies in culture and in the flow cytometer specifically.

### **3.5 Filtering**

Filtering is the oldest and one of the most commonly used methods of separating fluid from suspended particulates. It is also an essential element of many of the techniques discussed above (Gronthos, Mankani et al. 2000). When used correctly filtering can be very useful allowing the separation of large particles from smaller ones (Mach and Di Carlo 2010). It can also be used as the first in many enrichment steps in a separation methodology such as adherence assays. Another example is the work of Liu *et al*; the separation of cell types within murine livers, Kupffer cells from hepatic stellate cells, for example (Liu, Hou et al. 2011). Filtering can be compromised when the filter becomes clogged with organic debris. The filter substrate can also become damaged and allow the passage of particles larger than those prescribed. Finally, pressures dangerous to the integrity of the cells under investigation can build up (especially if the filter is clogged) and lyse the target cells. This was found to be an issue during the work of Zheng *et al* while trying to microfilter and selectively capture human tumour cells (Zheng, Lin et al. 2007). While filtering may appear simple and possibly old fashioned it is still the focus of research and new innovations are made with some regularity (Isabel, Boissinot et al. 2012).

### **3.6 Differential centrifugation**

Differential centrifugation is used primarily in microbiology to separate out cell fragments from whole cells (Weiss, Coolbaugh et al. 1975, Lodish, Berk et al. 2000) and to remove cells from a homogenised tissue sample (Eisenberg, Fox et al. 1982). It can also be used to separate saprophytic bacteria from their immediate environment (Hayakawa, Otoguro et al. 2000) or to separate bacteria based upon their specific buoyant densities (Zwilling,

Campolito et al. 1982). The process often involves many rounds of centrifugation with the particle mass decreasing with every round as cells and debris are removed.

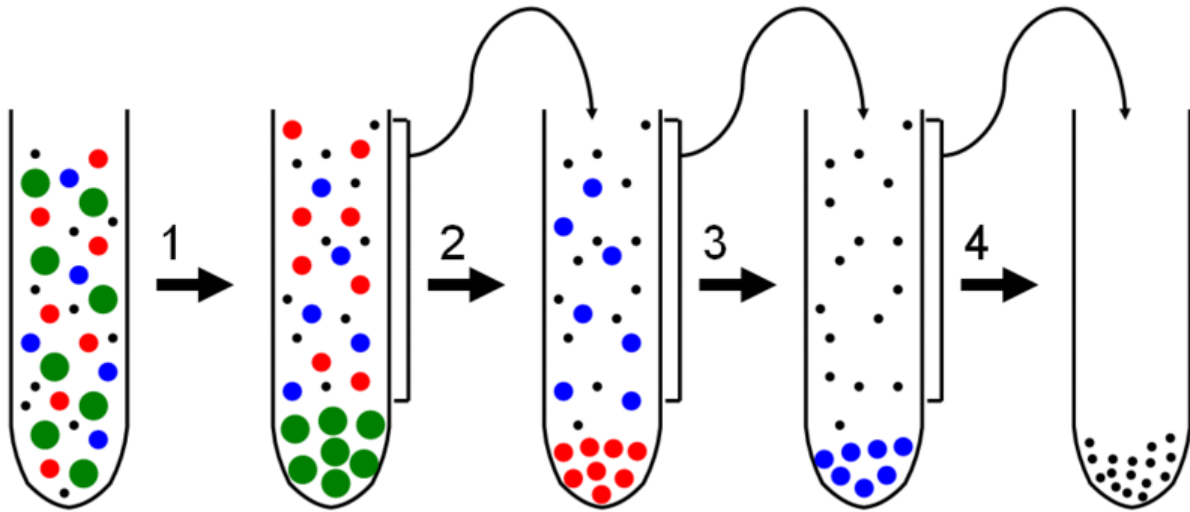


Figure 3.1. Schematic depicting differential centrifugation in action, sequentially removing larger particles with every round of centrifugation.

The separation of particles is based on their size and density with larger particles pelleting at the bottom of the tube more easily under less centrifugal force. The use of high g-forces makes the sedimentation of particles much faster and more efficient than if simple Brownian diffusion were to be used. Stokes law is used to determine the g-force applied to the sample with reference to the distance from the moment of inertia

$$D = \sqrt{\frac{18\eta \ln(R_f/R_i)}{(\rho_p - \rho_f)\omega^2 t}}$$

D is the particle diameter (cm)

$\eta$  is the fluid viscosity (poise)

$R_f$  is the final radius of rotation (cm)

$R_i$  is the initial radius of rotation (cm)

$\rho_p$  is particle density (g/mL)

$\rho_f$  is the fluid density (g/mL)

$\omega$  is the rotational velocity (radians/s)

$t$  is the time required to sediment from  $R_i$  to  $R_f$  (s)

### **3.7 Introduction to D<sub>2</sub>O separation (buoyancy dependant separation, BDS)**

#### **3.7.1 Isopycnic centrifugation**

Isopycnic centrifugation refers to a method wherein a density gradient is either pre-formed or forms during high speed centrifugation. After this gradient is formed particles move within the gradient to the position having a density matching their own.

Equilibrium sedimentation classically uses a gradient of a solution such as sucrose to separate particles based on their individual densities. It can be used as a purifying process for differential centrifugation. A methodology was developed that is based upon isopycnic centrifugation but without a centrifugation step. In the course of this work there has been a centrifugation step added to speed up the process.

To generate a density centrifugation gradient a solution is prepared with the densest portion of the gradient at the bottom. Particles to be separated are then added to the gradient and centrifuged at an appropriate speed (g) and time. Each particle proceeds (either up or down) until it reaches an environment of comparable density. Such a density gradient may be continuous or prepared in a stepped manner. For instance, when using sucrose to prepare density gradients, it is possible to carefully float a solution of 40% sucrose onto a layer of 45% sucrose and add further less dense layers above, the samples are then layered on top. After centrifugation it is possible to observe disks of cells at

different densities residing at the change in density from one layer to the next. By carefully adjusting the layer densities to match the cell type, one can enrich for specific cell types. For example it is common to separate erythrocytes from the 'buffy coat' (leucocytes and platelets) and the plasma in whole blood preparations.

Differences in buoyant density can be used to separate particles (HOLTER, OTTESEN et al. 1953, BALLENTINE and BURFORD 1960, Brakke and Daly 1965, Boogaerts, University Hospital (Hematology) Leuven et al. 1986), and the density-dependent cell sorting (DDCS) method has been applied to laboratory cultured bacteria (KURNICK, Department of Immunology et al. 1979).

Cells in different physiological states have been successfully separated using this approach (Makinoshima, Nishimura et al. 2002) because physiological changes alter cellular components and the subsequent buoyant density. The DDCS method has been applied mostly to pure cultures (Raposo 1996).

Natural bacterial communities are composed of physiologically and taxonomically different groups of cells, but it is not clear how these two factors affect the apparent buoyant density of each group.

### **3.7.2 Percoll ©**

Percoll is a matrix of colloidal silica particles approximately 15-30 nm in diameter. The silica particles have been coated in polyvinylpyrrolidone which makes them non-toxic to most cell types. Percoll has a low viscosity and a low osmolarity making it very good for biological

experimentation without interfering with the processes of the cells involved (Russmann, Jung et al. 1982, Vincent and Nadeau 1984, Berger, Marrs et al. 1985).

Experiments were conducted with Percoll (see section 3.7.2) and it was found that it was possible to separate cells due to their specific gravity, or density, however there were problems with the technique; primarily the extraction of the cells after they had been separated. To remove cells at layers below the meniscus the pipette tip has to be lowered through the upper layers. This forces Percoll up into the pipette tip and can carry with it cells other than the ones under investigation. Bubbling or holding air in the pipette tip under pressure did little to improve the yield and disrupted the layer under investigation.

### **3.7.3 D<sub>2</sub>O**

Deuterium oxide is a stable oxide of deuterium. Deuterium is a hydrogen atom with an extra neutron, giving it an atomic mass of 2 rather than hydrogen's usual 1. This accounts for the difference in the specific gravities of water and D<sub>2</sub>O. Pure D<sub>2</sub>O has a specific gravity of 1.11 g/cm<sup>3</sup>. Pure water has a specific gravity of 1.00 g/cm<sup>3</sup>. This means that a solution of D<sub>2</sub>O from 1% - 99% could have the range of specific gravities from 1.01 g/cm<sup>3</sup> - 1.10 g/cm<sup>3</sup>. Previous work has shown that the density of lipid rich mycobacterial cells lies within this range (Lipworth, Gillespie, unpublished).

A solution of D<sub>2</sub>O and pure water would not be subject to the difficulties of other liquid separation methodologies the chief of these being evaporation. A solution of sucrose and water will change its density if left uncovered overnight at room temperature due to the water evaporating off leaving comparatively more sucrose behind. Other problems inherent to liquid separation media are stability of the solute (present to increase density) and

toxicity to the operator. Stability is not a problem with D<sub>2</sub>O as it is not only chemically but atomically stable meaning no solute is going to precipitate out of suspension mid-experiment and change the density of the media. Percoll is a toxic substance that can cause serious injury if ingested (<http://www.bio-world.com/msds/41600001/Percoll-%E2%84%A2.html>), no such concern exists with D<sub>2</sub>O.

A problem specific to this work and to sucrose separation gradients is the presence of a carbon source. Mycobacteria are not fastidious and can utilise almost all simple carbohydrate carbon sources including sucrose (Tsukamura and Tsukamura 1965). The intention of the separation methodology was not only to separate the cells but also to keep them stressed so they do not resuscitate into lipid poor cells. A solution of D<sub>2</sub>O and water contains no carbon sources and keeps the cells under osmotic stress.

The final consideration that was taken into account was a practical one. Percoll and sucrose solutions are difficult to work with because of their components. Percoll is an oil-like substance that is viscous and liable to contaminate any substance into which it is placed. Sucrose solutions evaporate and leave a sticky residue on a benchtop. Neither of these scenarios are advantageous. In addition to this Percoll is classically used to create multi-layered systems, an aim of this work was to produce a system with a single layer of cells at the top and another at the bottom for ease of harvesting.

Because D<sub>2</sub>O is stable and fluid experiments were carried out to ascertain whether it would be possible to use D<sub>2</sub>O as a viable alternative to substances such as Percoll. These experiments proved successful. It was decided that a new technique based on D<sub>2</sub>O that would yield only two layers but would result in total separation of the cells under investigation should be developed. This technique would separate out the lipid rich cells



from the lipid poor cells with great efficiency, high purity and the resulting population of cells would be easily identifiable by simple staining methodologies.

## **3.8 Methods**

### **3.8.1 Buoyant density separation**

We have previously shown the density of lipid rich cells to be less than that of lipid poor cells- lipid rich cells have a specific gravity of approximately  $1.08 \text{ g/cm}^3$  whereas lipid poor cells have a specific gravity of approximately  $1.1 \text{ g/cm}^3$ . In order to create a separation medium with a specific gravity similar to the density of lipid rich cells we used a mixture of  $\text{D}_2\text{O}$  and pure  $\text{H}_2\text{O}$ . Given the above figures on the relative densities of pure  $\text{H}_2\text{O}$  ( $1.00 \text{ g/cm}^3$ ) and  $\text{D}_2\text{O}$  ( $1.11 \text{ g/cm}^3$ ) calculations were undertaken that demonstrated that a 3:1 solution of  $\text{D}_2\text{O} : \text{H}_2\text{O}$  gave a specific gravity of  $1.08325 \text{ g/cm}^3$ . This is slightly more dense than the lipid rich cells under investigation (see section 3.2). With a solution density of 3:1  $\text{D}_2\text{O} : \text{H}_2\text{O}$  a population of exclusively lipid rich cells gathered at the meniscus of the  $\text{D}_2\text{O}$  solution whereas all other cells sank to the bottom of the vessel used for the separation.

### **3.8.2 One g separation**

A 1mL aliquot of bacterial cells was harvested from middlebrook 7H9 culture (grown as previously described) and washed three times by centrifugation ( $20,000g$  for 3 minutes) with filter sterilised water ( $0.22\mu\text{m}$  filters, Millipore). Washed cells were re-suspended in  $200\mu\text{L}$  of filter sterilised  $\text{dH}_2\text{O}$  (Sigma Aldrich) which was then added to  $600\mu\text{L}$  of  $\text{D}_2\text{O}$  to give  $800\mu\text{L}$  of  $\text{D}_2\text{O}$  solution at 75%  $\text{D}_2\text{O} : 25\% \text{dH}_2\text{O}$ . This solution was then sealed and left to equilibrate for 24 hours without agitation. Figure 3.3 shows five standard cuvettes containing a separated mixture of lipid rich and lipid poor cells. For the purposes of this figure cuvettes were used to clearly show the different layers. In standard laboratory practise anti-static microcentrifuge tubes or microcentrifuge tubes that have been subjected to a de-static step are used. This is to prevent any electrostatic attraction of cells to the

inside walls of the tubes. Cells from the top layer (within 1mm of the meniscus) were removed by P200 pipette tips that had been laser cut to 8mm in length with an internal luminal bore of 5mm. 100µL of this layer was removed and stored in a sterile Microcentrifuge tube. The bottom layer (within 1mm of the bottom of the tube) was removed by a standard P200 pipette tip with bubbling through the D<sub>2</sub>O/H<sub>2</sub>O mixture until the correct depth was reached to prevent cells from other layers entering the pipette tip. 100µL was removed from this layer and stored in a sterile Microcentrifuge tube. When separations failed to achieve sufficient purity by fluorescent microscopic evaluation such samples were subjected to a further round of buoyant density separation.

### **3.8.3 Centrifuge (~200g) separation**

Cells for centrifugation were prepared as described in section 3.8.2. Two versions of the centrifugation technique were produced. These techniques were designed to elicit the same result but in different ways. The main difference between the techniques was the volume of liquid present. In a microcentrifuge tube the maximum safe volume of liquid to be used is 1200µL when centrifuging a sample. In a glass pipette it is possible to use up to 5mL of liquid. Both techniques are outlined below.

- 1) An anti-static microcentrifuge tube was prepared. A 1mL mixture of washed cells in a 3:1 D<sub>2</sub>O:H<sub>2</sub>O solution was aliquoted into the tube. The tube was sealed and centrifuged for 5 minutes at 252 g (1500 rpm in VWR microstar 17).

2) Standard short nosed glass pipette was heated in a Bunsen burner and the end of the pipette tip is gripped with forceps. When the glass of the pipette tip begins to soften the forceps are twisted and pulled to sever the end of the pipette tip and seal it in one movement. This sealed and shortened pipette is then used as the separation vessel. A 5mL solution of cells and 3:1 D<sub>2</sub>O:H<sub>2</sub>O was prepared as in section 3.8.2 and added to the sealed glass pipette. The pipette was then sealed with parafilm at the opening and placed into a 15mL falcon tube that has been padded with absorbent white tissue. More tissue is added around the pipette and above it before the cap of the falcon is sealed. The falcon tube complex was then placed into a centrifuge with appropriate rotor and spun at 200g for 5 minutes.

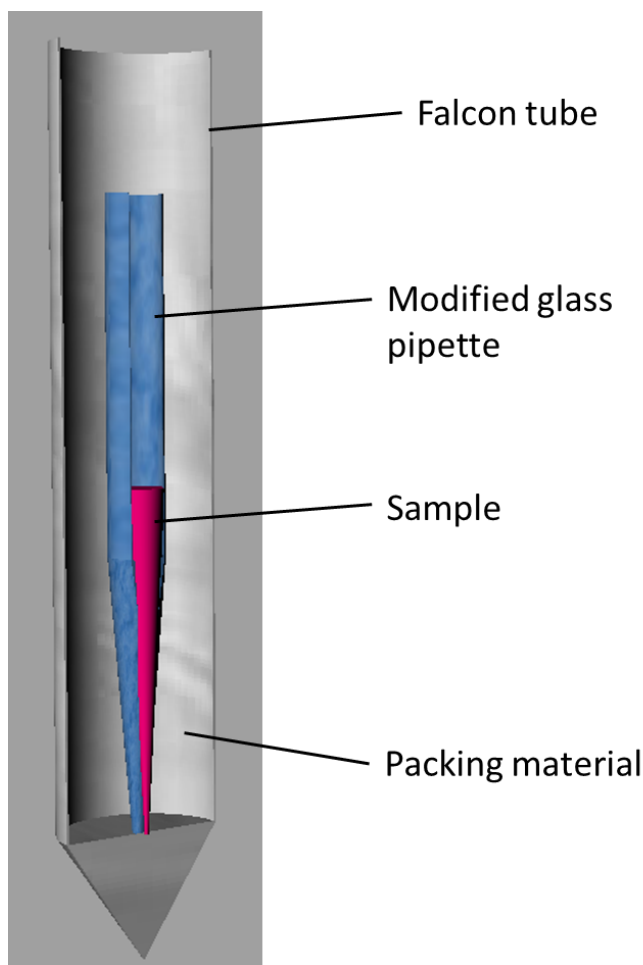


Figure 3.2 Schematic diagram of the assembly used to centrifuge D<sub>2</sub>O and bacterial samples for separation

### **3.8.4 Isolation and identification of different phenotypic states**

#### ***3.8.4.1 Lipid rich/Lipid poor analysis***

Bacteria were stained with Nile red and lipid bodies were identified by fluorescent microscopic analysis as in section 4.5.5.

#### ***3.8.4.2 Flow cytometry for purity analysis***

Fluorescent microscopic analysis was used when checking the presence or absence of lipid bodies in an experiment. If a global lipid body analysis was required then flow cytometry was used. The cells under investigation were stained with Nile red as in section 4.2 and then analysed by flow cytometry to glean an understanding of the global lipid body presence in a given sample. Samples that achieved  $\geq 90\%$  lipid rich cells (purity) after a single passage were identified and recorded. Samples that failed to achieve a  $\geq 90\%$  lipid rich cell purity were either discarded or subjected to a further BDS passage. Data shown in Figure 3.4.

#### ***3.8.4.3 Comparing efficiency to purity of the separation technique***

In flow cytometric analysis it was noted that the number of overall events (individual cells) was lower in lipid rich populations when compared to lipid poor populations for certain starting mixed cultures, namely young- mid exponential phase cultures. To demonstrate that the purity of the separation was still excellent despite the lower number of lipid rich cells the efficiency of the technique was quantified. Total even counts for each population were compared against lipid rich counts for each population (Figure 3.5A). These data were compared against each other to generate a percentage purity data set (Figure 3.5B).

### **3.8.5 Granularity data**

Samples of lipid rich cells and lipid poor cells were separated and left unstained. These samples were then analysed in the flow cytometer. Side scatter data was collected automatically as an adjunct to other data in the flow cytometer. Side scatter data was analysed to find a significant value over which the quantity of side scatter in lipid poor samples was consistently negligible. Increasing quantities of side scatter above the given threshold indicate higher levels of granularity in the samples. This data is displayed in Figure 3.7 and Figure 3.8.

### 3.9 Results

We had shown previously that lipid rich cells had a specific gravity of approximately  $1.08\text{g}/\text{cm}^3$ . We also found that lipid poor cells and cell debris had a higher density than  $1.08\text{g}/\text{cm}^3$  as they descended further in the Percoll. Pure water has a specific gravity of 1.00 whereas deuterium oxide ( $\text{D}_2\text{O}$ ) has a specific gravity of 1.11 exactly and is sold at 99.9% purity. Early experiments involving mixing pure  $\text{H}_2\text{O}$  and  $\text{D}_2\text{O}$  to create different density gradients were encouraging (data not shown).

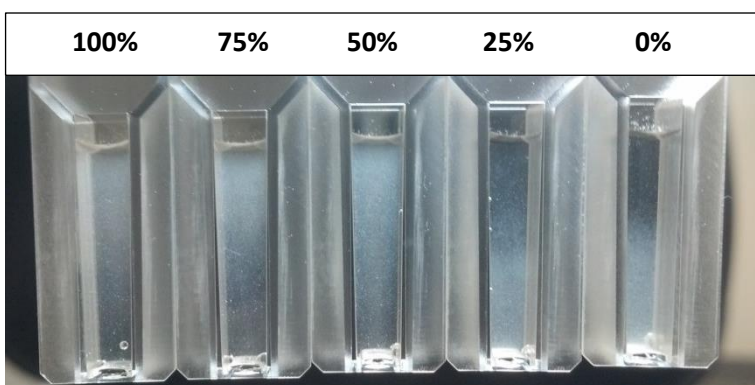


Figure 3.3. Less than 1 minute after inoculation with  $10^9$  cells/mL of *M. smegmatis* the difference in density is obvious, the samples are left for approximately 16 hours to equilibrate at 1g in a sterile plastic cuvette. Percentages refer to concentrations of  $\text{D}_2\text{O}$  present in cuvettes.

### 3.9.1 D<sub>2</sub>O

#### Isolation and identification of different phenotypic states

D<sub>2</sub>O separation method is highly successful; >90% purity of lipid rich cells is frequently attained. These data were collected over 20 individual experiments as peripheral data parallel to the main experiment (data shown in Figure 3.4). It was noted that the number of successful separations was excellent with >75% of the separations undertaken being successful. These data were collected by fluorescent microscopic analysis after staining with Nile red, the data is displayed in Figure 3.4.

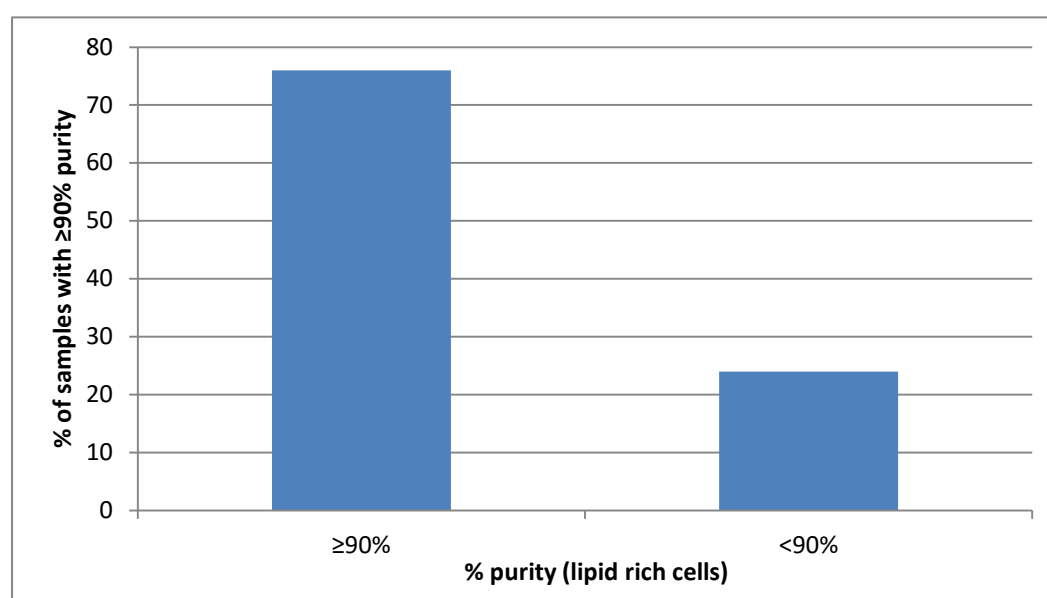


Figure 3.4. Percentage of samples extracted from top fraction of 75% D<sub>2</sub>O- 25% H<sub>2</sub>O solution that yield greater than or equal to 90% purity of lipid rich cells. Those samples that yield less than 90% could be resuspended to increase the yield.

Flow cytometry data was used to indicate the purity of samples extracted via a D<sub>2</sub>O separation. Removal of the top fraction of a 3:1 D<sub>2</sub>O:H<sub>2</sub>O solution yielded high proportions of lipid rich cells. The flow cytometry results showed that there was a high proportion of lipid rich cells in the fraction that had been designated 'lipid rich'- there was very high purity. But it also showed that the number of cells recovered from the lipid rich is low when



compared with the concentration of cells added to the separation. From a culture of  $\sim 1 \times 10^7$  CFU/mL we recover  $1 \times 10^3$  CFU/mL of cells. This was not true for the lipid poor fraction. Many more cells in total we extracted from the lipid poor fraction (approximately 10x as many). But the concentration of lipid rich cells present was very low. This means that the experiment was a success with each fraction yielding a high purity of the cell type expected to appear there.

Figure 3.5 displays two figures drawn from the same experiment. Figure 3.5A displays typical results from a separation of a culture containing an input concentration of approximately  $2 \times 10^7$  cells per millilitre. The lipid poor fraction contained considerably more cells than the lipid rich fraction. The red fluorescence represented the total number of cells and the green fluorescence represents the proportion of those cells that were lipid body positive. The lipid poor fraction contained, on average, approximately 1700 cells. Despite the considerably lower yield the lipid rich fraction is very pure, >90% purity. The LP fraction is also very pure containing very few lipid rich cells, <7%. This displays a fundamental problem with our separation technique. While the purity is excellent and the efficiency is good the yield is very poor. It is common to lose between 1000-10000 cells in a separation. A better extraction methodology would improve this and to that end we have developed wide-nosed pipette tips that will extract more efficiently from the top layer of the D<sub>2</sub>O solution.

### **3.9.2 Comparing efficiency to purity of the separation technique**

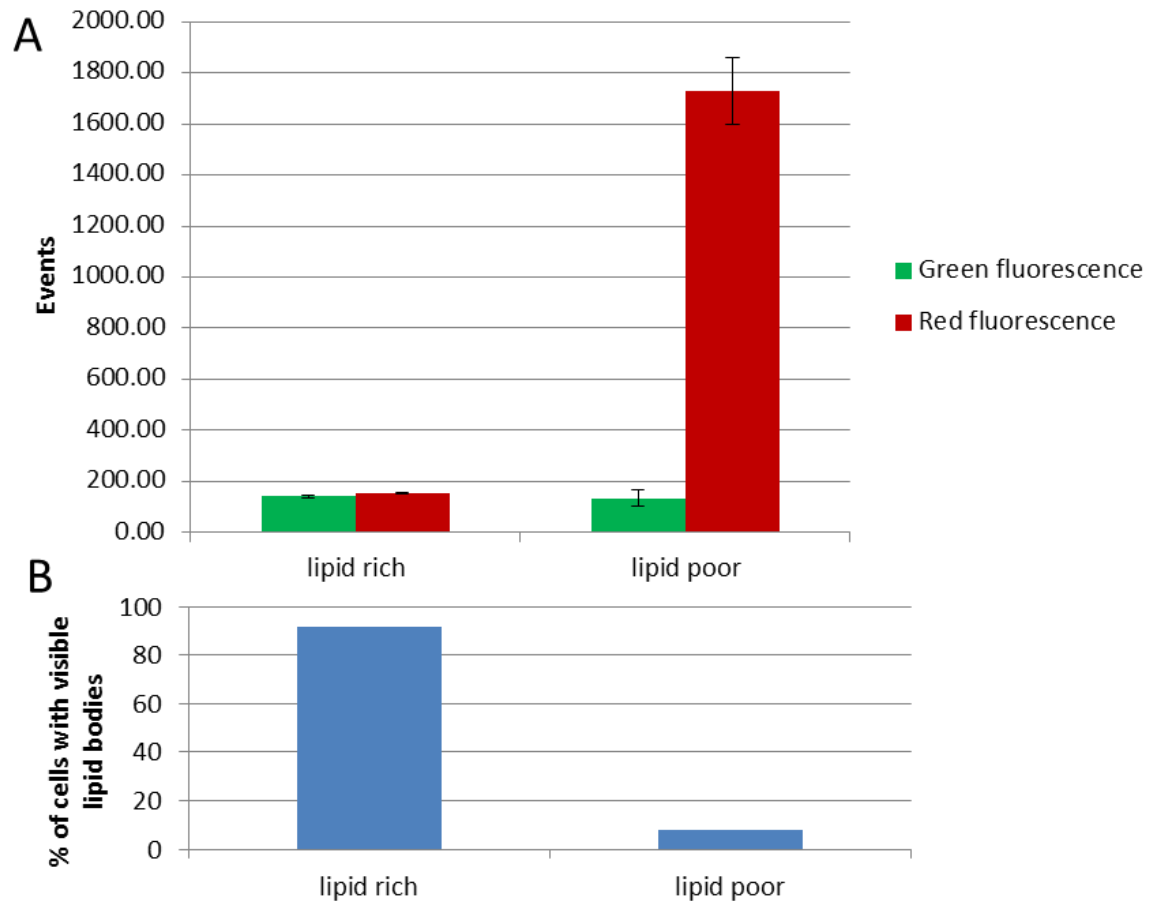


Figure 3.5. flow cytometry data depicting the differences between LR and LP extractions from the BDS methodology. A- Flow cytometry results for lipid rich and lipid poor cells separated by D<sub>2</sub>O buoyancy method stained with Nile red. Error bars= one standard error from the mean. p value green-red lipid rich 0.14 (2 s.f.), p value green-red lipid poor 0.00067 (2 s.f.). n= 3. Green fluorescence indicates the presence of lipid bodies, red fluorescence indicates the presence of cells. In the lipid rich fraction it can be seen that there are significantly fewer cells than in the lipid poor fraction but the proportion of those cells which are lipid rich is near 100% (B). In the lipid poor fraction we see a similar number of lipid rich cells as in the lipid rich fraction but the overall cell number is much higher. B- data from A showing the relative frequencies of lipid body occurrence as a percentage of total cells present

It is important to understand how the data displayed in Figure 3.5 is generated. There will always be a background of fluorescence whether from cellular auto-fluorescence or from impurities in the flow system. In order to generate reliable data the flow cytometer has mathematical operators that are used to properly define the areas of interest and to reduce the impact of the background. These operators are the capacity to 'gate' and apply 'gains' to the flow cytometry results. Figure 3.6 displays the raw data from the red and green detectors of the flow cytometer. These data display the differences between lipid rich and lipid poor samples analysed in this way. The lipid rich sample displays a large area of green fluorescence in the high intensity bands of the detectors sensitivity. The lipid poor fraction shows an obvious area of background in the lower right corner with a few events registering high red fluorescence and even fewer (~5) registering green fluorescence. These data show how pure the samples from the separation are; 5 events in 5000 represents a 0.1% error in the separation method.

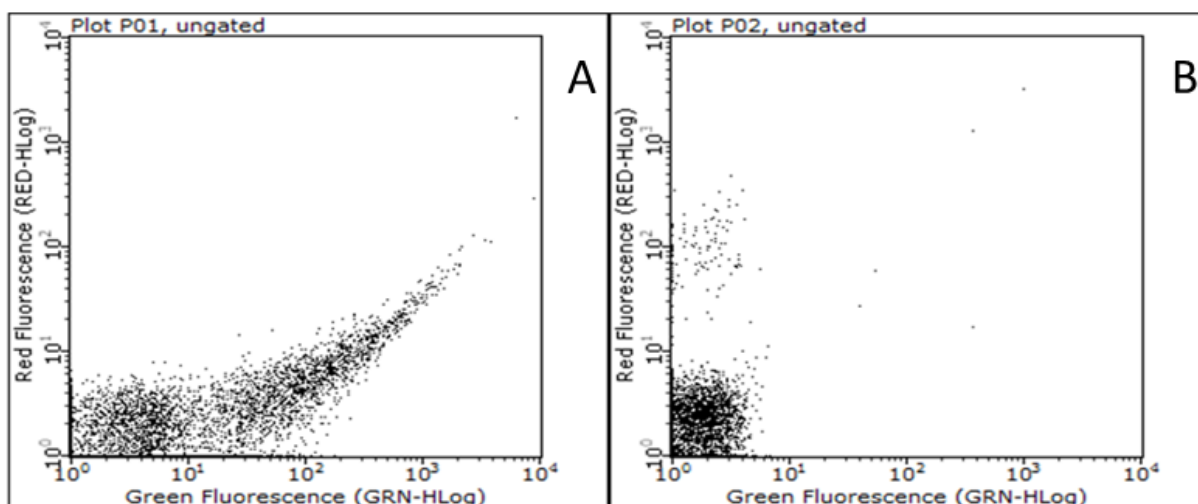


Figure 3.6. Representative raw flow cytometry dot plots. A and B- Raw flow cytometry dot plots demonstrating the difference between a lipid rich sample (A) and a lipid poor sample (B), the quantity and intensity of the green fluorescence indicating the presence of lipid bodies. These lipid bodies can be seen in Figure 4.2.

### 3.9.3 Confirmation – granularity results

When mycobacterial cells were separated by BDS methodology and left unstained they could be differentiated by side scatter alone (Figure 3.7 and Figure 3.8). The cells present in the lipid rich fraction of the 75% D<sub>2</sub>O samples are the most granular and therefore the most lipid rich. The cells immersed in the 100% D<sub>2</sub>O solution were not separated. Due to the high specific gravity of pure D<sub>2</sub>O (1.11 g/cm<sup>3</sup>) all the cells, lipid rich and lipid poor, and crucially, all the cell debris and any precipitated particles less dense than 1.11 g/cm<sup>3</sup> were floating on the surface of the 100% D<sub>2</sub>O solution. This cumulative effect is the reason for the apparent degree of side scatter present in the 100% D<sub>2</sub>O solution. It is also worth noting that the p value for the 75% versus the 100% D<sub>2</sub>O solutions is high indicating that there is no significant statistical difference between the two samples. This is not true of either the 100% or the 75% solutions versus the 50%, 25% or 0% solutions, these p values are low indicating statistical differences between these two cohorts.

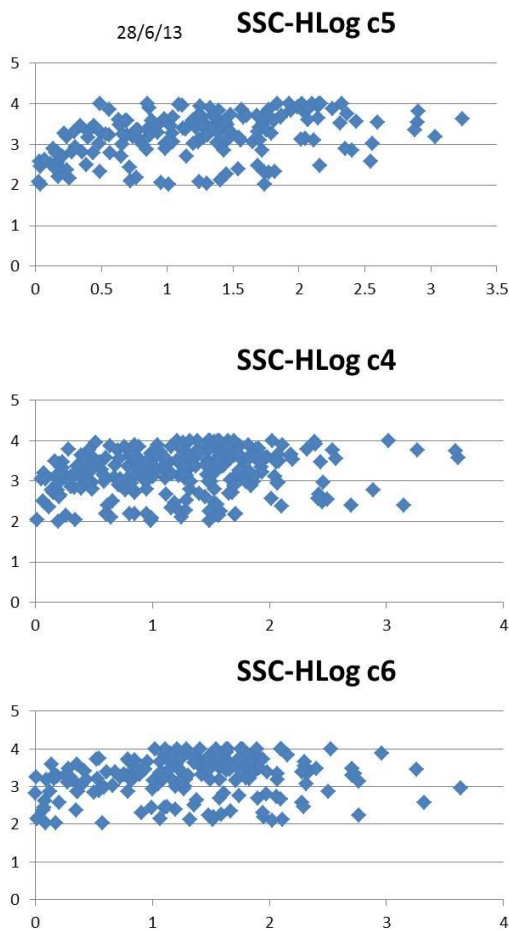
Side scatter was measured in every flow cytometry experiment and functioned as a quality checking step. We showed that in lipid rich cells the quantity of side scatter was considerably higher than in the lipid poor cells. This is due to the presence of lipid bodies that scatter the light differently due to both their general granularity but also because of their distance from the refractive indices of the rest of the bacterial cell matrix. With this quality checking step in place we could be confident that the cells we have separated are lipid rich and, moreover, we can begin to build a database of characteristics by which to judge lipid rich/poor separation efficiencies such as the degree of side scatter (Figure 3.6) and the intensity of red/green fluorescence.

After using Nile red extensively it was hypothesised that it might be possible to differentiate lipid rich from lipid poor cells using other means. To generate the required n numbers to make the study robust the use of a flow cytometer was again selected. Instead of using Nile red or any other staining regimen it was decided that using a natural feature of the cells themselves could be advantageous. Cells containing lipid bodies by their nature must scatter light at a different angle than cells without lipid bodies. We used this information to discriminate LR from LP using only the side scattering data collected by the flow cytometer on unstained samples. The results are displayed in Figure 3.7.

What Figure 3.7 shows is that above a threshold (set at 2 arbitrary units) the lipid rich samples scatter considerably more light sideways than the lipid poor samples. This is shown in Table 3.1. p values indicate that there are significant statistical differences between lipid rich and lipid poor samples *only* at the 100% and 75% concentrations of D<sub>2</sub>O. This means that there is no significant separation at 50%, 25% or 0%, by this metric.

Figure 3.8 displays the differences between side scattering of lipid rich and lipid poor samples over a range of D<sub>2</sub>O concentrations. Different concentrations of D<sub>2</sub>O were used, the levels of side scatter sharply decline after 75% D<sub>2</sub>O which is concordant with microscopic evaluations of the same samples (data not shown). The samples at 50%, 25% and 0% show an event number of approximately 50, this is 1% of the total number of events and represents the total error with using a non-staining based discriminatory methodology. While it would be expected the purist cultures of lipid rich cells in a 75% solution of D<sub>2</sub>O the results of the 100% solution are not surprising. In the 100% solution, theoretically, all the cells will float with only dense clumps of mycobacteria sinking. Because of this we were able to recover a higher yield of both lipid rich and lipid poor cells giving us a higher side scattering result. However it is important not to interpret this data as meaning that 100% D<sub>2</sub>O is the best solution for lipid rich cell retrieval. The 75% solution has a comparable degree of side scatter and therefore LR cell material but is much more pure as the density of the solution means all the LP cells will have sunk to the bottom of the vessel.

Lipid rich cells



lipid poor cells

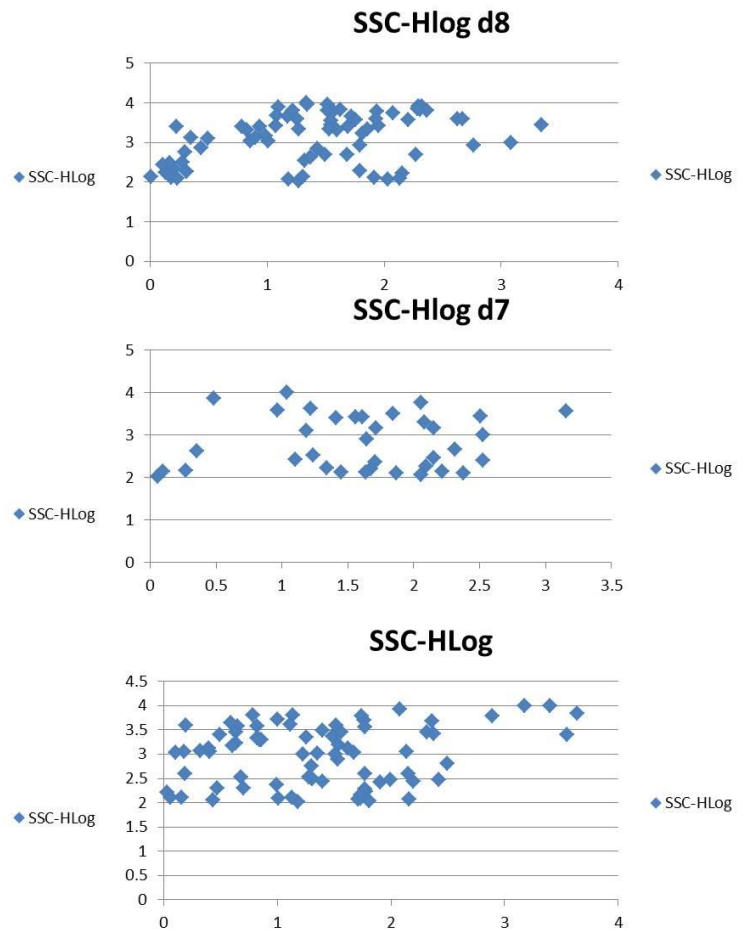


Figure 3.7. Raw flow cytometry side scatter data. Lipid rich samples show an increase in the quantity of side scatter detected above a given threshold (2 arbitrary units- y axis) indicating a higher degree of granularity within the cells. This corresponds to the formation of lipid bodies.

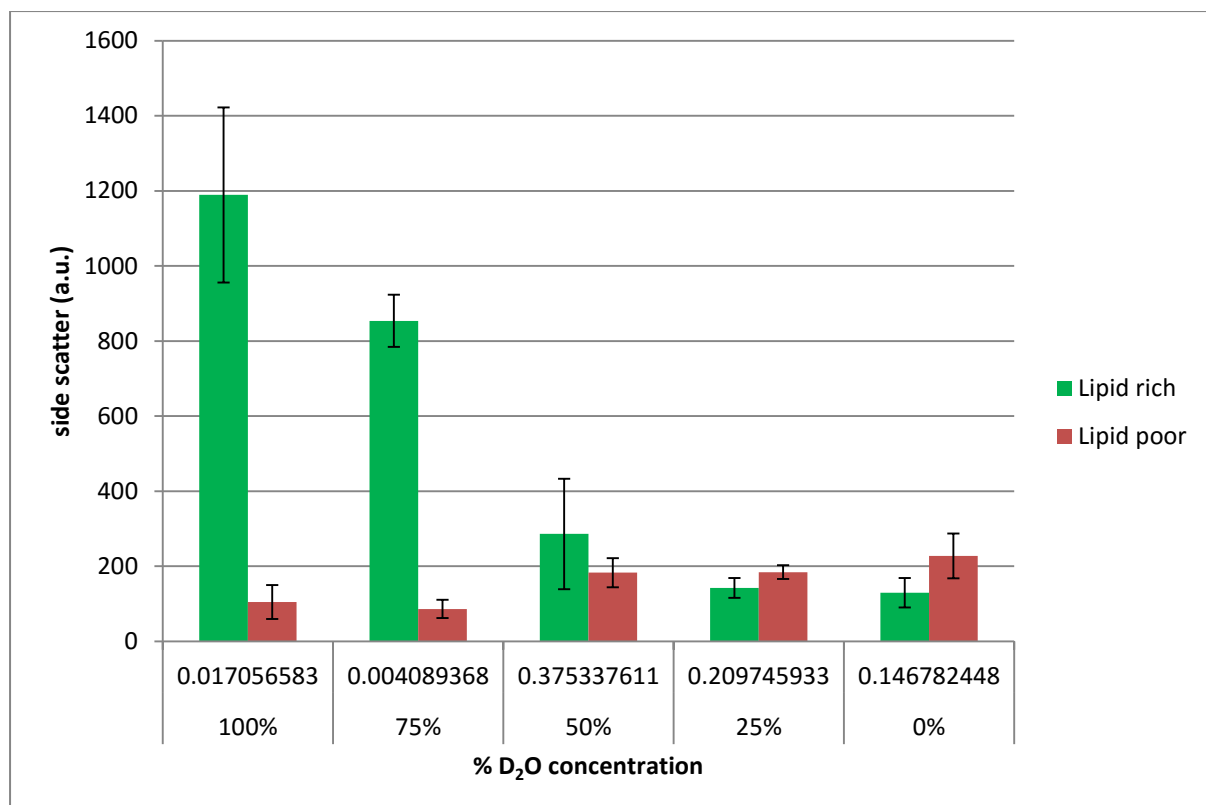


Figure 3.8. *M. smegmatis* cells separated by D<sub>2</sub>O fractionation and measured for side scatter (granularity) in a flow cytometer when unstained. Lipid bodies account for the granularity in the 100% and 75% samples. Error bars = 2 standard deviations from the mean. n=3.

% D2O concentration	100%	75%	50%	25%	0%
p value	0.017057	0.004089	0.375338	0.209746	0.146782

Table 3.1. Student's T-test p values for data displayed in Figure 3.8. p values indicate that there is a significant difference between lipid rich and lipid poor samples for side scattering at 100% and 75% D<sub>2</sub>O concentrations



### **3.10 Discussion**

In this chapter I set out to show that different subpopulations of mycobacteria exist and can be separated easily and quickly with very high purity. I wanted to demonstrate that using physical features of the cells to be separated it is possible to generate pure cultures of mycobacteria in different phenotypic states and that these populations would be measurably different from each other and identifiable. We originally used standard BDS separation media such as Percoll® but quickly found that it was ill suited to our needs. This was due to the inherent inaccuracies, difficulty of the method and its potential as a bacterial carbon (food) source (see section 3.7.2). We then moved on to other BDS theories and methods and decided to peruse the material with the least chance of affecting the mycobacteria in suspension, water. Deuterium dioxide was decided upon as a stable, cheap and easily manipulated substance that would allow us to create the required density gradient.

#### **3.10.1 Mycobacterial separation via D<sub>2</sub>O solution**

What we have achieved is to demonstrate that lipid rich cells can be separated from their lipid poor cohorts easily and rapidly. We have shown that buoyant density separation methodologies are effective in separating cells containing lipid bodies from those lacking lipid bodies and that a methodology using D<sub>2</sub>O is a viable alternative to other methods such as Percoll and sucrose gradients. In addition to this we have shown that a single layer D<sub>2</sub>O gradient confers numerous advantages for this cell type such as ease and cheapness. Numerous studies (Russmann, Jung et al. 1982, Vincent and Nadeau 1984, Arrowood and Sterling 1987, Makinoshima, Nishimura et al. 2002) found that Percoll and sucrose gradients both could affect the quality of the cells (mammalian or bacterial) and change their

morphology or cell state. As far as we are aware the D<sub>2</sub>O method does not have these problems.

### **3.10.2 Yields and efficiencies of BDS methodologies**

Many groups write about the importance of high yields and good efficiencies in cellular separation methods (Tomlinson, Tomlinson et al. 2013), however few do the necessary experiments to ascertain whether the efficiencies of their techniques could be improved. Zhu and Murthy (Zhu and Murthy) show that with microfluidic methods it is possible to generate  $\geq 95\%$  efficiency with a through put of  $10^{11}$  cells per hour. This is comparable with our methodology as we do not separate cells individually as Zhu and Murthy do but in large batches of  $10^8$ - $10^{10}$  cells per passage and many passages can occur simultaneously. Chang *et al* (Chang, Hsieh et al. 2009) compare the efficiencies of two commercially available separation media, Percoll and Ficoll but do not compare them to other methods. Chang *et al* found that for human leukocytes Ficoll was more efficient with a higher yield than Percoll. No other groups known to be working with mycobacteria were found that separated their cells in this way after an exhaustive literature search.

Arrowood and Stirling (Arrowood and Sterling 1987) conducted experiments attempting to ascertain the recovery efficiencies of different isopycnic centrifugation methods. They found that they were able to recover  $\sim 60\%$  ( $\pm \sim 10\%$ ) of *Cryptosporidium* oocysts from a discontinuous sucrose gradient after a single passage and  $\sim 70\%$  ( $\pm \sim 10\%$ ) from a second passage. However they were able to recover  $>70\%$  ( $\pm \sim 15\%$ ) oocysts from a properly constructed Percoll gradient. This experiment was then further tested to discover the levels of intact (and therefore viable) oocysts recovered. It was found that while it was possible to recover  $>80\%$  of oocyst walls the quantity of intact oocysts was nearer 25%. *Cryptosporidia*

oocysts are roughly spherical and approximately 4-6  $\mu\text{m}$  in diameter (Vesey, Slade et al. 1993). While mycobacteria are not spherical the size measurement (4-6  $\mu\text{m}$ ) is comparable with a late stage, non-replicating mycobacterium.

Another study by Martin and MacDonald (MARTIN, Department of Microbiology et al. 2015) showed that saprophytic bacteria extracted from soil could be separated based on their density in Percoll but with very poor efficiencies, 10-20% of the bacteria found in the raw soil samples were extracted post-centrifugation.

These studies show that the separation efficiencies of isopycnic centrifugation methods are difficult to predict and often poor. Our separation purity is excellent with >90% purity after a signal passage. Zhu and Murthy were able to generate a comparable purity using a much more sophisticated and expensive methodology- microfluidics.

When compared with the above studies our separation efficiencies are not as good as Arrowood and Stirling's but are better than Martin and MacDonald's. This will be, in part, due to the differing nature of the material being separated, oocysts versus bacteria. In Martin and MacDonald's study the extraction efficiency was reported as 10-20%. It is not reported if this was the total cell number or the viable cell number recovered. This is an important metric for our work because we lose up to 2 log of biomass per passage. The important distinction is biomass, not viable bacteria. Most of the separations we undertake occur on cultures in stationary or death phase. This means there is a lot of cell debris present in the culture. Measurement by spectrophotometry indicates that we lose 2 log of biomass but measurement by PCR shows that the concentration of viable cells present in the extracted lipid rich and lipid poor layers is similar to that of the original culture with a

loss of <40%. This means that our extraction efficiency is >60%, a significant improvement on the Percoll system used by Martin and Macdonald.

### **3.10.3 Significance of our findings**

The significance of these findings are global in the mycobacterial research world. With this simple method of separating cells which are expressing lipid bodies into 100% pure culture we are now able to investigate numerous objectives relating to the mycobacterial accumulation of lipids. Some of the experiments that are now possible include; investigations into the reason for lipid body formation, what effect lipid bodies have on bacterial cells, such as drug susceptibility, metabolic activity and probability of becoming part of a latent disease state. These are all important and significant questions still unanswered in the mycobacterial research community.

The data from Figure 3.4 and Figure 3.5 showed that it is possible to purify mycobacterial cells to a high degree after only one passage. In the event another passage was required the maximum attempted on a single sample was 2. This allowed for a >99% purity to be achieved. It was also shown that Nile red was an effective stain for the identification of lipid bodies both microscopically and in a flow cytometer. These data were confirmed by Figure 3.6, Figure 3.7 and Figure 3.8. While no staining was used in the generation of the data for Figure 3.7 and Figure 3.8 the granularity results showed conclusively that there was a significant difference in the scattering patterns of samples designated lipid rich versus those designated lipid poor. This difference has been attributed to the presence of lipid bodies. We believe that this is a reasonable conclusion. All of these data were confirmed again by the routine sampling and staining of populations throughout the work, if there was ever

confusion about the lipid body purity status of a sample it was destroyed and the experiment was restarted.

#### **3.10.4 Relevance to presence of mycobacterial lipid bodies**

Work conducted by Deb *et al* (Deb, Lee *et al.* 2009), Daniel *et al* (Daniel, Deb *et al.* 2004, Daniel, Maamar *et al.* 2011) and the Barer group at Leicester University, UK (Christensen, Garton *et al.* 1999, Garton, Christensen *et al.* 2002, Garton, Waddell *et al.* 2008, Mukamolova, Turapov *et al.* 2010, Barer, University of Leicester Medical School *et al.* 2015) has shown the concentrations of lipid bodies in mycobacterial cells rises as the culture ages. The Barer group in particular have managed to produce lipid bodies artificially by manipulating the nitrogen concentrations in their cultures. Our work compares favourably with these experiments as it shows that lipid rich cells exist in mycobacterial species, that they seem to appear spontaneously and they can be positively identified through direct observation or via an indirect method such as flow cytometry. Beyond this we have shown that total separation is possible and have shown more clearly than the above studies that a difference exists in the antibiotic resistance characteristics of lipid rich bacteria (see section 4.6.1).

Where our work is different (and advantageous) from other reported findings in this area is the purity of the separation we are able to achieve. A  $\geq 99\%$  purity of lipid rich cells has not been achieved before. This achievement opens up possibilities of what we can accomplish with pure lipid rich cultures. With a  $\geq 99\%$  purity of lipid rich cells we are able to experiment on a subpopulation of mycobacteria without interference from another subpopulation. An example of work suffering from contamination by an unwanted subpopulation is the work conducted by numerous groups such as Rodriguez *et al* (Rodríguez, Ruiz *et al.* 2002) Wallis

*et al* (Wallis, Patil et al. 1999) and Wanger *et al* (Wanger and Mills 1996). These groups all tested the MIC or MBC of anti-tuberculosis compounds and all found similar data for similar drugs. As none of these groups included a separation step they were experimenting on a heterogeneous mixture of lipid rich and lipid poor cells and as such were only able to produce MBC<sub>90</sub> and MIC<sub>90</sub> data without using huge concentrations of drug that are well above the standard guidelines for such an experiment. The effect of the mixed population may have been profound. If the above groups had included a separation step, as we have, they would have been able to experiment on lipid rich and lipid poor cultures separately and discover the differences (if any) between their respective MIC and MBC values. This is what we went on to do in this study (see section 4.6.1).

There are no direct comparisons to be made with this work as few single layer separation methodologies exist. Those that do don't rely upon the intrinsic nature of the cells they are separating but instead on an additive such as an antibody (see above).

### **3.10.5 Disadvantages of BDS methods**

There are numerous disadvantages to this BDS method. The primary disadvantage is the loss of cells in the lipid rich layer. This has been addressed with the modification of standard P200 pipette tips to have shortened, blunt ends that allow more of the surface volume of the sample to be extracted at once but even with this innovation we are still losing approximately 2 log of biomass with every passage (see above). Numerous concepts have been explored to remedy this such as snap freezing the D<sub>2</sub>O solution and cryotoming the top few layers off. Another possibility would be to conduct the separation in a larger vessel and extract the lipid rich layer through the side of the vessel with a needle and syringe. While these are both possible it was decided that they were not practical solutions as snap

freezing will undoubtedly alter the metabolism and structure of the cells being separated. It is also likely that the same problems encountered with our current extraction methodology would plague a needle and syringe extraction.

The problem is that our D<sub>2</sub>O technique is limited to a few cell types. This is due to the fact that it contains stages in which the cells are suspended in pure water. This would cause serious osmotic imbalance in many cell types and cause them to lyse. This does not appear to be a concern for mycobacteria, however, as mycobacteria have a thick mycolic acid outer envelope and a robust cell wall that allows the cells to resist severe osmotic imbalance for an extended period of time (Hatzios, Baer et al. 2013), this they have in common with all bacteria.

There are inefficiencies and problems with the methods described above. Reasons for the inefficiencies shown in Figure 3.4 have not been explored in depth, however, some hypotheses have been proposed. One possibility could be due to the quality checking methodology we use (see below). Staining with Nile red is effective however we cannot be sure that every lipid rich cell is observable. For high throughput screening a flow cytometer was used. Advantages of this machine include labour saving and rapid time to result. A serious disadvantage however is that it cannot differentiate between a fluorescing crystal of Nile red and a cell displaying a lipid body. It is possible that the flow cytometer is producing erroneous results leading to incorrect efficiency calculations as it is returning false negatives. As the 1g sedimentation separation technique requires an extended period of time (~16 hours) and for the vessel containing the separation to be undisturbed during this time it is also possible that the vessels have been agitated in some way during incubation, this could lead to excessive Brownian motion in the vessel. Establishment of convection

currents is also a potential problem if the immediate area surrounding the vessel is too warm. A warming of the immediate environment would also cause a slight decrease in the density of the D<sub>2</sub>O solution again causing issues. Other potential sources of error are operator based in origin. Pipetting inaccuracies and disturbing the sample prior to extraction could both cause the sampling to go awry. The last significant source of error we have explored is the idea that there may be in some samples no or at least very few lipid rich cells present in the first place. This seems unlikely as we have tracked the growth of lipid rich cells and shown that they can be extracted in young cultures as well as established cultures where one would expect to find them but it remains a possibility until further investigated.

### **3.10.6 Flow cytometry data**

With regard to the flow cytometry data in Figure 3.6, the reasons for the high background in the data and the number of high intensity red or green events in the lipid poor fraction can be explained hence. The most likely that we have evidence for is due to Nile red's hydrophobicity. In aqueous solutions Nile red readily precipitates out of solution and forms needle-like crystals. These have very high natural fluorescence in both the red and green ranges. If they were to form in the flow cytometer they would be read as events and therefore give a false positive reading. The only way to avoid this problem would be to use a non-aqueous solution in the flow cytometer or to find a different stain with all of Nile red's properties. Neither of these are appealing options as to put a volatile fluid into the flow cytometer would be dangerous, risking a fire. In addition after extensive literature searching we have found no suitable alternative to Nile red so we must proceed with our current method which has appreciably small margins of error.



### 3.10.7 Centrifuge separation

In relation to the centrifugation method within the BDS separation there are reasons that the two different techniques exist and are both used. The glass pipette method could accommodate a larger volume, 5mL in contrast with 1.2mL in a microcentrifuge tube. This greater volume allowed for a greater quantity of bacteria to be separated at once, however, it has a major drawback. The glass pipette method was used when collection of the lipid rich fraction *only* was required as the cell debris and lipid poor cells were pelleted to the conical end of the glass pipette and very difficult to remove. A benefit of the glass pipette, however, is that glass does not require anti-static treatment in the same way that polystyrene microcentrifuge tubes do meaning a time consuming step can be removed from the process.

The advantages of this method, we believe, far outweigh the disadvantages. For the first time we have been able to generate pure lipid rich cultures for experimentation which allow us to gather data solely on these subpopulations and attempt to understand why they exist and how they affect human disease. We have also shown that staining is not necessary to discover if lipid rich cells are present. In the absence of a staining agent such as Nile red the granularity (side scatter) data collected from a flow cytometric analysis can indicate the lipid body presence in a mycobacterial cell. Added to this we have shown that Nile red is an effective stain for identifying internal lipid droplets and that this technique is not just applicable to microscopic analysis but also to flow cytometry. This may allow future researchers and clinicians to examine *mycobacterium tuberculosis* infect tissue or sputum without the addition of a staining reagent shortening the time to detection and making the process faster and less expensive.

### 3.10.8 Conclusion

With this tool it becomes possible to experiment on only one population of mycobacteria at a time. This means that inefficient data collected in the past, when only  $MBC_{90}$ s were possible because of the heterogeneous mixture of cells, can be repeated with a homogenous cell population. This will allow an accurate determination of drug susceptibility in lipid rich and lipid poor cells to be gathered (see chapter 4). This is important as we have shown in section 4.6.6 lipid rich cells, morphologically identical to those found *in vitro* are found in *ex vivo post mortem* human lung tissue. If we can experiment solely on lipid rich cells we can discover whether they truly have a higher drug tolerance to the standard drug regimen. We can also test new and different classes of drugs on them to see if it is possible to kill them more easily. This will mean that we can eradicate one possible source of persistent relapse in patients.

## 4 Lipid rich Mycobacteria

### 4.1 Introduction to Bacterial Dormancy

Many species of bacteria enter a quiescent stage in their life cycle (ANDREWS and HENRY 1935) or sporulate (Spudich and Kornberg 1968) meaning they become immune to many forms of bacterial killing (Ceragioli, Cangiano et al. 2009). Mycobacteria appear to do something different, however. They can become 'dormant' within the host and within host phagocytes (namely macrophages) (Goren, D'Arcy Hart et al. 1976, Daniel, Maamar et al. 2011). These cells are viable but non-replicating and therefore non-culturable until they resuscitate. Prior to resuscitation they also display a lowered metabolic rate and a resistance to antibiotics (Loebel, Shorr et al. 1933, Betts, Lukey et al. 2002, Betts, and et al. 2014). There is evidence to suggest that there is an up-regulation of lipid metabolism in mycobacterial cells that are entering dormancy (Reed, Gagneux et al. 2007) and this could account for the presence of lipid bodies found in many stressed mycobacterial cultures (Deb, Burnett School of Biomedical Sciences et al. 2009). Where cells have become stressed and are expressing lipid bodies we have termed these cells 'lipid-rich' whereas their counterparts lacking lipid bodies are 'lipid poor'. Lipid richness can be thought of as a phenotypic marker of dormancy. As cells move towards this phenotype they begin to sequester environmental lipids (Neyrolles, Hernandez-Pando et al. 2006, Daniel, Maamar et al. 2011) as well as produce lipids from their own metabolites (D'Avila, Melo et al. 2006). This leads to lipid bodies being formed from, among other substances; triacylglycerides, waxy esters and free fatty acids (Daniel, Maamar et al. 2011).

Being able to detect these cells and work with them exclusively (to the exclusion of actively multiplying cells) has been a research challenge (see chapter 3)

Novel use of the well-studied lipophilic stain Nile Red has allowed us to elucidate the lipid rich cells in a mixed culture and to be able to track their change from lipid poor to lipid rich over time.

## 4.2 Nile red

Nile red is a benzophenoxazine dye (structure shown in Figure 4.1). Table 4.1 lists some properties of Nile red. Nile red is highly soluble in ethanol but is negligibly soluble in water which makes its use in biological situations difficult. One way to eliminate this problem is to bathe cells to be stained in a highly polar substance such as ethanol. This however can damage or change to properties of the cells under investigation so is generally avoided. Another method is to use DMSO (dimethylsulphoxide) as the solvent for the dye. Nile red is readily soluble in DMSO and DMSO will aid in the carriage of Nile red across biological membranes. Nile red is a dye that exhibits solvatochromism; its absorption band varies in spectral position, shape and intensity with the nature of its solvent environment, it will fluoresce intensely red in polar environment and blue shift with the changing polarity of its solvent. This makes it ideal for the detection of lipid bodies within mycobacteria as the lipid bodies are made of non-polar lipids such as triacylglycerols but the cell membranes are made up of polar lipid species.

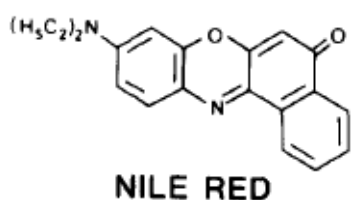


Figure 4.1. Molecular structure of Nile red.

Molecular formula	C <sub>20</sub> H <sub>18</sub> N <sub>2</sub> O <sub>2</sub>	
Molecular weight (Molar Mass)	318.369 g/mol	
Melting point	192-193°C	
Solubility	acetone	1 mg/mL
	n-heptane	62 µg/mL
	water	<1 µg/mL
Partition coefficient (4°C)	xylene/water	210
	chloroform/water	196
	iso-amylacetate/water	198
	n-heptane/water	58
Absorption maxima (HCCl <sub>3</sub> , solvent)	ultraviolet, 264 nm; visible, 538 nm	
Infrared maxima (HCCl <sub>3</sub> solvent)	1000, 1105, 1265, 1305, 1550, 1580, 1612 (C=O), 1710 cm <sup>-1</sup>	
Fluorescence intensity relative to rhodamine B (HCCl <sub>3</sub> solvent)	0.36	

Table 4.1. Physical properties of Nile red

Separating lipid rich from lipid poor cells has been achieved via a simple density dependant method which allows us to conduct studies on lipid rich cells alone (section 3, Separation). Studies such as antibiotic susceptibility experiments have allowed us to ascertain whether the dormancy phenotype has any advantage in terms of antibiotic resistance within a population; this has important implications for many millions of tuberculosis sufferers worldwide.

Some of the markers we have found in lipid rich cells include; a short and fat appearance under a microscope, a green lipid droplet(s) and red cell membrane (when stained with Nile red and observed fluorescently at ~530nm/645nm). Lipid rich cells also appear more granular to a flow cytometer (more side scatter) and they are less dense than their counterparts, this forms the basis of our separation methodology. Most interestingly of all

perhaps is the lipid rich cell's inherent resistance to antibiotics, which goes some way to explain the phenomenon of 'persister cells' and the latent nature of many treated MTB infections.

### **4.3 Lipids**

Lipid droplets in algae and other microscopic organisms have recently become of interest to many researchers as they carry the capacity to produce bio-oil for the mass market (Chen, Zhang et al. 2009, Feng, Zhang et al. 2013). This has led to a lot of research into non-polar lipids or 'neutral' lipids in microorganisms. We have been researching this area as well but for a different purpose. We believe that when mycobacteria are becoming 'dormant' they produce lipid bodies that contain non-polar lipids. We have conducted microscopic analyses (light, fluorescence and transmission electron) of mycobacteria and discovered that there do appear to be internal vacuoles which are concurrent in morphology and placement with literature reports of lipid bodies in bacteria. Other groups have found these same vacuoles and have similarly named them lipid bodies (Garton, Christensen et al. 2002). We have also found that these lipid bodies appear to be in the concurrent locations in differing species of mycobacteria but subject to change if the cells are stressed in some way. We also have observed that these lipid bodies fluoresce green/yellow with Nile red which indicates their contents.

As a lipophilic stain Nile red is used widely to elucidate the presence of extra- and intracellular lipids and lipid inclusion bodies. This is of use to us as it allows us to reveal the presence of lipid bodies in mycobacterial cells. When Nile red enters the cell it is dissolved in the fluid phospholipid cell membrane and fluoresces red. The atypical cell wall that mycobacteria possess is also be a factor. This cell wall is composed largely of mycolic acids,

long chain fatty acids ranging from 60-90 carbons in length. This mycolic acid out layer contains various functional groups (Takayama, Wang et al. 2005) which are polar (MINNIKIN, PATEL et al. 1977, Liu, Barry et al. 1996) and therefore also fluoresce red with Nile red. The lipid bodies we wish to discover, however, are made of non-polar substances. Most likely these are triacylglycerols and waxy esters which cause the Nile red to blue shift and fluoresce a yellow/green.

It is possible that the formation of lipid bodies is a survival mechanism and the lipids within the droplets allow the lipid-rich cells to resuscitate faster than if the lipid bodies were not present. It is also possible that the lipid bodies have a second, related, use. When a tuberculosis infection is established in a human lung there is commonly a granuloma formed. These can eventually caseate and rupture which can cause severe morbidity (Co, Hogan et al. 2004). The internal structure of a caseatic granuloma is semi-liquid and necrotic. It is hypoxic (or anoxic) and with high concentrations of cell debris and reactive oxygen species (Silva Miranda, Breiman et al. 2012). This is a highly hostile environment for the MTB bacillus. We theorise that the MTB bacillus will convert to its lipid-rich form (sequestering lipids from the foamy macrophages which form the necrotic core of the granuloma) and float to the top of the caseateous fluid. At the air-liquid interface of the granuloma the bacillus can resuscitate in the presence of oxygen and be the first to emerge if the granuloma ruptures. This process may occur many times over the course of the granuloma's existence. This allows the lipid rich cell to survive and re-infect the same host or be expelled and infect a new host. There is also evidence (Gillespie, Baron *et al*, unpublished) that there is no difference between lipid rich and lipid poor cell's lag phase in

solid and liquid media meaning that dormant cells are not necessarily eponymously named and are simply awaiting the opportunity to re-grow in favourable surroundings.

The lipids present in a mycobacterial cell range from common bacterial lipids (or phospholipids) such as phosphatidylglycerol and phosphatidylethanolamine to lipids unique to the mycobacterial clade such as mycolic acid (these are shared by the *Rhodococcus* family as well which belong to the mycolata taxon (Butler, Ahearn et al. 1986)). This has made these unique lipids that form an essential part of the mycobacterial cell wall a popular target for antibiotic therapy (Takayama, Schnoes et al. 1975, Takayama, Armstrong et al. 1979).

#### **4.4 Chemotherapy**

The standard drug regimen for pulmonary human tuberculosis consists of four drugs given in tandem over 6-8 months (Botha, Sirgel et al. 1996). These drugs are; rifampicin (rifampin), isoniazid, ethambutol and pyrazinamide. All of these drugs work in different ways to attempt to combat the MTB infection.

Rifampicin inhibits bacterial DNA dependant RNA synthesis by inhibiting RNA polymerase (Levin, Department of Biological Sciences et al. 2014). The *rpoB* gene has been identified as the resistance gene in MTB (Chang, Lu et al. 2012).

Isoniazid is a prodrug that is activated by catalase- peroxide (KatG in MTB (Suarez, Rangelova et al. 2009)) (Ng, Cox et al. 2004). Once activated isoniazid inhibits fatty acid synthesis and thereby mycolic acid synthesis. Because of this it is bacteriostatic if the



mycobacteria are slow-growing but can be bactericidal to rapidly dividing organisms (Davidson and Takayama 1979)

Ethambutol obstructs the formation of the mycolic 'cell wall'. It disrupts arabinogalactan synthesis by inhibiting the enzyme arabinosyl transferase. Mycolic acids attach to the 5'-hydroxyl groups of D-arabinose residues of arabinoglycan which forms mycolyl-arabinogalactan-peptidoglycan complexes. This leads to an inhibition of the peptidoglycan complex and an incomplete cell wall which has increased permeability compared to the wild type. (Wolucka, McNeil et al. 1994)

Pyrazinamide is another prodrug which is converted to pyrazinoinic acid by pyrazinamidase enzyme. Under acidic conditions the pyrazinoic acid leaks out of the cell where it converts to a protonated conjugate acid which can easily diffuse back into the cell and accumulate. The overall effect of this is that more pyrazinoic acid is present on the inner face of the cell membrane at lower pH and at a neutral pH (Zhang and Mitchison 2003). The exact mechanism of action of pyrazinamide has not been fully elucidated but the best theory currently states that the pyrazinamide by-products interfere with FAS (fatty acid synthase) I. The FAS I from MTB was tested against pyrazinamide and its analogues and it was found that the drug and its analogues all had the effect of inhibiting purified FAS I (Ngo, Zimhony et al. 2007). It has also been found that pyrazinoic acid binds to the ribosomal protein S1 (RpsA) and inhibits tmRNA activity, this may explain its *in vivo* activity against 'dormant' MTB (Shi, Zhang et al. 2011).

Not in clinical use for tuberculosis is ciprofloxacin, a fluoroquinolone with a wide spectrum of activity. It inhibits bacterial growth by inhibiting DNA gyrase which is necessary to separate the DNA strands in the double helix. This therefore inhibits bacterial cell division (Drlica and Zhao 1997). Ciprofloxacin is included here as it was used throughout the experiments detailed herein because of its broad spectrum activity and its mechanism of action which could promote mutants to arise in a population treated with a sub-MIC concentration.

Standard chemotherapy for tuberculosis last 6-9 months and is very costly both to the patient as the side effects can be unpleasant (Garner, Smith et al. 2007) and to the global economy as the drugs can be expensive to produce, transport and the infrastructure necessary to disseminate them to the people who need them needs to be in place (Loddenkemper, Sagebiel et al. 2002). A better, more targeted drug therapy is needed.

We have reason to believe that the current therapy and the current research are addressing the wrong issues we regard to standard MBC and MIC assays. Many papers (Collins and Uttley 1985, Casal, Ruiz et al. 2000, Rodríguez, Ruiz et al. 2002, Tato, de la Pedrosa et al. 2006) cite that they use an MIC<sub>90</sub> technique when establishing the effectiveness of a drug against MTB. This is even the case with new experimental drugs (Molina-Torres, Ocampo-Candiani et al. 2010). We believe that this methodology is neglecting a small but significant sub-population of bacteria within a tuberculosis infection. The experiments in the above papers are conducted on exponential phase bacteria, with no stresses upon them. This environment is not analogous to the *in vivo* environment found in a patient. The 10% left alive after treatment in the above papers could be the lipid rich cell we have been

separating and working on as they have lower drug susceptibility than the lipid poor cells which are more common in an exponentially dividing culture.

## **4.5 Methods**

### **4.5.1 Lipid-rich bacteria analysis**

#### **4.5.1.1 Bacteria and culture.**

Isolates of *M. smegmatis* (NCTC 9159), *M. fortuitum* (CIP 104534), *M. marinum* (M-strain) and *M. bovis* (BCG)(NCTC 5692) were grown to defined stages of maturity by inoculating them into sealed tubes in Middlebrook 7H9 (Fluka) with 0.05% Tween (Sigma Aldrich) incubating at 37°C for all species but *M. marinum* which was incubated at 30°C for the appropriate duration. The viable count was determined using a modified Miles and Misra method by serial dilution and inoculation on Middlebrook 7H10 agar (Fluka) and brain-heart infusion agar (Oxoid) as described previously. (Billington, McHugh et al. 1999)

### **4.5.2 FitC staining**

Preparations of bacteria were grown to mid stationary phase and stained with a final concentration of 2µg/mL of FitC suspended in DMSO for 30 minutes. This culture was then subcultured into fresh sterile media containing 0.05% Tween 80. After 24 hours this subculture was again subcultured into fresh sterile media containing 0.05% Tween 80. After a further 24 hours this twice passaged culture was separated as described into LR and LP fractions. These fractions were run through the flow cytometer to establish whether there was a bias of non-dividing cells present in either of the fractions.

### **4.5.3 Determination of antibiotic susceptibility**

Preparations of bacteria (between 300-700 cells) were incubated for 16 hours at 37°C (30°C for *M. marinum*) with relevant antibiotics (ciprofloxacin (Sigma), rifampicin (Sigma), Isoniazid (Sigma) and ethambutol (Sigma)) at concentrations from below published MIC to

100x MIC. After incubation cells were centrifuged and washed twice in sterile PBS then re-suspended in sterile 7H9 media plus 0.05% Tween. These preparations were incubated at 37°C (30°C for *M. marinum*) in a shaking incubator at 210RPM for 72 hours. Viability was determined by inoculation onto 7H10 agar. The plates were then incubated for up to 72 hours at 37°C (30°C for *M. marinum*) and results were scored as positive or negative. All experiments were conducted as either MBC or MBC<sub>90</sub>. MBC<sub>90</sub> experiments were carried out to establish whether the MBC<sub>90</sub> of exponential cultures was comparable to the MBC of a lipid poor culture as described previously. (Gomez and McKinney 2004, Tato, de la Pedrosa et al. 2006)

#### **4.5.4 Staining**

##### **4.5.4.1 Microscopic analysis**

Mycobacterial cells were stained with Nile red 2mg/mL (Sigma Aldrich) by adding to the separated fractions of cells at a 1:1 ratio with a final concentration of 1mg/mL and incubated at room temperature with constant agitation for 20 minutes. Samples were then centrifuged for 3 minutes at 20,000g to pellet the cells. The supernatant was removed and discarded and 200µL of 100% ethanol was added and vortexed for 1 minute. The samples were again centrifuged for 3 minutes at 20,000g and the supernatant discarded. 100µL of PBS was then added and vortexed for 1 minute. The samples (10µl) were applied to a clean glass slide and heat-fixed. Bacterial preparations were viewed by fluorescence microscopy (Leica DM5500) (excitation; 480/40, 540/40. Emission 527/30, 645/75) to determine the proportion of lipid body positive cells.

Direct fluorescent microscopy was used to measure the quality of the preparations. A 10µL suspension of stained cells was removed and heat fixed on a glass slide. This spot was

washed with 70% ethanol to remove any Nile red crystals and visualised under fluorescent microscopy at 530nm and 645nm emission for green (neutral lipid) and red (polar lipid) fluorescence respectively. Cells in the field of view were counted and the numbers of cells expressing green fluorescence were counted to give a percentage of cells expressing green fluorescence versus cells expressing only red fluorescence. This process was repeated until 300 cells in total were counted. Example preparations are illustrated in Figure 4.2

#### **4.5.5 Flow cytometry**

Flow cytometry was carried out on a Millipore Guava easyCyte™ HT as an independent method of determining the proportion of lipid rich and poor cells. Cells were stained as above and loaded into a round-bottomed 96 well plate. This was loaded into the flow cytometer which excited the samples at 488nm and read the samples at 525/30nm and 690/50nm. Microscopic analysis of Nile red stained preparations (Figure 4.2) was used to validate the results of flow cytometric analysis.

#### **4.5.6 Human lung tissue**

The same Nile red protocol that was used with the microscopic analysis and for flow cytometry was used to stain mounted sections of human lung tissue that were removed as part of a post mortem biopsy. The slides were originally mounted with paraformaldehyde after sequential dehydration in increasing concentrations of ethanol. They were then stained with ZN stained to establish the presence of MTB cells. In order to analyse the slides there were destained with xylene and methanol and then allowed to air dry. The slides were then immersed in a 1mg/mL (dissolved in 100% ethanol) Nile red bath for 20 minutes after

which the slides were rinsed with deionised water and 70% ethanol to remove precipitated Nile red crystals.

#### **4.5.7 Old Lipid-rich cells versus young lipid-rich cells**

Samples of all species were grown to late stationary phase ('old'). Cultures were also grown to mid exponential phase ('young'). Samples from both old and young cultures were taken at the same time points throughout the experiment.

Samples of the four species were then separated as above and split into lipid rich and lipid poor fractions. Each of these samples was then treated with each of four antibiotics; rifampicin, isoniazid, ethambutol and ciprofloxacin. These antibiotics were administered at a range of concentrations from well below the MBC to >10x the MBC (See Table 4.5).

The samples were incubated with the drug and bacteria resuspended in PBS overnight (~16hours). The 96-well plates were then centrifuged at 3000 RPM for 10 minutes and the drug-containing supernatant removed. Middlebrook 7H9 media was then added and the plates were incubated for a further 72 hours. The MBC was defined as the lowest concentration that produced a sterile sample. A 96-well plate reader (600nm) was used to establish the presence of growth. Results reported with a greater O.D. than the blank plate containing sterile media were considered positive. Constant and equal inoculum sizes were maintained by on-site growth analysis.

## 4.5.8 Long term experiments

### 4.5.8.1 Preparation of bacteria for long term experiments

Cultures of mycobacteria were measured using spectrophotometry ( $OD_{600}$ ) and, if necessary, diluted to a measurement corresponding to  $10^3$  CFU/mL. These cultures were then aliquoted into sterile 1.5mL Microcentrifuge tubes and incubated at 37° C until they were harvested. Harvesting consisted of; 100µL being taken for DNA sampling, 500µL taken for RNA sampling, 100µL taken for microscopic investigation, 30µL were spotted onto middlebrook 7H9 agar plates for CFU counting and the remaining 270µL kept for lipidomic investigation. All harvested samples were centrifuged at 20,000g for 3 minutes and the supernatant removed and discarded. The DNA and microscopy samples were kept at -20° C, RNA samples were kept at -80° C and the lipidomics samples went straight into Blight and Dyer lipid extraction.

As MTB has such a long generation time some experiments on MTB analogues which also have long doubling times had to take place over long periods. BCG has a roughly similar doubling time as MTB (24h) so to stress or age the cells took time, 100 day cultures of MTB are a laboratory standard for late stationary phase (Hu, Department of Medical Microbiology et al. 2014). In rapidly dividing species (*M. smegmatis* and *M. fortuitum*) long term experiments were carried out to see the generation of lipid bodies in real time and the increase or decrease in certain nucleic acid markers as a sign of dormancy. These species allow us to see a speeded up version of experiments yet to be carried out in the slowly growing species.

Some experiments brought together elements already discussed herein and introduced new ones. DNA and RNA polymerase chain reaction (PCR) was performed to establish bacteria numbers and to corroborate other cell counting measures used such as spectrophotometry.



RNA PCR was undertaken to attempt to find a nucleic acid marker of dormancy that would be an indicator of a dormancy phenotype.

## **4.5.9 PCR**

### **4.5.9.1 DNA**

#### **4.5.9.1.1 Lysate generation**

Lysates of the cells were created by the following protocol: 100µL of cells from each time point were harvested and centrifuged at 10,000g for 10 minutes. Supernatant was removed and the pellet was resuspended in 100µL of TE buffer. This suspension was incubated at 95°C and 1000 rpm for 20 min. Once removed from the heat block the samples were vortexed and centrifuged at 13,000g for 3 minutes. The supernatant was removed and retained and the pellet (cell debris) is discarded.

### **4.5.9.2 RNA**

#### **4.5.9.2.1 Extraction**

0.65g of 0.1 mm glass beads were loaded into as many 2mL homogenisation tubes as there were samples. β-mercaptoethanol was added to lysis buffer (Quigen) to a final concentration of 1%. 600µL of this mixture was added to the homogenisation tubes along with 1mL of cells in sterile water suspension (at  $<10^8$  CFU/ml). Samples were homogenised at 6000rpm for 2 x 30 seconds in Precellys' homogeniser or similar. Samples were centrifuged at 12,000g for 5 minutes at room temperature. 400µL of supernatant was removed and placed into a sterile Microcentrifuge tube with 400µL of ethanol to a final volume of 800µL. 500µL of this homogenate was then transferred to a spin cartridge with a collection tube. The spin assembly was centrifuged at 12,000g for 15 seconds at room temperature. The flow-through was discarded and the spin assembly retained, the remaining 300µL of homogenate was then loaded into the spin cartridge with its collecting

tube and centrifuged again at 12,000g for 15 seconds. 700µL of wash buffer I was then added to the spin assembly and centrifuged at 12,000g for 15 seconds. The flow through and collection tubes were discarded and a new collection tube was fitted below the spin cartridge. 500µL of wash buffer II was added to the spin cartridge and centrifuged at 12,000g for 15 seconds, the flow-through was discarded. This was repeated once so 1000µL of wash buffer II had passed through the spin cartridge. The spin assembly was then centrifuged once with no added buffer to dry the membrane. The collection tube was discarded along with any further flow-through. The spin cartridge was then placed into an Microcentrifuge tube (or collection tube with a lid) and 50µL of RNase-free water was added. This was incubated at room temperature for 60 seconds. The spin assembly was then centrifuged at 12,000 g for one minute at room temperature. ~50µL of RNA suspended in water was recovered in the Microcentrifuge tube and the spin cartridge discarded. The Microcentrifuge tube was stored at -80° C until needed.

2µL of this lysate solution is used per reaction. In quantitative PCR (qPCR) a master mix of Eva Green (BioRad), forward and reverse primers and sterile water are combined to a final volume of 20µl. This is aliquoted into tubes and loaded into a rotor which is in turn placed into the qPCR machine (Rotorgene). Software then controls the Rotorgene and heats the tubes to the required temperature for the PCR reaction to take place (95° C for 2 minutes, then 40-45 repeats of; 95° C 15seconds, 60° C 60seconds) with fluorescence measurements being taken in the green range ( $\lambda_{\text{abs}}/\lambda_{\text{em}} = 500/530 \text{ nm}$  (DNA bound) (see Figure 4.2  $\lambda_{\text{abs}} = 471 \text{ nm}$  (without DNA)).

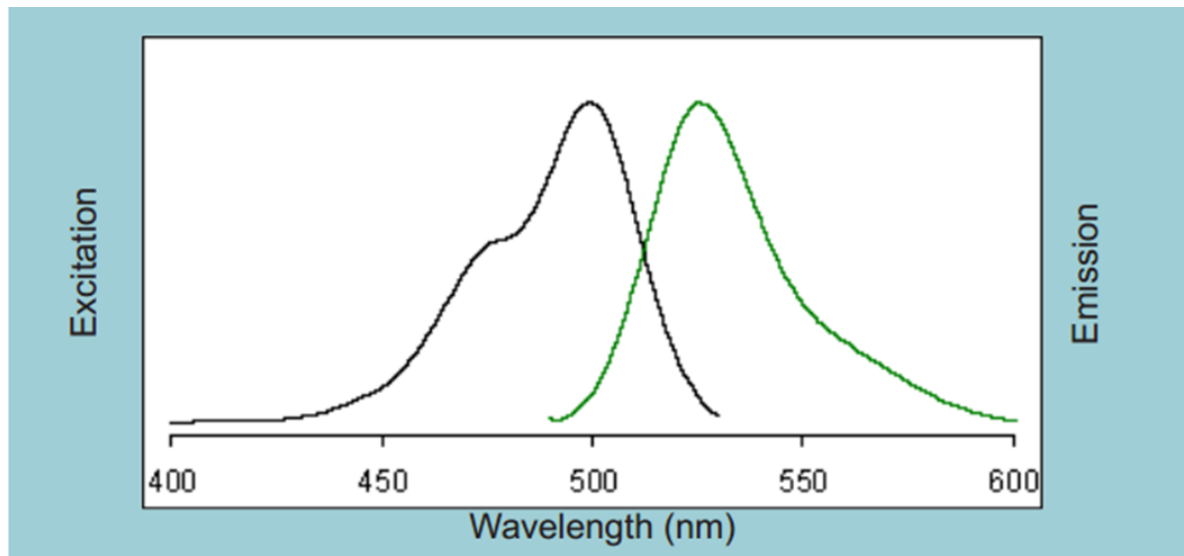


Figure 4.2. Excitation and emission spectra of EvaGreen dye bound to dsDNA in pH 7.3 buffer. Adapted from figure found at - <http://www.fishermolecularbiology.com/uploads/files/EVA%20GREEN%20q-PCR%20REAL%20Time%20Master%20Mix%20Plus.pdf>

$C_t$  (threshold cycle) numbers are used to calculate the quantity of DNA (or other nucleic acid) present in the sample (with reference to a previously generated standard curve). An example data set is displayed below. This figure shows the comparison between a high (red) and a low (green) quantity of DNA being detected in a qPCR reaction. The point at which the lines rise above a predetermined threshold (on the Y-axis) the  $C_t$  value is read from the X-axis. This gives us our value and subsequently the quantity of DNA present in a sample.

As with DNA PCR 2  $\mu$ L of RNA was used per reaction and the specificity of the PCR reaction comes from the primers used. PCRs carried out included mRNA, tmRNA, 16s RNA and pre16s RNA.

The qPCR protocol for RNA is largely the same as for DNA with the exception of the RNA extraction technique.

## 4.5.10 qPCR protocol

### 4.5.10.1 RNA

Oligonucleotides for the *M. smegmatis* 16s rRNA, tmRNA and pre16s RNA quantitative real-time PCR were designed and optimized (Table 4.3). The optimized *M. smegmatis* qPCR protocol contents can be found in Table 4.4.

Ingredient	Sample	IC F+R	IC Probe	M.smeg F+R	M.smeg Probe	Rt mix	Multiplex mix	H <sub>2</sub> O	Total
Volume (μl)	2	0.2	0.2	0.2	0.2	0.1	5	2.1	10

Table 4.2. ingredients and volumes for all constituents of all RNA qPCR reactions. IC= internal control. F+R = forward and reverse primers together. Rt mix= reverse transcriptase mix from Qiagen. Multiplex mix also from Qiagen. H<sub>2</sub>O = deionised, RNAase free water

The reactions were performed in a RotorGene 3000 apparatus (Qiagen, United Kingdom) under cycling conditions of 50°C for 20 min, 95°C for 15 mins followed by 40 cycles of 94°C for 45 seconds and 60°C for 45 seconds at which time the acquisition of the reaction was taken at multiple fluorescent wavelengths. The probes used fluoresce at different wavelengths; HEX- yellow probe Fam- green, ROX- orange. Results were analysed with the cycle threshold set at 0.03. The standard curves were constructed in two independent experiments on serial 10-fold dilutions of *M. smegmatis* DNA in triplicate samples. The specificity of the assay was confirmed by the amplification of 1 ng of DNA from a control sample of mycobacteria, in duplicate.

		Sequence
pre16s	Forward	TTT TGG CCA TGC TCT TGA T
	Reverse	AAA GGG AGC CAA AGG TAT TT
tmRNA	Forward	CGT CAT CTC GGC TAG TTC
	Reverse	CTA CGG CAT TCC CTC AAG
16s RNA	Forward	CTG GGA AAC TGG GTC TAA
	Reverse	CAC CAA CAA GCT GAT AGG
Internal control	Forward	GCC ATG CTA CCC CTG TGC GG
	Reverse	GCG TGG CAA CCA TGA GGT GC

Table 4.3. Sequences for the primers used including the internal control devised and optimised in house.

#### 4.5.11 DNA

Aliquots of 2  $\mu$ L of template DNA were amplified in a 20  $\mu$ L reaction mixture with 10 $\mu$ L Sso Fast mix (Bio-Rad, United Kingdom) and 200 nM each primer (Table 4.3). The PCRs were carried out in a RotorGene Q thermocycler set to a thermal cycling program of 95°C for 2 min, 40 cycles of 95°C for 15 s and 60°C for 1 min, with fluorescence detection at an excitation wavelength of 470nm and an emission wavelength of 510 nm, and a final melt curve analysis. DNA data is not displayed below, it was used primarily as a means of corroborating CFU and SLIC data on cell numbers.

Ingredient	DNA	Primers F+R	EvaGreen Mix	H <sub>2</sub> O	volume
Volume ( $\mu$ l)	2.5	0.8	10	6.70	20

Table 4.4. Ingredients and volumes for all constituents of all DNA qPCR reactions. F+R = forward and reverse primers together. EvaGreen mix = mix containing probe, dNTPs and magnesium required for reaction, from BioRad. H<sub>2</sub>O = deionised, RNAase free water.

To be certain we had separated cells effectively a quality checking step was required. This was carried out using Nile red. Red and green fluorescence was observed under a fluorescent microscope (Figure 4.2) and in a flow cytometer (Figure 4.4).

In parallel to the flow cytometry the same cultures are used under a fluorescent microscope to quality check the samples. Flow cytometry is high throughput but lack specificity; this was overcome using the microscope.

## **4.6 Results**

### **4.6.1 Determination of antibiotic susceptibility**

The phenotypic changes that the cells underwent when accumulating lipid bodies gave them a higher resistance to at least three of the front line anti-TB antibiotics in addition to ciprofloxacin (Table 4.5). We found that in the case of the lipid poor cells the susceptibility to the three front line drugs used, rifampicin, isoniazid and ethambutol, was the same as the published literature but the resistances shown by the lipid rich cells were far higher than the in the literature. The literature values were based upon exponentially growing cultures containing a mixed population of lipid rich and lipid poor cells. We found that up to >30x the dose required to kill all lipid poor cells and >30x the reported dosage (LD100, MBC – minimum bactericidal concentration) (Table 4.5). There was the same pattern with ciprofloxacin with the lipid poor cells reacting as predicted but the lipid rich cells requiring much higher amounts of drug to achieve MBC. Susceptibility studies were performed on lipid rich *or* lipid poor samples, not mixed cultures.

Cells separated into lipid rich and lipid poor fractions display different susceptibilities to frontline anti-tuberculosis drugs.

Drugs	Literature MBC values for <i>M. smegmatis</i> (µg/ml)	Lipid poor MBC values for <i>M. smegmatis</i> (µg/ml)	Lipid rich MBC values for <i>M. smegmatis</i> (µg/ml)
Rifampicin	16	50	1000
Isoniazid	32	30	1000
Ethambutol	30	30	200
Ciprofloxacin	32	30	100

Table 4.5. Minimum bactericidal concentration (MBC) for *M. smegmatis* from published literature versus the lipid poor and lipid rich samples obtained for this study treated with the same regimen as described in the literature.

Drugs	<i>M. smegmatis</i>	<i>M. fortuitum</i>	<i>M. marinum</i>	BCG
Rifampicin	40	20	5	5
Isoniazid	33.3	20	15	16.7
Ethambutol	33.3	na	15	5
Ciprofloxacin	2.9	5	5	5

Table 4.6. Fold increase in MBC concentration required to clear LR cells compared with LP cells. All mycobacterial species tested against all drugs tested. In all cases the quantity of drug required to clear all LR bacteria is significantly higher than the amount required to clear all LP bacteria. There was no data for ethambutol and *M. fortuitum* because we found the strain of *M. fortuitum* tested was wholly resistant to ethambutol.

#### 4.6.2 Staining

Nile red has been used for many years to visualise intracellular lipids. The classic Nile red protocol as adapted in this study and used to visualise and quantify lipid bodies within mycobacterial cells. This was useful not only in microscopy but also in flow cytometry where



it was possible to further adapt the Nile red staining protocol to a high through put screening method to allow for rapid quantification of the lipid body load in a particular sample. Figure 4.2 below demonstrates what a lipid rich cell from each of the species studied looks like and how they were identified microscopically.

It is clear that lipid bodies within lipid rich cells appear to fluoresce vividly green with Nile red while the rest of the cell (specifically the polar lipids of the cell wall and membranes) stay a bright red. This allows for good separation in the flow cytometer and allows for only one stain to be used. This is rather than a mixture of others meaning the acid-alcohol detaining that gives mycobacteria one of their classifications (acid fast) is not necessary greatly reducing the complexity and difficulty of the procedure

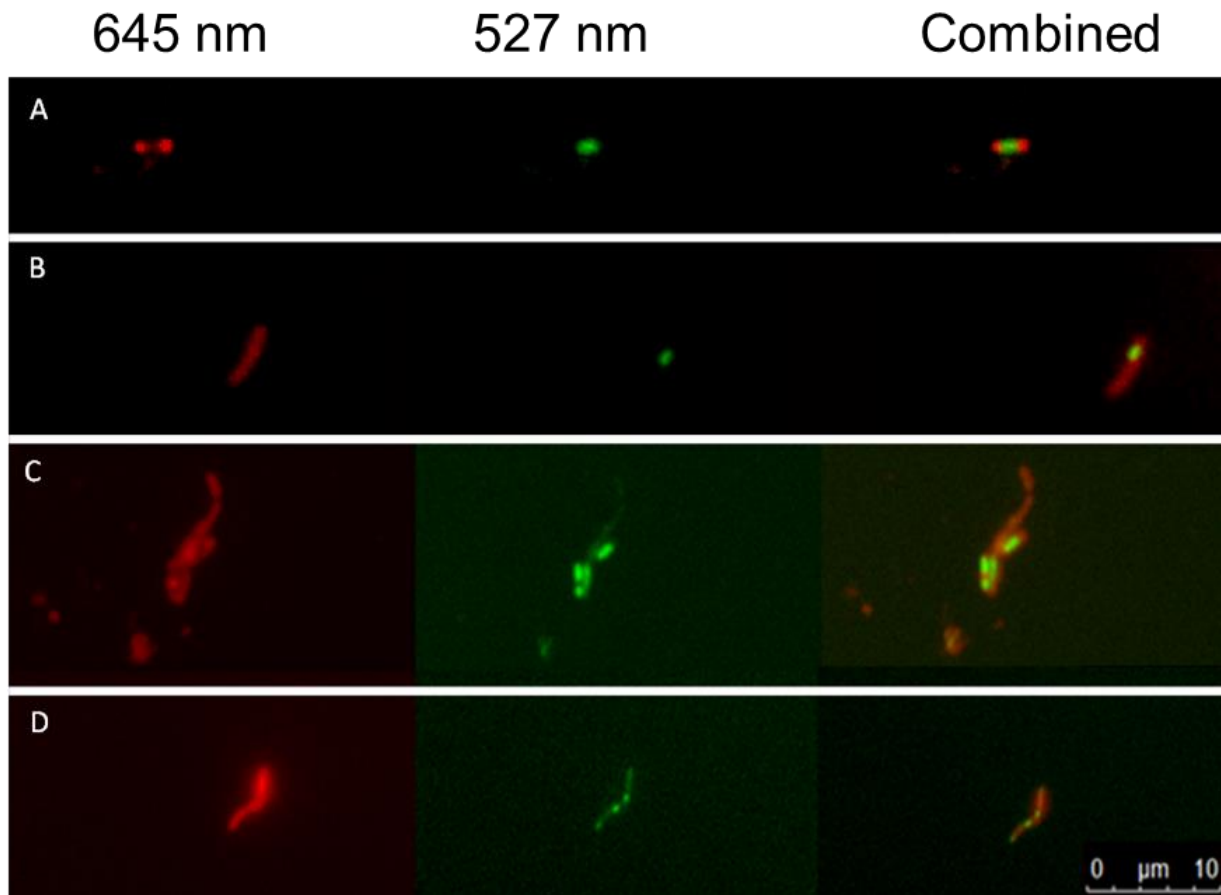


Figure 4.2. Left to right; Nile red fluorescence of polar lipids at 645 nm, Nile red fluorescence of non-polar lipids at 527 nm, composite image lipid rich cells extracted from D2O separation top layer. A; *M. marinum*, B; BCG, C; *M. smegmatis*, D; *M. fortuitum*. It can be seen that in *M. marinum* the lipid body is single and large in the centre of the cell. In BCG the lipid body (or bodies) is found at the polar end of the cell. *M. smegmatis* is similar to *M. marinum* in that it will have large lipid bodies situated in the centre of the cell but *M. smegmatis* regularly displays more than one lipid body. *M. fortuitum* is similar again to BCG as it shows lipid bodies at the poles of the cells but much more commonly there will be two lipid bodies rather than one.

### 4.6.3 FitC

Studies with Fluorescein isothiocyanate (FitC) were undertaken to establish whether lipid rich cells found in young cultures were in fact older cells left over from a previous passage. FitC binds to the cell membranes of bacteria and halves its fluorescence every time the bacteria divide. If there was a bias towards non-replicating cells in a fraction of cells this would show up as a peak in the number of cells fluorescing intensely. Data shown in Figure 4.3 shows that there is no bias towards brightly fluorescing events in either the lipid rich or lipid poor fractions. This supports our hypothesis that lipid rich cells occur spontaneously in cultures of any age under few or many stressors. The older fraction is a negative control of mixed LR and LP cells that were stained at the same time as the test LR and LP samples. The young fraction is a positive control that was stained just prior to the sample measurement. It displays the data expected if there was a bias present in either of the LR or LP samples.

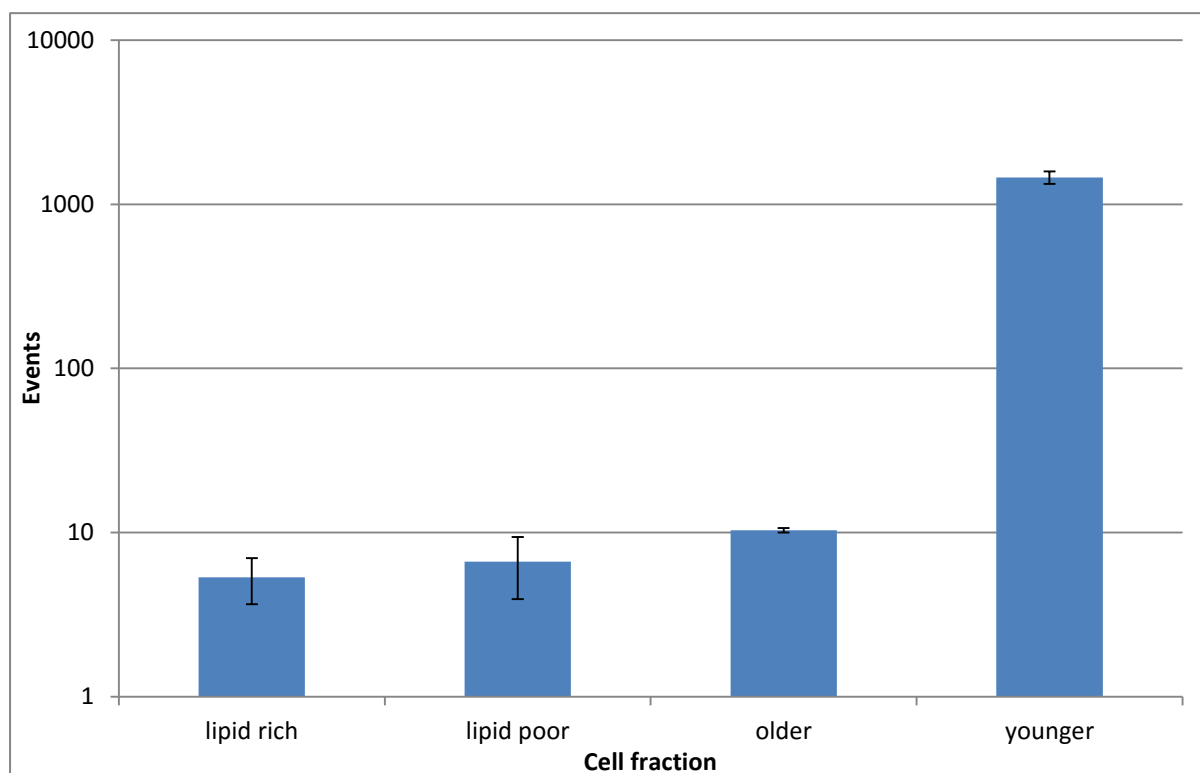


Figure 4.3. Graph displaying the number of flow cytometry events of an intensity greater or equal to 3 arbitrary units of *Mycobacterium smegmatis* after FitC staining and incubation for either 72 hours (LR, LP and 'older') or less than 1 hour ('younger'). Measurement took place in a Millipore Guava EasyCyte flow cytometer. Data for all other species used (*M. fortuitum*, *M. marinum* and BCG) was similar and not shown. Error bars represent  $\pm 1$  standard deviation from the mean.  $n=3$ .

#### 4.6.4 Long term experiments

DNA and RNA PCR of mycobacterial samples on a long time scale can allow us to see changes occurring within the cells as they age. This coupled with microscopic and lipidomic investigations can reveal a more complete picture than is currently available of the dormancy phenotype and the progression of lipid richness in mycobacterial species as a whole.

##### **4.6.4.1 400 hour PCR DNA/RNA *Mycobacteria smegmatis* profile**

Figure 4.5 displays the results for a 400+ hour experiment to determine if there was a class of easily identifiable RNA in *M. smegmatis* that would serve as a marker for dormancy or the cell entering a state of lowered metabolic activity. It was expected that 16s ribosomal RNA would become less common as the cells became quiescent but it appears that only the pre16s RNA concentrations decrease over the length of the experiment.

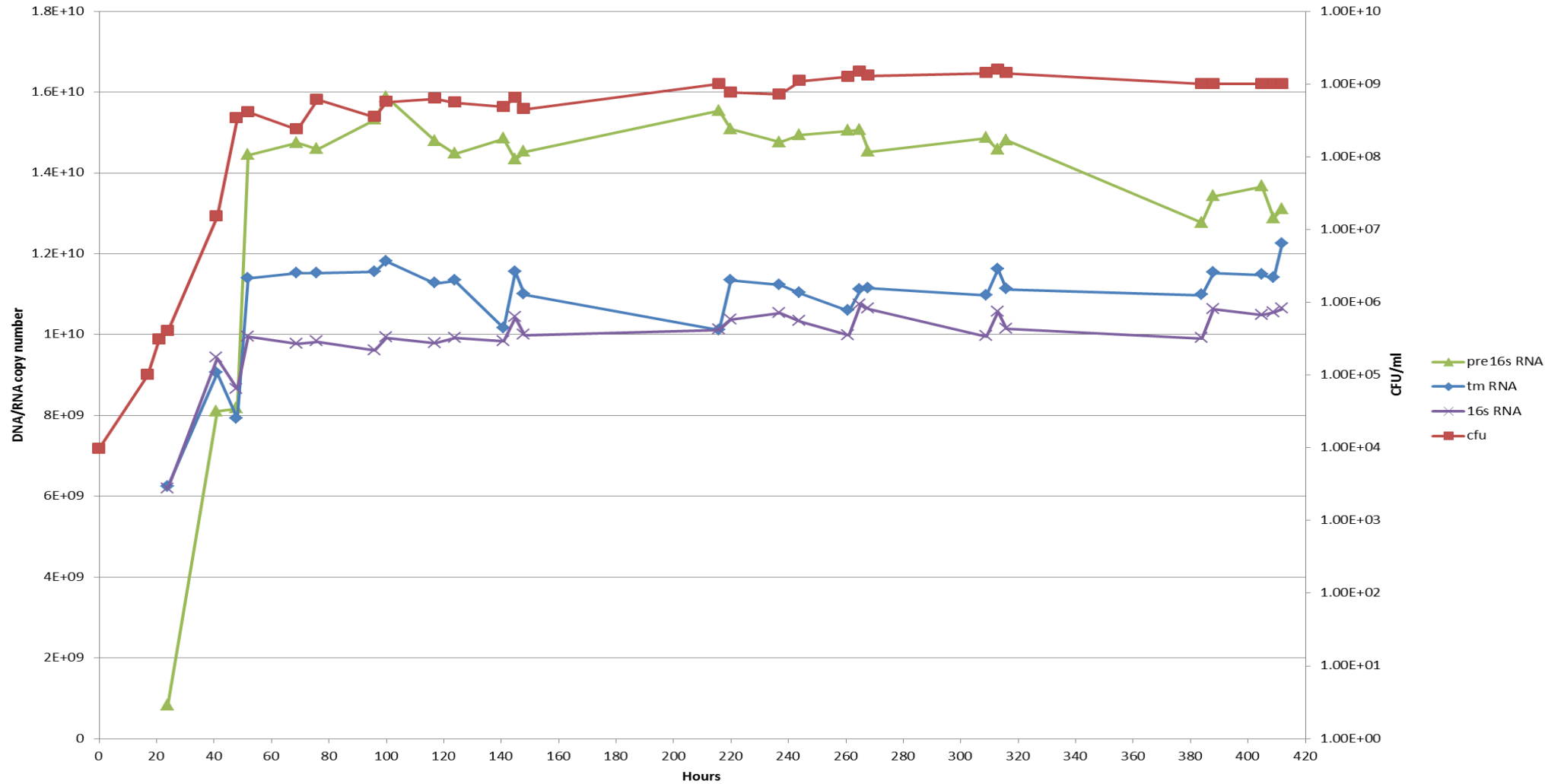
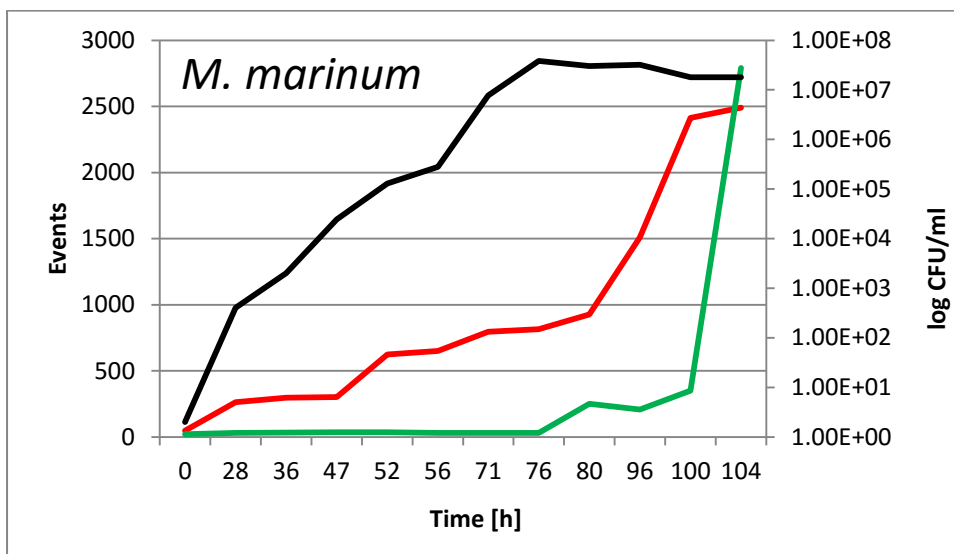
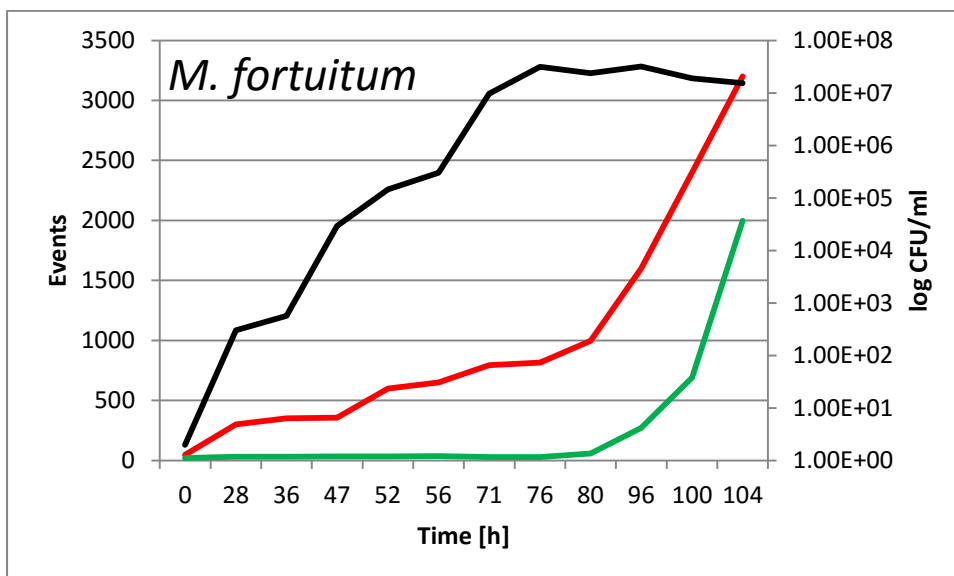
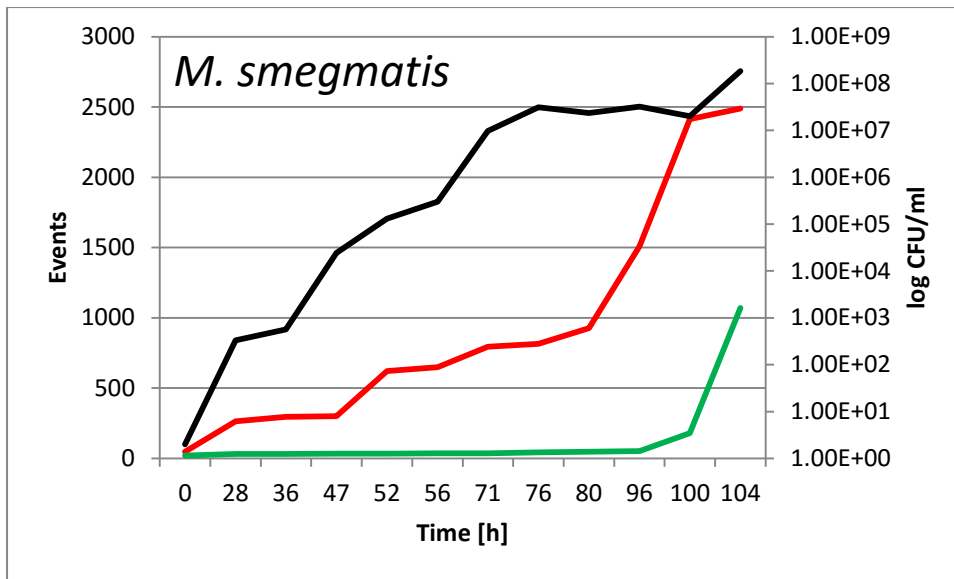


Figure 4.5. Graph of a 400h long experiment displaying the relative concentrations detected of pre16S RNA, tmRNA, 16S RNA and the CFU value of *M. smegmatis*. Data suggests that after ~300h the quantity of pre16S RNA begins to decline.

#### **4.6.4.2 100+ hour lipid body formation experiments**

Figure 4.4 displays the results for a series of 100+ hour experiment to determine if it were possible to track the accumulation of lipid bodies in a culture via Nile red staining and flow cytometry in near-real time. The literature on the subject suggests that lipid rich cells occur only in later stages of culture. We have shown here that the levels of lipid rich cells detected are low but present. For example at the 28 hour mark in the *M. smegmatis* experiment there was an average of ~20 'green events' (lipid rich cells) detected indicating that a population of young lipid rich cells exists. This is the case for all species tested. The expected result was that over time the level of green fluorescence rose and tracked well with what we predicted, as the cells entered stationary phase at around the 70h mark (for *M. smegmatis*, for example) the amount of detected lipid rich cells rose sharply. This rise in lipid rich cells is not as obvious or dramatic in the BCG samples tested but we did find that the red fluorescence (total cell number) tracked well with the CFU count that was made alongside all flow cytometry measurements in the BCG cohort. This is less true of the other species tested.

A longer-term study was undertaken with only *M. smegmatis* and the results from Figure 4.4 were corroborated – see Figure 4.5.





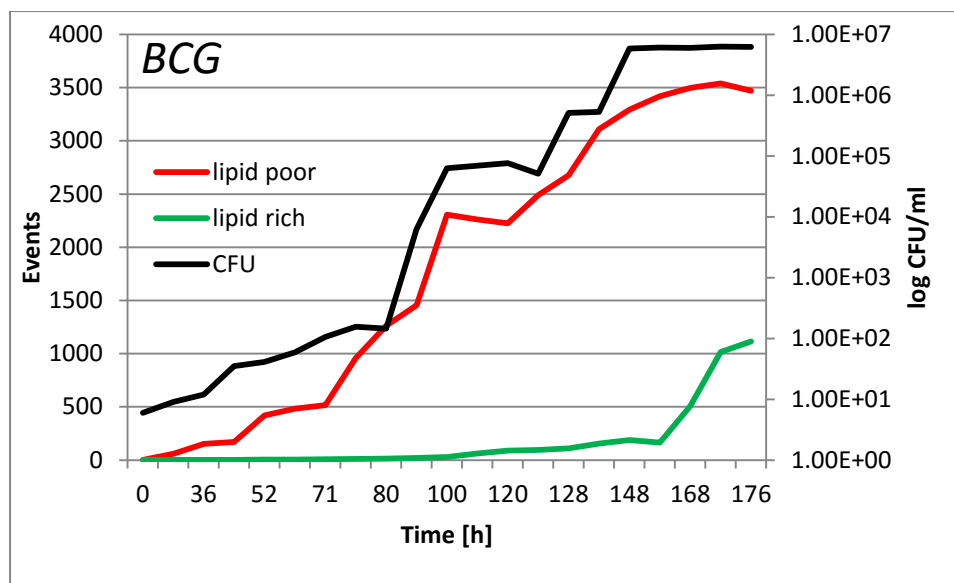


Figure 4.4. Quantity of non-polar lipid fluorescence increasing over time relative to the quantity of detected red fluorescence and the CFU value.

In a 288 hour experiment samples of *M. smegmatis* were taken at six intervals and stained with Nile red. Their relative quantities of green and red fluorescence were measured by flow cytometry and the results are displayed below. At 72 hours the quantity of non-polar (green) fluorescence is lower than the quantity of polar (red) fluorescence and is statistically close to 0. This indicates that there were few lipid bodies present at this stage however at 96 hours the quantity of green fluorescence has increased to levels comparable with red fluorescence. By 120 hours the quantity of green fluorescence has risen to a degree statistically higher than that of the red fluorescence indicating that 120 hours is the threshold for extracting cells to attempt to separate lipid rich from lipid poor; before this time point there were too few cells to make a high enough yield viable.

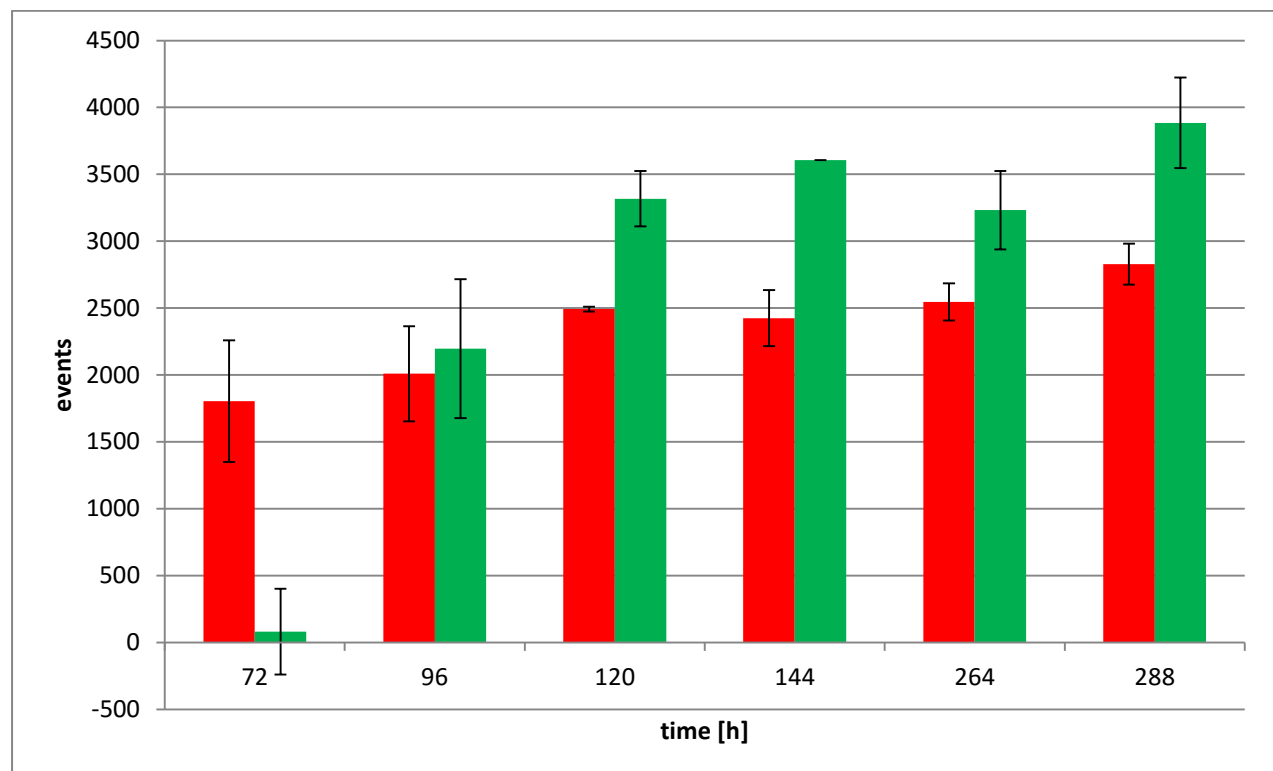


Figure 4.5. lipid profiles across 6 time points from 72-288 hours. The green bars indicate green (non-polar) fluorescence and red bars indicate red (polar) fluorescence. Quantities of green fluorescence rise to statistically significant levels after 120 hours. Error bars = 2 standard deviations from the mean. n = 3.

#### **4.6.5 Old Lipid-rich cells versus young lipid-rich cells**

In order to ascertain whether the presence of a lipid body in a mycobacterial cell or the cell's (culture's) age was the deciding factor for antibiotic resistance conducted experiments on young and old cultures separated into their LR and LP fractions. Table 4.7 clearly shows that irrespective of the age of the cells under investigation the LP cells not expressing lipid bodies have a significantly lower tolerance for all the drugs used in this study. The most striking difference is between old LP cells and old LR cells treated with rifampicin; old LP cells require 25µg/mL of rifampicin to clear all cells in culture whereas the same number of LR cells requires 1000µg/mL (1mg/ml) of rifampicin to get the same result.

Drugs	Old	Young	Old	Young	Old	Young	Old	Young	Old	Young	Old	Young	Old	Young	Old	Young
	Lipid poor MBC values for <b>M. smegmati s</b>	Lipid poor MBC values for <b>M. smegmati s</b>	Lipid rich MBC values for <b>M. smegmati s</b>	Lipid rich MBC values for <b>M. smegmati s</b>	Lipid poor MBC values for <b>M. marinum</b>	Lipid poor MBC values for <b>M. marinum</b>	Lipid rich MBC values for <b>M. marinum</b>	Lipid rich MBC values for <b>M. marinum</b>	Lipid poor MBC values for <b>M. fortuitu m</b>	Lipid poor MBC values for <b>M. fortuitu m</b>	Lipid rich MBC values for <b>M. fortuitu m</b>	Lipid rich MBC values for <b>M. fortuitu m</b>	Lipid poor MBC values for <b>BCG</b>	Lipid poor MBC values for <b>BCG</b>	Lipid rich MBC values for <b>BCG</b>	Lipid rich MBC values for <b>BCG</b>
Rifampicin (µg/mL)	25	50	1000	500	100	50	500	500	50	35	1000	100	1	2.5	5	5
Isoniazid (µg/mL)	30	50	1000	1000	50	35	750	1000	50	50	1000	1000	15	12.5	250	250
Ethambutol (µg/mL)	30	25	1000	500	10	25	150	250	na	na	na	na	50	50	250	500
Ciprofloxacin (µg/mL)	35	10	100	50	50	30	250	75	50	75	250	200	5	1	25	5

Table 4.7. Table displaying the raw values for the data shown in

Figure 4.6. For every species tested the same trend is true- the cells containing lipid bodies, irrespective of age, are the cells that are more resistant to the antibiotics used.

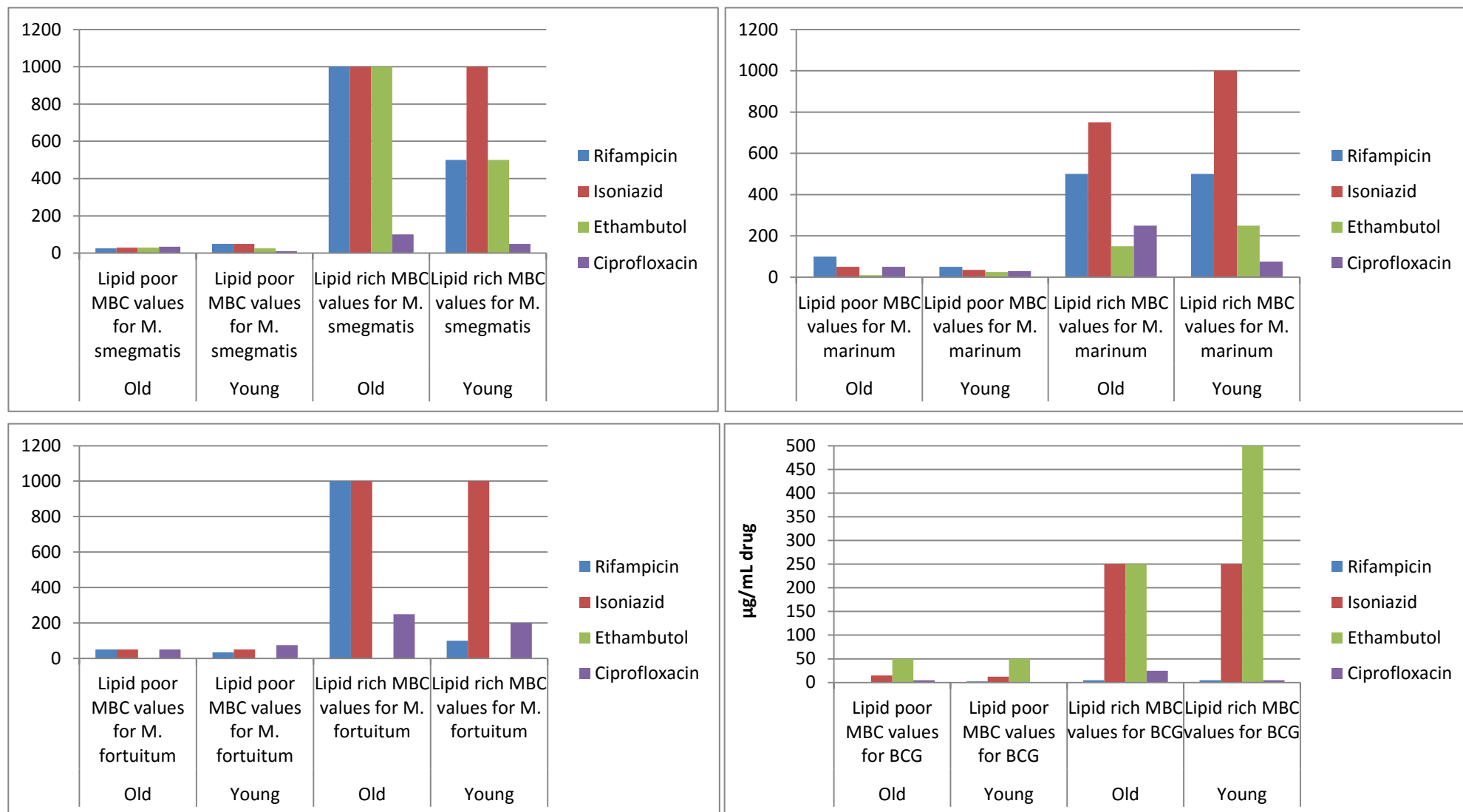


Figure 4.6. Concentrations of drugs required to completely sterilise cultures of mycobacteria, LR and LP Vs. old and young cultures

#### **4.6.6 Human lung tissue exhibiting LR cells**

Human lung tissue was examined microscopically after being stained with Nile red. Figure 4.7 shows the results of this staining regimen. While the staining was effective it also highlighted structures we were not investigating such as the large round objects in Figure 4.7C. It is difficult to know that these structures are without proper histopathological staining but in all images the arrows indicate structures we are confident are mycobacterial cells that are exhibiting lipid bodies. Some of these are free as in Figure 4.7A and Figure 4.7C but some (as in Figure 4.7B) seem to be within other small round objects. As above it is difficult to know what these objects are but it is possible given the close, straight constraints of the rest of the image that Figure 4.7B is a bronchiole and the round objects are alveolar macrophages that have phagocytosed the lipid rich cells.

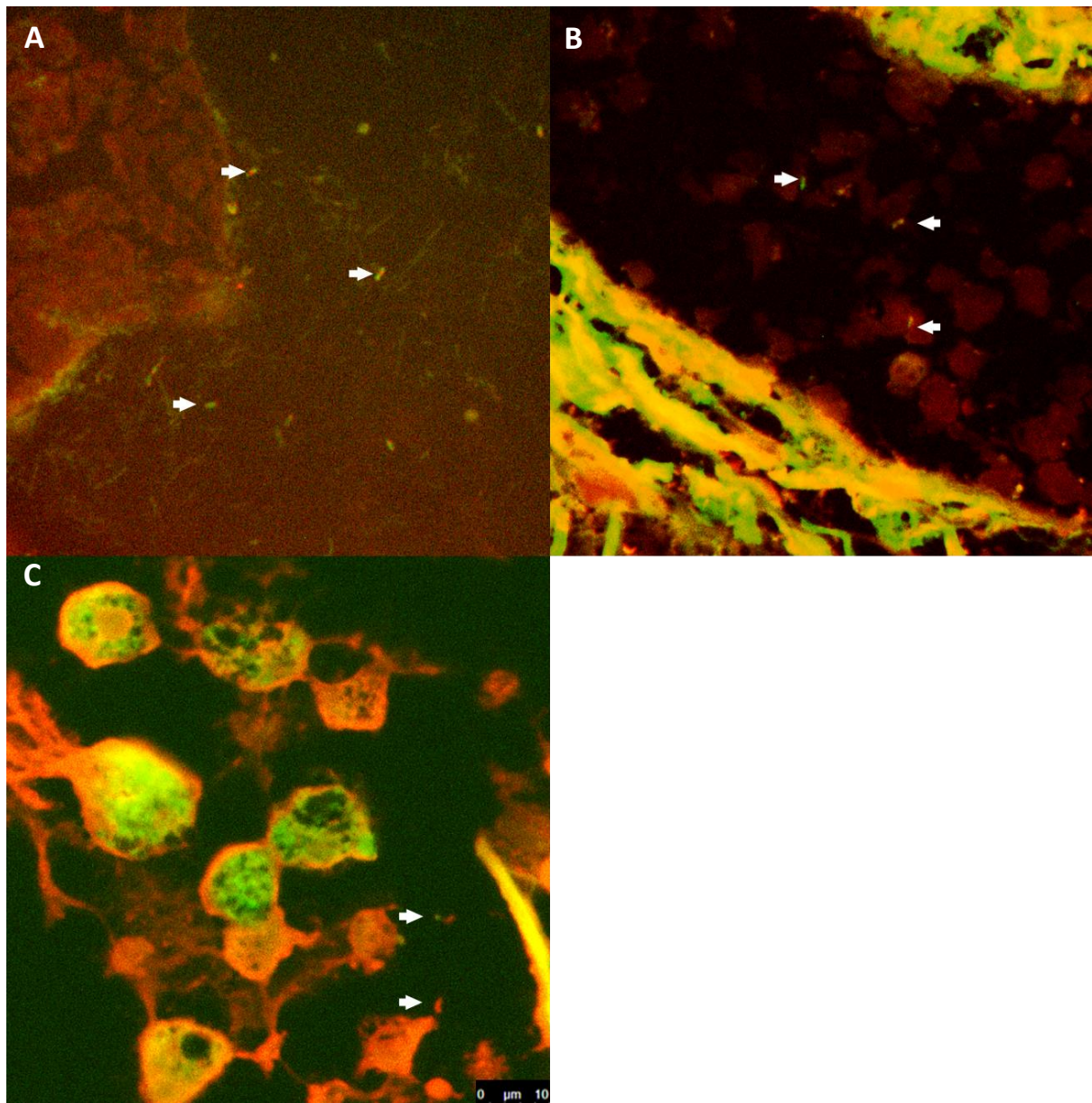


Figure 4.7. Images of human lung sections stained with Nile red. A shows a large open region, possibly a cavity containing many lipid rich cells besides those indicated. B shows lipid rich cells encapsulated within objects that are possibly macrophages in a bronchus. C shows one lipid rich and one lipid poor cell out with any host cells or obvious structures in addition to a number of structures that could be foamy macrophages. All images at 100X magnification.

Drug	MBC Lipid rich OLD μg/ml	MBC Lipid rich YOUNG μg/ml
Rifampicin	1000	500
Isoniazid	1000	1000
Ethambutol	1000	500
Ciprofloxacin	100	50

Table 4.8. Values for MBCs of cultures of *M. smegmatis* grown to either later stationary phase (old) or mid exponential phase (young), separated into LR and LP (LR only show here) and treated with increasing quantities of drugs until there was no detectable growth



## 4.7 Discussion

### 4.7.1 Susceptibility

We found that the presence of lipid bodies was correlated with an increase in resistance to the actions of the four antibiotics we used. This was found to be a function of the lipid body presence and was not correlated with the age of the culture.

The presence of lipid bodies could, in and of itself be the cause of the marked differences seen in drug tolerance between lipid rich and lipid poor cultures. It is known that lipid rich tissue can sequester drugs directly in mammals (Minder, Daniel et al. 1994). It is possible that in prokaryotes could have lipid rich regions that preferentially sequester drugs. This theory is lent credence by the fact that rifampicin, a frontline TB drug, has good lipid solubility (Singh, Bhandari et al. 2013) and we see the largest difference in drug susceptibility in *M. smegmatis* treated with rifampicin. Some of the other drugs used in this study have limited lipid solubility such as ethambutol (Ino-Ue and Yamamoto 2008) and ciprofloxacin (Maurer, Wong et al. 1998). If this is the case then it raises the question of what happens to the drug if and when it comes out of suspension in the lipid body. Does the cell have a mechanism by which it can shuttle the drug to the lipid vesicle and then jettison the vesicle as it is now toxic to the cell? Are the lipid bodies a survival mechanism for responding to antibiotic chemicals *in vivo* in which the cell has a detoxifying mechanism that it can use in the lipid body to render the antibiotics harmless? These are questions we have not set out to discover the answers to but they could form part of a new study in the future that could involve deep sequencing of the mycobacterial clade genome to discover the upregulated genes and promotion factors in the lipid rich cell.

If we reject the idea that the lipid bodies are themselves the mechanism of antibiotic resistance but simply a marker of a wider phenotypic change then we have to again address

the concept of dormancy. Lipid rich cells are thought to be in a form metabolic shutdown or dormancy. Whether lipid bodies being present is a sign of dormancy is still up for debate and something we hope to address in the future. Accepting that lipid bodies are a marker of dormancy (Daniel, Deb et al. 2004, Deb, Lee et al. 2009, Daniel, Maamar et al. 2011) we can begin to understand some of the data. A metabolic shut/slowdown occurring would affect the whole metabolome of the cell meaning that nutrients and other environmental factors were no longer being taken up from the surroundings. This means that drugs would no longer be effective against these non-replicating bacteria. This is especially true of isoniazid. Isoniazid is a prodrug meaning it must be metabolised, either by the infective agent or the host, to become an active pharmaceutical agent. Isoniazid is activated by a bacterial catalase-peroxidase enzyme called KatG that is found in MTB (Suarez, Rangelova et al. 2009). KatG couples the isonicotinic acyl with NADH to form isonicotinic acyl-NADH complex. This complex binds tightly to the enoyl-acyl carrier protein reductase known as InhA, thereby blocking the natural enoyl-AcpM substrate and the action of fatty acid synthase. This process inhibits the synthesis of mycolic acid, required for the mycobacterial cell wall (Master, Springer et al. 2002). Isoniazid is bactericidal to rapidly dividing mycobacteria, but is bacteriostatic if the mycobacteria are slow-growing (Ahmad, Klinkenberg et al. 2009).

If there was a global metabolic shutdown rather than a slowdown none of the cells would be metabolising at all. The drugs that simply diffuse passively across the cell membranes would still act upon the cells they are within but isoniazid, a pro-drug, would not be taken up and metabolised and therefore its action would be completely neutralised. This would also be true of two drugs not used in this study, pyrazinamide- a highly effective frontline

anti-TB drug that is difficult to use *in vitro* is also a prodrug as is PA-824, an experimental drug that shows great promise in clinical trials.

One of the most interesting results from the piece of work is the discovery of young lipid rich cells. It has been thought for a long time that lipid rich cells were an artefact of an aged culture in which cells are old and stressed; lacking in nutrients and oxygen they form storage vesicles to allow them to resuscitate in more favourable conditions. We have shown that even in a young, well oxygenated exponential culture with plenty of carbon sources there are lipid rich cells. This indicates that the formation of lipid bodies is a natural part of the cell cycle and occurs without the need of external stimuli such as oxygen or pH stress.

The discovery of exponential phase lipid rich cells and their similar reactions to more 'classical' (stationary phase) lipid rich cells demonstrates that it is the presence of lipid bodies, not the age of a culture that dictates whether there will be a strong antibiotic resistance in that culture. As mentioned above (page 171) the association solely between mycobacterial cells containing lipid inclusion vesicles and aged cultures has been disputed by our findings. There could be wider biological and clinical implications for this data. As lipid bodies exist in younger cultures of all mycobacterial species tested it is likely that they exist in MTB, indeed we have shown in Figure 4.7 that MTB does include lipid bodies and in *in vivo* samples. If these lipid rich cells are present from the initiation of infection then these could be a missing population of latent mycobacterial cells in human infection that are resistant to chemotherapy that have been hypothesised before (Wayne and Sohaskey 2001, Cosma, Sherman et al. 2003, Daniel, Maamar et al. 2011). Another, linked, possibility is that the lipid rich cells could be a source of relapse amongst patients that diligently keep to their

drug regimen but after it has ended the cells, resistant due to their status as lipid rich cells, are able to re-emerge and effectively re-infect.

In order to be sure that when we tested the lipid rich fraction from a young culture that we weren't testing old cells from a previous inoculum that had been 'carried over' we used FitC to detect if the cells in the LR or LP fractions were old or young. We found that there was a comparable number of bright green events in both LR and LP fractions meaning that there is no statistical difference between the two fractions in terms of the number of non-dividing cells present. This means that we can be sure that it is not the presence of old cells carried over into young cultures that are the source of the young lipid rich cells we see meaning the phenomenon of a young lipid rich cell is genuine.

## **4.7.2 Staining**

### **4.7.2.1 NR/DAPI**

Numerous staining regimens were used during this study. Bodipy 356, Oil red O, and Nile red were all used as lipophilic stains and combined in some cases with DAPI, Hoechst or SYTOX green to indicate the boundaries of the cell. These regimens were assessed both combined and separate until the final regimen was decided upon- Nile red alone. Nile red has the benefit of being both lipophilic and a polarity indicator. When combined with Sytox green the DNA of the cell was visible as a bright green smear but this occluded the view of the lipid bodies as we theorised at the time that the lipid bodies would appear as blue-shifted (from crimson red) internal vesicles. When Hoechst was used the DNA was clearly visible as an intense blue fluorescent but there seemed to be some unknown interaction with the Nile red causing a bright halo to appear around the cells. In dilute samples this was

acceptable but in concentrated samples this represented a significant problem so this regimen was abandoned. When combining Nile red with DAPI another interesting reaction took place; there seemed to be bodies appearing at the polar ends of the cell in some cases, these were very abundant and in others they were scarce. As can be seen in Figure 4.2 these bodies appear yellow/gold and can also appear on the medial line of the cell. These structures were at first thought to be lipid bodies but as they did not change in size, density or granularity as the cultures were stressed or aged this theory was dismissed. Literature searching garnered better results (Kapuscinski 1990), we found that RNA is known to fluoresce at a red-shifted wavelength with DAPI. This answered the question of what the bodies seen were but not why they were there. As this was not pertinent to the investigation this line of inquiry was dropped but it remains an interesting mystery.

We found Nile red alone to be the best stain as it allows us to see the whole cell envelope in red and allows us to see the internal lipid droplets in green. This allows for a good degree of disparity between the two structures and for our purposes was quite sufficient. Accepted Nile red protocols exist and these are what were followed when this study was first undertaken however there was room for improvement. We experimented with numerous solvents to dissolve the Nile red and have it cross the cell membranes and wall easily but in the end we adapted our own regimen to include Dimethyl sulfoxide (DMSO (sigma)) to facilitate entry to the cell. Nile red is also readily soluble in DMSO. When staining human tissue and artificial sputum there are added difficulties. The background fluorescence of a clean glass slide is negligible, not so for tissue samples. When staining with NR, especially in lung tissue, there is a large background of both green and red fluorescence as there are many host cells present containing lipids or other polar/non-polar substances. Some of these substances are excreted surfactant which stains green as it is a lipoprotein (Goerke

1998) and cell membranes of host cells that stain red as they contain a high proportion of phospholipids. We have yet to use genuine human sputum but we have a laboratory analogue made with porcine mucin and various salts to imitate human sputum. With this artificial media the background issues are not as obvious as with lung tissue but there is still significant background fluorescence and bacterial clumping. This issue will have to be rectified if further human biopsy studies are to be carried out or it might be possible to use the same NR staining protocol but use consecutive, successive cryotome slices through a lesion or cavity in a lung sample and stain each slice with a different stain such as ZN, NR and sudan black. This would allow us to see the presence of the tubercle bacilli with ZN staining, see the lipid bodies with NR but with significant background and then see lipid rich regions in a non-fluorescent format with sudan black staining. This work is currently possible and ready to begin but has yet to.

Another way around the problem of very high background would be to use immunofluorescence with antibodies specific for MTB surface antigens conjugated to a fluorescent probe. This has the drawback of non-specific binding being a potential issue with so much unquantified tissue in a biopsy sample it is possible that the antibodies would bind to random pieces of human tissue.

### **4.7.3 Flow Cytometry data**

Staining for use of the flow cytometer presented a new set of challenges. When using NR the solvent environment is important to consider. NR will readily and rapidly come out of solution in aqueous solvents so mixed NR in any solvent with bacteria in standard media causes an immediate precipitation of a large portion of the dissolved NR. As flowing volatile

compounds through the flow cytometer is discouraged we tried different methods for detecting lipid bodies in the flow cytometer with varying degrees of success.

As the lipid bodies are non-transparent at the flow cytometers excitation wavelength (488nm) we can use the sideways scattering to differentiate them from their lipid poor cohorts. The sideways scattering angle (broadly speaking) is a measure of the granularity of the cell in the beam line. As the lipid bodies cause more scattering this seemed a reasonable measurement for differentiation. After some experimentation we found it was difficult to get good discrepancy between LP and LR cells so this method was not used. We tried the same methods as were used in the microscopy staining but found the same as before; that NR is the best stain for the job.

In order to reduce the issue of crystals of NR coming out of solution we added various wash steps and tightened the acceptance thresholds on the flow cytometer meaning that we are now confident that any crystals that are washed through the flow cytometer are not counted or if they are they are in a negligible quantity.

#### **4.7.4 As a function of time – when to LBs form?**

The data displayed here show the stages of the growth cycle at which lipid bodies begin to appear. We have found that lipid bodies appear only after the cultures have reached stationary phase. In the case of a mid-exponential phase plateau there will be a small rise in lipid bodies present which does not diminish, only growing in number once the culture reached it's true stationary phase.

This could be due to a number of factors such as lipid bodies being a stress response- the cells getting ready to 'hibernate'- become dormant and wait until the situation has become

more favourable. It could also be that it is a natural part of the cell cycle, once a threshold is reached of bacteria forming lipid bodies it begins a chain reaction via quorum sensing until all or most of the cells in a population are expressing lipid bodies. This could be because of an evolutionary advantage to being in the host; in a stressful environment (a necrotic lesion, for example) some cells begin to become dormant and generate lipid bodies. These cells send out chemical messages to other cells in the area that do the same, thus allowing this second wave of bacteria to form better, more robust lipid bodies in their comparably favourable environment. These lipid bodies will be used as a carbon source later when the environment becomes more favourable. This also allows the cells a longer time to exist out with the host in an external environment after being expelled from the host via a cough or sneeze, meaning that infection of new host is easier and more likely.

In parallel with the previous experiment into the timing of the formation of lipid bodies RNA expression profile experiments were undertaken.

These two sets of experiments largely agree on the timing of stationary phase occurring in *M. smegmatis*; approximately 70 hours after first inoculation with <1000 cells. Beyond that we were hoping to observe an obvious change in the expression of one of the RNA species we chose around the time that lipid bodies form. We were unsuccessful in that endeavour but we did observe something interesting. At approximately 200 hours the concentrations of pre-16sRNA begin to fall. This could be an indication of the cells beginning to enter a dormant state although this seems unlikely given our previous experiments showing that lipid body formation spikes at around 100 hours. Another explanation could be simply that the cells in culture are aging. At 200 hours the cells have been at stationary phase for 100 hours or 25 generations without the cell number changing. Either the cells are not dividing anymore and are aging, possibly moving towards a dormant phenotype, or there is still



some cell division going on and the level of fission is equal to the level of cell death. The drop in pre-16sRNA could be an indication that the culture was about to enter the death phase as the cells are completely bereft of nutrients or oxygen.

This gives us important data. If we want to experiment on cells that are lipid rich and 'dormant' but are not entering another phase of the cell cycle, the death phase, we have a window of approximately 25 generations in which to experiment on them while the quantities of the RNA species we investigated are relatively stable; between the beginning of the stationary phase, after 25 generations, and before the beginning of the death phase, after 50 generations.

#### **4.7.5 Lung**

The images of the lung tissue are a tantalizing insight into lipid rich cells in human disease. The three images displayed here show lipid rich cells inside human lung tissue. Some of the tubercle bacilli appear to be in open space, likely a cavity. Some are inside a channel of some kind, possibly a bronchiole, and within other cellular structures, possibly alveolar macrophages. We cannot say with any degree of certainty what these structures are given the problems with NR staining of tissue delineated above. Ways of addressing this problem are also addressed above but these images do show one thing certainly- after a patient has died, their biopsied tissue removed and dehydrated, mounted and stained with ZN some of the lipid rich cells remain even after a further round of staining with NR in ethanol.

#### **4.7.6 Old Lipid-rich cells versus young lipid-rich cells**

The data displayed in Table 4.7 clearly shows that irrespective of age the cells that contain lipid bodies are more resistant to drugs than the cells that are not expressing lipid bodies, as separated by our separation technique. There is a discrepancy between the data for old and young lipid rich cells can be seen in Table 4.8. This discrepancy can be explained by the dilution method employed for this study. The concentrations of drugs used were in relatively small increments at low concentrations but became more massive as the concentrations became higher. The dilution regimen was such that large increments existed between drug concentrations. This explains the large differences between, of example, the result for old LR cells treated with ethambutol versus the young LR cells treated with ethambutol. The true answer probably lies somewhere between the two values of 500 $\mu$ g/mL and 1000 $\mu$ g/mL of drug.

# 5 Lipidomics

## 5.1 Introduction to lipidomics

Lipidomics is the study of cellular lipids in living systems (Wenk 2005). Like genomics which is the global study of an organism's genome lipidomics is the global study of all the lipids within a given organism - its lipidome. Lipidomics is concerned with the structure, function and metabolism of lipids and compliments the related fields of genomics and proteomics to complete the picture of systems biology in an organism (Han 2007) (arguably along with the 'metabolome' which is concerned with carbohydrates and lipids in the cell). Lipidomics is a relatively new field and has been accelerated by the advances in mass spectrometry and fluorescence spectroscopy, among others.

Lipidomics research involves the identification and quantification of the thousands of cellular lipid molecular species and their interactions with other lipids, proteins, and other metabolites. An investigator into lipidomics will examine the structures, functions, interactions, and dynamics of cellular lipids and the changes that occur if a cell is damaged or in some other way perturbed.

Han and Gross (Han and Gross 2003) first defined the field of lipidomics through investigating the specific chemical properties of lipid species and using a new mass spectrometric approach; electrospray ionisation mass spectrometry (ESI/MS). Although lipidomics is under the umbrella of the more general field of "metabolomics", lipidomics is itself a distinct discipline due to the uniqueness and functional specificity of lipids relative to other metabolites.

There are numerous ways to go about establishing the lipidome of an organism. We knew that MTB contains unusual and unique lipids and wanted to establish whether other strains

we were working with had the same or similar lipid profiles. We decided to address one of the simplest means of establishing a lipid profile first and perform whole cell lipid extractions (Bligh and Dyer extraction (Bligh and Dyer 1959)) and investigate these extracts with thin layer chromatography (TLC).

### **5.1.1 TLC**

Thin-layer chromatography (TLC) is a chromatography technique used to separate non-volatile mixtures of substances in a volatile mobile phase. Thin-layer chromatography is performed on a sheet of glass, plastic, or aluminium foil, which is coated with a thin layer of adsorbent material, usually silica gel, aluminium oxide, or cellulose. This layer of adsorbent is known as the stationary phase.

After the sample has been applied on the plate, a solvent or solvent mixture (mobile phase) is drawn up the plate via capillary action. Because different substances will ascend the TLC plate at different rates, separation is achieved

### **5.1.2 Mass Spectrometry**

Mass spectrometry (MS) is an analytical technique that allows identification of the amount and type of chemicals present in a sample by measuring the mass-to-charge ratio and abundance of gas-phase ions (Boggess 2001).

The read out from a mass spectrometer is in the form of a mass spectrum. It is a plot of the ion signal as a function of the mass to charge ratio.

The mass to charge ratio is the relationship between the size of a particle in atomic mass units and the ease with which it is ionised in the mass spectrometer. The  $m$  refers to the

molecular or atomic mass number and  $z$  to the charge number of the ion. The charge number is the amount by which an ion can be charged and related to its valency.

In a typical MS procedure, a sample, which may be solid, liquid, or gas, is ionized by bombarding it with high energy particles or waves such as electrons. This may cause some of the sample's molecules to break into charged fragments. These ions are then separated according to their mass-to-charge ratio, typically by accelerating them and subjecting them to an electric or magnetic field. Ions of the same mass-to-charge ratio will undergo the same amount of deflection (Boggess 2001). The ions are detected by a mechanism capable of detecting charged particles, such as an electron multiplier. Results are displayed as spectra of the relative abundance of detected ions as a function of the mass-to-charge ratio. The resulting data can be interpreted by existing knowledge of the mass and characteristic ionization of individual ions and molecules.

## 5.2 Methods

### 5.2.1 Lipidomics

#### 5.2.1.1 TLC

Bacteria were regrown to late stationary phase and centrifuged and washed in PBS three times. They were then subjected to lipid extraction as described by Bligh and Dyer (Bligh and Dyer 1959). Once dried onto glass vials the whole lipid contents were resuspended in 2:1 (v/v) mixture of chloroform and methanol and vortexed to ensure all lipid residue had left the glass.

Aluminium-backed silica TLC plates were used (Merck). These were pre-run in a tank containing chloroform/methanol (1:1, v/v) up to the top to remove any contaminant from the silica gel. Clean plates were stored in another glass tank. A line was drawn *gently* on the plate 10 mm from the base of the plate in pencil to mark where the lipid would be spotted on. Concentrate solutions of lipids in chloroform/methanol mixtures (2/1, v/v) are applied (1 to 10  $\mu$ L per spot) as fine rows at 2.5 cm of the bottom of the plate and separated from each other by 1 cm. After evaporation with the help of a nitrogen flow or a cool air blowing plates were placed immediately in the elution tank (height of solvent: 5 mm, eluent mixture hexane/diethyl ether/ glacial acetic acid (60/40/2, v/v)) and the solvent was allowed to ascend to within about 2 cm of the top of the plate. Plates were then removed from the tank and the solvent was allowed to evaporate in the fume hood.

When the solvent has evaporated (~10 mins), the primuline solution (5 mg in 100 mL of acetone/water (80/20, v/v)) is sprayed with an all-glass atomizer and the plate is viewed under ultraviolet light (340 nm). Lipids appear as bright yellow spots on a clear background, neutral lipids are at a low distance from the solvent front and polar lipids remain at the deposit line (see Figure 5.2 and Figure 5.8).

#### **5.2.1.2 TLC purification of lipids**

Once the plates have been viewed the spots were cut out of the plate and the lipids recovered from the silica gel by eluting the spots in glass tubes with 2 x 1.5 mL hexane/diethyl ether (1/1, v/v). These samples were allowed to evaporate and were then sent for mass spec analysis.

#### **5.2.1.3 Mass spec**

Cells were harvested and washed in PBS and extracted according to the Bligh-Dyer method (Bligh and Dyer 1959), dried under N<sub>2</sub>, and stored at 4°C until analysed by electrospray mass spectrometry (ES-MS and ES-MS/MS). Total lipid extracts were dissolved in 100 µl of chloroform:methanol (1:2) and analysed with a Absciex 4000 QTrap – a triple quadrupole mass spectrometer equipped with a nanoelectrospray source. Samples (15 µl) were delivered using a Nanomate interface (Advion, Inc.) in direct infusion mode (~ 125 nl min<sup>-1</sup>). The lipid extracts were analysed in both positive and negative ion modes using a capillary voltage of 1.25 kV. MS/MS scanning (daughter and precursor scans) were performed using nitrogen as the collision gas with collision energies between 35–100 V. Each spectrum encompasses at least 50 repetitive scans. Tandem mass spectra (MS/MS) were obtained with collision energies as follows: 35–55 V, inositol containing lipids in negative ion mode, parent-ion scanning of m/z 241; 35–65 V, PE in negative ion mode, parent-ion scanning of m/z 196; 40–100 V, for all glycerophospholipids (including PG and CL) detected by precursor scanning for m/z 153 in negative ion mode. MS/MS fragmentation/daughter ion scanning was performed with collision energies between 35–100 V. For each sample data was acquired in three distinct scan windows 600-1000 m/z, 1000-2000 m/z and 2000-2800 m/z.

The assignment of lipid species is based upon a combination of survey, daughter, and precursor scans, as well as previous assignments (Rhoades, Hsu et al. 2003, Layre, Sweet et al. 2011, Sartain, Dick et al. 2011, Pacheco, Hsu et al. 2013). The identity of lipid peaks was also supported by using the *M. tuberculosis* species-specific database at the LIPID MAPS: Nature Lipidomics Gateway (<http://www.lipidmaps.org>). In order to compare the peak heights relative to each other, peaks (detectable above background) were measured by ion intensities and their relative ratios were calculated.

### **5.2.2 Artificial lipid accumulation**

Cultures of mycobacteria were grown to mid exponential phase (see Figure 5.1) in round bottomed 14mL incubation tubes and then aliquoted in their original media into two separate 14mL incubation tubes. To one tube 500µL of a mixture of known lipids was added (the 'fed' population) and the contents vortexed. To the other tube 500µL of PBS was added as a control (the 'unfed' population). These samples were then placed back into the incubator at 37°C for 48 hours. After this time the cultures were removed from the incubator and samples were taken into sterile 1.5mL microcentrifuge tubes. These samples were then stained with Nile red as discussed previously (see section 4.2). Stained samples of both populations were heat fixed to clean glass slides and visualised under fluorescent microscopy to assess the presence of lipid bodies and the relative abundance of lipid bodies when comparing the 'fed' to the 'unfed' population. Cells from these samples were isolated by centrifugation (20,000g for 3 minutes to pellet the cells) and TLC was then carried out alongside the original lipid mixture.



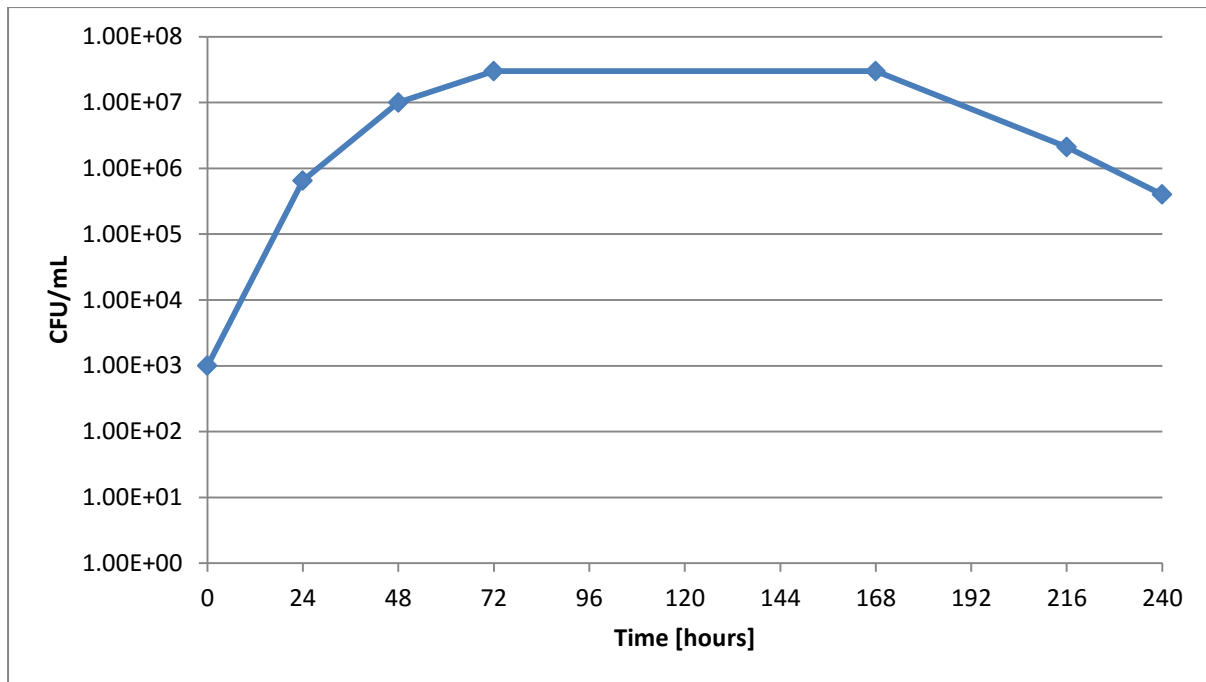


Figure 5.1. Figure displaying a growth curve of *M. smegmatis* over 10 days. The logarithmic phase is between 0 and 72 hours, the stationary phase is between 72 and 168 hours and the death or decline phase is from 168-240 hours. This growth curve was conducted with bacteria already in exponential phase growth so the lag phase is small or non-existent.

## 5.3 Results

### 5.3.1 TLC

TLC experiments show that there is a difference in the lipid content of old (late stationary phase) and young (mid-exponential phase, see Figure 5.1) mycobacteria. Some of the lipid spots appear to be similar in both old and young cultures of the same species but some are clearly different; present in the older culture but not in the younger (see BCG and *M. marinum*).

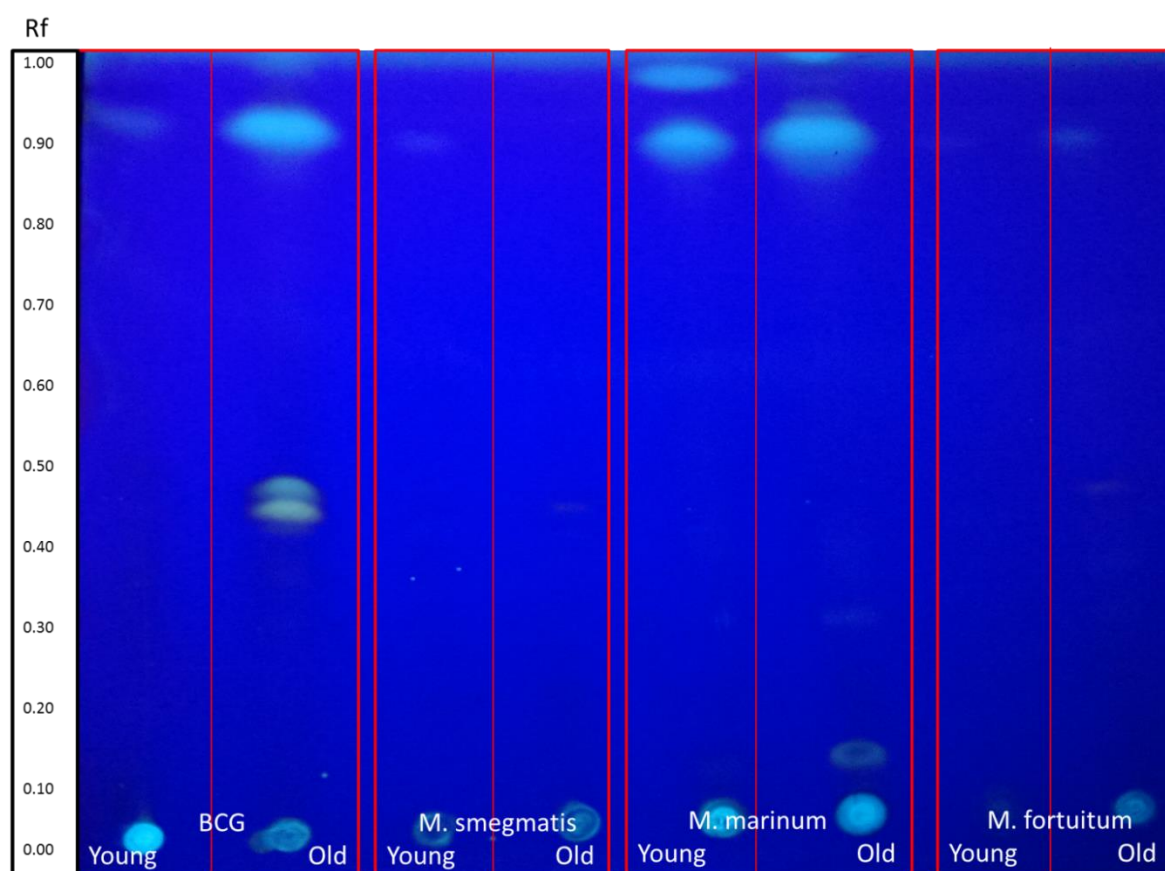


Figure 5.2. Comparison of TLC results from a whole lipid extraction of four mycobacterial species in different culture stages; young (mid-exponential phase) and old (late stationary phase). Bright spots at the bottom indicate the position of the polar lipids which in this solvent system do not move. Solvent system; 60:40:2 hexane : diethyl ether : glacial acetic acid. Rf refers to Rf values; the measurement of the movement of the lipids and there relative polarity (see Table 5.1). NB not all spots are visible on this image, some are very faint.

Lipid (family)	Rf value
Cholesterol ester	0.965-0.97
steryl esters	0.94-0.96
wax esters	0.86-0.92
fatty acid methyl esters	0.81-0.84
triacylglycerols	0.69-0.73
fatty acids	0.33-0.58
fatty alcohols	0.28-0.29
1,3-diacylglycerols	0.24-0.255
sterols	0.24-0.26
1,2-diacylglycerols	0.21-0.23
carotenoids	0.0-0.2

Table 5.1. Table showing the accepted Rf values for the solvent system used in Figure 5.2 and the associated predicted lipid position. The Rf values displayed here are derived from standardised tables of Rf values for any given solvent system.

The data displayed in Figure 5.2 and

Table 5.1 when taken together allow us to examine the lipids found in the TLC analysis of these mycobacteria. Figure 5.3 displays all the Rf values derived from successful TLC experiments over the course of this study. It is important to note that in Figure 5.2 there are numerous groups of interest, especially in the 'old' samples. In the BCG sample there is a double band at approximately Rf ~0.45. This double band corresponds to two distinct fatty acid groups, the lower being of a longer chain fatty acid than the upper. There is also

evident a dramatic increase in the quantity of the lipid present at  $R_f \sim 0.91$ . This band corresponds to wax esters or sterol esters both of which have been noted before in older cultures of mycobacteria (Garton, Christensen et al. 2002, Deb, Lee et al. 2009, Sirakova, Burnett School of Biomedical Sciences et al. 2012). The other samples shown follow similar patterns with the exception of *M. marinum*. Older cultures of *M. marinum* are known to turn yellow in colour on exposure to sunlight (see Table 1.1), this is what has occurred here and the resulting spot on the TLC plate indicated that at least one of the coloured compounds is likely a carotenoid.

0.0	0.1	0.2	0.3	0.4	0.5	0.6	0.7	0.8	0.9		
0.076	0.123	0.211	0.300	0.413	0.507	0.644		0.814	0.900		
	0.137	0.211	0.300	0.414	0.534	0.644		0.833	0.902	Cholesterol ester	0.965-0.97
	0.137	0.214	0.300	0.455	0.535	0.644		0.841	0.909	steryl esters	0.94-0.96
	0.153	0.214	0.301	0.463	0.563	0.644		0.859	0.913	wax esters	0.86-0.92
		0.220	0.301	0.463	0.575	0.645		0.859	0.913	fatty acid methyl esters	0.81-0.84
		0.233	0.303		0.589	0.645		0.863	0.919	triacylglycerols	0.69-0.73
		0.233	0.306			0.647		0.871	0.925	fatty acids	0.33-0.58
		0.247	0.306			0.647		0.873	0.925	fatty alcohols	0.28-0.29
		0.247	0.313			0.647		0.887	0.927	1,3-diacylglycerols	0.24-0.255
		0.247	0.314			0.647		0.888	0.932	sterols	0.24-0.26
		0.250	0.319			0.649		0.888	0.932	1,2-diacylglycerols	0.21-0.23
		0.250	0.324			0.657		0.889	0.932	carotenoids	0.0-0.2
		0.250	0.324			0.659			0.943		
		0.254	0.324			0.659			0.944		
		0.260	0.331						0.944		
		0.260	0.331						0.951		
		0.260	0.338						0.952		
		0.260	0.350						0.959		
		0.260	0.356						0.963		
		0.263	0.356						0.963		
		0.263	0.356						0.963		
		0.264	0.363						0.963		
		0.264	0.363						0.965		
		0.274	0.363						0.966		
		0.274	0.363						0.972		
		0.274	0.370						0.973		
		0.288	0.375						0.975		
		0.292	0.375						0.979		
		0.295	0.375						0.985		
		0.295	0.390						0.986		
		0.296	0.397						0.986		
		0.296	0.397						0.986		
		0.296							0.988		

Figure 5.3. Figure displaying the Rf values for every successful TLC experiment colour coded to their respective lipid family (as in Table 5.1). The most abundant detected lipid group was the free fatty acids (Rf 0.33-0.58) but many of the lipid families previously reported in mycobacteria are represented, importantly the triacylglycerols and wax esters (Garton, Christensen et al. 2002, Deb, Lee et al. 2009, Sirakova, Burnett School of Biomedical Sciences et al. 2012).

### 5.3.2 Mass spectrometry

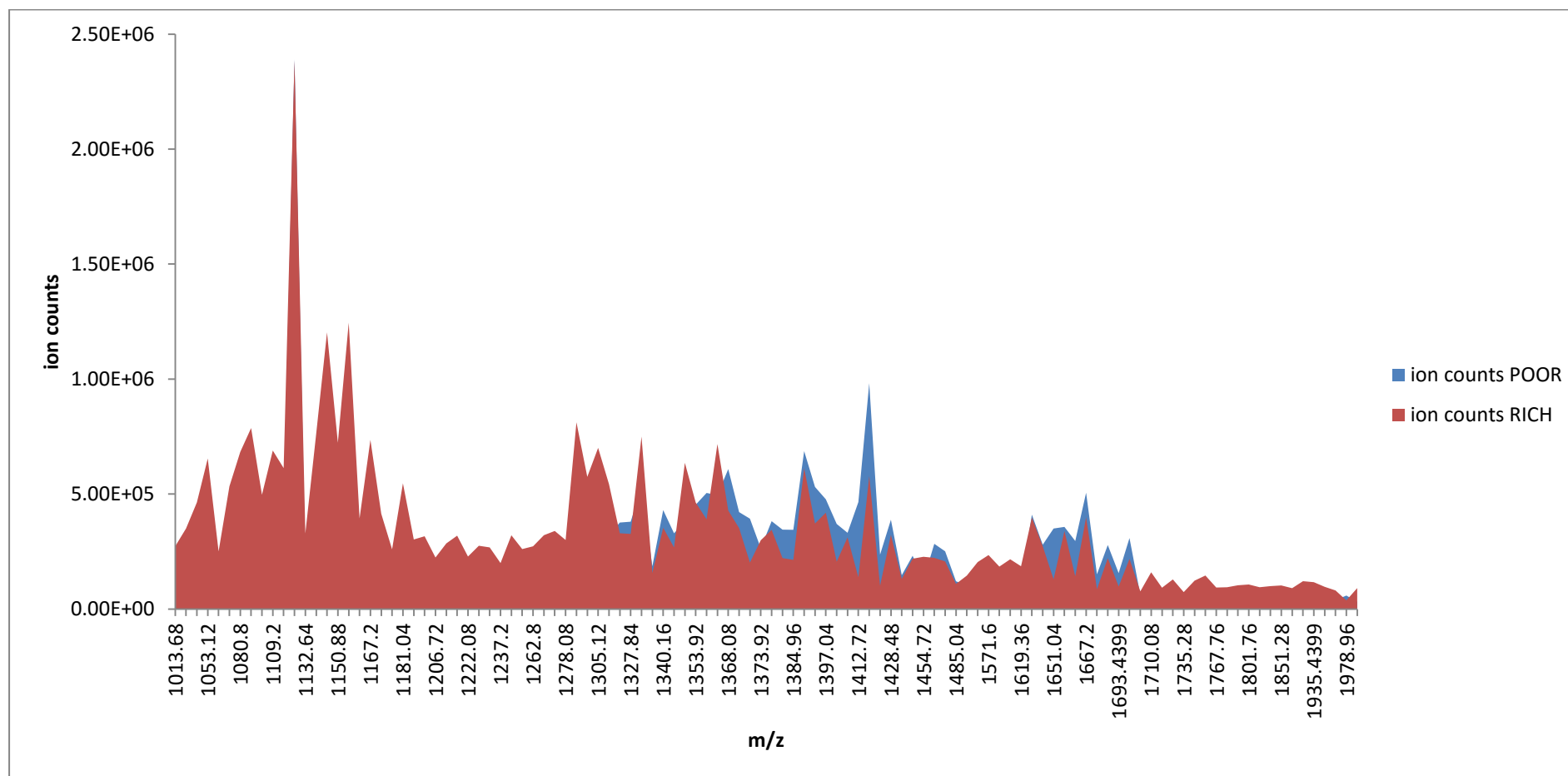


Figure 5.4. Gross ion counts for numerous lipid species recovered from a Bligh and Dyer extraction of lipid rich and lipid poor BCG. It appears that the larger and smaller mass-to-charge species are more present in the lipid rich sample with the species in the middle range more abundant in the lipid poor sample. This work was conducted by Dr Simon Young.

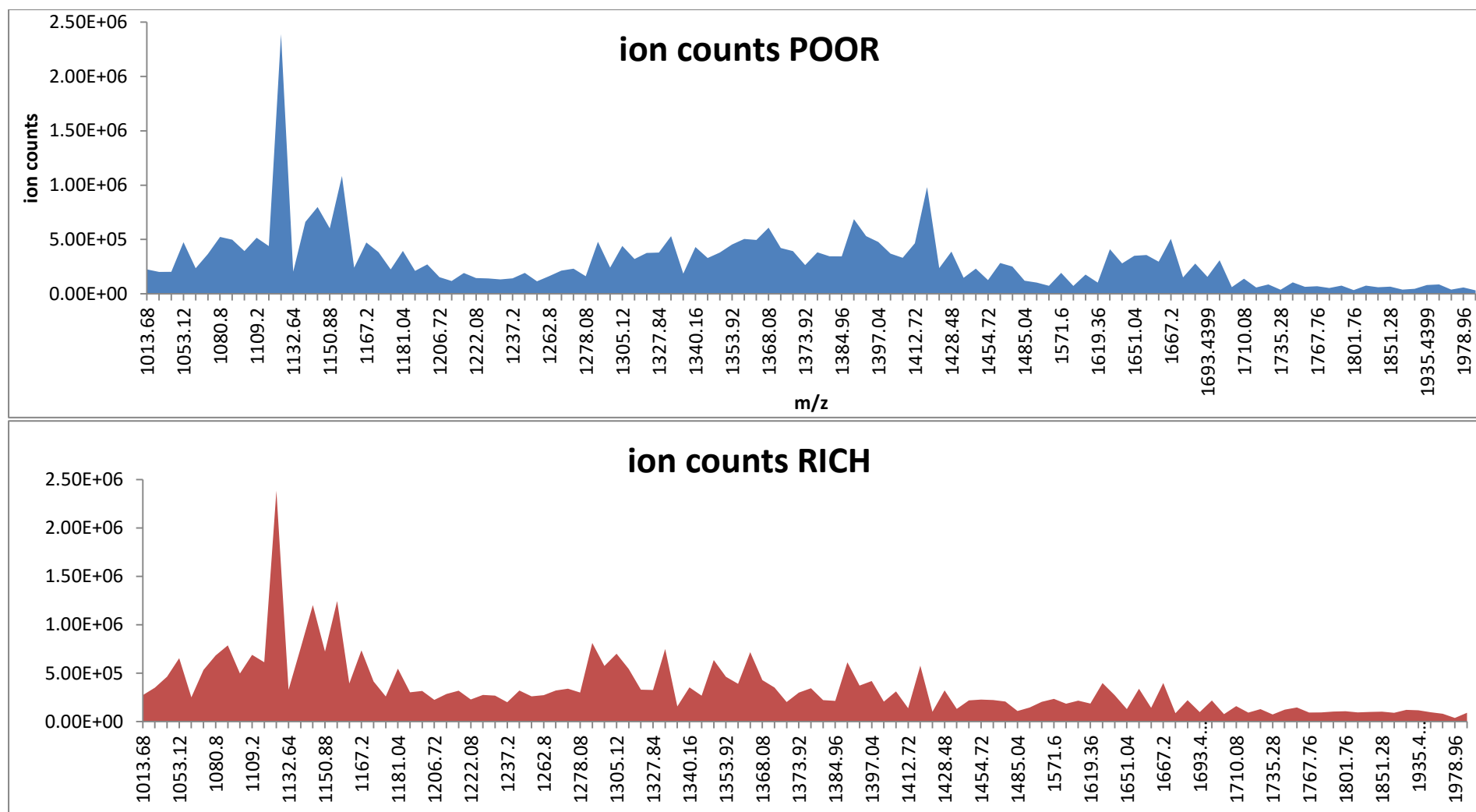


Figure 5.4. Data from Figure 5.4 displayed separately. It is possible to see that there are higher peaks in certain regions corresponding to discrete lipids, this is shown more obviously in

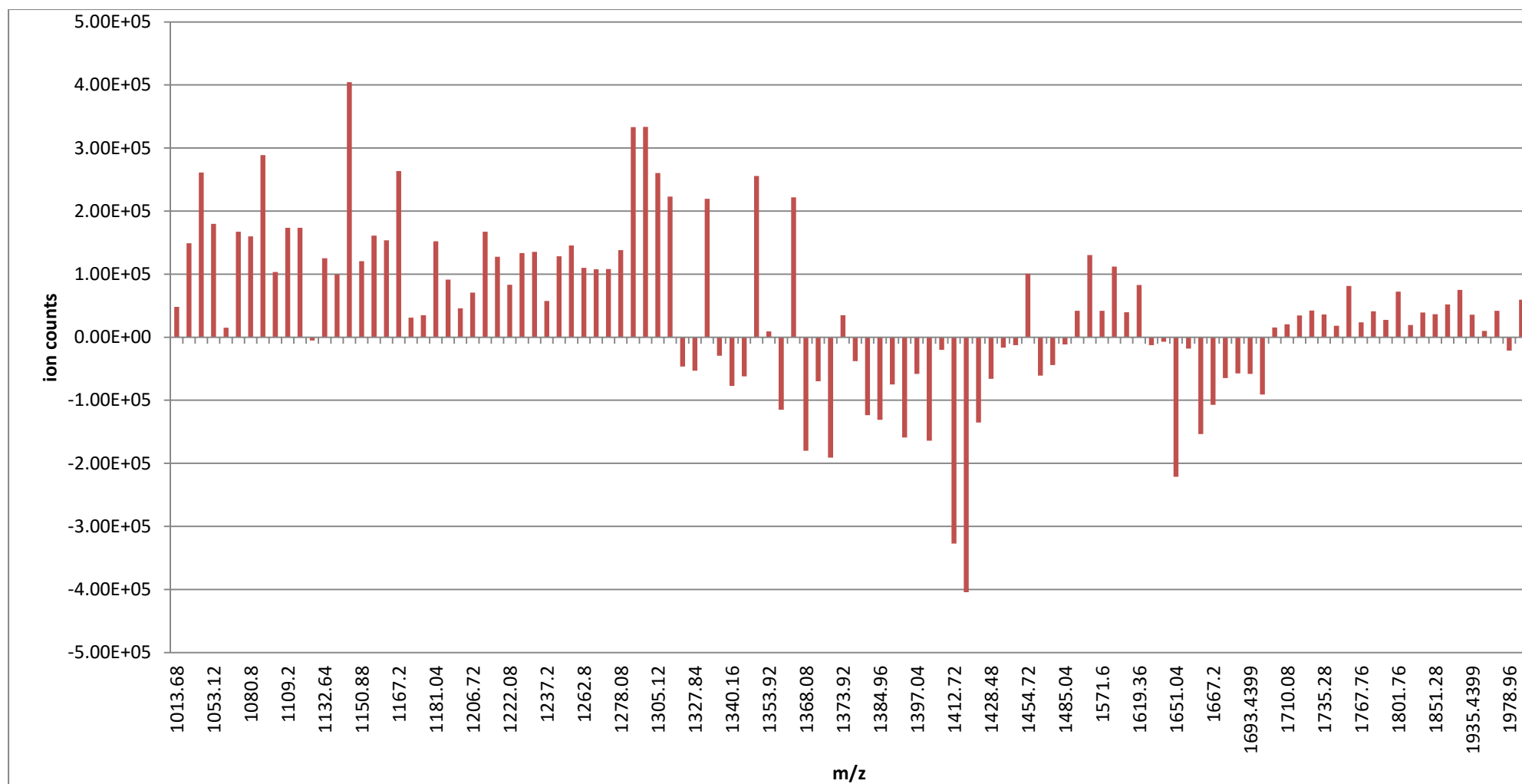


Figure 5.5. Data from Figure 5.4 displayed in terms of the absolute difference in the relative ion counts. Where a peak is negative it indicates that that lipid is more abundant in the lipid poor fraction. Where a peak is positive it indicates that lipid is more abundant in the lipid rich fraction.



Figures 5.4, 5.5 and 5.6 all display data from a single experiment performed by Dr Simon Young of the BSRC Annex at St Andrews University. This data displays the relative differences in abundance of various lipids between 1000-2000 m/z (mass to charge ratio). This is only a portion of all the available data but even so it lends some interesting insights. It can be seen that there are definitely lipids which are more abundant in the lipid poor fraction. These lipids are primarily members of the Glucose monomycolate (GMM) family and are known to elicit a strong immune response (see section 6.5). Many other lipids are, as expected, upregulated in the lipid rich fraction such as mycolic acids (MAs) and phosphatidylmyo-inositol mannosides (PIMs). Mycolic acids being upregulated is expected as a thickening of the cell wall is well documented in older mycobacterial cultures and PIMs have been shown to have anti-phagolysosome effects *in vivo*.

mass to charge ratio <b>m/z</b>	Lipid acronym (carbon chain length)
1013.68	PIM1(C35)
1026.8	Carboxy-MA (C70)
1039.6	PIM1(C37:1)
1053.12	Alpha-MA(C72)
1066.88	Alpha-MA(C73)
1079.28	Alpha-MA(C74:1)
1080.8	Alpha-MA(C74)
1095.2	Alpha-MA(C75)
1107.12	Alpha-MA(C76:1)
1109.2	Alpha-MA(C76)
1111.12	Keto-MA(C75)
1123.28	Alpha-MA(C77)
1132.64	PIM2(C32)
1137.36	Alpha-MA(C78)
1139.04	Keto-MA(C77)
1150.88	Alpha-MA(C79)
1153.2	Keto-MA(C78)
1164.72	Alpha-MA(C80)
1167.2	Keto-MA(C79)
1176.08	PIM2(C35)
1179.4399	Alpha-MA(C81)
1181.04	Keto-MA(C80)
1194.96	Keto-MA(C81)
1205.84	Alpha-MA(C83)
1206.72	Keto-MA(C82:1)
1208.96	Keto-MA(C82)

1220.16	Alpha-MA(C84)
1222.08	Keto-MA(C83:1)
1223.92	Keto-MA(C83)
1235.52	Keto-MA(C84:1)
1237.2	Keto-MA(C84)
1249.28	Keto-MA(C85:1)
1251.12	Keto-MA(C85)
1262.8	Keto-MA(C86:1)
1264.08	Keto-MA(C86)
1275.92	Keto-MA(C87:1)
1278.08	Keto-MA(C87)
1290	Alpha-MA (C89)
1291.8	Keto-MA(C88)
1305.12	Alpha-MA (C90)
1318.3199	Alpha-MA (C91)
1325.84	GMM(Alpha-MA)(C80)
1327.84	GMM(keto-MA)(C79)
1331.6	Alpha-MA (C92)
1337.52	PIM3(C35)
1340.16	GMM(Alpha-MA)(C81)
1341.6801	GMM(keto-MA)(C80)
1346.24	Alpha-MA (C93)
1353.92	GMM(Alpha-MA)(C82)
1355.76	GMM(keto-MA)(C81)
1359.92	Alpha-MA (C94)
1368.08	GMM(Alpha-MA)(C83)
1370.16	GMM(keto-MA)(C82)
1371.76	Ac1PIM2(C48:1)
1373.92	Ac1PIM2(C48)
1382.48	GMM(Alpha-MA)(C84)
1384.16	GMM(keto-MA)(C83)
1384.96	Ac1PIM2(C49:1)
1386.8	Ac1PIM2(C49)
1395.6	GMM(Alpha-MA)(C85)
1397.04	GMM(keto-MA)(C84)
1399	Ac1PIM2(50:1)
1401.28	Ac1PIM2(50:0)
1412.72	Ac1PIM2(51:1)
1414.8	Ac1PIM2(51:0)
1426.8	Ac1PIM2(C52:1)
1428.48	Ac1PIM2(C52)
1439.92	Ac1PIM2(C53:1)
1441.6801	Ac1PIM2(C53)
1454.72	Ac1PIM2(C54:1)
1456.72	Ac1PIM2(C54)
1471.84	Ac1PIM2(C55)
1485.04	Ac1PIM2(C56)
1543.04	Lyso-PIM6(C16)
1557.04	Lyso-PIM6(C17)
1571.6	Lyso-PIM6(C18)
1585.76	Lyso-PIM6(C19)
1610.08	Ac2PIM2(C64)
1619.36	PIM5(C32)
1625.28	Ac2PIM2(65:0)
1638.8	Ac2PIM2(C66)
1651.04	Ac2PIM2(67:1)
1652.88	Ac2PIM2(C67)

1664.88	Ac2PIM2(68:1)
1667.2	Ac2PIM2(C68)
1679.52	Ac2PIM2(69:1)
1681.52	Ac2PIM2(C69)
1693.4399	Ac2PIM2(C70:1)
1695.92	Ac2PIM2(C70)
1707.76	Ac2PIM2(C71:1)
1710.08	Ac2PIM2(C71)
1721.4399	Ac2PIM2(C72:1)
1723.04	Ac2PIM2(C72)
1735.28	Ac2PIM2(C73:1)
1737.36	Ac2PIM2(C73)
1754	PIM6(C30)
1767.76	PIM6(C31)
1782.48	PIM6(C32)
1786.48	Ac2PIM3(C65)
1801.76	Ac1PIM5(C44)
1819.6	Ac1PIM4(57:1)
1829.52	Ac1PIM5(C46)
1851.28	PIM6(C37)
1885.76	Ac1PIM5(C50)
1919.52	Ac2PIM4(C63)
1935.4399	Ac2PIM4(C64)
1950.96	Ac2PIM4(C65)
1971.04	Ac1PIM5(C56)
1978.96	Ac1PIM6(C45)
1985.52	Ac1PIM5(C57)

Table 5.2. Mass to charge ratios for all lipid species displayed in Figure 5.4 and accompanying identifiers

### 5.3.3 Artificial lipid accumulation

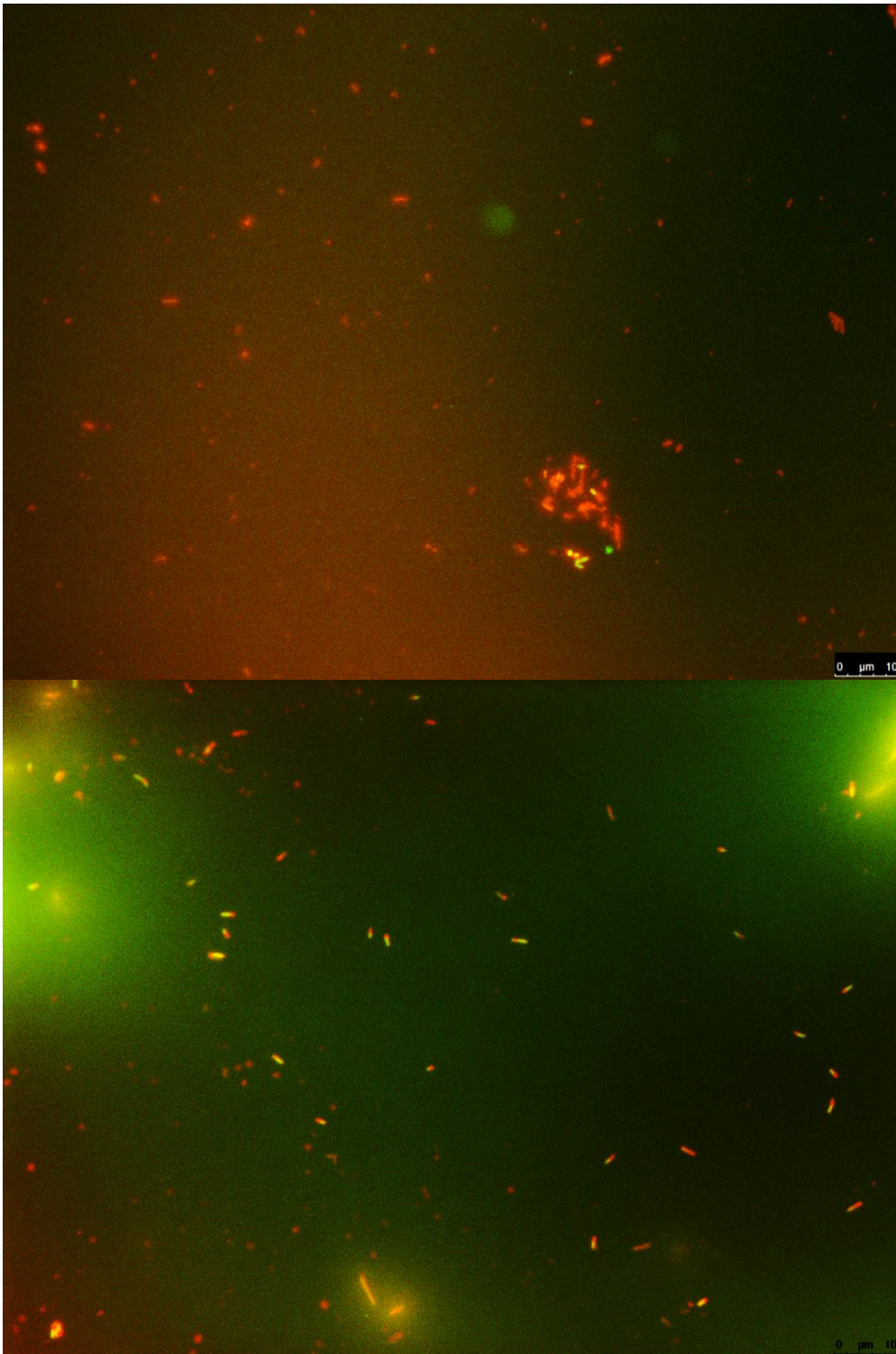


Figure 5.6. Nile red stained fluorescence micrograph of the difference between 'fed' and 'unfed' cultures. A is the control 'unfed' population. B is the 'fed' population. Only a few cells are expressing lipid bodies in the control but >90% of the cells in the 'fed' population are expressing lipid bodies.

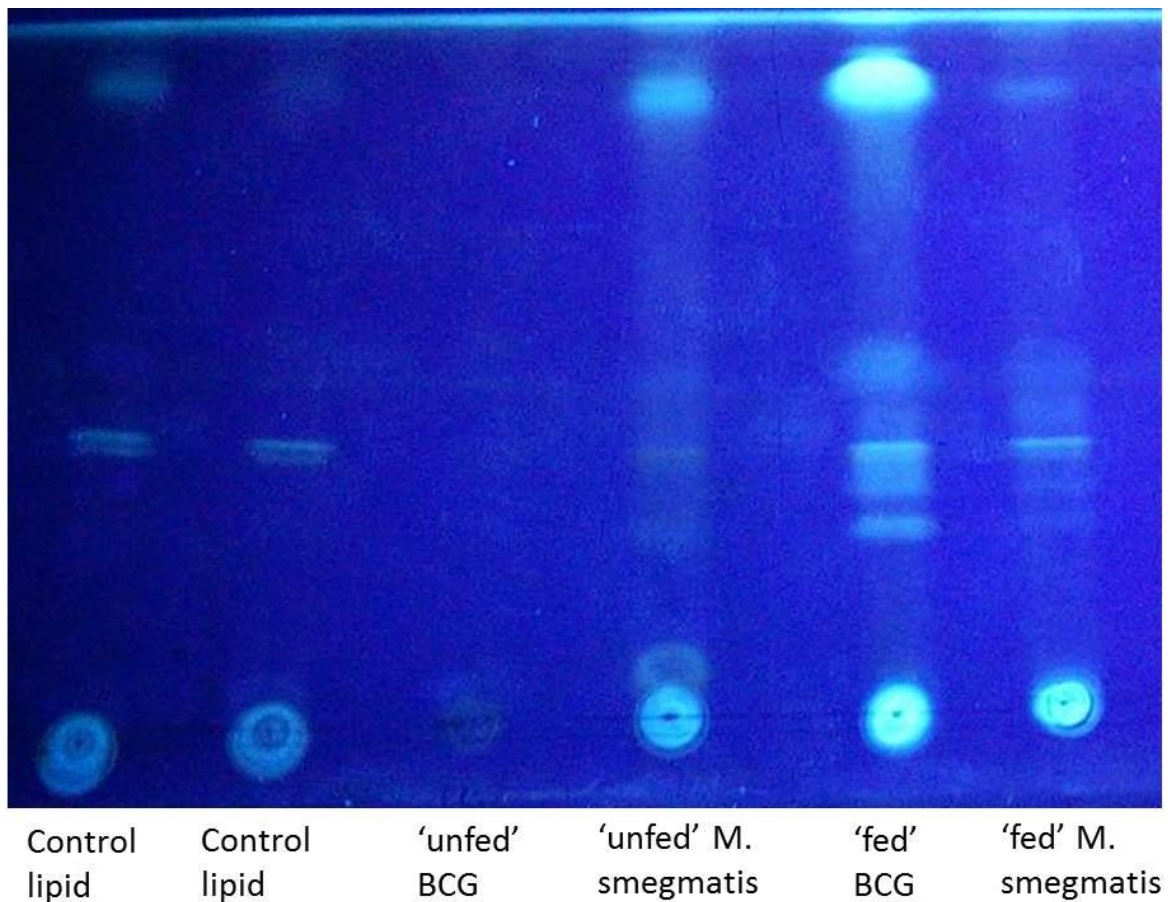


Figure 5.8. TLC of Bligh and Dyer extracted whole cell lipids from samples of 'fed' and 'unfed' BCG and *M. smegmatis* against the control lipid that was fed to the cells. It is clear that the three distinct bands that appearing in the control lipid samples are also found in the extracted bacterial lipids after the bacteria were given the lipid mixture. Of interest is that the 'unfed' *M. smegmatis* appears to have the same or similar lipid species naturally occurring at the same regions on the TLC plate.

## 5.4 Discussion

During the analysis of the lipidome of the examined mycobacterial species Bligh and Dyer lipid extraction methodology was used extensively. Bligh and Dyer method is for the extraction of whole cell lipids, both polar and non-polar. This is both an advantage and a disadvantage of the technique. As we were interested only in the non-polar lipids we had to be able to differentiate them. TLC seemed like the obvious technique to use as it is quick, cheap and easy. As we were not able to separate out lipid species in the liquid phase of the extraction we accomplished it in the solid phase of the silica after TLC. Although some of the whole lipid extract was used in our preliminary mass spectrometry data we hope to be able to use solely non-polar lipids in the future. This may increase the quality of resolution and allow us to see more subtle shifts in the lipidome profile.

TLC was performed on numerous occasions and, as mentioned above, worked efficiently differentiating different lipid species. The TLC work we undertook has revealed some interesting data to begin further work with but it is a blunt tool for a fine job. TLC lacks sensitivity and its specificity is dependent upon the operator's ability to accurately mix solutions of volatile compounds. The sensitivity is an issue as if there is only a small quantity of lipid present that sample can be lost as it may not stain the TLC plate enough to be seen by the naked eye. Another issue with our technique was the use of primuline as the resolving agent. Primuline photobleaches quickly meaning that if a faint signal was originally visible it might be lost as the plate is being read. TLC is not quantifiable and therefore we were not able to see clearly the quantity of each lipid species present. This could be important data and future experimental protocols should take this into account. Another issue with TLC is that TLC is a very gross analysis- only lipid present in overt abundance are seen and other more subtle quantities of lipid could easily be overlooked. Again future

experiments need to account for this but mass spectrometry largely solves these problems although it is slow and expensive.

In order to visualise the TLCs a fluorescent stain was used to bind to the lipids in the silica and reveal them. The dye used was primuline. It is sensitive to UV light and will photobleach therefore all experiments had to be undertaken in the dark after the primuline was administered. Inconsistencies in handling procedures could have caused originally less visible spots to become dimmer meaning that they were not observed in some cases but were in others. A way to address this problem is with sulphuric acid vapour, a standard method for discovering TLC results. However vaporising sulphuric acid at the concentrations required over the surface area required was deemed too dangerous so primuline was used. It is possible that sulphuric acid vapour would give a higher resolution but this has not been tested.

Another alternative that was not explored due to time constraints was the use of an alternative solvent system in the liquid phase of the TLC. We experimented with differing concentrations of ethyl ether, acetic acid and hexane to get the best results but it is possible that an entirely different solvent system could be superior. A recommended system is petrol. This is, however, highly volatile and dangerous to use in the lab as well as highly toxic. With the correct protective equipment (fume hood and appropriate gloves etc.) however it might be worth trying in future experiments.

Some of the  $R_f$  values collected from our TLC data do not correspond exactly to the scale for this solvent system. The reference samples all corresponded as they should be we have had to make some estimations when it has come to the mycobacterial lipids. This could be due to numerous things but the most likely is that mycobacteria, especially as they age, produce

fatty acids with longer chains of hydrocarbons than is typical. This will make the lipid associated with these extended tails more polar and therefore they will move differently on the silica plate. Another good explanation of the appearance of lipid species in unusual places on the Rf scale is that mycobacteria produce an entirely unique classes of lipids. One example of these are the mycolic acids that make up a large percentage of the dry weight of the cell wall (Schweizer and Hofmann 2004, Takayama, Wang et al. 2005, Bhatt, Molle et al. 2007) as well as unique subclasses of lipids such as sulfolipids (Rhoades, Streeter et al. 2011) that are also found in the outer cell envelope. These unique lipids are difficult if not impossible to get reliable Rf values for as the work may have never been done on them, hence the need for mass spectrometry to ascertain the presence of certain lipid families and species.

The mass spectrometry data we have is only of a small fraction of the total cellular lipids in any given Bligh and Dyer extraction. As mentioned above, mycobacteria produce many unique lipid classes. Mycolic acids are an obvious example of the unique lipids that mycobacteria produce, mycolic acids are believed to lend rigidity to the bacterial cell envelope as well as protect against hydrophobic antibiotics by making the cell membrane more hydrophilic (ASSELINEAU and LEDERER 1950, Barry, Lee et al. 1998). Some mycobacterial lipids are hypothesised to function as a permeability barrier (Bansal-Mutalik and Nikaido 2014). Bansal-Mutalik and Nikaido further posit that, through their experimentation, they have discovered that some of the lipids that form this permeability barrier consist of close relatives of PIMs namely diacyl phosphatidylinositol dimannoside ( $\text{Ac}_2\text{PIM}_2$ ). They suggest that because  $\text{Ac}_2\text{PIM}_2$  contains four fatty acid chains in a single lipid molecule it could produce an area of unusually low fluidity within the plasma membrane of



the bacteria. Such a robust and ridged membrane would be more resistant to the natural influx of large molecule drugs and therefore contribute significantly to the level of drug resistance in mycobacteria (Bansal-Mutalik and Nikaido 2014). Interestingly as we found heightened levels of PIMs in cultures that were more resistant to antimicrobial drugs it is possible that this conclusion could be confirmed by the data we have collected so far as well as forthcoming data from other mass spec experiments.

The presence of unique lipid classes makes mass spectrometric analysis difficult as the lipid types must be identified individually and manually by a skilled operator with a wealth of experience. The effort of analysing mycobacterial data is worthwhile as it produces much more valuable data than TLC. TLC is a useful tool for establishing a lipid extraction methodology and obtaining a gross picture of the lipids present in a sample but mass spec allows much deeper probing and more thorough interrogation of any material used.

The data presented here is preliminary, many more samples have yet to be analysed and it is thought that these will elucidate more of what is occurring in the mycobacterial lipidome. For example we expect to be able to characterise the contents the lipid bodies we observe. This will consist of discovering whether there are differences in the composition between lipid bodies of cells that have been under pH stress, oxidative stress, hypoxia or anoxia, nutrient starvation or a combination therein. These insights will allow us to discover if specific drug regimens will have more of an effect of mycobacteria that have recently ruptured from a caseated lesion of an advanced stage patient. In this case the cells will have been under multiple stresses and may, for instance, be expressing large quantities of PIMs and are therefore more resistant the standard drug regimen and an alternative must be prescribed. In addition to this we wish to discover if lipids ‘fed’ to cultures (as in Figure 5.8)

undergo any catabolism or if they are simply shuttled into lipid vacuoles. This will allow us to more effectively treat not only pulmonary TB but also extrapulmonary TB as the lipids available to bacterial cells will necessarily change in different host environments. This could also be true of TB sufferers in different geographic locations. Palmitic acid is a large constituent of palm oil which is used for cooking in the tropics and South East Asia where there is a serious problem with endemic TB. Palmitic acid may affect the structure of the lipid bodies within the mycobacterial cells and therefore the phenotype of the bacillus therefore requiring a novel drug treatment regimen. Another benefit is the gaining of insight into other lipid body forming species such as *Rhodococcus opacus*, *Acinetobacter* spp and *Streptomyces lividans*.

The Mass Spec data presented above also consists largely of polar lipids, not the families we are hoping to investigate. Even so there are still some interesting trends emerging (discussed more thoroughly in the general discussion- section 6). Once the non-polar lipid range has been analysed and lipid rich and lipid poor samples have been compared we will have more data to discuss.

Some of the samples we hope to receive the analysis for were non-polar lipids separated by TLC on the silica plates. These samples were treated identically to the others meaning that they will be contaminated with primuline, acetone, silica, possibly aluminium from the plate backing and likely trace amounts of the TLC liquid phase (hexane, diethyl ether and acetic acid). This is likely to contaminate the data from these samples but as we have yet to receive this data we can only speculate at this point.

### 5.4.1 Mass Spectrometry

We would expect to see large differences between the lipid rich and lipid poor fractions in the non-polar lipid range and would expect to see largely similar relationships between the young and old cultures. We would expect young cultures to have few lipid rich cells, similar to the lipid poor fraction. We would also expect the older cultures to contain more lipid rich cells but not as many proportionally as the lipid rich fraction which should show higher quantities of all non-polar lipids as the level of lipid rich cells is near 100%

When the mycobacterial cells (in this case only *M. smegmatis* and BCG) were dosed with a mixture of reference lipids they ingested them as they would inside a macrophage (Daniel, Maamar et al. 2011). It is clear that these lipids were metabolised by the cells as the reference bands were then visible in the TLC after whole cell lipid extraction. What is less clear is why there are more than three bands in the 'fed' cells when there were only 3 lipids and therefore 3 bands in the reference lipid. This can be explained in one or both of two ways. The cells when up-taking the lipid converted some of it to another form of lipid, or possibly were in the process of metabolising it when they were killed and their lipids extracted. The other explanation is that these other bands not present in the reference lipid represent the naturally occurring species of lipid that will occur in any culture of BCG or *M. smegmatis* allowed to grow to maturity with any carbon source. This theory is backed up by the observation that the sample of *M. smegmatis* also showed the same regions of lipid banding prior to being 'fed' indicating that these lipid species will naturally occur in all mycobacterial species. A future experiment could focus utilise a species of lipid that does not naturally occur in the mycobacterial lipidome, this would cause an obvious difference in the banding pattern and show that the foreign lipid was truly up-taken.

In the micrograph of the cells after being 'fed' or left 'unfed' displays some clear features. There is a cluster of cells in the 'unfed' image that appear to be lipid rich. This is a common occurrence when clumps of cells form and are found as it is thought that the internal face of clump is like a micro-granuloma. It becomes a hypoxic and unpleasant environment and the cells react in the same fashion they do in a true granuloma, they become lipid rich. This is by contrast with the 'fed' image where all the cells are free of clumps yet almost all of them display large lipid bodies.

During the course of this work experiments were conducted on the growth of mycobacteria under hypoxic conditions. We found that without exception the mycobacteria had retarded growth but almost all displayed lipid bodies similar to those shown in Figure 5.6B (see Figure 5.7 )

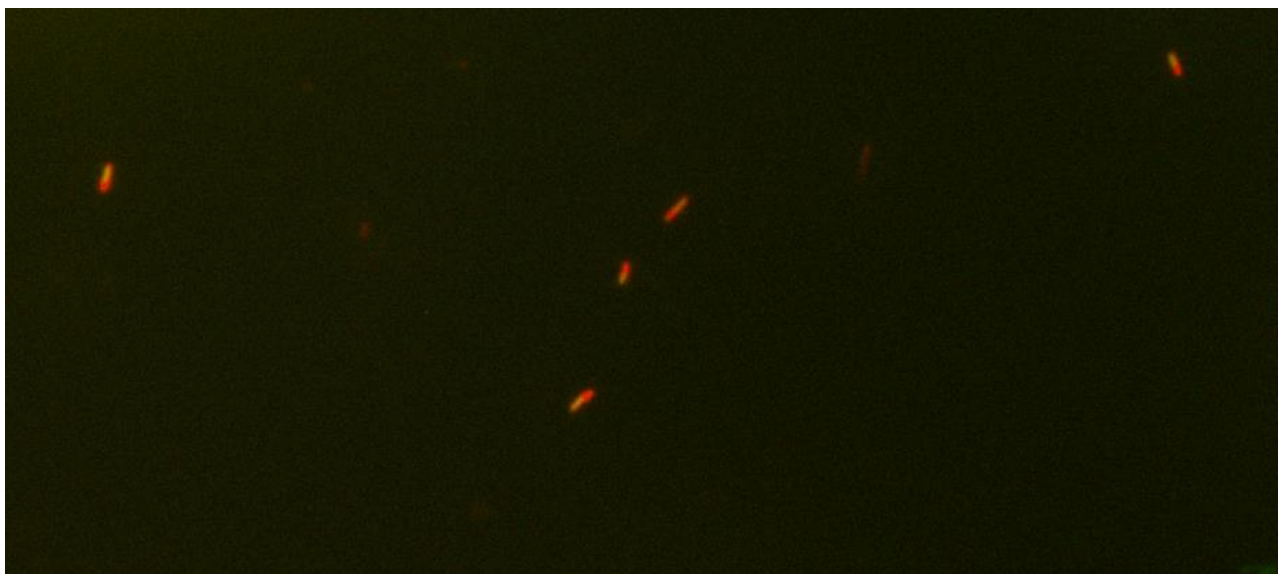


Figure 5.7. *M. fortuitum* cells grown under hypoxic conditions. Few cells were found and many were non-viable on solid agar. Spectrophotometric analysis indicated that there was a small rise in the bacterial biomass indicating that the cells did divide in highly unfavourable conditions. All cells observed expressed large lipid bodies at the cellular poles. Preparation was stained with Nile red as previously described and observed at  $527\pm30$  nm and  $645\pm75$  nm

When the cells are fed in this way the distinctiveness of the placement of the lipid bodies within the cells is lost. Ordinarily it is possible to discern, for instance, *M. fortuitum* from *M. marinum* by the placement of the lipid body. This discrepancy is lost when the lipid bodies are 'artificially' created as in this experiment.

The BCG culture extracted for this experiment was in the same growth stage as the *M. smegmatis* but seems to have acquired significantly more lipid in the upper region of the TLC plate. This area of the plate roughly correlates with wax esters. These are a common lipid found within mycobacterial lipid bodies (Waltermann, Stoveken et al. 2007, Deb, Lee et al. 2009, Sirakova, Burnett School of Biomedical Sciences et al. 2012) and it is reasonable to assume that these were accumulated naturally and had little to do with the reference lipid which had a band in the same region.

Another way to conduct this experiment would be in a pulse-chase experiment with a mildly radioactive form of a lipid or mixture of lipids. Palmitic acid is naturally radioactive and contains many of the fatty acids that are known to be readily up-taken by mycobacteria (Daniel, Maamar et al. 2011). This would allow us to conduct an experiment to obtain data on the rate at which mycobacteria up-take foreign lipids and if mass spectrometry was used we could establish how quickly the bacteria convert the lipids into other cellular products or if they do this at all.

## 6 General Discussion

The current study investigated two main research topics. The first was the capacity of a static light scattering array to detect differences in morphology (phenotype) of bacterial samples. This is discussed below (section 6.1- SLIC). The second research topic was investigating specific factors that affect the susceptibility of mycobacteria to antibiotics.

The factors investigated were the presence or absence of lipid bodies. A range of techniques and methodologies were developed and used in the attempt to discover the nature of mycobacterial lipid bodies and their effect on the overall metabolism of mycobacteria in relation to current frontline TB treatment regimens.

Fluorescent microscopy was used in conjunction with a modified Nile red methodology in order to visualise lipid bodies. This was vital for identification of lipid rich cells both in mixed cultures and once separated into LR and LP. The Nile red methodology that was used for the bulk of this investigation was adapted from a general literature search (Fowler and Greenspan 1985, Greenspan, Mayer et al. 1985) into the identification of lipid accumulations in a wide range of organisms such as algae (Chen, Zhang et al. 2009, Feng, Zhang et al. 2013, Pullammanappallil 2013), protozoa (Ramoino, Margallo et al. 1996) and prokaryotes (Waltermann and Steinbuchel 2005). The Nile red method was adapted because of a problem with permeability of Nile red into cells over a short time frame. Originally samples were stained for 20 minutes with constant agitation, however after the addition of DMSO to the Nile red mixture the staining time was reduced to less than 5 minutes and the agitation was no longer required. Other modifications made to the staining procedure were the concentration at which Nile red was administered, up to 1000 fold the concentration used for other studies (Garton, Christensen et al. 2002, Garton, Waddell et al.

2008, Anuchin, Mulyukin et al. 2009, Chen, Zhang et al. 2009). This led to issues common to all Nile red procedures- the formation of hydrophobic crystals. This was accommodated for by the addition of two ethanol wash steps. The first step took place in the tube containing the sample in liquid phase. The second ethanol was took place once the sample had been fixed to the slide; in the solid phase. These two additions reduced the amount of Nile red crystals to a negligible amount and allowed for greater visual acuity of the bacterial samples than was previously possible. This effectivity abolished any problems with background fluorescence.

In the case of *ex vivo* samples there was a significant amount of background to contend with and this was a source of serious consideration for these samples. Unfortunately the number of samples we had to work with was limited. It was therefore impractical to experiment on the *ex vivo* tissue without running the risk of destroying potentially valuable data. Because of this the lung tissue staining regimen is still in its infancy however we have still made some important observations. The most significant of these being the discovery of lipid rich cells in the cavity and on the inner face of structures thought to be pulmonary immune cells. These lipid rich cells are identical to *in vitro* MTB lipid rich cells that have been observed from general culture. This information lends three insights;

1. Lipid rich cells occur in MTB.
2. It is reasonable to assume that lipid rich cells occurring in the lung of a diseased patient are similar to lipid rich cells found in culture.
3. The acquisition of a lipid body seems to be a natural part of the mycobacterial cell cycle

The first two of these insights is straightforward; we have shown that lipid bodies are accumulated in mycobacterial cultures over time from cultures that contained cells with no lipid bodies at T0. We have also shown that lipid bodies occur in MTB in both heat killed samples from pure culture and in biopsy tissue harvested from a diseased patient. It is reasonable to assume, therefore, that lipid bodies found in mycobacterial species closely related to MTB will have a degree of similarity to one another. If this last point is true then the next research step is to characterise the lipid bodies found in patients in various stages of disease progression. Once complete the next step would be to characterise lipid bodies from all category 2 mycobacterial species in various states of stress. This would be in an attempt to compare them to find the lipid body composition that most closely resembles that of a MTB bacillus that, for example, was found in the foamy macrophage in a caseated granuloma. Once this is established a model organism for a specific life-stage of MTB has been created. Providing that it reacts in a predictable manner to antibiotic therapy the model could be used to predict treatment outcomes on a more personalised level in a biohazard safety level 2 laboratory; more safely that is currently done.

The third insight listed above pertains to lipid body acquisition as a simple function of mycobacteria as a clade. All mycobacteria species tested over the course of this study have produced lipid bodies. This indicates that it is a common phenomenon. Mycobacterial cultures that have had their media changed on a regular basis, had their cell population split and were cultured with agitation to allow atmospheric oxygen to dissolve into culture were still found to form lipid bodies strongly indicating that it is simply a function of mycobacterial growth. The argument against that is that even with vigorous agitation there will still always be a degree of settling in a culture tube, this means that the bacteria



collected at the bottom of the tube will be in a hypoxic environment and/or in a biofilm. Something the present study has not explored is the possibility of a biofilm/lipid body complex in mycobacterial culture. This study would be interesting and merits further work.

These insights lend credibility to our discoveries having real clinical significance and allow us to start the formulation of a model of lipid rich cell mediated disease resistance, recurrence and relapse. In the event that our insights prove to be true this allows us to use this data and other data from future studies on similar topics to begin to model using category 2 biohazard organisms such as *M. smegmatis*, *M. fortuitum*, *M. komossense* and BCG. We can also model *in silico* with more confidence than before as we have more of the important parameters in place. Ongoing work at the University of St Andrews in collaboration with Dr Ruth Bowness involves the *in silico* modelling of TB progression, oxygen gradients and drug metabolism. Adding the data we have on lipid rich MTB cells may allow us to produce a model accurate model of disease progression than was possible before this work was conducted. In addition to this we can also work practically with MTB and its surrogates *in vitro* and *ex vivo*. Samples of H37Rv grown to produce lipid bodies compared against *ex vivo* samples that are already expressing lipid bodies and their respective drug susceptibility profiles would be fascinating and important clinically.

We found significant correlations between lipid body positivity and resistance to antibiotics.

This has led us to two possible conclusions:

1. The presence of lipid bodies is a reflection of the cell's state (stress, metabolic down-shift, dormancy) - if a lipid body is present then the cell is stressed and beginning a metabolic shutdown process.
2. Lipid bodies are somehow protective in and of themselves.

This first conclusion, if proven true, lends itself to the concept of a lipid storage vesicle within the MTB bacillus that allows rapid resuscitation after any stressors have been removed. We have shown that once stressors are removed the mycobacterial species tested did resuscitate to lipid poor cells rapidly and ongoing work with Mr Vincent Baron has shown that there is little to no difference between LR and LP cells in terms of their lag phase in ideal conditions.

The second conclusion above is possible (as mentioned above 1.15.2) as some of the drugs we used are lipid soluble. There is, however, little evidence of a drug-shuttling chaperone within the cell that would be able to translocate the drug crossing the cell membrane to the lipid body. It is theoretically possible that the lipid bodies reside so close to the outer cell envelope that the drugs naturally move towards regions of high lipid content but then the cell would have to have specific drug detoxifying machinery or a way to jettison the 'toxic' lipid body and evidence for either of these is lacking.

We have also shown that lipid bodies are lost when the cell is placed into media with adequate oxygen and nutrients this leads us to believe that the primary use of the lipid body is as a carbon source for long-term survival. There are many theories supporting this

argument (see section 1.15.2). These concepts support the former rather than the latter of the two above theories as to the effect of the lipid body for the cell.

Other techniques used or developed during the lifetime of this work include:

- Flow cytometry for the high through-put measurement of lipid rich cells in culture
- MIC and MBC studies of mixed cultures and cultures containing only LR and LP cells
- Novel separation methodology based on the specific buoyant densities of individual populations of cells
- Standard PCR and qPCR reactions with novel primers to specific regions of the mycobacterial genome and transcriptome
- Lipidomic studies we conducted including TLC of non-polar lipids and mass spectrometry of said lipids

The MBC and MIC studies conducted as part of this work yielded exciting results. We have shown that the level of antibiotic resistance is up to 40 fold higher in mycobacteria expressing a lipid body. Specifically the species displaying this susceptibility pattern was *M. smegmatis* and the resistance was to rifampicin. The presence of lipid bodies had a marked effect on all species tested. Without exception all species, when expressing one or more lipid bodies, became significantly more resistant to all drugs tested which include three of the frontline anti-tuberculosis drugs the WHO recommends (WHO , WHO 2001, 2012). This finding has significant implications for clinical practise and the treatment of tuberculosis worldwide. As we have found lipid rich cells *in vivo* in patients with TB which appear similar to lipid rich cells found *in vitro* we can assume these cells are similar in composition and

phenotype. In addition to this we need not assume a similarity between *in vivo* and *in vitro* lipid rich cells as various groups (Goble, Iseman et al. 1993, Garton, Christensen et al. 2002, Garton, Waddell et al. 2008) have extracted resistant cells from patient sputum and one of these groups (Garton *et al*) have identified some of the extracted cells as lipid rich. If we are correct that lipid richness and the associated loss of acid fastness (Deb, Lee et al. 2009, Kapoor, Pawar et al. 2013) and intracellular lipid bodies is a marker of a type of dormancy and/or a type of antimicrobial resistance we need to re-examine how tuberculosis therapy is applied to patients, especially those patients that have chronic disease with necrotic lesions. A possible way to address this issue would be to continue the work we have been performing, assessing each antibiotic separately and in combination, including new antibiotics such as bedaquiline and pretomanid (PA824), against early and late phase cultures as well as against specifically separated lipid rich and lipid poor cells of all mycobacterial species including MTB. Full genetic profiling, using RNAseq and metabolic profiling using SILAC (Stable isotope labelling by amino acids in cell culture) would also allow us to probe further into the specific state of each lipid rich population within a species or strain.

## 6.1 SLIC

When the SLIC was first developed testing and calibrating was required. We did this using the same material that would later be used for measuring; bacteria. In order to ascertain whether the SLIC was functioning as it was developed to do we tested it against differing phenotypic populations for bacteria. What was found was, once everything else was controlled for, the SLIC was unable to differentiate between samples of bacteria with wildly differing phenotypes such as a gram positive coccus (a *Streptococcus spp.*) and a flagellated

gram negative bacillus (*Proteus mirabilis*). This is atleast the case with our current limited data analysis capabilities. As a prototype device SLIC is still being trialled and we are still assessing it capabilities. As such we have yet to fully discover all of its potential, it is certain that scattering patterns between species and between the same species at different concentrations are subtly different but we have yet to develop the correct tools to determine the meaning of these differences. We are taking some cues from a group at Purdue University in the USA. They developed a technique called BARDOT (BACTERIAL Rapid Detection using Optical scatter Technology)(Huff 2006) that allowed them to differentiate bacterial colonies on solid agar by their unique growth and morphological characteristics. The task facing us is more complex as we will be attempting to identify the scattering pattern of a system moving under Brownian motion however we believe that it is possible.

In the first instance this work focused on the creation of a technology that could detect phenotypic changes in bacterial populations. We have achieved this but not in the manner we were expecting to. We have created a device that is both useful and marketable that could potentially replace current spectrophotometer technology.

From this invention sprung the notion of being able to detect very tiny changes in bacterial populations. The original sphere of activity for this project was to detect phenotypic changes but we have found it easier to detect changes in bacterial population. This allows us to detect growth/non-growth at an earlier stage than current technology meaning we can perform drug susceptibility testing faster and more accurately.

One of the few problems with SLIC as a technology is the current dampening effect we see at high concentrations of particles. This is due to the interfacing of the digital oscilloscope

and the lock-in amplifier and the nature of the lock-in amplifier. The signals received by the lock-in are typically in the 10-100 mV range but the lock-in can measure with accuracy up to 500 mV. Beyond this figure the signal is too strong and the lock-in is overloaded. When we have cultures of bacteria that are visibly cloudy (a McFarland rating of 2 or greater, approximately  $6 \times 10^8$  cells) SLIC can measure them effectively but when cultures are in the range of  $10^9 - 10^{10}$  cells the lock-in becomes overloaded. This is not typically a problem as clinical samples are rarely this concentrated. However the imperfect interfacing between the lock-in amplifier and the digital oscilloscope means that the effective range of the SLIC is limited to approximately  $10^1 - 10^8$  cells per millilitre inclusive. The reason for this problem is the inflexibility of the oscilloscope firmware. The oscilloscope will only measure at one given range in a single experiment (at between 0.1 - 10 mV, for example) therefore the range must be set prior to recording and kept constant between experiments, which is what has been done. The mathematical conversion of the number the oscilloscope produces to the number the lock-in produces is simple but imprecise. This is because, as the number the lock-in produces rises the oscilloscope is only measuring a reduced range of this value. An example is;

Lock-in readout	Oscilloscope readout
1.1 mV	1.1 mV
10 mV	10 mV
150 mV	1.5 mV
500 mV	5 mV

Table 6.1. Discrepancy between the numerical readout from the lock-in amplifier and the digital oscilloscope which is the presumed source of the distortions in the SLIC data found at high mV ranges.

The conversion that is required to gain the 'true' value from the experiment means we lose sensitivity at high millivolt ranges. This problem could be remedied in the future with a more flexible oscilloscope or an integrated digital lock-in and oscilloscope array mounted together, this work has been undertaken and is largely complete (see Figure 6.1).

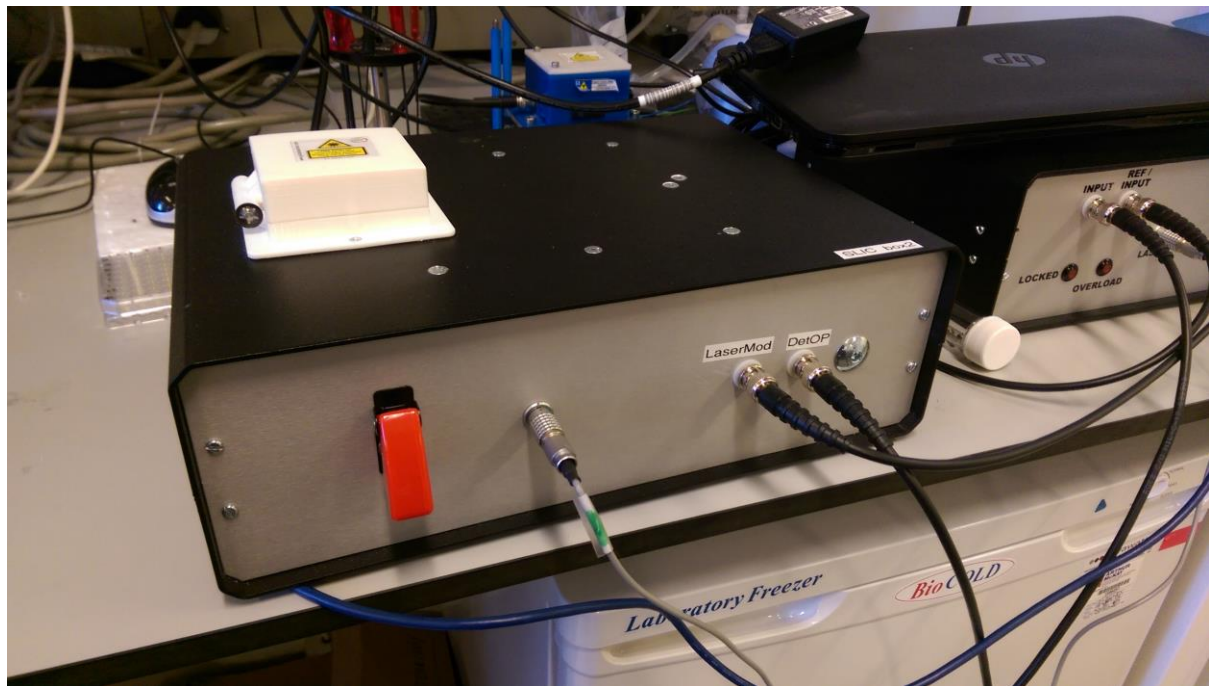


Figure 6.1. The newest version of the SLIC, created for us by SAIL (St Andrews Instrumentation Ltd). This is the penultimate prototype before we attempt to make SLIC a commercial entity. It is currently undergoing beta testing and debugging.

The development of SLIC has allowed us detect bacterial growth at a lower bacterial concentrations than was previously possible. This is of particular use when measuring TTP of slow growing cultures of mycobacteria such as BCG or MTB.

From this we decided that we could use our highly sensitive technology to investigate the drug tolerances of lipid rich bacteria.

Before we could do this we had to find a way of identifying lipid rich cells in a mixed culture. This was already possible with various direct and indirect observation methods using light and fluorescence. We took a known method (Nile red staining) and adapted it for use with our microscope hardware. This gave us startling results that showed lipid rich cells clearly in the environments we were expecting to find them and in some instances where we were not expecting to find them. Next we needed a way of enriching or selecting for lipid rich cells. Again, a method existed (Percoll) but we found it not as functional as we had hoped. We took the basic principal and adapted it and invented the D<sub>2</sub>O separation methodology. The D<sub>2</sub>O methodology created during the course of this work has far reaching potential. We have proven its effectiveness in pure culture; the next step would logically be to use it with biologically derived samples such as patient sputum containing lipid rich cells. In addition to this we could use it for the separation of different mammalian cell types in tissue culture. This would require adapting the technique so that the mammalian cells were not put under osmotic stress but the principal would remain constant. Another application would be to adapt the technique to industry. The separation of particles by their density is common in industries such as mineral mining and water purity treatment. While not suitable for large scale industrial applications due to the cost of D<sub>2</sub>O an adapted BDS methodology could be applicable for site managers on a small scale in the field.

Once we had created a robust separation methodology and an effective Nile red staining regimen we had all the tools necessary to conduct novel experiments with pure samples of lipid rich and lipid poor cells individually, identify them accurately with microscopy or flow cytometry and measure their responses to common antimicrobial treatments more accurately than was previously possible.



In addition to these goals we wanted a more rounded view of the lipid rich cell. To this end we conducted genetic and lipidomic studies on lipid rich and lipid poor populations to try and generate a more general view of the phenotypic, genetic and metabolic state of these cells.

## **6.2 Detection methodologies**

The studies and experiments detailed herein were aiming towards the goal of 'Detecting cell states using photonics'. This was ostensibly meant to refer to mycobacteria but the technology we developed has applications outside mycobacterial microbiology and therefore some of the work detailed herein was conducted on more rapidly growing pathogenic bacteria.

In order to detect bacterial cells and to discern their states we developed several technologies and methodologies.

The data from the SLIC surpasses anything before achieved with rapid photonic methodologies in the field of bacterial quantification. We have a greater sensitivity and because of this we are able to generate faster TTPs for all the species tested so far.

For rapidly dividing organisms such as *E. coli* or *S. aureus* the TTP has been established at approximately 2 generations from a starting concentration of <1000 cells. For slowly growing organisms such as BCG the TTP is, relatively, faster. Because we can sample more times during one generation phase we have found that we can generate a significant TTP in less than two generations. The lower limit of detection for all species appears to be between 100 and 10 cells.

As BCG is a biohazard category 2 analogue for MTB it is encouraging that we will be able to, from pure culture, generate data on the susceptibility of MTB many times faster than was possible before the invention of SLIC. MTB cells from sputum or tissue present more of a

challenge. It is possible, with established decontamination techniques, to remove most of the debris and bacterial contaminants from a sputum sample leaving only MTB cells behind. In this way human biological samples could be treated to be used in SLIC and drug susceptibility testing could be transformed. This is of particular importance in poor and rural settings as SLIC can be used in resource poor environments due to its mobility and low cost. SLIC has been tested and calibrated against numerous particles and compounds. This was done to establish whether the technology was specific to bacterial growth systems or if any colloidal substance would provide a result. We found that a non-opaque colloidal suspension of any particle(s) was measurable. This has lead us to hypothesise that SLIC might have applications in industry such as the detection of pollutants in liquid food and drink products or in fluids that must be sterile such as drugs or liquid (saline) solutions for hospitals.

### **6.3 Separation**

The separation methodology was borne out of very simple physics- a less dense substance floats in a more dense substance - oil floats on water.

We decided to attempt to separate lipid rich from lipid poor cells as it had never been done to our satisfaction in the literature. Percoll methodologies were somewhat effective but involved a lot of mess and we wanted a cleaner method that would allow *total* separation. We decided upon the use of deuterium oxide (D<sub>2</sub>O) as it is atomically stable and not prone to issues associated with other density gradients such as evaporation. The density of D<sub>2</sub>O is well known (1.108 g/cm<sup>3</sup> (Neuefeind, Benmore et al. 2002)) and easily controlled meaning we could be confident of the density of any gradient we made and that it would remain as we made it. This is pertinent is the same is not true of sucrose gradients that present a ready source of carbon thereby keeping the cells unstressed when to gain an effective

separation the cells must remain stressed to arrest their resuscitation back to being lipid poor.

The isolation of different phenotypes based upon whether they were lipid rich or lipid poor was simple once the technique was established. The top layer of any given solution of D<sub>2</sub>O between 60-75% D<sub>2</sub>O : H<sub>2</sub>O contained lipid rich cells only and the bottom layer (within 1mm of the bottom of the vessel) contained only lipid poor cells and clumps of cells that had not been adequately homogenised. In this way we sometimes encountered issues with lipid rich contamination in the lipid poor fraction but 75% of separations were successful.

The physics behind the BDS methodology are simple, the cells that contain lipid float in a substance that is more dense than they are. Previous work (Lipworth *et al*, unpublished) established the density of a lipid rich cell at approximately 1.08 g/cm<sup>3</sup>. A solution of D<sub>2</sub>O more dense than 1.08 g/cm<sup>3</sup> will cause the lipid rich cells to float and the lipid poor cells to sink. It is possible there is a biological imperative for this to occur. Obviously mycobacteria do not encounter deuterium oxide regularly in nature but MTB cells will encounter fluids more dense than water in the host. As was alluded to earlier, it is possible that a cell, loaded with lipid from time spent inside a macrophage, could become inactive and be released into caseous fluid. The need to float to the top to be able to escape as soon as possible from this inhospitable environment would be a biological imperative.

So it may be that the lipid body serves many purposes. It might be a carbon store, a floatation device, a drug sequestering and detoxifying area, linked to the capacity to evade the immune system, a means of surviving in the open environment out with a host and a marker of antibiotic resistance.

Is it possible that the mycobacterial lipid body, one of MTB's greatest weapons, might end up being its downfall with these discoveries? Once we have fully elucidated the role of the lipid body, what its true functions really are, we may be able to design drugs that target the enzymes and processes that allow lipid body formation and use this versatile and multifaceted organelle as the tool of MTB's eventual defeat.

Something that this study first set out to discover that we have not yet achieved is the relatively simple question of if lipid-richness is indicative of dormancy. The question is simple but the means of answering the question are complex and difficult. In section 7 (Future work) it is proposed that we undertake RNAseq or similar whole genome/whole metabolome experiments (SILAC- Stable isotope labelling by amino acids in cell culture, for example) be undertaken in order to answer this question.

#### **6.4 Lipid accumulation**

Understanding how phenotypic resistance arises in mycobacteria is important if we are to improve treatments against tuberculosis. We have addressed this question by investigating the relationship between the presence of lipid bodies in mycobacterial cells and phenotypic resistance to antibiotics.

We have monitored the accumulation of lipid bodies in growing cultures and show that the concentration of lipid rich cells increases over time and that the development is similar in all species allowing for the different generation times. We have also shown that cells from old cultures are more resistant to antibiotics than exponentially growing cultures as has been described previously (Gomez and McKinney 2004, Ahmad, Klinkenberg et al. 2009,

Hammond, Baron et al. 2015). We have expanded this observation by demonstrating that culture samples with >95% lipid rich cells share this resistance pattern. In contrast lipid poor cells behave like the exponentially growing cultures. An important point to be taken from the data in Table 4.8 is the lack of difference between old and young lipid rich and lipid poor cells. Within a margin of error the lipid rich and lipid poor cells reacted similarly to the drugs irrespective of whether they came from a young or old culture.

As *in vitro* mycobacterial cultures grow and age the supernatant becomes more acidic (Vandal, Nathan et al. 2009). If left unopened the concentration of oxygen available to the bacteria reduces (Filippini, Iona et al. 2010). The quantity of nutrients available to the organism will also reduce (Hampshire, Soneji et al. 2004) and the population density of the bacteria obviously increases. All of these things can have detrimental effects on the growth and replication of mycobacteria. In these circumstances it would be reasonable to state that the bacteria are stressed or at least in a stressful environment as in a granuloma *in vivo*. This can be seen in the work of Kapoor *et al* (Kapoor, Pawar et al. 2013) wherein they put forward an *in vitro* model of granuloma formation, drug penetration and disruption. A review paper by Lipworth *et al* (Lipworth, Hammond et al. 2016) organises the models, including Kapoor's work and agrees with our above assessments.

The production of lipid bodies has been linked to a stress response in mycobacteria (Deb, Lee et al. 2009, Daniel, Maamar et al. 2011, Piccaro, Giannoni et al. 2013). We let all our cultures age and generate lipid bodies 'naturally' – this is similar to the Wayne model of microaerophilic conditions (Wayne 1976). Where we differ from Wayne however, is our ability to separate 'dormant' from 'non-dormant' cells – lipid rich from lipid poor. When these cells are separated we have shown that the individual drug susceptibilities are vastly different. In all cases it requires more drug to sterilise a culture of lipid rich cells than the

same number of lipid poor cells. As mentioned previously (and later in more detail (page 228) this means that we have possibly identified a mechanism for relapse in treatment adherent patients who are not co-infected or immunocompromised.

In a culture containing both lipid rich and lipid poor cells (a mixed culture, presumably normal for *in vivo* and most *in vitro* work) we have shown what those before us have demonstrated; that an older mycobacterial culture can tolerate a higher quantity of drug before 90% of the cells are killed. However when attempting to cure a patient of disease clearing 90% of the cells is of little use and could cause further morbidity to the patient and others through the production of drug resistant organisms, therefore MBC<sub>100</sub> assays were used for the majority of our work.

Using our separation technique we separated lipid rich cells from young logarithmic phase cultures and older stationary phase cultures. Our data indicates that the presence of lipid bodies is not merely a feature of aged cultures but that lipid rich cells are present at every stage of the mycobacterial cell cycle although in different proportions. In addition to this we have shown that, irrespective of where in the growth cycle the lipid rich cells are, these LB containing cells are phenotypically resistant to the four antibiotics tested and that this phenomenon is similar in all four species tested. We have further expanded on this with the addition of a bedaquiline regimen and we plan to use pretomanid in the future.

The advantages of this study were mainly due to our two novel methodologies. We are now able to separate with high efficiency but low yield lipid rich and lipid poor cells and identify them rapidly. Working with a defined cell population with high purity allowed us to identify the specific drug susceptibilities of the four species of bacteria tested. This, for the first time,

has allowed the use of MBC methodologies to elucidate a more accurate and clinically relevant end point for drug resistances in four species of mycobacteria and produce compelling evidence for the presence of a highly resistant sub-population of bacteria that could be the source of latent disease.

It is possible that the results we have obtained are influenced by the D<sub>2</sub>O separation technique. The method provides preparations with a >95% pure population but there is a significant loss of cells in the process. This may mean that our results do not from a representative population of cells. It is possible some lipid rich cells resuscitate and convert back to lipid poor and some are stressed or naturally form lipid bodies during the incubation period. This is largely unimportant however as we are not concerned with how the lipid rich cells are produced but simply if they are lipid rich. It is possible that cells that are completely metabolically inactive are the cells we are collecting, all those with metabolic activity metabolise their lipid bodies and appear to resuscitate but those that are inactive stay on the top layer of the D<sub>2</sub>O separation and are collected. Similar results were achieved with samples separated using D<sub>2</sub>O and a centrifugation period. This indicates that the incubation period is not as significant factor or that the cells are able to change state rapidly or nearly instantaneously of the course of a 4 minute centrifugation step.

The D<sub>2</sub>O separation methodology is currently very low throughput, we have attempted to increase the yields with centrifugation as mentioned above and this has been successful. This has allowed us to hypothesise that the D<sub>2</sub>O methodology may have a place in clinical practise one day. We envision a similar method being used to quickly establish the lipid-rich content of a patient's bacterial load and this informing the clinician of the correct drug

regimen to use as we have also shown the resistance lipid rich cells show to frontline anti-tuberculosis drugs.

We have shown that lipid rich cells do in fact occur in the human host out with macrophages, something that was hypothesised prior to this study but not confirmed. This discovery gives credence to the theory that has been touched on previously that our drug resistance profile results could be a reason for or a contributing factor towards relapse in human TB.

Relapse in TB is considered to occur in several ways. However only one of these is true relapse; the others are misnomers.

The first form of returning disease is reinfection from another individual (exogenous reinfection). This is usually confirmed by serotyping or SNP profiling of the causative organism. If the SNPs are confirmed to be a threshold number different a case of exogenous reinfection is confirmed.

The second form of disease recurrence is endogenous reinfection; usually this occurs when an unknown lesion or granuloma ruptures reintroducing viable bacteria to a previously smear/culture negative patient. This is confirmed as with exogenous reinfection but the SNPs are usually identical indicating the same strain has reinfected an individual. It is important to note that this can also occur in hospitals, clinics or small communities where the same strain is passed rapidly between individuals without any SNP variation taking place.

The third type reappearing disease is false positive relapse where a patient was never truly cured but was no longer showing positive results on the tests used. Tests include becoming



smear negative and culture negative. The patient may also no longer show any symptoms but was always infected and infectious. This type of 'relapse' can often be confused with endogenous reinfection and for most intents and purposes it is the same thing, epidemiologists attempt to differentiate the two but for clinicians the meaning is similar if not identical.

The fourth type TB recurrence is the only true relapse. This occurs when the patient was smear/culture negative, clear of both live and dead bacteria in sputum and bronchial lavage, no bacterial DNA or RNA could be found in sputum or other samples and symptoms had abated. In this case when the disease comes back it is most likely to be classified as an endogenous reinfection or a false positive relapse. True relapse is very difficult to identify and diagnose. In the case of true relapse there is little known (for the above reasons) as to how it occurs, however there are many theories.

It is possible that the bacteria were walled away effectively in macro- or micro granulomas which have since lysed and released viable bacteria back into the lung cavities.

It is also possible that bacteria, inside or outside of a granuloma were lying dormant in biofilms or singly in areas of the lung. Why they would awaken to cause active disease again is unknown but it could be due to the host becoming immunocompromised because of a secondary infection, stress or poor diet.

Another theory consists of these previous two combined where dormant bacteria were walled away in a granuloma and once released were able to cause relapse by escaping the (foamy) macrophages they were dormant within.

If any of these models is true remains to be seen but there is an obvious roll for lipid rich cells in all of the above theories. In any scenario where dormancy is mentioned lipid rich cells can fill the same niche as we have shown that they are not only highly drug resistant but that they are in a degree of metabolic shutdown with RNA activity declining; they are becoming quiescent. This being the case lipid rich cells are a fruitful area of research within the Mycobacterial research field and could, in time, prove to be the lynch pin of MTB's infectivity model.

## **6.5 Lipidomics**

The lipidomics section of this work was originally meant to be an adjunct to the other work, a way to confirm or refute our ideas about what was happening in the cell at the time of lipid body formation and afterwards. The TLC analysis, while crude, has produced significant and important data because of our other methodologies, namely the separation technique. The data shown in Figure 5.2 and Figure 5.8 indicate some interesting phenomena that are occurring in the mycobacterial metabolome when the cell is expressing a lipid body. Figure 5.2 displays the differences between old and young cultures of the same species. These cultures were, in fact, identical cultures matured for more than 3 weeks until they had reached the 'old' criteria we used previously for our susceptibility experiments (mid stationary phase). The data indicates that levels of certain lipids are increased as the cultures age. This is in line with our earlier observations that older cultures express more lipid bodies. TLC, a rather crude method of identifying lipid species, has allowed us to elucidate the lipid species once they are present in abundance.

This work compliments the mass spectrometry data on BCG. The first column in Figure 5.2 displays the obvious differences in cellular lipid content between old and young BCG. Figure 5.4 displays data from the mass spectrometry of a Bligh and Dyer extraction of whole cell

lipids. In the lipid poor fractions analysed it was apparent that there are lipids that are more abundant. These lipids are primarily members of the Glucose monomycolate (GMM) family. These glycolipids are known to elicit a strong immune response from the human host (Matsunaga, Naka et al. 2008, Nguyen, Koets et al. 2009, Morita, Hattori et al. 2013). Additionally GMMs are being trailed as potential sources of immune therapy and targets for vaccines (Enomoto, Sugita et al. 2005, Matsunaga, Naka et al. 2008, Nguyen, Koets et al. 2009). This raises serious concerns if our data is correct. We have shown that in an older culture of mycobacteria and in a population of lipid rich cells GMMs are less common than other lipids. This means that future vaccine targets may not vaccinate patients against the lipid rich ('dormant') cells that are the hidden population we are also failing to eradicate with standard and new experimental chemotherapies.

Many of the species of lipid that are upregulated are mycolic acids, this is not surprising as a thickening of the cell wall is often noted in cells from older cultures and cells expressing lipid bodies (Sarathy, Dartois et al. 2012). Even though this is preliminary data it reveals something interesting; many of the lipids that are more abundant in the old fraction are Phosphatidylmyo-inositol mannosides (PIMs). These glycolipids are strongly associated with MTB's ability to evade and subvert the human immune system especially regarding the fusion of the lysosome with the phagosome (Kaplan, Gandhi et al. 1987, Sibley, Adams et al. 1990, Fratti, Backer et al. 2001, Vergne, Chua et al. 2003, Vergne, Fratti et al. 2004). New fluorescent spots are found on the TLC plate indicating a new lipid or a higher quantity of one that was previously noted at approximately R<sub>f</sub> values of 0.92 and 0.58 (corresponding to wax esters and fatty acids, respectively). These are the most obvious differences between old and young BCG lipids found in this study. The above information in conjunction with the

TLC data leads us to an interesting conclusion; older cells, specifically older BCG cells, are expressing high levels of glycolipids that allow them to evade the immune system while also expressing high levels of wax esters and free fatty acids often associated with lipid bodies. We can conclude that old cultures contain lipid rich cells and that these cells are not only rich in non-polar lipid body lipids but also in immune evasion lipids meaning that lipid bodies could be a possible marker of cells that can *persist in the host* (see above page 228). This explains why we see lipid rich cells in the biopsy tissue of a deceased patient that died with TB, these cells were the ones that not only could withstand antibiotic treatment but could also evade the immune system and persist inside macrophages or interstitial spaces.

Our data on artificial lipid accumulation mirrors work done by Daniel *et al* (Daniel, Maamar et al. 2011). They found that in cell culture models MTB be phagocytosed by macrophages. Following this the MTB cells would accumulate lipids the group had labelled and artificially incorporated into the macrophages demonstrating that MTB cells will sequester lipid from host cells. This is interesting when taken with our previous conclusion. It is possible that cells that are expressing anti-lysosome factors are the cells that are up taken by macrophages and not destroyed. These cells then go on to become lipid rich cells. When the degradation resistant cells are inside the phagosome they start to sequester lipid from their host cell. This is analogous to our artificially 'fed' cells. These artificially lipid rich cells that have gathered lipid from their surroundings rather than generate it themselves, are then able to become dormant in the macrophage safe from the immune system. The method by which it is evading the phagolysosome fusion is passive, the mere presence of the PIMs on its surface discourage phagolysosome fusion so the cell need not be active. The macrophage the cell(s) is residing in may become part of a lesion or granuloma which may caseate and

necrose releasing the lipid rich cell into the toxic fluid of the granuloma. This might kill a cell that was active and multiplying. A dormant cell however could float to the top of this toxic fluid and thereby be in the best possible position to be released from the granuloma when it eventually ruptures. This allows the dormant bacilli to either re-infect new areas of the same host's lung, move through the host body to become a renal or hepatic infection or to be released through coughing to infect a new host. The lipid bodies the cell is carrying allow it to survive longer in the open and give it a better chance of being ingested into a new host and being able to establish an infection once there as the lipid body acts as a carbon source.

## 6.6 Conclusions

We have shown that-

- Phenotypic antibiotic resistance is associated with the appearance of lipid bodies and may be driven by the changes in gene expression that have also been found associated with this change. Future studies should investigate the metabolome of similar separated preparations
- Lipid bodies occur not only in old cultures but in young, mid-exponential phase, cultures as well
- The presence of lipid bodies and not the age of the cell is the deciding factor in the antibiotic resistance characteristics of the lipid rich phenotype
- Separating lipid rich from lipid poor cells can be accomplished with a simple mixture of D<sub>2</sub>O and water in plastic vessels for very little cost
- These separated cultures have different morphological characteristics and can be differentiated with both fluorescent microscopy and flow cytometry
- Our adapted Nile red protocol is more effective than previous iterations of the protocol and allows greater resolution of mature lipid bodies

- Lipid rich cells are more rich in PIM glycolipids which are linked to the ability to evade the human immune system
- Old cultures contain many more lipid rich cells than young cultures
- Old cultures display more wax esters and free fatty acids than young ones indicating that these could be significant components of the lipid body
- SLIC might be the most efficient and cost effective way to establish pathogen susceptibility currently available.

## 7 Future work

The work presented herein has shown significant correlations between the lipid body status of a mycobacterial cell and its ability to resist antibiotics. In order to further this work it is necessary to establish whether the presence of a lipid body is indicative of anything other than a high degree of lipid in the cell's immediate environment. To demonstrate that lipid bodies are a marker of dormancy or not we must undertake to investigate the metabolome of separated cultures. The tools with which we approach this task are significant. In order to get a full profile of a cell expressing lipid bodies versus one expressing none we can first separate them with high purity which we can do. We must then use techniques such as RNAseq or SILAC. Deep sequencing of the whole mycobacterial genome in different phenotypic conditions would also be exciting and worth perusing in the future. In order to establish if different circumstances (hypoxia, low pH etc.) effect the content of lipid bodies and therefore their effect on antibiotic resistance and patient treatment outcomes we should also undertake a mass spectrometric study of the whole cell lipidome. These measures should help us to answer the question of whether metabolic shut down equals dormancy and if lipid bodies always present in a 'dormancy-like phenotype'?

The lipidomic work we have begun is still in its nascent stage and can, in the future, grow to become much more complex. In order to not have contamination with lipid species we are not interested in (polar lipids) a new lipid extraction technique could be employed. The Bligh and Dyer technique is dependent upon various volatile solvents to lyse the cell and solubilise the lipids within. A more constrained array of solvents that would only dissolve the non-polar lipids would be beneficial. Alternatively the Bligh and Dyer methodology is well known and accepted by many. It may be what we need only change or add a single step

to ensure that we do not gather any polar lipids. This step could be the inclusion of a more polar solvent to dissolve the polar lipids or simply a larger sample vessel to allow greater resolution of the aqueous and non-polar layers in the extraction thereby reducing the risk of extracting a layer that is not required.

Another lipidomic requirement in future studies will be the quantification of lipids present. This is impossible with TLC or even HPTLC (high performance thin layer chromatography). It may be possible however with gas chromatography to a degree as well as with qHPLC (quantifiable high performance liquid chromatography) (Laxman Sawant 2015). We can quantify the lipids in the lipid bodies with mass spectrometry and this work is ongoing.

If we were to continue to employ TLC as a gross measurement it might in future be worth using a different mobile phase to get greater resolution over the TLC plate and elucidate the lipid species present more accurately. We may also want to employ a different resolving agent such as vaporised sulphuric acid as this does not photo bleach or in other ways fade over time. The last TLC experiment that should be undertaken is a repeat of the 'fed' and 'unfed' bacteria work where we chose a single lipid or a mixture of lipids that do not occur naturally in the mycobacterial metabolome. We could also radio label these lipids for ease of tracking. This would allow us to establish whether certain lipids are up taken more readily than others and if adding lipids or restricting them from the bacteria's 'diet' with drugs or nutritional methods could improve treatment outcomes.

We have had access to some human lung tissue and this has granted us insights into the presence of lipid bodies in human lung tissue. There is ongoing work into numerous human sputum samples which will also contribute new data into the presence of lipid bodies in A



vertically orientated version of the SLIC is also under development which will hopefully give us an even greater stratum of sensitivity in samples with minimal bacterial growth.

human disease. If we are able to extract viable cells from the sputum it is possible we will be able to conduct *ex vivo* susceptibility tests with real-world significance as to the sensitivity of individual patients to individual drugs. If this is possible and tracking patients is also possible it might be that we can change the treatment outcome for future patients by understanding the phenotypical characteristics of the bacteria in their effluent.

SLIC is a potent technology but we are only in the prototype stages and are only beginning to understand what it is capable of. Other methods of bacterial and particle detection such as MALDI-TOF (matrix-assisted laser desorption/ionisation- time of flight) and electrical methods such as resistance (as in a coulter counter), capacitance and electrical and/or magnetic alignment are all potent in their own right but if combined with SLIC they could allow near-instantaneous identification of bacteria in a range of solutions and matrices and allow for non-nucleic acid based susceptibility testing which is more relevant and useful in a real-world environment. Of these none have been attempted with the exception of resistance and capacitance measurements which were effective in established particle number at high concentrations. A detection methodology that is specifically useful to this work and to tuberculosis research would be the high throughput quantification of lipid rich cells in human tissue and effluent. To this end we developed the FLIC (fluorescent light integrating collector). This device is based on the same technology as SLIC but is optimised for discovering the quantity of lipid bodies present in a liquid or solid preparation of bacteria.

Another addition to the SLIC technology we have developed is the heated SLIC. This allows for benchtop incubation of samples and real-time growth curves to be generated without the need to use an external incubator. While a small step forward in the development and the technology of SLIC this represents the proof of concept that benchtop analysis is possible and accurate.

With the further development of SLIC we hope in time to be able to differentiate between different species of bacteria based only on their scattering patterns. Once we have achieved this then the next task is to be able to differentiate between the same species of bacteria but different stains with a good degree of accuracy. The final hurdle would be to be able to differentiate different phenotypic states of the same strain of bacteria such as the 'long thin' active phenotype of mycobacteria versus the 'short fat' dormant phenotype.

The final future development we see currently is the addition of lasers of different wavelengths to SLIC. This would allow for the scattering and absorption measurements of numerous different aspects of a culture and cells which might point towards a species or strain for identification purposes. A blue laser absorbed by the nucleic acids of the cell whereas a yellow laser would be absorbed by the proteins and a green laser by the chromophores of some bacteria. The scattering from these lasers would also allow us to build a detailed database of scattering patterns of bacteria in different media under different conditions allowing us to potentially, eventually, to have an automated system that could identify bacteria by photonics alone. The addition of different wavelengths of laser would also allow for SLIC to be used for colourimetry. This would mean the automatic identification of a media in which bacteria are suspended or the identification of a drug or a change that the bacteria have caused to their environment.

While still in the very early stages of development we have shown that the SLIC/FLIC technology is applicable across a range of photon gathering disciplines.

A fourth version of the SLIC is currently under development in which we can incubate sample on the bench top and generate real-time growth curves with no operator intervention and produce real-time antibiotic susceptibility data.

## 8 References

- (2012). "WHO | Tuberculosis." WHO.
- Adams, A. A., P. I. Okagbare, J. Feng, M. L. Hupert, D. Patterson, J. Gottert, R. L. McCarley, D. Nikitopoulos, M. C. Murphy and S. A. Soper (2008). "Highly efficient circulating tumor cell isolation from whole blood and label-free enumeration using polymer-based microfluidics with an integrated conductivity sensor." J Am Chem Soc **130**(27): 8633-8641.
- Adams, J. D., U. Kim and H. T. Soh (2008). Multitarget magnetic activated cell sorter. Proc Natl Acad Sci U S A. **105**: 18165-18170.
- Ahmad, Z., L. G. Klinkenberg, M. L. Pinn, M. M. Fraig, C. A. Peloquin, W. R. Bishai, E. L. Nuermberger, J. H. Grosset and P. C. Karakousis (2009). "Biphasic kill curve of isoniazid reveals the presence of drug-tolerant, not drug-resistant, Mycobacterium tuberculosis in the guinea pig." J Infect Dis **200**(7): 1136-1143.
- Alliance, T. (2015). "Economic Impact of TB." Retrieved 19/03/2015, 2015, from <http://www.tballiance.org/why/economic-impact.php>.
- Alonso-Echanove, J., R. M. Granich, A. Laszlo, G. Chu, N. Borja, R. Blas, A. Olortegui, N. J. Binkin and W. R. Jarvis (2001). "Occupational Transmission of Mycobacterium tuberculosis to Health Care Workers in a University Hospital in Lima, Peru."
- Alvarez, H. M. and A. Steinbuchel (2002). "Triacylglycerols in prokaryotic microorganisms." Appl Microbiol Biotechnol **60**(4): 367-376.
- Amann, R. I., B. J. Binder, R. J. Olson, S. W. Chisholm, R. Devereux and D. A. Stahl (1990). "Combination of 16S rRNA-targeted oligonucleotide probes with flow cytometry for analyzing mixed microbial populations."
- Anderson, C., N. Inhaber and D. Menzies (1995). "Comparison of sputum induction with fiber-optic bronchoscopy in the diagnosis of tuberculosis." Am J Respir Crit Care Med **152**(5 Pt 1): 1570-1574.
- ANDREWS, E. and L. D. HENRY (1935). "BACTERIOLOGY OF NORMAL AND DISEASED GALLBLADDERS." Archives of Internal Medicine **56**(6): 1171-1188.
- Anuchin, A. M., A. L. Mulyukin, N. E. Suzina, V. I. Duda, G. I. El-Registan and A. S. Kaprelyants (2009). Dormant forms of Mycobacterium smegmatis with distinct morphology. Microbiology. England. **155**: 1071-1079.
- Arrowood, M. J. and C. R. Sterling (1987). "Isolation of Cryptosporidium oocysts and sporozoites using discontinuous sucrose and isopycnic Percoll gradients." J Parasitol **73**(2): 314-319.
- ASSELINAEU, J. and E. LEDERER (1950). "Structure of the Mycolic Acids of Mycobacteria." Nature **166**(4227): 782-783.
- Austrian, R. (1960). "THE GRAM STAIN AND THE ETIOLOGY OF LOBAR PNEUMONIA, AN HISTORICAL NOTE1." Bacteriol Rev **24**(3): 261-265.
- Auty, M. A. E., G. E. Gardiner, S. J. McBrearty, E. O. O'Sullivan, D. M. Mulvihill, J. K. Collins, G. F. Fitzgerald, C. Stanton and R. P. Ross (2001). "Direct In Situ Viability Assessment of Bacteria in Probiotic Dairy Products Using Viability Staining in Conjunction with Confocal Scanning Laser Microscopy."
- Baek, S. H., A. H. Li and C. M. Sasseti (2011). "Metabolic regulation of mycobacterial growth and antibiotic sensitivity." PLoS Biol **9**(5): e1001065.
- Balasubramanian, V., E. H. Wiegshauss, B. T. Taylor and D. W. Smith (1994). Pathogenesis of tuberculosis: pathway to apical localization. Tuber Lung Dis. Scotland. **75**: 168-178.
- BALLENTINE, R. and D. D. BURFORD (1960). "Differential density separation of cellular suspensions." Anal Biochem **1**: 263-268.
- Bansal-Mutalik, R. and H. Nikaido (2014). Mycobacterial outer membrane is a lipid bilayer and the inner membrane is unusually rich in diacyl phosphatidylinositol dimannosides. Proc Natl Acad Sci U S A. **111**: 4958-4963.

Barer, M. R., M. S. B. University of Leicester Medical School, U. H. o. L. N. Trust, mrb19@le.ac.uk, N. J. Garton, M. S. B. University of Leicester Medical School and njg17@le.ac.uk (2015). "Mycobacterial Lipid Bodies and the Chemosensitivity and Transmission of Tuberculosis." 3185-3193.

Barry, C. E., 3rd, R. E. Lee, K. Mdluli, A. E. Sampson, B. G. Schroeder, R. A. Slayden and Y. Yuan (1998). "Mycolic acids: structure, biosynthesis and physiological functions." Prog Lipid Res **37**(2-3): 143-179.

Berg, S., R. Firdessa, M. Habtamu, E. Gadisa, A. Mengistu, L. Yamuah, G. Ameni, M. Vordermeier, B. D. Robertson, N. H. Smith, H. Engers, D. Young, R. G. Hewinson, A. Aseffa and S. V. Gordon (2009). "The burden of mycobacterial disease in ethiopian cattle: implications for public health." PLoS One **4**(4): e5068.

Berger, T., R. P. Marrs and D. L. Moyer (1985). "Comparison of techniques for selection of motile spermatozoa." Fertil Steril **43**(2): 268-273.

Bermudez, L. E. and J. Goodman (1996). "Mycobacterium tuberculosis invades and replicates within type II alveolar cells." Infect Immun **64**(4): 1400-1406.

Betts, J. C., R. P. and, P. T. Lukey, R. P. and, L. C. Robb, G. Statistical Sciences, Gunnels Wood Road, Stevenage, Herts SG1 2NY, UK., R. A. McAdam, R. P. and, K. Duncan and R. P. and (2014). "Evaluation of a nutrient starvation model of Mycobacterium tuberculosis persistence by gene and protein expression profiling." Molecular Microbiology **43**(3): 717-731.

Betts, J. C., P. T. Lukey, L. C. Robb, R. A. McAdam and K. Duncan (2002). "Evaluation of a nutrient starvation model of Mycobacterium tuberculosis persistence by gene and protein expression profiling." Mol Microbiol **43**(3): 717-731.

Bhatt, A., V. Molle, G. S. Besra, W. R. Jacobs, Jr. and L. Kremer (2007). "The Mycobacterium tuberculosis FAS-II condensing enzymes: their role in mycolic acid biosynthesis, acid-fastness, pathogenesis and in future drug development." Mol Microbiol **64**(6): 1442-1454.

Bianchi, A. and L. Giuliano (1996). "Enumeration of viable bacteria in the marine pelagic environment."

BICK, H. (1963). "A REVIEW OF CENTRAL EUROPEAN METHODS FOR THE BIOLOGICAL ESTIMATION OF WATER POLLUTION LEVELS." Bull World Health Organ **29**: 401-413.

Billington, O. J., T. D. McHugh and S. H. Gillespie (1999). Physiological Cost of Rifampin Resistance Induced In Vitro in Mycobacterium tuberculosis. Antimicrob Agents Chemother. **43**: 1866-1869.

Bligh, E. G. and W. J. Dyer (1959). "A rapid method of total lipid extraction and purification." Can J Biochem Physiol **37**(8): 911-917.

BOGEN, E. (1948). "Streptomycin treatment for tuberculosis." J Natl Med Assoc **40**(1): 32.

Boggess, B. (2001). Mass Spectrometry Desk Reference (Sparkman, O. David), Division of Chemical Education.

Bonner, W. A., H. R. Hulett, R. G. Sweet and L. A. Herzenberg (1972). "Fluorescence activated cell sorting." Rev Sci Instrum **43**(3): 404-409.

Boogaerts, M. A., B. University Hospital (Hematology) Leuven, G. Vercelotti, M. University of Minnesota, USA, C. Roelant, B. University Hospital (Hematology) Leuven, S. Malbrain, B. University Hospital (Hematology) Leuven, R. L. Verwilghen, B. University Hospital (Hematology) Leuven, H. S. Jacob and M. University of Minnesota, USA (1986). "Platelets augment granulocyte aggregation and cytotoxicity: uncovering of their effects by improved cell separation techniques using Percoll gradients." Scandinavian Journal of Haematology **37**(3): 229-236.

Boon, C. and T. Dick (2002). Mycobacterium bovis BCG Response Regulator Essential for Hypoxic Dormancy. J Bacteriol. **184**: 6760-6767.

Boshoff, H. I. and C. E. Barry, 3rd (2005). Tuberculosis - metabolism and respiration in the absence of growth. Nat Rev Microbiol. England. **3**: 70-80.

Botha, F. J., F. A. Sirgel, D. P. Parkin, B. W. van de Wal, P. R. Donald and D. A. Mitchison (1996). "Early bactericidal activity of ethambutol, pyrazinamide and the fixed combination of isoniazid, rifampicin and pyrazinamide (Rifater) in patients with pulmonary tuberculosis." S Afr Med J **86**(2): 155-158.

Bowden, K. M. and M. A. McDiarmid (1994). "Occupationally acquired tuberculosis: what's known." J Occup Med **36**(3): 320-325.

Brakke, M. K. and J. M. Daly (1965). "Density-Gradient Centrifugation: Non-Ideal Sedimentation and the Interaction of Major and Minor Components." Science **148**(3668): 387-389.

Brathwaite, C. E., S. E. Ross, R. Nagele, A. J. Mure, K. F. O'Malley and F. A. García-Perez (1993). "Bacterial translocation occurs in humans after traumatic injury: evidence using immunofluorescence." J Trauma **34**(4): 586-589; discussion 589-590.

Brennan, P. J. (2003). Structure, function, and biogenesis of the cell wall of *Mycobacterium tuberculosis*. Tuberculosis (Edinb). England. **83**: 91-97.

Brown, H. A. and L. J. Marnett (2011). "Introduction to lipid biochemistry, metabolism, and signaling." Chem Rev **111**(10): 5817-5820.

Brown-Elliott, B. A. and R. J. Wallace, Jr. (2002). "Clinical and taxonomic status of pathogenic nonpigmented or late-pigmenting rapidly growing mycobacteria." Clin Microbiol Rev **15**(4): 716-746.

Bruckner, M. Z. (2012). "Viability and Quantification Stains."

Burdon, K. L. (1946). "Fatty Material in Bacteria and Fungi Revealed by Staining Dried, Fixed Slide Preparations 1." J Bacteriol **52**(6): 665-678.

Butler, W. R., D. G. Ahearn and J. O. Kilburn (1986). "High-performance liquid chromatography of mycolic acids as a tool in the identification of *Corynebacterium*, *Nocardia*, *Rhodococcus*, and *Mycobacterium* species." J Clin Microbiol **23**(1): 182-185.

Cantwell, M. F., M. T. McKenna, E. McCray and I. M. Onorato (1998). "Tuberculosis and race/ethnicity in the United States: impact of socioeconomic status." Am J Respir Crit Care Med **157**(4 Pt 1): 1016-1020.

Carlson, J., H. Helmbj, A. V. Hill, D. Brewster, B. M. Greenwood and M. Wahlgren (1990). "Human cerebral malaria: association with erythrocyte rosetting and lack of anti-rosetting antibodies." Lancet **336**(8729): 1457-1460.

Casal, M., P. Ruiz, A. Herreras and S. Spanish Study Group of *M. tuberculosis* resistance (2000). "Study of the in vitro susceptibility of *M. tuberculosis* to ofloxacin in Spain." The International Journal of Tuberculosis and Lung Disease **4**(6).

Castro-Malaspina, H., R. E. Gay, G. Resnick, N. Kapoor, P. Meyers, D. Chiarieri, S. McKenzie, H. E. Broxmeyer and M. A. Moore (1980). "Characterization of human bone marrow fibroblast colony-forming cells (CFU-F) and their progeny." Blood **56**(2): 289-301.

Caviedes, L., T. S. Lee, R. H. Gilman, P. Sheen, E. Spellman, E. H. Lee, D. E. Berg and S. Montenegro-James (2000). "Rapid, efficient detection and drug susceptibility testing of *Mycobacterium tuberculosis* in sputum by microscopic observation of broth cultures. The Tuberculosis Working Group in Peru." J Clin Microbiol **38**(3): 1203-1208.

Ceragioli, M., G. Cangiano, S. Esin, E. Ghelardi, E. Ricca and S. Senesi (2009). "Phagocytosis, germination and killing of *Bacillus subtilis* spores presenting heterologous antigens in human macrophages." Microbiology.

Chan, J., Y. Tian, K. E. Tanaka, M. S. Tsang, K. Yu, P. Salgame, D. Carroll, Y. Kress, R. Teitelbaum and B. R. Bloom (1996). "Effects of protein calorie malnutrition on tuberculosis in mice."

Chang, K., W. Lu, J. Wang, K. Zhang, S. Jia, F. Li, S. Deng and M. Chen (2012). "Rapid and effective diagnosis of tuberculosis and rifampicin resistance with Xpert MTB/RIF assay: a meta-analysis." J Infect **64**(6): 580-588.

Chang, Y., P. H. Hsieh and C. C. Chao (2009). "The efficiency of Percoll and Ficoll density gradient media in the isolation of marrow derived human mesenchymal stem cells with osteogenic potential." Chang Gung Med J **32**(3): 264-275.

Chao, M. C. and E. J. Rubin (2010). "Letting sleeping dos lie: does dormancy play a role in tuberculosis?" Annu Rev Microbiol **64**: 293-311.

Chen, W., C. Zhang, L. Song, M. Sommerfeld and Q. Hu (2009). "A high throughput Nile red method for quantitative measurement of neutral lipids in microalgae." J Microbiol Methods **77**(1): 41-47.

Cheney, W. F. (1909). "Tuberculosis of the Kidneys\*." Cal State J Med **7**(6): 212-216.

Chintu, C. and P. Mwaba (2003). Is there a role for chest radiography in identification of asymptomatic tuberculosis in HIV-infected people? Lancet. England. **362**: 1516.

Christensen, H., N. J. Garton, R. W. Horobin, D. E. Minnikin and M. R. Barer (1999). "Lipid domains of mycobacteria studied with fluorescent molecular probes." *Mol Microbiol* **31**(5): 1561-1572.

Clemens, D. L. and M. A. Horwitz (1995). "Characterization of the Mycobacterium tuberculosis phagosome and evidence that phagosomal maturation is inhibited." *J Exp Med* **181**(1): 257-270.

Co, D. O., L. H. Hogan, S. I. Kim and M. Sandor (2004). "Mycobacterial granulomas: keys to a long-lasting host-pathogen relationship." *Clin Immunol* **113**(2): 130-136.

Coker, R. and R. Miller (1997). "HIV associated tuberculosis."

Cole, S. T., R. Brosch, J. Parkhill, T. Garnier, C. Churcher, D. Harris, S. V. Gordon, K. Eiglmeier, S. Gas, C. E. Barry, 3rd, F. Tekaia, K. Badcock, D. Basham, D. Brown, T. Chillingworth, R. Connor, R. Davies, K. Devlin, T. Feltwell, S. Gentles, N. Hamlin, S. Holroyd, T. Hornsby, K. Jagels, A. Krogh, J. McLean, S. Moule, L. Murphy, K. Oliver, J. Osborne, M. A. Quail, M. A. Rajandream, J. Rogers, S. Rutter, K. Seeger, J. Skelton, R. Squares, S. Squares, J. E. Sulston, K. Taylor, S. Whitehead and B. G. Barrell (1998). "Deciphering the biology of Mycobacterium tuberculosis from the complete genome sequence." *Nature* **393**(6685): 537-544.

Cole, S. T., R. Brosch, J. Parkhill, T. Garnier, C. Churcher, D. Harris, S. V. Gordon, K. Eiglmeier, S. Gas, C. E. Barry, F. Tekaia, K. Badcock, D. Basham, D. Brown, T. Chillingworth, R. Connor, R. Davies, K. Devlin, T. Feltwell, S. Gentles, N. Hamlin, S. Holroyd, T. Hornsby, K. Jagels, A. Krogh, J. McLean, S. Moule, L. Murphy, K. Oliver, J. Osborne, M. A. Quail, M.-A. Rajandream, J. Rogers, S. Rutter, K. Seeger, J. Skelton, R. Squares, S. Squares, J. E. Sulston, K. Taylor, S. Whitehead and B. G. Barrell (1998). "Deciphering the biology of Mycobacterium tuberculosis from the complete genome sequence." *Nature* **393**(6685): 537-544.

Collins, C. H. and A. H. Uttley (1985). "In-vitro susceptibility of mycobacteria to ciprofloxacin." *J Antimicrob Chemother* **16**(5): 575-580.

Comstock, G. W., V. T. Livesay and S. F. Woolpert (1974). "The prognosis of a positive tuberculin reaction in childhood and adolescence." *Am J Epidemiol* **99**(2): 131-138.

Conde, M. B., A. C. Loivos, V. M. Rezende, S. L. Soares, F. C. Mello, A. L. Reingold, C. L. Daley and A. L. Kritski (2003). Yield of sputum induction in the diagnosis of pleural tuberculosis. *Am J Respir Crit Care Med*. United States. **167**: 723-725.

Corbett, E. L., C. J. Watt, N. Walker, D. Maher, B. G. Williams, M. C. Raviglione and C. Dye (2003). The growing burden of tuberculosis: global trends and interactions with the HIV epidemic. *Arch Intern Med*. United States. **163**: 1009-1021.

Cosma, C. L., D. R. Sherman and L. Ramakrishnan (2003). "The secret lives of the pathogenic mycobacteria." *Annu Rev Microbiol* **57**: 641-676.

Coulombel, L. (2004). "Identification of hematopoietic stem|[sol]|progenitor cells: strength and drawbacks of functional assays." *Oncogene* **23**(43): 7210-7222.

Crofton, J. and D. A. Mitchison (1948). "Streptomycin Resistance in Pulmonary Tuberculosis." *Br Med J* **2**(4588): 1009-1015.

Cundall, D. B. (1986). "The diagnosis of pulmonary tuberculosis in malnourished Kenyan children." *Ann Trop Paediatr* **6**(4): 249-255.

D'Avila, H., R. C. Melo, G. G. Parreira, E. Werneck-Barroso, H. C. Castro-Faria-Neto and P. T. Bozza (2006). "Mycobacterium bovis bacillus Calmette-Guérin induces TLR2-mediated formation of lipid bodies: intracellular domains for eicosanoid synthesis in vivo." *J Immunol* **176**(5): 3087-3097.

Daniel, J., C. o. M. Burnett School of Biomedical Sciences, University of Central Florida, Orlando, Florida, United States of America, H. Maamar, C. o. M. Burnett School of Biomedical Sciences, University of Central Florida, Orlando, Florida, United States of America, C. Deb, C. o. M. Burnett School of Biomedical Sciences, University of Central Florida, Orlando, Florida, United States of America, T. D. Sirakova, C. o. M. Burnett School of Biomedical Sciences, University of Central Florida, Orlando, Florida, United States of America, P. E. Kolattukudy and C. o. M. Burnett School of Biomedical Sciences, University of Central Florida, Orlando, Florida, United States of America (2011). "Mycobacterium tuberculosis Uses Host Triacylglycerol to Accumulate Lipid Droplets and Acquires a Dormancy-Like Phenotype in Lipid-Loaded Macrophages." *PLOS Pathogens* **7**(6).

Daniel, J., C. Deb, V. S. Dubey, T. D. Sirakova, B. Abomoelak, H. R. Morbidoni and P. E. Kolattukudy (2004). Induction of a novel class of diacylglycerol acyltransferases and triacylglycerol accumulation in *Mycobacterium tuberculosis* as it goes into a dormancy-like state in culture. *J Bacteriol*. United States. **186**: 5017-5030.

Daniel, J., H. Maamar, C. Deb, T. D. Sirakova and P. E. Kolattukudy (2011). "Mycobacterium tuberculosis uses host triacylglycerol to accumulate lipid droplets and acquires a dormancy-like phenotype in lipid-loaded macrophages." *PLoS Pathog* **7**(6): e1002093.

Dannenberg, A. M., Jr. (1991). Delayed-type hypersensitivity and cell-mediated immunity in the pathogenesis of tuberculosis. *Immunol Today*. England. **12**: 228-233.

Dannenberg, A. M., Jr. and M. Sugimoto (1976). "Liquefaction of caseous foci in tuberculosis." *Am Rev Respir Dis* **113**(3): 257-259.

David, H. L., W. D. Jones and C. M. Newman (1971). "Ultraviolet Light Inactivation and Photoreactivation in the Mycobacteria." *Infect Immun* **4**(3): 318-319.

Davidson, L. A. and K. Takayama (1979). "Isoniazid Inhibition of the Synthesis of Monounsaturated Long-Chain Fatty Acids in *Mycobacterium tuberculosis* H37Ra." *Antimicrob Agents Chemother* **16**(1): 104-105.

de Wit, D., M. Wootton, J. Dhillon and D. A. Mitchison (1995). The bacterial DNA content of mouse organs in the Cornell model of dormant tuberculosis. *Tuber Lung Dis*. Scotland. **76**: 555-562.

Deb, C., C. o. M. Burnett School of Biomedical Sciences, University of Central Florida, Orlando, Florida, United States of America, C.-M. Lee, C. o. M. Burnett School of Biomedical Sciences, University of Central Florida, Orlando, Florida, United States of America, V. S. Dubey, C. o. M. Burnett School of Biomedical Sciences, University of Central Florida, Orlando, Florida, United States of America, J. Daniel, C. o. M. Burnett School of Biomedical Sciences, University of Central Florida, Orlando, Florida, United States of America, B. Abomoelak, C. o. M. Burnett School of Biomedical Sciences, University of Central Florida, Orlando, Florida, United States of America, T. D. Sirakova, C. o. M. Burnett School of Biomedical Sciences, University of Central Florida, Orlando, Florida, United States of America, S. Pawar, C. o. M. Burnett School of Biomedical Sciences, University of Central Florida, Orlando, Florida, United States of America, L. Rogers, C. o. M. Burnett School of Biomedical Sciences, University of Central Florida, Orlando, Florida, United States of America, P. E. Kolattukudy and C. o. M. Burnett School of Biomedical Sciences, University of Central Florida, Orlando, Florida, United States of America (2009). "A Novel In Vitro Multiple-Stress Dormancy Model for *Mycobacterium tuberculosis* Generates a Lipid-Loaded, Drug-Tolerant, Dormant Pathogen." *PLOS ONE* **4**(6).

Deb, C., C. M. Lee, V. S. Dubey, J. Daniel, B. Abomoelak, T. D. Sirakova, S. Pawar, L. Rogers and P. E. Kolattukudy (2009). "A novel in vitro multiple-stress dormancy model for *Mycobacterium tuberculosis* generates a lipid-loaded, drug-tolerant, dormant pathogen." *PLoS One* **4**(6): e6077.

Debye, P. (1944). "Light Scattering in Solutions." *Journal of Applied Physics* **15**: 338-342.

Deng, L., K. Mikusova, K. G. Robuck, M. Scherman, P. J. Brennan and M. R. McNeil (1995). "Recognition of multiple effects of ethambutol on metabolism of mycobacterial cell envelope." *Antimicrob Agents Chemother* **39**(3): 694-701.

Deretic, V., S. Singh, S. Master, J. Harris, E. Roberts, G. Kyei, A. Davis, S. de Haro, J. Naylor, H. H. Lee and I. Vergne (2006). *Mycobacterium tuberculosis* inhibition of phagolysosome biogenesis and autophagy as a host defence mechanism. *Cell Microbiol*. England. **8**: 719-727.

Diel, R., S. Rutz, S. Castell and T. Schaberg (2012). "Tuberculosis: cost of illness in Germany." *European Respiratory Journal*.

Diseases, W. H. O. D. o. C. and W. I. G. P. o. A.-T. D. R. Surveillance (2000). "Anti-tuberculosis drug resistance in the world / the WHO/IUATLD Global Project on Anti-Tuberculosis Drug Resistance Surveillance. Report 2, Prevalence and trends."

Driscoll, J. R. (2009). "Spoligotyping for molecular epidemiology of the *Mycobacterium tuberculosis* complex." *Methods Mol Biol* **551**: 117-128.



Drlica, K. and X. Zhao (1997). "DNA gyrase, topoisomerase IV, and the 4-quinolones." Microbiol Mol Biol Rev **61**(3): 377-392.

Ducati, R. G., A. Ruffino-Netto, L. A. Basso and D. S. Santos (2006). The resumption of consumption -- a review on tuberculosis. Mem Inst Oswaldo Cruz. Brazil. **101**: 697-714.

Ducharme, A., A. Daniels, E. Grann and G. Boreman (1997). "Design of an integrating sphere as a uniform illumination source." Ieee Transactions on Education **40**(2): 131-134.

Dutta, N. K., M. L. Pinn and P. C. Karakousis (2014). "Reduced emergence of isoniazid resistance with concurrent use of thioridazine against acute murine tuberculosis." Antimicrob Agents Chemother **58**(7): 4048-4053.

Dye, C., A. Bassili, A. L. Bierrenbach, J. F. Broekmans, V. K. Chadha, P. Glaziou, P. G. Gopi, M. Hosseini, S. J. Kim, D. Manissero, I. Onozaki, H. L. Rieder, S. Scheele, F. van Leth, M. van der Werf and B. G. Williams (2008). Measuring tuberculosis burden, trends, and the impact of control programmes. Lancet Infect Dis. United States. **8**: 233-243.

EASTWOOD, J. B., C. M. CORBISHLEY and J. M. GRANGE (2001). "Tuberculosis and the Kidney." Journal of the American Society of Nephrology.

Eisenberg, R., A. Fox, J. J. Greenblatt, S. K. Anderle, W. J. Cromartie and J. H. Schwab (1982). "Measurement of bacterial cell wall in tissues by solid-phase radioimmunoassay: correlation of distribution and persistence with experimental arthritis in rats." Infect Immun **38**(1): 127-135.

Eisert, W. G., R. Ostertag, E. Niemann, x and G (1975). "Simple flow microphotometer for rapid cell population analysis." Review of Scientific Instruments **46**(8): 1021-1024.

Enomoto, Y., M. Sugita, I. Matsunaga, T. Naka, A. Sato, T. Kawashima, K. Shimizu, H. Takahashi, Y. Norose and I. Yano (2005). "Temperature-dependent biosynthesis of glucose monomycolate and its recognition by CD1-restricted T cells." Biochem Biophys Res Commun **337**(2): 452-456.

Ewer, K., J. Deeks, L. Alvarez, G. Bryant, S. Waller, P. Andersen, P. Monk and A. Lavani (2003). Comparison of T-cell-based assay with tuberculin skin test for diagnosis of Mycobacterium tuberculosis infection in a school tuberculosis outbreak. Lancet. England. **361**: 1168-1173.

Farnia, P., R. M. Mohammad, M. A. Merza, P. Tabarsi, G. K. Zhavnerko, T. A. Ibrahim, H. O. Kuan, J. Ghanavei, R. Ranjbar, N. N. Poleschuyk, L. P. Titov, P. Owlia, M. Kazampour, M. Setareh, M. Sheikolsami, G. B. Migliori and A. A. Velayati (2010). "Growth and cell-division in extensive (XDR) and extremely drug resistant (XXDR) tuberculosis strains: transmission and atomic force observation." Int J Clin Exp Med **3**(4): 308-314.

Feng, G. D., F. Zhang, L. H. Cheng, X. H. Xu, L. Zhang and H. L. Chen (2013). "Evaluation of FT-IR and Nile Red methods for microalgal lipid characterization and biomass composition determination." Bioresour Technol **128**: 107-112.

Ferrero, E., P. Biswas, K. Vettoretto, M. Ferrarini, M. Uguccioni, L. Piali, B. E. Leone, B. Moser, C. Rugarli and R. Pardi (2003). "Macrophages exposed to Mycobacterium tuberculosis release chemokines able to recruit selected leucocyte subpopulations: focus on  $\gamma\delta$  cells." Immunology **108**(3): 365-374.

Filippini, P., E. Iona, G. Piccaro, P. Peyron, O. Neyrolles and L. Fattorini (2010). "Activity of Drug Combinations against Dormant Mycobacterium tuberculosis."

Firdessa, R., S. Berg, E. Hailu, E. Schelling, B. Gumi, G. Erenso, E. Gadisa, T. Kiros, M. Habtamu, J. Hussein, J. Zinsstag, B. D. Robertson, G. Ameni, A. J. Lohan, B. Loftus, I. Comas, S. Gagneux, R. Tschoop, L. Yamuah, G. Hewinson, S. V. Gordon, D. B. Young and A. Aseffa (2013). Mycobacterial Lineages Causing Pulmonary and Extrapulmonary Tuberculosis, Ethiopia. Emerg Infect Dis. **19**: 460-463.

Flynn, J. L. and J. Chan (2001). Tuberculosis: Latency and Reactivation. Infect Immun. **69**: 4195-4201.

Fountain, J. R. (1954). "Blood Changes Associated with Disseminated Tuberculosis." Br Med J **2**(4879): 76-79.

Fowler, S. D., W. J. Brown, J. Warfel and P. Greenspan (1987). "Use of nile red for the rapid in situ quantitation of lipids on thin-layer chromatograms." J Lipid Res **28**(10): 1225-1232.

Fowler, S. D. and P. Greenspan (1985). "Application of Nile red, a fluorescent hydrophobic probe, for the detection of neutral lipid deposits in tissue sections: comparison with oil red O." J Histochem Cytochem **33**(8): 833-836.

Fratti, R. A., J. M. Backer, J. Gruenberg, S. Corvera and V. Deretic (2001). Role of phosphatidylinositol 3-kinase and Rab5 effectors in phagosomal biogenesis and mycobacterial phagosome maturation arrest. J Cell Biol. United States. **154**: 631-644.

Frieden, T. R., T. Sterling, A. Pablos-Mendez, J. O. Kilburn, G. M. Cauthen and S. W. Dooley (1993). "The emergence of drug-resistant tuberculosis in New York City." N Engl J Med **328**(8): 521-526.

Gandhi, N. R., A. Moll, A. W. Sturm, R. Pawinski, T. Govender, U. Lalloo, K. Zeller, J. Andrews and G. Friedland (2006). "Extensively drug-resistant tuberculosis as a cause of death in patients co-infected with tuberculosis and HIV in a rural area of South Africa." Lancet **368**(9547): 1575-1580.

Garner, P., H. Smith, S. Munro and J. Volmink (2007). "Promoting adherence to tuberculosis treatment." Bull World Health Organ **85**(5): 404-406.

Garton, N. J., H. Christensen, D. E. Minnikin, R. A. Adegbola and M. R. Barer (2002). "Intracellular lipophilic inclusions of mycobacteria in vitro and in sputum." Microbiology **148**(Pt 10): 2951-2958.

Garton, N. J., S. J. Waddell, A. L. Sherratt, S. M. Lee, R. J. Smith, C. Senner, J. Hinds, K. Rajakumar, R. A. Adegbola, G. S. Besra, P. D. Butcher and M. R. Barer (2008). Cytological and Transcript Analyses Reveal Fat and Lazy Persister-Like Bacilli in Tuberculous Sputum. PLoS Med. **5**.

Garton, N. J., S. J. Waddell, A. L. Sherratt, S. M. Lee, R. J. Smith, C. Senner, J. Hinds, K. Rajakumar, R. A. Adegbola, G. S. Besra, P. D. Butcher and M. R. Barer (2008). "Cytological and transcript analyses reveal fat and lazy persister-like bacilli in tuberculous sputum." PLoS Med **5**(4): e75.

Gawne-Cain, M. L. and D. M. Hansell (1996). "The pattern and distribution of calcified mediastinal lymph nodes in sarcoidosis and tuberculosis: a CT study." Clin Radiol **51**(4): 263-267.

Getahun, H., M. Harrington, R. O'Brien and P. Nunn (2007). Diagnosis of smear-negative pulmonary tuberculosis in people with HIV infection or AIDS in resource-constrained settings: informing urgent policy changes. Lancet. England. **369**: 2042-2049.

Githui, W., F. Kitui, E. S. Juma, D. O. Obwana, J. Mwai and D. Kwamanga (1993). "A comparative study on the reliability of the fluorescence microscopy and Ziehl-Neelsen method in the diagnosis of pulmonary tuberculosis." East Afr Med J **70**(5): 263-266.

Goble, M., M. D. Iseman, L. A. Madsen, D. Waite, L. Ackerson and C. R. Horsburgh, Jr. (1993). "Treatment of 171 patients with pulmonary tuberculosis resistant to isoniazid and rifampin." N Engl J Med **328**(8): 527-532.

Goebel, D. G. (1967). "Generalized Integrating-Sphere Theory." Applied Optics, Vol. 6, Issue 1, pp. 125-128.

Goerke, J. (1998). "Pulmonary surfactant: functions and molecular composition." Biochim Biophys Acta **1408**(2-3): 79-89.

Goldburg, W. (1999). "Dynamic light scattering." American Journal of Physics **67**(12): 1152-1160.

Gomez, J. E. and J. D. McKinney (2004). "M. tuberculosis persistence, latency, and drug tolerance." Tuberculosis (Edinb) **84**(1-2): 29-44.

Gonzalez-Mariscal, I., E. Garcia-Teston, S. Padilla, A. Martin-Montalvo, T. Pomares Vician, L. Vazquez-Fonseca, P. Gandolfo Dominguez and C. Santos-Ocana (2014). The regulation of coenzyme q biosynthesis in eukaryotic cells: all that yeast can tell us. Mol Syndromol. Switzerland. **5**: 107-118.

Goodfellow, M. and J. G. Magee (1998). Mycobacteria: basic aspects, Springer US.

Goodfellow, M., D. E. Minnikin, C. Todd, G. Alderson, S. M. Minnikin and M. D. Collins (1982). "Numerical and chemical classification of *Nocardia amarae*." J Gen Microbiol **128**(6): 1283-1297.

Gordon, R. E. and M. M. Smith (1953). "RAPIDLY GROWING, ACID FAST BACTERIA I. : Species' Descriptions of *Mycobacterium phlei* Lehmann and Neumann and *Mycobacterium smegmatis* (Trevisan) Lehmann and Neumann1." J Bacteriol **66**(1): 41-48.

Goren, M. B., P. D'Arcy Hart, M. R. Young and J. A. Armstrong (1976). "Prevention of phagosome-lysosome fusion in cultured macrophages by sulfatides of *Mycobacterium tuberculosis*." Proc Natl Acad Sci U S A **73**(7): 2510-2514.

Gosling, R. D., L. O. Uiso, N. E. Sam, E. Bongard, E. G. Kanduma, M. Nyindo, R. W. Morris and S. H. Gillespie (2003). The bactericidal activity of moxifloxacin in patients with pulmonary tuberculosis. Am J Respir Crit Care Med. United States. **168**: 1342-1345.

Gram, C. (1884). "The differential staining of Schizomycetes

in tissue sections and in

dried preparations." General Microbiology.

Gratama, J. W., D. d. H. K. Department of Clinical and Tumor Immunology, Rotterdam, The Netherlands, D. d. H. C. C. Department of Clinical and Tumor Immunology, P.O. Box 5201, 3008 AE Rotterdam, The Netherlands, J. L. D'hautcourt, B. H pital de Warquignies, Belgium, F. Mandy, H. P. B. National Laboratory for Analytical Cytology, Health Canada, Ottawa, Canada, G. Rothe, K. d. U. t. R. Institut f r Klinische Chemie und Laboratoriumsmedizin, Regensburg, Germany, D. Barnett, R. H. H. Department of Haematology, Sheffield, England, G. Janossy, R. F. H. S. o. M. Department of Clinical Immunology, London, England, S. Papa, U. d. U. Istituto di Scienze Morfologiche, Urbino, Italy, G. Schmitz, K. d. U. t. R. Institut f r Klinische Chemie und Laboratoriumsmedizin, Regensburg, Germany, R. Lenkei, S. t. G. r. S. CALAB Research, Stockholm, Sweden and T. E. W. G. o. C. C. Analysis (1999). "Flow cytometric quantitation of immunofluorescence intensity: Problems and perspectives." Cytometry **33**(2): 166-178.

Greenspan, P. and S. D. Fowler (1985). "Spectrofluorometric studies of the lipid probe, Nile red." J Lipid Res **26**(7): 781-789.

Greenspan, P., E. P. Mayer and S. D. Fowler (1985). "Nile red: a selective fluorescent stain for intracellular lipid droplets." J Cell Biol **100**(3): 965-973.

Griffith, D. E. and C. M. Kerr (1996). Tuberculosis: disease of the past, disease of the present. J Perianesth Nurs. United States. **11**: 240-245.

Gronthos, S., M. Mankani, J. Brahimi, P. G. Robey and S. Shi (2000). "Postnatal human dental pulp stem cells (DPSCs) in vitro and in vivo." Proc Natl Acad Sci U S A **97**(25): 13625-13630.

Grossman, W. J., J. W. Verbsky, W. Barchet, M. Colonna, J. P. Atkinson and T. J. Ley (2004). "Human T regulatory cells can use the perforin pathway to cause autologous target cell death." Immunity **21**(4): 589-601.

Hall-Stoodley, L. and H. Lappin-Scott (1998). Biofilm formation by the rapidly growing mycobacterial species *Mycobacterium fortuitum*. FEMS Microbiol Lett. Netherlands. **168**: 77-84.

Hammond, R. J. H., V. O. Baron, K. Oravcova, S. Lipworth and S. H. Gillespie (2015). "Phenotypic resistance in mycobacteria: is it because I am old or fat that I resist you?" Journal of antimicrobial chemotherapy.

Hampshire, T., S. Soneji, J. Bacon, B. W. James, J. Hinds, K. Laing, R. A. Stabler, P. D. Marsh and P. D. Butcher (2004). "Stationary phase gene expression of *Mycobacterium tuberculosis* following a progressive nutrient depletion: a model for persistent organisms?" Tuberculosis (Edinb) **84**(3-4): 228-238.

Han, X. (2007). "Neurolipidomics: challenges and developments." Front Biosci **12**: 2601-2615.

Han, X. and R. W. Gross (2003). Global analyses of cellular lipidomes directly from crude extracts of biological samples by ESI mass spectrometry: a bridge to lipidomics. J Lipid Res. United States. **44**: 1071-1079.

Hanna, B. A., A. Ebrahimzadeh, L. B. Elliott, M. A. Morgan, S. M. Novak, S. Rusch-Gerdes, M. Acio, D. F. Dunbar, T. M. Holmes, C. H. Rexer, C. Savthyakumar and A. M. Vannier (1999). "Multicenter Evaluation of the BACTEC MGIT 960 System for Recovery of *Mycobacteria*."

Harmoinen, A., O. H llstr m and P. Gr nroos (2009). "Rapid quantitative determination of C-reactive protein using laser-nephelometer."

Harries, A. D., D. Maher and P. Nunn (1998). "An approach to the problems of diagnosing and treating adult smear-negative pulmonary tuberculosis in high-HIV-prevalence settings in sub-Saharan Africa." Bull World Health Organ **76**(6): 651-662.

Hatzios, S. K., C. E. Baer, T. R. Rustad, M. S. Siegrist, J. M. Pang, C. Ortega, T. Alber, C. Grundner, D. R. Sherman and C. R. Bertozzi (2013). Osmosensory signaling in *Mycobacterium tuberculosis* mediated by a eukaryotic-like Ser/Thr protein kinase. *Proc Natl Acad Sci U S A*. **110**: E5069-5077.

Hayakawa, M., M. Otoguro, T. Takeuchi, T. Yamazaki and Y. Iimura (2000). "Application of a method incorporating differential centrifugation for selective isolation of motile actinomycetes in soil and plant litter." *Antonie Van Leeuwenhoek* **78**(2): 171-185.

Heesemann, J. and R. Laufs (1985). "Double immunofluorescence microscopic technique for accurate differentiation of extracellularly and intracellularly located bacteria in cell culture."

Hett, E. C. and E. J. Rubin (2008). Bacterial growth and cell division: a mycobacterial perspective. *Microbiol Mol Biol Rev*. United States. **72**: 126-156, table of contents.

Hobby, G. L., A. P. Holman, M. D. Iseman and J. M. Jones (1973). "Enumeration of Tubercle Bacilli in Sputum of Patients with Pulmonary Tuberculosis." *Antimicrob Agents Chemother* **4**(2): 94-104.

HOLTER, H., M. OTTESEN and R. WEBER (1953). "Separation of cytoplasmic particles by centrifugation in a density-gradient." *Experientia* **9**(9): 346-348.

Honer zu Bentrup, K. and D. G. Russell (2001). Mycobacterial persistence: adaptation to a changing environment. *Trends Microbiol*. England. **9**: 597-605.

Hu, Y., S. G. s. H. M. S. Department of Medical Microbiology, London SW17 0RE, UK, A. R. M. Coates and S. G. s. H. M. S. Department of Medical Microbiology, London SW17 0RE, UK (2014). "Increased levels of sigJ mRNA in late stationary phase cultures of *Mycobacterium tuberculosis* detected by DNA array hybridisation." *FEMS Microbiology Letters* **202**(1): 59-65.

Huang, Y., X. Zhou, Y. Bai, L. Yang, X. Yin, Z. Wang and D. Zhao (2012). "Phagolysosome maturation of macrophages was reduced by PE\_PGRS 62 protein expressing in *Mycobacterium smegmatis* and induced in IFN-gamma priming." *Vet Microbiol* **160**(1-2): 117-125.

Hudelson, P. (1996). Gender differentials in tuberculosis: the role of socio-economic and cultural factors. *Tuber Lung Dis*. Scotland. **77**: 391-400.

Huff, K., Banada, P., Bae, E., Bayraktar, B., Rajwa, B., Robinson, J., Bhunia, A. (2006). Detection and Identification of Foodborne Pathogens to Genus and Species Levels Using a Noninvasive Modified Light Scatterometer-Bardot. American Society for Microbiology., American Society for Microbiology.

Hunter, R. L., M. R. Olsen, C. Jagannath and J. K. Actor (2006). "Multiple Roles of Cord Factor in the Pathogenesis of Primary, Secondary, and Cavitory Tuberculosis, Including a Revised Description of the Pathology of Secondary Disease."

Ichiyama, S., K. Shimokata and J. Takeuchi (1993). "Comparative study of a biphasic culture system (Roche MB Check system) with a conventional egg medium for recovery of mycobacteria. Aichi Mycobacteriosis Research Group." *Tuber Lung Dis* **74**(5): 338-341.

Ino-Ue, M. and M. Yamamoto (2008). "Toxic Optic Neuropathy: Psychotropics and Ethambutol Inhibit Myelin Basic Protein Phosphorylation." *Cutaneous and Ocular Toxicology*.

Isabel, S., M. Boissinot, I. Charlebois, C. M. Fauvel, L. E. Shi, J. C. Lévesque, A. T. Paquin, M. Bastien, G. Stewart, É. Leblanc, S. Sato and M. G. Bergeron (2012). Rapid Filtration Separation-Based Sample Preparation Method for Bacillus Spores in Powdery and Environmental Matrices. *Appl Environ Microbiol*. **78**: 1505-1512.

IUATLD (2000). Sputum examination for tuberculosis by direct microscopy in low income countries. 5th ed. Paris.

Jeong, Y. J. and K. S. Lee (2008). Pulmonary tuberculosis: up-to-date imaging and management. *AJR Am J Roentgenol*. United States. **191**: 834-844.

Jones-Lopez, E. C., O. Namugga, F. Mumbowa, M. Ssebidiandi, O. Mbabazi, S. Moine, G. Mboowa, M. P. Fox, N. Reilly, I. Ayakaka, S. Kim, A. Okwera, M. Joloba and K. P. Fennelly (2013). Cough aerosols of *Mycobacterium tuberculosis* predict new infection: a household contact study. *Am J Respir Crit Care Med*. United States. **187**: 1007-1015.

Jula, A., P. Puukka and H. Karanko (1999). "Multiple Clinic and Home Blood Pressure Measurements Versus Ambulatory Blood Pressure Monitoring."

Jung, T., U. Schauer, C. Heusser, C. Neumann and C. Rieger (1993). "Detection of intracellular cytokines by flowcytometry." **159**(Issues 1–2): 197–207.

Kachan, S., A. Ponyavina, V. Borisenko, S. Gaponenko and V. Gurin (2001). "Optical properties of layer-periodic metal nanoparticle systems in the visible." Physics, Chemistry and Application of Nanostructures: 235-238.

Kahnert, A., U. E. Hopken, M. Stein, S. Bandermann, M. Lipp and S. H. Kaufmann (2007). Mycobacterium tuberculosis triggers formation of lymphoid structure in murine lungs. J Infect Dis. United States. **195**: 46-54.

Kannaperuman, J., G. Natarajarathinam, A. V. Rao and S. Palanimuthu (2013). Primary tuberculous osteomyelitis of the mandible: A rare case report. Dent Res J (Isfahan). **10**: 283-286.

Kaplan, G., R. R. Gandhi, D. E. Weinstein, W. R. Levis, M. E. Patarroyo, P. J. Brennan and Z. A. Cohn (1987). "Mycobacterium leprae antigen-induced suppression of T cell proliferation in vitro." J Immunol **138**(9): 3028-3034.

Kapoor, N., S. Pawar, T. D. Sirakova, C. Deb, W. L. Warren and P. E. Kolattukudy (2013). "Human granuloma in vitro model, for TB dormancy and resuscitation." PLoS One **8**(1): e53657.

Kaprelyants, A. S. and D. B. Kell (1993). "Dormancy in Stationary-Phase Cultures of Micrococcus luteus: Flow Cytometric Analysis of Starvation and Resuscitation." Appl Environ Microbiol **59**(10): 3187-3196.

Kapuscinski, J. (1990). "Interactions of nucleic acids with fluorescent dyes: spectral properties of condensed complexes." J Histochem Cytochem **38**(9): 1323-1329.

Kawaguchi, S., G. Imai, J. Suzuki, A. Miyahara, T. Kitano and K. Ito (1997). "Aqueous solution properties of oligo- and poly(ethylene oxide) by staticlightscattering and intrinsic viscosity." **38**(12): 2885–2891.

Kawamura, L. M., J. A. Grinsdale, C. S. Ho and J. A. Jereb (2012). Interferon-gamma release assays for prediction of tuberculosis. Lancet Infect Dis. United States. **12**: 584.

Kawkab Adris Mahmod, B. A. A. ك. ا. ب. م. ا. ع. ل. "Detection of Mycobacterium tuberculosis in sputum using conventional methods and PCR التحري الصديات عن ال  
ال قشع في (ال سل) ال تدرن ع صديات عن ال  
ال م تسلسل ال بالمره ت فاعل وت قذية ال تقل يدي هب ال طرائق

Kenyon, T. A., S. E. Valway, W. W. Ihle, I. M. Onorato and K. G. Castro (1996). "Transmission of multidrug-resistant Mycobacterium tuberculosis during a long airplane flight." N Engl J Med **334**(15): 933-938.

Keren, I., N. Kaldalu, A. Spoering, Y. Wang and K. Lewis (2004). Persister cells and tolerance to antimicrobials. FEMS Microbiol Lett. Netherlands. **230**: 13-18.

King, L. (2001). "Minimising the risk of hospital transmission of pulmonary TB." Nurs Stand **16**(4): 45-52; quiz 54-45.

Kivihya-Ndugga, L. E., M. R. van Cleeff, W. A. Githui, L. W. Nganga, D. K. Kibuga, J. A. Odhiambo and P. R. Klatser (2003). "A comprehensive comparison of Ziehl-Neelsen and fluorescence microscopy for the diagnosis of tuberculosis in a resource-poor urban setting." Int J Tuberc Lung Dis **7**(12): 1163-1171.

Knaysi, G. (1945). ON THE ORIGIN AND FATE OF THE FATTY INCLUSIONS IN A STRAIN OF BACILLUS CEREUS. Science. United States. **102**: 424.

Knight, R. K. and M. H. Pritchard (1982). "Nephelometry compared with differential antibody titre in routine rheumatoid factor measurements."

Kornberg, H. L. and H. Beevers (1957). "A mechanism of conversion of fat to carbohydrate in castor beans." Nature **180**(4575): 35-36.

Kremer, L., C. de Chastellier, G. Dobson, K. J. Gibson, P. Bifani, S. Balor, J. P. Gorvel, C. Loch, D. E. Minnikin and G. S. Besra (2005). Identification and structural characterization of an unusual mycobacterial monomeromycyl-diacylglycerol. Mol Microbiol. England. **57**: 1113-1126.

KUPPENHEIM, J. A. J. H. F. (1955). "Theory of the Integrating Sphere." JOSA, Vol. 45, Issue 6, pp. 460-466.

KURNICK, J. T., U. U. Department of Immunology, Uppsala, Sweden, L. ÖSTBERG, U. U. Department of Immunology, Uppsala, Sweden, M. STEGAGNO, U. U. Department of Immunology, Uppsala, Sweden, A. K. KIMURA, U. U. Department of Immunology, Uppsala, Sweden, A. ÖRN, U. U. Department of Immunology, Uppsala, Sweden, O. SJÖBERG and U. U. Department of Immunology, Uppsala, Sweden (1979). "A Rapid Method for the Separation of Functional Lymphoid Cell Populations of Human and Animal Origin on PVP-Silica (Percoll) Density Gradients." Scandinavian Journal of Immunology **10**(6): 563-573.

Laifangbam, S., H. L. Singh, N. B. Singh, K. M. Devi and N. T. Singh (2009). "A comparative study of fluorescent microscopy with Ziehl-Neelsen staining and culture for the diagnosis of pulmonary tuberculosis." Kathmandu Univ Med J (KUMJ) **7**(27): 226-230.

Lalvani, A. (2007). "Diagnosing Tuberculosis Infection in the 21st Century: New Tools To Tackle an Old Enemy." CHEST Journal **131**(6): 1898-1906.

Lawn, S. D. and A. I. Zumla (2011). "Tuberculosis." Lancet **378**(9785): 57-72.

Laxman Sawant, B. P. a. N. P. (2015). "Quantitative HPLC Analysis of Ascorbic Acid and Gallic Acid in *Phyllanthus Emblica*." Journal of Analytical & Bioanalytical Techniques.

Layre, E., L. Sweet, S. Hong, C. A. Madigan, D. Desjardins, D. C. Young, T. Y. Cheng, J. W. Annand, K. Kim, I. C. Shamputa, M. J. McConnell, C. A. Debono, S. M. Behar, A. J. Minnaard, M. Murray, C. E. Barry, I. Matsunaga and D. B. Moody (2011). "A comparative lipidomics platform for chemotaxonomic analysis of *Mycobacterium tuberculosis*." Chem Biol **18**(12): 1537-1549.

LEIFSON, E. (1951). "Staining, shape and arrangement of bacterial flagella." J Bacteriol **62**(4): 377-389.

Levin, M. E., U. o. P. Department of Biological Sciences, Pittsburgh, Pennsylvania 15260, USA., G. F. Hatfull and U. o. P. Department of Biological Sciences, Pittsburgh, Pennsylvania 15260, USA. (2014). "Mycobacterium smegmatis RNA polymerase: DNA supercoiling, action of rifampicin and mechanism of rifampicin resistance." Molecular Microbiology **8**(2): 277-285.

Lewis, K. (2006). "Persister cells, dormancy and infectious disease." Nature Reviews Microbiology **5**(1): 48-56.

Lewis, K. (2008). "Multidrug tolerance of biofilms and persister cells." Curr Top Microbiol Immunol **322**: 107-131.

Li, L. M., L. Q. Bai, H. L. Yang, C. F. Xiao, R. Y. Tang, Y. F. Chen, S. M. Chen, S. S. Liu, S. N. Zhang, Y. H. Ou and T. I. M. Niu (1999). "Sputum induction to improve the diagnostic yield in patients with suspected pulmonary tuberculosis [Notes from the Field]."

Lienhardt, C., P. Glaziou, M. Uplekar, K. Lönnroth, H. Getahun and M. Raviglione (2012). "Global tuberculosis control: lessons learnt and future prospects." Nature Reviews Microbiology **10**(6): 407-416.

Lin, P. L. and J. L. Flynn (2010). "Understanding Latent Tuberculosis: A Moving Target." J Immunol **185**(1): 15-22.

Lipworth, S., R. J. Hammond, V. O. Baron, Y. Hu, A. Coates and S. H. Gillespie (2016). "Defining dormancy in mycobacterial disease." Tuberculosis (Edinb) **99**: 131-142.

Liu, J., C. E. Barry, G. S. Besra and H. Nikaido (1996). "Mycolic acid structure determines the fluidity of the mycobacterial cell wall." J Biol Chem **271**(47): 29545-29551.

Liu, W., Y. Hou, H. Chen, H. Wei, W. Lin, J. Li, M. Zhang, F. He and Y. Jiang (2011). "Sample preparation method for isolation of single-cell types from mouse liver for proteomic studies." Proteomics **11**(17): 3556-3564.

Loddenkemper, R., D. Sagebiel and A. Brendel (2002). "Strategies against multidrug-resistant tuberculosis." Eur Respir J Suppl **36**: 66s-77s.

Lodish, H., A. Berk, S. L. Zipursky, P. Matsudaira, D. Baltimore and J. Darnell (2000). "Purification of Cells and Their Parts."

Loebel, R. O., E. Shorr and H. B. Richardson (1933). "The Influence of Adverse Conditions upon the Respiratory Metabolism and Growth of Human Tubercle Bacilli 1." J Bacteriol **26**(2): 167-200.

Lonroth, K., E. Jaramillo, B. G. Williams, C. Dye and M. Raviglione (2009). Drivers of tuberculosis epidemics: the role of risk factors and social determinants. *Soc Sci Med*. England. **68**: 2240-2246.

Lorenz, M. C. and G. R. Fink (2002). Life and Death in a Macrophage: Role of the Glyoxylate Cycle in Virulence. *Eukaryot Cell*. **1**: 657-662.

Mach, A. J. and D. Di Carlo (2010). "Continuous scalable blood filtration device using inertial microfluidics." *Biotechnol Bioeng* **107**(2): 302-311.

Makinoshima, H., A. Nishimura and A. Ishihama (2002). Fractionation of Escherichia coli cell populations at different stages during growth transition to stationary phase. *Mol Microbiol*. England. **43**: 269-279.

Mangili, A. and M. A. Gendreau (2005). Transmission of infectious diseases during commercial air travel. *Lancet*. England. **365**: 989-996.

Mangtani, P., D. J. Jolley, J. M. Watson and L. C. Rodrigues (1995). "Socioeconomic deprivation and notification rates for tuberculosis in London during 1982-91." *BMJ* **310**(6985): 963-966.

Marais, B. J., W. Brittle, K. Painczyk, A. C. Hesselring, N. Beyers, E. Wasserman, D. van Soolingen and R. M. Warren (2008). "Use of light-emitting diode fluorescence microscopy to detect acid-fast bacilli in sputum." *Clin Infect Dis* **47**(2): 203-207.

MARTIN, N. J., W. o. S. A. C. Department of Microbiology, Auchincruive, Ayr KA65HW, U.K., R. M. MACDONALD and R. E. S. Department of Soil Microbiology, Harpenden AL52JQ, U.K. (2015). "Separation of Non-filamentous Micro-organisms from Soil by Density Gradient Centrifugation in Percoll." *Journal of Applied Bacteriology* **51**(2): 243-251.

Master, S. S., B. Springer, P. Sander, E. C. Boettger, V. Deretic and G. S. Timmins (2002). "Oxidative stress response genes in Mycobacterium tuberculosis: role of ahpC in resistance to peroxynitrite and stage-specific survival in macrophages." *Microbiology* **148**(Pt 10): 3139-3144.

Matsunaga, I., T. Naka, R. S. Talekar, M. J. McConnell, K. Katoh, H. Nakao, A. Otsuka, S. M. Behar, I. Yano, D. B. Moody and M. Sugita (2008). Mycolyltransferase-mediated Glycolipid Exchange in Mycobacteria\*. *J Biol Chem*. **283**: 28835-28841.

Mattos, K. A., F. A. Lara, V. G. Oliveira, L. S. Rodrigues, H. D'Avila, R. C. Melo, P. P. Manso, E. N. Sarno, P. T. Bozza and M. C. Pessolani (2011). "Modulation of lipid droplets by Mycobacterium leprae in Schwann cells: a putative mechanism for host lipid acquisition and bacterial survival in phagosomes." *Cell Microbiol* **13**(2): 259-273.

Maurer, N., K. F. Wong, M. J. Hope and P. R. Cullis (1998). Anomalous solubility behavior of the antibiotic ciprofloxacin encapsulated in liposomes: a 1H-NMR study. *Biochim Biophys Acta*. Netherlands. **1374**: 9-20.

Mboowa, G., C. Namaganda and W. Ssengooba (2014). "Rifampicin resistance mutations in the 81 bp RRDR of rpoB gene in Mycobacterium tuberculosis clinical isolates using Xpert® MTB/RIF in Kampala, Uganda: a retrospective study." *BMC Infectious Diseases* **14**(1): 481.

McKinney, J. D., K. Honer zu Bentrup, E. J. Munoz-Elias, A. Miczak, B. Chen, W. T. Chan, D. Swenson, J. C. Sacchetti, W. R. Jacobs, Jr. and D. G. Russell (2000). "Persistence of Mycobacterium tuberculosis in macrophages and mice requires the glyoxylate shunt enzyme isocitrate lyase." *Nature* **406**(6797): 735-738.

Mehta, J. B., A. Dutt, L. Harvill and K. M. Mathews (1991). "Epidemiology of extrapulmonary tuberculosis. A comparative analysis with pre-AIDS era." *Chest* **99**(5): 1134-1138.

Middlebrook, G. and M. L. Cohn (1958). "Bacteriology of Tuberculosis: Laboratory Methods." *Am J Public Health Nations Health* **48**(7): 844-853.

Miller, L. G., S. M. Asch, E. I. Yu, L. Knowles, L. Gelberg and P. Davidson (2000). "A Population-Based Survey of Tuberculosis Symptoms: How Atypical Are Atypical Presentations?".

Miller, R. G. and R. A. Phillips (1969). "Separation of cells by velocity sedimentation." *J Cell Physiol* **73**(3): 191-201.

Millington, K. A., S. Gooding, T. S. Hinks, D. J. Reynolds and A. Lalvani (2010). "Mycobacterium tuberculosis-specific cellular immune profiles suggest bacillary persistence decades after spontaneous cure in untreated tuberculosis." *J Infect Dis* **202**(11): 1685-1689.

Miltenyi, S., W. Muller, W. Weichel and A. Radbruch (1990). "High gradient magnetic cell separation with MACS." *Cytometry* **11**(2): 231-238.

Minder, S., W. A. Daniel, J. Clausen and M. H. Bickel (1994). "Adipose tissue storage of drugs as a function of binding competition. In-vitro studies with distribution dialysis." *J Pharm Pharmacol* **46**(4): 313-315.

MINNIKIN, D. E., P. V. PATEL, L. ALSHAMAONY and M. GOODFELLOW (1977). "Polar Lipid Composition in the Classification of Nocardia and Related Bacteria." *International Journal of Systematic and Evolutionary Microbiology* **27**(2): 104-117.

Molina-Torres, C. A., J. Ocampo-Candiani, A. Rendón, M. J. Pucci and L. Vera-Cabrera (2010). "In vitro activity of a new isothiazoloquinolone, ACH-702, against Mycobacterium tuberculosis and other mycobacteria." *Antimicrob Agents Chemother* **54**(5): 2188-2190.

Molloy, P., L. Brydon, A. J. Porter and W. J. Harris (1995). "Separation and concentration of bacteria with immobilized antibody fragments." *J Appl Bacteriol* **78**(4): 359-365.

Morawska, L. (2006). Droplet fate in indoor environments, or can we prevent the spread of infection? *Indoor Air*. Denmark. **16**: 335-347.

Morita, D., Y. Hattori, T. Nakamura, T. Igarashi, H. Harashima and M. Sugita (2013). "Major T cell response to a mycolyl glycolipid is mediated by CD1c molecules in rhesus macaques." *Infect Immun* **81**(1): 311-316.

Mukamolova, G. V., O. Turapov, J. Malkin, G. Woltmann and M. R. Barer (2010). Resuscitation-promoting factors reveal an occult population of tubercle Bacilli in Sputum. *Am J Respir Crit Care Med*. United States. **181**: 174-180.

Munoz-Elias, E. J. and J. D. McKinney (2005). Mycobacterium tuberculosis isocitrate lyases 1 and 2 are jointly required for in vivo growth and virulence. *Nat Med*. United States. **11**: 638-644.

Munoz-Elias, E. J. and J. D. McKinney (2006). Carbon metabolism of intracellular bacteria. *Cell Microbiol*. England. **8**: 10-22.

Murphy, D. J. and J. Vance (1999). Mechanisms of lipid-body formation. *Trends Biochem Sci*. England. **24**: 109-115.

Murray, M. J., A. B. Murray, M. B. Murray and C. J. Murray (1978). "The adverse effect of iron repletion on the course of certain infections." *Br Med J* **2**(6145): 1113-1115.

Narayana, A. (1982). "Overview of renal tuberculosis." *Urology* **19**(3): 231-237.

Nardell, E. A., J. Keegan, S. A. Cheney and S. C. Etkind (1991). "Airborne infection. Theoretical limits of protection achievable by building ventilation." *Am Rev Respir Dis* **144**(2): 302-306.

Naya, H., H. Romero, A. Zavala, B. Alvarez and H. Musto (2002). "Aerobiosis increases the genomic guanine plus cytosine content (GC%) in prokaryotes." *J Mol Evol* **55**(3): 260-264.

Neuefeind, J., C. J. Benmore, B. Tomberli and P. A. Egelstaff (2002). "Experimental determination of the electron density of liquid H<sub>2</sub>O and D<sub>2</sub>O - IOPscience." *Journal of Physics: Condensed Matter*.

Neyrolles, O., R. Hernandez-Pando, F. Pietri-Rouxel, P. Fornes, L. Tailleux, J. A. Barrios Payan, E. Pivert, Y. Bordat, D. Aguilar, M. C. Prevost, C. Petit and B. Gicquel (2006). "Is adipose tissue a place for Mycobacterium tuberculosis persistence?" *PLoS One* **1**: e43.

Ng, V. H., J. S. Cox, A. O. Sousa, J. D. MacMicking and J. D. McKinney (2004). "Role of KatG catalase-peroxidase in mycobacterial pathogenesis: countering the phagocyte oxidative burst." *Mol Microbiol* **52**(5): 1291-1302.

Ngo, S. C., O. Zimhony, W. J. Chung, H. Sayahi, W. R. Jacobs and J. T. Welch (2007). "Inhibition of isolated Mycobacterium tuberculosis fatty acid synthase I by pyrazinamide analogs." *Antimicrob Agents Chemother* **51**(7): 2430-2435.

Nguyen, T. K. A., A. P. Koets, W. J. Santema, W. van Eden, V. P. Rutten and I. Van Rhijn (2009). The mycobacterial glycolipid glucose monomycolate induces a memory T cell response comparable to a model protein antigen and no B cell response upon experimental vaccination of cattle. *Vaccine*. **27**: 4818-4825.

Nicas, M., W. W. Nazaroff and A. Hubbard (2005). Toward understanding the risk of secondary airborne infection: emission of respirable pathogens. *J Occup Environ Hyg*. United States. **2**: 143-154.



Nicoletti, I., G. Migliorati, M. C. Pagliacci, F. Grignani and C. Riccardi (1991). "A rapid and simple method for measuring thymocyte apoptosis by propidium iodide staining and flow cytometry." *J Immunol Methods* **139**(2): 271-279.

Nikfarjam, L. and P. Farzaneh (2012). "Prevention and Detection of Mycoplasma Contamination in Cell Culture." *Cell J* **13**(4): 203-212.

OPIE, E. L. and F. M. McPHEDRAN (1926). "SPREAD OF TUBERCULOSIS WITHIN FAMILIES." *Journal of the American Medical Association* **87**(19): 1549-1551.

Organisation, W. H. (2013). "WHO | Tuberculosis." [WHO](#).

Organization, W. H. (2013). "Tuberculosis." **34**.

Otte, S. C. M., U. o. Leiden, E. J. v. d. Meent, U. o. Leiden, P. A. v. Veelen, U. o. Leiden, A. S. Pundsnes, U. o. Leiden, J. Amesz and U. o. Leiden (2012). "Identification of the major chlorosomal bacteriochlorophylls of the green sulfur bacteria *Chlorobium vibrioforme* and *Chlorobium phaeovibrioides*; their function in lateral energy transfer." *Photosynthesis Research* **35**(2): 159-169.

Pacheco, S. A., F. F. Hsu, K. M. Powers and G. E. Purdy (2013). "MmpL11 protein transports mycolic acid-containing lipids to the mycobacterial cell wall and contributes to biofilm formation in *Mycobacterium smegmatis*." *J Biol Chem* **288**(33): 24213-24222.

Panchuk-Voloshina, N., R. P. Haugland, J. Bishop-Stewart, M. K. Bhalgat, P. J. Millard, F. Mao and W. Y. Leung (1999). "Alexa dyes, a series of new fluorescent dyes that yield exceptionally bright, photostable conjugates." *J Histochem Cytochem* **47**(9): 1179-1188.

Papineni, R. S. and F. S. Rosenthal (1997). "The size distribution of droplets in the exhaled breath of healthy human subjects." *J Aerosol Med* **10**(2): 105-116.

Parrish, N. M., J. D. Dick and W. R. Bishai (1998). Mechanisms of latency in *Mycobacterium tuberculosis*. *Trends Microbiol*. England. **6**: 107-112.

Parry, C. M., O. Kamoto, A. D. Harries, J. J. Wirima, C. M. Nyirenda, D. S. Nyangulu and C. A. Hart (1995). The use of sputum induction for establishing a diagnosis in patients with suspected pulmonary tuberculosis in Malawi. *Tuber Lung Dis*. Scotland. **76**: 72-76.

Paul A. Jensen, L. A. L., Michael F. Iademarco, Renee Ridzon. (2015). "Guidelines for Preventing the Transmission of *Mycobacterium tuberculosis* in Health-Care Settings, 2005." from <http://www.cdc.gov/MMWR/Preview/mmwrhtml/rr5417a1.htm>.

Penney, D. P., J. M. Powers, M. Frank, C. Willis and C. Churukian (2009). "Analysis and testing of biological stains-- The Biological Stain Commission Procedures." <http://dx.doi.org/10.1080/bih.77.5-6.237.275>.

Peters, W. and J. D. Ernst (2003). Mechanisms of cell recruitment in the immune response to *Mycobacterium tuberculosis*. *Microbes Infect*. France. **5**: 151-158.

Peyron, P., J. Vaubourgeix, Y. Poquet, F. Levillain, C. Botanch, F. Bardou, M. Daffe, J. F. Emile, B. Marchou, P. J. Cardona, C. de Chastellier and F. Altare (2008). "Foamy macrophages from tuberculous patients' granulomas constitute a nutrient-rich reservoir for *M. tuberculosis* persistence." *PLoS Pathog* **4**(11): e1000204.

Piccaro, G., F. Giannoni, P. Filippini, A. Mustazzolu and L. Fattorini (2013). "Activities of drug combinations against *Mycobacterium tuberculosis* grown in aerobic and hypoxic acidic conditions." *Antimicrob Agents Chemother* **57**(3): 1428-1433.

Porter, J., J. Diaper, C. Edwards and R. Pickup (1995). "Direct measurements of natural planktonic bacterial community viability by flow cytometry."

Prashant K. Jain, Kyeong Seok Lee, Ivan H. El-Sayed, ‡ and and Mostafa A. El-Sayed\* (2006). "Calculated Absorption and Scattering Properties of Gold Nanoparticles of Different Size, Shape, and Composition: Applications in Biological Imaging and Biomedicine."

Pullammanappallil, R. D. a. P. (2013). "Liquid, Gaseous and Solid Biofuels - Conversion Techniques."

Pusey, P. N. (1999). "Suppression of multiple scattering by photon cross-correlation techniques." **4**(3): 177-185.

Putman, M., R. Burton and M. H. Nahm (2005). "Simplified method to automatically count bacterial colony forming unit." *J Immunol Methods* **302**(1-2): 99-102.

Quy, H. T., N. T. Lan, M. W. Borgdorff, J. Grosset, P. D. Linh, L. B. Tung, D. van Soolingen, M. Raviglione, N. V. Co and J. Broekmans (2003). "Drug resistance among failure and relapse cases of tuberculosis: is the standard re-treatment regimen adequate?" *Int J Tuberc Lung Dis* **7**(7): 631-636.

R. Ananthanarayan, C. J. P. (2009). *Ananthanarayan and Paniker's Textbook of Microbiology*, Universities Press.

Ragno, S., M. Romano, S. Howell, D. J. Pappin, P. J. Jenner and M. J. Colston (2001). Changes in gene expression in macrophages infected with *Mycobacterium tuberculosis*: a combined transcriptomic and proteomic approach. *Immunology*. England. **104**: 99-108.

Ramakrishnan, L. (2012). "Revisiting the role of the granuloma in tuberculosis." *Nature Reviews Immunology* **12**(5): 352-366.

Ramoino, P., E. Margallo and G. Nicolo (1996). "Age-related changes in neutral lipid content of *Paramecium primaurelia* as revealed by Nile red." *J Lipid Res* **37**(6): 1207-1212.

Rao, S. (2009). Sputum smear microscopy in DOTS: Are three samples necessary? An analysis and its implications in tuberculosis control. *Lung India*. **26**: 3-4.

Raposo, G., Nijman, H. W., Stoorvogel, W. et al. (1996). "B lymphocytes secrete antigen-presenting vesicles." *J. Exp. Med.* **183**(3).

Raviglione, M. C. (2009). *Tuberculosis : the essentials*. New York, Informa Healthcare USA.

Reed, M. B., S. Gagneux, K. DeRiemer, P. M. Small and C. E. B. III (2007). "The W-Beijing Lineage of *Mycobacterium tuberculosis* Overproduces Triglycerides and Has the DosR Dormancy Regulon Constitutively Upregulated." *Journal of Bacteriology*.

Rhoades, E., F. Hsu, J. B. Torrelles, J. Turk, D. Chatterjee and D. G. Russell (2003). "Identification and macrophage-activating activity of glycolipids released from intracellular *Mycobacterium bovis* BCG." *Mol Microbiol* **48**(4): 875-888.

Rhoades, E. R., C. Streeter, J. Turk and F. F. Hsu (2011). "Characterization of sulfolipids of *Mycobacterium tuberculosis* H37Rv by multiple-stage linear ion-trap high-resolution mass spectrometry with electrospray ionization reveals that the family of sulfolipid II predominates." *Biochemistry* **50**(42): 9135-9147.

Rieder, H. L. (2009). "The infectiousness of laryngeal tuberculosis: appropriate public health action based on false premises." *Int J Tuberc Lung Dis* **13**(1): 4-5.

Rodríguez, J. C., M. Ruiz, M. López and G. Royo (2002). "In vitro activity of moxifloxacin, levofloxacin, gatifloxacin and linezolid against *Mycobacterium tuberculosis*." *Int J Antimicrob Agents* **20**(6): 464-467.

Rogall, T., T. Flohr and E. C. Bottger (1990). "Differentiation of *Mycobacterium* species by direct sequencing of amplified DNA." *J Gen Microbiol* **136**(9): 1915-1920.

Roy, C. J. and D. K. Milton (2004). Airborne transmission of communicable infection--the elusive pathway. *N Engl J Med*. United States. **350**: 1710-1712.

Russell, D. G. (2007). Who puts the tubercle in tuberculosis? *Nat Rev Microbiol*. England. **5**: 39-47.

Russell, D. G. (2011). "Mycobacterium tuberculosis and the intimate discourse of a chronic infection." *Immunol Rev* **240**(1): 252-268.

Russell, D. G., C. E. Barry, 3rd and J. L. Flynn (2010). Tuberculosis: what we don't know can, and does, hurt us. *Science*. United States. **328**: 852-856.

Russmann, L., A. Jung and H. G. Heidrich (1982). "The use of percoll gradients, elutriator rotor elution, and mithramycin staining for the isolation and identification of intraerythrocytic stages of *Plasmodium berghei*." *Z Parasitenkd* **66**(3): 273-280.

Rustad, T. R., M. I. Harrell, R. Liao and D. R. Sherman (2008). "The enduring hypoxic response of *Mycobacterium tuberculosis*." *PLoS One* **3**(1): e1502.

Sakula, A. (1983). "Robert Koch: Centenary of the Discovery of the Tubercle Bacillus, 1882." *Can Vet J* **24**(4): 127-131.

Salina, E. G., S. J. Waddell, N. Hoffmann, I. Rosenkrands, P. D. Butcher and A. S. Kaprelyants (2014). "Potassium availability triggers *Mycobacterium tuberculosis* transition to, and resuscitation from, non-culturable (dormant) states." *Open Biol* **4**(10).

Salton, M. R. J. and K.-S. Kim (1996). "Structure."

Sarathy, J. P., V. Dartois and E. J. D. Lee (2012). The Role of Transport Mechanisms in Mycobacterium Tuberculosis Drug Resistance and Tolerance. *Pharmaceuticals (Basel)*. **5**: 1210-1235.

Sartain, M. J., D. L. Dick, C. D. Rithner, D. C. Crick and J. T. Belisle (2011). "Lipidomic analyses of Mycobacterium tuberculosis based on accurate mass measurements and the novel "Mtb LipidDB"." *J Lipid Res* **52**(5): 861-872.

Saunders, B. M. and A. M. Cooper (2000). "Restraining mycobacteria: Role of granulomas in mycobacterial infections." *Immunology and Cell Biology* **78**(4): 334-341.

Schaefer, W. B. and C. W. Lewis (1965). "Effect of Oleic Acid on Growth and Cell Structure of Mycobacteria." *J Bacteriol* **90**(5): 1438-1447.

Schatzel, K., M. Drewel and J. Ahrens (1999). "Suppression of multiple scattering in photon correlation spectroscopy."

Schmidt, M., M. K. Hourfar, S. B. Nicol, H. P. Spengler, T. Montag and E. Seifried (2006). "FACS technology used in a new rapid bacterial detection method." *Transfus Med* **16**(5): 355-361.

Schubert, G. E., T. Haltaufderheide and R. Golz (1992). "Frequency of urogenital tuberculosis in an unselected autopsy series from 1928 to 1949 and 1976 to 1989." *Eur Urol* **21**(3): 216-223.

Schweizer, E. and J. Hofmann (2004). "Microbial type I fatty acid synthases (FAS): major players in a network of cellular FAS systems." *Microbiol Mol Biol Rev* **68**(3): 501-517, table of contents.

Shata, A. M., J. B. Coulter, C. M. Parry, G. Ching'ani, R. L. Broadhead and C. A. Hart (1996). "Sputum induction for the diagnosis of tuberculosis." *Arch Dis Child* **74**(6): 535-537.

Sherman, D. R., P. J. Sabo, M. J. Hickey, T. M. Arain, G. G. Mahairas, Y. Yuan, C. E. Barry and C. K. Stover (1995). "Disparate responses to oxidative stress in saprophytic and pathogenic mycobacteria." *Proc Natl Acad Sci U S A* **92**(14): 6625-6629.

Shi, C. and E. G. Pamer (2011). "Monocyte recruitment during infection and inflammation." *Nature Reviews Immunology* **11**(11): 762-774.

Shi, L., C. D. Sohaskey, B. D. Kana, S. Dawes, R. J. North, V. Mizrahi and M. L. Gennaro (2005). "Changes in energy metabolism of Mycobacterium tuberculosis in mouse lung and under in vitro conditions affecting aerobic respiration."

Shi, W., X. Zhang, X. Jiang, H. Yuan, J. S. Lee, C. E. Barry, 3rd, H. Wang, W. Zhang and Y. Zhang (2011). "Pyrazinamide inhibits trans-translation in Mycobacterium tuberculosis." *Science* **333**(6049): 1630-1632.

Shuler, M. L., R. Aris and H. M. Tsuchiya (1972). "Hydrodynamic focusing and electronic cell-sizing techniques." *Appl Microbiol* **24**(3): 384-388.

Sibley, L. D., L. B. Adams and J. L. Krahenbuhl (1990). "Inhibition of interferon-gamma-mediated activation in mouse macrophages treated with lipoarabinomannan." *Clin Exp Immunol* **80**(1): 141-148.

Silva Miranda, M., A. Breiman, S. Allain, F. Deknuydt and F. Altare (2012). "The tuberculous granuloma: an unsuccessful host defence mechanism providing a safety shelter for the bacteria?" *Clin Dev Immunol* **2012**: 139127.

Singh, H., R. Bhandari and I. P. Kaur (2013). "Encapsulation of Rifampicin in a solid lipid nanoparticulate system to limit its degradation and interaction with Isoniazid at acidic pH." *Int J Pharm* **446**(1-2): 106-111.

Sirakova, T. D., U. o. C. F. Burnett School of Biomedical Sciences, Orlando, Florida, United States of America, C. Deb, U. o. C. F. Burnett School of Biomedical Sciences, Orlando, Florida, United States of America, J. Daniel, U. o. C. F. Burnett School of Biomedical Sciences, Orlando, Florida, United States of America, H. D. Singh, U. o. C. F. Burnett School of Biomedical Sciences, Orlando, Florida, United States of America, H. Maamar, U. o. C. F. Burnett School of Biomedical Sciences, Orlando, Florida, United States of America, V. S. Dubey, U. o. C. F. Burnett School of Biomedical Sciences, Orlando, Florida, United States of America, P. E. Kolattukudy and U. o. C. F. Burnett School of Biomedical Sciences, Orlando, Florida, United States of America (2012). "Wax Ester Synthesis is Required for Mycobacterium tuberculosis to Enter In Vitro Dormancy." *PLOS ONE* **7**(12).

Sirakova, T. D., V. S. Dubey, C. Deb, J. Daniel, T. A. Korotkova, B. Abomoelak and P. E. Kolattukudy (2006). "Identification of a diacylglycerol acyltransferase gene involved in accumulation of triacylglycerol in *Mycobacterium tuberculosis* under stress." Microbiology.

Smith, I. (2003). "Mycobacterium tuberculosis pathogenesis and molecular determinants of virulence." Clin Microbiol Rev **16**(3): 463-496.

Soukos, N. S., S. Som, A. D. Abernethy, K. Ruggiero, J. Dunham, C. Lee, A. G. Doukas and J. M. Goodson (2005). "Phototargeting Oral Black-Pigmented Bacteria."

Spudich, J. A. and A. Kornberg (1968). "Biochemical Studies of Bacterial Sporulation and Germination." The Journal of Biological Chemistry **246**: 4600 - 4605.

Ssengooba, W., D. P. Kateete, A. Wajja, E. Bugumirwa, G. Mboowa, C. Namaganda, G. Nakayita, M. Nassolo, F. Mumbowa, B. B. Asiimwe, J. Waako, S. Verver, P. Musoke, H. Mayanja-Kizza and M. L. Joloba (2012). "An Early Morning Sputum Sample Is Necessary for the Diagnosis of Pulmonary Tuberculosis, Even with More Sensitive Techniques: A Prospective Cohort Study among Adolescent TB-Suspects in Uganda." Tuberc Res Treat **2012**: 970203.

Stead, W. W. and J. P. Lofgren (1983). "Does the risk of tuberculosis increase in old age?" J Infect Dis **147**(5): 951-955.

Steen, T. W. and G. N. Mazonde (1998). "Pulmonary tuberculosis in Kweneng District, Botswana: delays in diagnosis in 212 smear-positive patients." Int J Tuberc Lung Dis **2**(8): 627-634.

Steingart, K. R., M. Henry, V. Ng, P. C. Hopewell, A. Ramsay, J. Cunningham, R. Urbanczik, M. Perkins, M. A. Aziz and M. Pai (2006). Fluorescence versus conventional sputum smear microscopy for tuberculosis: a systematic review. Lancet Infect Dis. United States. **6**: 570-581.

Su, X.-z., V. M. Heatwole, S. P. Wertheimer, F. Guinet, J. A. Herrfeldt, D. S. Peterson, J. A. Ravetch and T. E. Wellems (1995). "The large diverse gene family var encodes proteins involved in cytoadherence and antigenic variation of plasmodium falciparum-infected erythrocytes."

Suarez, J., K. Ranguelova, A. A. Jarzecki, J. Manzerova, V. Krymov, X. Zhao, S. Yu, L. Metlitsky, G. J. Gerfen and R. S. Magliozzo (2009). "An oxyferrous heme/protein-based radical intermediate is catalytically competent in the catalase reaction of *Mycobacterium tuberculosis* catalase-peroxidase (KatG)." J Biol Chem **284**(11): 7017-7029.

Takayama, K., E. L. Armstrong, K. A. Kunugi and J. O. Kilburn (1979). "Inhibition by ethambutol of mycolic acid transfer into the cell wall of *Mycobacterium smegmatis*." Antimicrob Agents Chemother **16**(2): 240-242.

Takayama, K., H. K. Schnoes, E. L. Armstrong and R. W. Boyle (1975). "Site of inhibitory action of isoniazid in the synthesis of mycolic acids in *Mycobacterium tuberculosis*." J Lipid Res **16**(4): 308-317.

Takayama, K., C. Wang and G. S. Besra (2005). "Pathway to synthesis and processing of mycolic acids in *Mycobacterium tuberculosis*." Clin Microbiol Rev **18**(1): 81-101.

Tang, J. W., Y. Li, I. Eames, P. K. Chan and G. L. Ridgway (2006). Factors involved in the aerosol transmission of infection and control of ventilation in healthcare premises. J Hosp Infect. England. **64**: 100-114.

Tanoue, S., S. Mitarai and H. Shishido (2002). Comparative study on the use of solid media: Lowenstein-Jensen and Ogawa in the determination of anti-tuberculosis drug susceptibility. Tuberculosis (Edinb). England. **82**: 63-67.

Tato, M., E. G. de la Pedrosa, R. Cantón, I. Gómez-García, J. Fortún, P. Martín-Davila, F. Baquero and E. Gomez-Mampaso (2006). "In vitro activity of linezolid against *Mycobacterium tuberculosis* complex, including multidrug-resistant *Mycobacterium bovis* isolates." Int J Antimicrob Agents **28**(1): 75-78.

Teramoto, K., T. Tamura, S. Hanada, T. Sato, H. Kawasaki, K.-i. Suzuki and H. Sato (2013). "Simple and rapid characterization of mycolic acids from *Dietzia* strains by using MALDI spiral-TOFMS with ultra high mass-resolving power." The Journal of Antibiotics **66**(12): 713-717.

Thadepalli, H., K. Rambhatla and I. H. Niden (1977). "Transtacheal Aspiration in Diagnosis of Sputum-Smear—Negative Tuberculosis." JAMA **238**(10): 1037-1040.

Tombolini, R., A. L. f. N. S. Department of Biochemistry, Stockholm University, Sâ€™10691 Stockholm, Sweden, A. Unge, A. L. f. N. S. Department of Biochemistry, Stockholm University, Sâ€™10691 Stockholm, Sweden, M. S. U. NSF Center for Microbial Ecology, East Lansing, MI 48824, USA, M. E. Davey, M. S. U. NSF Center for Microbial Ecology, East Lansing, MI 48824, USA, M. S. U. Department of Microbiology, East Lansing, MI 48824, USA, F. J. Bruijn, M. S. U. NSF Center for Microbial Ecology, East Lansing, MI 48824, USA, M. S. U. Department of Microbiology, East Lansing, MI 48824, USA, M. S. U. MSUâ€™DOE Plant Research Laboratory, East Lansing, MI 48824, USA, J. K. Jansson and A. L. f. N. S. Department of Biochemistry, Stockholm University, Sâ€™10691 Stockholm, Sweden (2006). "Flow cytometric and microscopic analysis of GFPâ€™tagged *Pseudomonas fluorescens* bacteria." *FEMS Microbiology Ecology* **22**(1): 17-28.

Tomlinson, M. J., S. Tomlinson, X. B. Yang and J. Kirkham (2013). "Cell separation: Terminology and practical considerations." *J Tissue Eng* **4**: 2041731412472690.

Tortoli, E. (2006). The new mycobacteria: an update. *FEMS Immunol Med Microbiol*. Netherlands. **48**: 159-178.

Tripathi, R. P., N. Tewari, N. Dwivedi and V. K. Tiwari (2005). "Fighting tuberculosis: an old disease with new challenges." *Med Res Rev* **25**(1): 93-131.

Trojan, J., H. T. Duc, L. C. Upegui-Gonzalez, F. Hor, Y. Guo, D. Anthony and J. Ilan (1996). "Presence of MHC-I and B-7 molecules in rat and human glioma cells expressing antisense IGF-I mRNA." **212**(1): 9-12.

Truant, J. P., W. A. Brett and W. Thomas, Jr. (1962). "Fluorescence microscopy of tubercle bacilli stained with auramine and rhodamine." *Henry Ford Hosp Med Bull* **10**: 287-296.

Tsukamura, M. and S. Tsukamura (1965). "[GROUPING OF MYCOBACTERIA BY UTILIZATION OF PROPYLENE GLYCOL, GLUCOSE, FRUCTOSE, AND SUCROSE AS SOLE CARBON SOURCES]." *Nihon Saikingaku Zasshi* **20**: 229-232.

Tunney, M. M., S. Patrick, M. D. Curran, G. Ramage, D. Hanna, J. R. Nixon, S. P. Gorman, R. I. Davis and N. Anderson (1999). "Detection of Prosthetic Hip Infection at Revision Arthroplasty by Immunofluorescence Microscopy and PCR Amplification of the Bacterial 16S rRNA Gene."

Urban, C. and P. Schurtenberger (1998). "Characterization of Turbid Colloidal Suspensions Using Light Scattering Techniques Combined with Cross-Correlation Methods ☆." **207**(1): 150-158.

van Cleeff, M., L. Kivihya-Ndugga, H. Meme, J. Odhiambo and P. Klatser (2005). "The role and performance of chest X-ray for the diagnosis of tuberculosis: A cost-effectiveness analysis in Nairobi, Kenya." *BMC Infectious Diseases* **5**(1): 111.

Van Deun, A., A. Hamid Salim, K. J. M. Aung, M. A. Hossain, N. Chambugonj, M. A. Hye, A. Kawria and E. Declercq (2005). "Performance of variations of carbolfuchsin staining of sputum smears for AFB under field conditions."

van Ingen, J., R. E. Aarnoutse, P. R. Donald, A. H. Diacon, R. Dawson, G. Plemper van Balen, S. H. Gillespie and M. J. Boeree (2011). Why Do We Use 600 mg of Rifampicin in Tuberculosis Treatment? *Clin Infect Dis*. United States. **52**: e194-199.

Vandal, O. H., C. F. Nathan and S. Ehrt (2009). "Acid resistance in *Mycobacterium tuberculosis*." *J Bacteriol* **191**(15): 4714-4721.

Varma, R., H. Moosmiller and W. P. Arnott (2003). "Toward an ideal integrating nephelometer." *Optics Letters*, Vol. 28, Issue 12, pp. 1007-1009.

Velayati, A. A., P. Farnia, M. A. Merza, G. K. Zhavnerko, P. Tabarsi, L. P. Titov, J. Ghanavei, M. Setare, N. N. Poleschuyk, P. Owlia, M. Sheikolslami, R. Ranjbar and M. R. Masjedi (2010). New insight into extremely drug-resistant tuberculosis: using atomic force microscopy. *Eur Respir J*. Switzerland. **36**: 1490-1493.

Vercellotti, G. M., J. B. McCarthy, P. Lindholm, P. K. Peterson, H. S. Jacob and L. T. Furcht (1985). "Extracellular matrix proteins (fibronectin, laminin, and type IV collagen) bind and aggregate bacteria." *Am J Pathol* **120**(1): 13-21.

Vergne, I., J. Chua and V. Deretic (2003). Tuberculosis Toxin Blocking Phagosome Maturation Inhibits a Novel Ca<sup>2+</sup>/Calmodulin-PI3K hVPS34 Cascade. *J Exp Med*. **198**: 653-659.

Vergne, I., R. A. Fratti, P. J. Hill, J. Chua, J. Belisle and V. Deretic (2004). Mycobacterium tuberculosis Phagosome Maturation Arrest: Mycobacterial Phosphatidylinositol Analog Phosphatidylinositol Mannoside Stimulates Early Endosomal Fusion. *Mol Biol Cell*. **15**: 751-760.

Verver, S., R. M. Warren, Z. Munch, M. Richardson, G. D. van der Spuy, M. W. Borgdorff, M. A. Behr, N. Beyers and P. D. van Helden (2004). Proportion of tuberculosis transmission that takes place in households in a high-incidence area. *Lancet*. England. **363**: 212-214.

Vesey, G., J. S. Slade, M. Byrne, K. Shepherd and C. R. Fricker (1993). "A new method for the concentration of Cryptosporidium oocysts from water." *J Appl Bacteriol* **75**(1): 82-86.

Via, L. E., P. L. Lin, S. M. Ray, J. Carrillo, S. S. Allen, S. Y. Eum, K. Taylor, E. Klein, U. Manjunatha, J. Gonzales, E. G. Lee, S. K. Park, J. A. Raleigh, S. N. Cho, D. N. McMurray, J. L. Flynn and C. E. Barry (2008). Tuberculous Granulomas Are Hypoxic in Guinea Pigs, Rabbits, and Nonhuman Primates<sup>▽</sup>. *Infect Immun*. **76**: 2333-2340.

Vilcheze, C. and W. R. Jacobs, Jr. (2007). "The mechanism of isoniazid killing: clarity through the scope of genetics." *Annu Rev Microbiol* **61**: 35-50.

Viljanen, M. K., T. Nurmi and A. Salminen (1983). "Enzyme-linked immunosorbent assay (ELISA) with bacterial sonicate antigen for IgM, IgA, and IgG antibodies to Francisella tularensis: comparison with bacterial agglutination test and ELISA with lipopolysaccharide antigen." *J Infect Dis* **148**(4): 715-720.

Vincent, R. and D. Nadeau (1984). "Adjustment of the osmolality of Percoll for the isopycnic separation of cells and cell organelles." *Anal Biochem* **141**(2): 322-328.

Vollmer, W., D. Blanot and M. A. de Pedro (2008). Peptidoglycan structure and architecture. *FEMS Microbiol Rev*. England. **32**: 149-167.

Voskuil, M. I., I. L. Bartek, K. Visconti and G. K. Schoolnik (2011). "The Response of Mycobacterium Tuberculosis to Reactive Oxygen and Nitrogen Species." *Front Microbiol* **2**.

Wallis, R. S., S. Patil, S. H. Cheon, K. Edmonds, M. Phillips, M. D. Perkins, M. Joloba, A. Namale, J. L. Johnson, L. Teixeira, R. Dietze, S. Siddiqi, R. D. Mugerwa, K. Eisenach and J. J. Ellner (1999). Drug Tolerance in Mycobacterium tuberculosis. *Antimicrob Agents Chemother*. **43**: 2600-2606.

Waltermann, M. and A. Steinbuchel (2005). Neutral lipid bodies in prokaryotes: recent insights into structure, formation, and relationship to eukaryotic lipid depots. *J Bacteriol*. United States. **187**: 3607-3619.

Waltermann, M., T. Stoveken and A. Steinbuchel (2007). Key enzymes for biosynthesis of neutral lipid storage compounds in prokaryotes: properties, function and occurrence of wax ester synthases/acyl-CoA: diacylglycerol acyltransferases. *Biochimie*. France. **89**: 230-242.

Wanger, A. and K. Mills (1996). "Testing of Mycobacterium tuberculosis susceptibility to ethambutol, isoniazid, rifampin, and streptomycin by using Etest." *J Clin Microbiol* **34**(7): 1672-1676.

Wayne, L. G. (1976). "Dynamics of submerged growth of Mycobacterium tuberculosis under aerobic and microaerophilic conditions." *Am Rev Respir Dis* **114**(4): 807-811.

Wayne, L. G. (1994). "Dormancy of Mycobacterium tuberculosis and latency of disease." *Eur J Clin Microbiol Infect Dis* **13**(11): 908-914.

Wayne, L. G. and L. G. Hayes (1996). "An in vitro model for sequential study of shutdown of Mycobacterium tuberculosis through two stages of nonreplicating persistence." *Infect Immun* **64**(6): 2062-2069.

Wayne, L. G. and K. Y. Lin (1982). "Glyoxylate metabolism and adaptation of Mycobacterium tuberculosis to survival under anaerobic conditions." *Infect Immun* **37**(3): 1042-1049.

Wayne, L. G. and C. D. Sohaskey (2001). Nonreplicating persistence of mycobacterium tuberculosis. *Annu Rev Microbiol*. United States. **55**: 139-163.

Weiss, E., J. C. Coolbaugh and J. C. Williams (1975). "Separation of viable Rickettsia typhi from yolk sac and L cell host components by renografin density gradient centrifugation." *Appl Microbiol* **30**(3): 456-463.

Wenk, M. R. (2005). "The emerging field of lipidomics." *Nat Rev Drug Discov* **4**(7): 594-610.

WHO Revised international definition in tuberculosis control. *Int J Tuberc Lung Dis*. **5**: 213-215.

WHO (2001). "Revised international definitions in tuberculosis control." Int J Tuberc Lung Dis **5**(3): 213-215.

WHO (2006). "WHO | WHO Global Task Force outlines measures to combat XDR-TB worldwide." WHO.

Wolucka, B. A., M. R. McNeil, E. de Hoffmann, T. Chojnacki and P. J. Brennan (1994). "Recognition of the lipid intermediate for arabinogalactan/arabinomannan biosynthesis and its relation to the mode of action of ethambutol on mycobacteria." J Biol Chem **269**(37): 23328-23335.

Wood, R., S. Johnstone-Robertson, P. Uys, J. Hargrove, K. Middelkoop, S. D. Lawn and L. G. Bekker (2010). "Tuberculosis transmission to young children in a South African community: modeling household and community infection risks." Clin Infect Dis **51**(4): 401-408.

Wu, Z., W. L. Wang, Y. Zhu, J. W. Cheng, J. Dong, M. X. Li, L. Yu, Y. Lv and B. Wang (2013). "Diagnosis and treatment of hepatic tuberculosis: report of five cases and review of literature." Int J Clin Exp Med **6**(9): 845-850.

Yeager, H., Jr., J. Lacy, L. R. Smith and C. A. LeMaistre (1967). "Quantitative studies of mycobacterial populations in sputum and saliva." Am Rev Respir Dis **95**(6): 998-1004.

Yimer, S. A., M. Agonafir, Y. Derese, Y. Sani, G. A. Bjune and C. Holm-Hansen (2012). "Primary drug resistance to anti-tuberculosis drugs in major towns of Amhara region, Ethiopia." APMIS **120**(6): 503-509.

Young, D. B., H. P. Gideon and R. J. Wilkinson (2009). "Eliminating latent tuberculosis." Trends in Microbiology **17**(5): 183-188.

Zar, H., E. Tannenbaum, P. Apolles, P. Roux, D. Hanslo and G. Hussey (2000). "Sputum induction for the diagnosis of pulmonary tuberculosis in infants and young children in an urban setting in South Africa." Arch Dis Child **82**(4): 305-308.

Zborowski, M., L. R. Moore, S. Reddy, G. H. Chen, L. Sun and J. J. Chalmers (1996). "Magnetic flow sorting using a model system of human lymphocytes and a colloidal magnetic label." Asaio j **42**(5): M666-671.

Zhang, Y. (2004). "Persistent and dormant tubercle bacilli and latent tuberculosis." Front Biosci **9**: 1136-1156.

Zhang, Y. and D. Mitchison (2003). "The curious characteristics of pyrazinamide: a review." Int J Tuberc Lung Dis **7**(1): 6-21.

Zhang, Y., M. M. Wade, A. Scorpio, H. Zhang and Z. Sun (2003). Mode of action of pyrazinamide: disruption of Mycobacterium tuberculosis membrane transport and energetics by pyrazinoic acid. J Antimicrob Chemother. England. **52**: 790-795.

Zhao, L., D. Wu, L.-F. Wu and T. Song (2007). "A simple and accurate method for quantification of magnetosomes in magnetotactic bacteria by common spectrophotometer." **70**(3): 377-383.

Zheng, S., H. Lin, J. Q. Liu, M. Balic, R. Datar, R. J. Cote and Y. C. Tai (2007). "Membrane microfilter device for selective capture, electrolysis and genomic analysis of human circulating tumor cells." J Chromatogr A **1162**(2): 154-161.

Zhou, S., C. Burger, B. Chu, M. Sawamura, N. Nagahama, M. Toganoh, U. E. Hackler, H. Isobe and E. Nakamura (2001). "Spherical Bilayer Vesicles of Fullerene-Based Surfactants in Water: A Laser Light Scattering Study."

Zhu, B. and S. K. Murthy "Stem Cell Separation Technologies." Curr Opin Chem Eng **2**(1): 3-7.

Zimm, B. H. (1945). "Molecular Theory of the Scattering of Light in Fluids." Journal of Chemical Physics **13**: 141-145.

Zumla, A. I., S. H. Gillespie, M. Hoelscher, P. P. Philips, S. T. Cole, I. Abubakar, T. D. McHugh, M. Schito, M. Maeurer and A. J. Nunn (2014). "New antituberculosis drugs, regimens, and adjunct therapies: needs, advances, and future prospects." Lancet Infect Dis **14**(4): 327-340.

Zwilling, B. S., L. B. Campolito and N. A. Reiches (1982). "Alveolar macrophage subpopulations identified by differential centrifugation on a discontinuous albumin density gradient." Am Rev Respir Dis **125**(4): 448-452.

